Skoltech
Skolkovo Institute of Science and Technology

Jury Member Report – Doctor of Philosophy thesis.

Name of Candidate: Nadezhda Khaustova

PhD Program: Petroleum Engineering

Title of Thesis: Uranium accumulation in marine source rocks: role of redox conditions and correlation with productivity

Supervisor: Professor Mikhail Spasennykh
Co-supervisors: Professor Yuri Popov
Dr. Elena Kozlova

Name of the Reviewer: Professor D. N. Singh

I confirm the absence of any conflict of interest	09-08-2022 **Date: DD-MM-YYYY**

The purpose of this report is to obtain an independent review from the members of PhD defense Jury before the thesis defense. The members of PhD defense Jury are asked to submit signed copy of the report at least 30 days prior the thesis defense. The Reviewers are asked to bring a copy of the completed report to the thesis defense and to discuss the contents of each report with each other before the thesis defense.

If the reviewers have any queries about the thesis which they wish to raise in advance, please contact the Chair of the Jury.

Reviewer's Report

Reviewers report should contain the following items:

- Brief evaluation of the thesis quality and overall structure of the dissertation.
- The relevance of the topic of dissertation work to its actual content
- The relevance of the methods used in the dissertation
- The scientific significance of the results obtained and their compliance with the international level and current state of the art
- The relevance of the obtained results to applications (if applicable)
- The quality of publications

The summary of issues to be addressed before/during the thesis defense

Doctoral Thesis: Nadezhda Khaustova

Title: Uranium Accumulation in Marine Source Rocks: Role Of Redox Conditions and Correlation With Productivity

General Comments:

The thesis presents the factors influencing the uranium accumulation in the oil-source rocks and its relationship with the productivity of the oil-source rocks. The factor influencing uranium accumulation, considered in this work, is redox conditions. The way of writing shall be better. Grammar and spelling mistakes shall be avoided. The results of tests shall be represented more pictorially and graphically. The analysis of the figures and graphs shall be given more emphasis instead of providing statistics. More details on thermodynamic modeling like the governing equations shall be included. The mismatch in the text and the data provided shall be avoided.

Section-wise specific comments:

Abstract:

1. The type of studies conducted (experimental, numerical or both) shall be mentioned.
2. It is mentioned as 'other' in the factors influencing uranium accumulation. Clarify.

Chapter 1: Introduction:

1. What is the reason for considering uranium for characterizing the oil source rock?
2. It is mentioned that data was obtained on core samples from 13 wells but only data for 9 wells is provided. The data for the remaining 4 wells shall be included.

Chapter 2: Review of Literature

1. The reason for the higher mobility of uranium during weathering shall be specified.
2. It is mentioned that the transition of U^{+6} to U^{+4} depends on pH and E_h. Is there any effect of pressure and temperature conditions in this transition?
3. It is mentioned that the anaerobic scheme of organic matter decomposition takes place at low E_h values. A range shall be mentioned from the literature studies.
4. The depth of various zones presented in Figures 5 and 6 shall be included.
5. The explanation on what is V I Vernadsky assumption shall be provided.
6. In figure 9, the sedimentation rates are qualitatively mentioned. The quantification of slow, high, and maximum sedimentation rates shall be included.
7. Why phosphate enriched organic matter adsorbs more uranium?
8. In the second figure of Figure 13, why the uranium concentration decreases at the same E_h value? In the text below, it is mentioned that organic matter concentration changes from 5 to 10% when E_h changes from 200 to -120mV. But the figure shows otherwise. Clarification is required.

9. From the literature review, how it is concluded that the influence of redox condition on uranium accumulation is maximum or dominant?

Chapter 3: Uranium accumulation in marine sediments under different redox conditions on the example of the White, East Siberian, and Black Seas, as well as the Laptev Sea

1. The criteria for selection of the sites that have been studied shall be included.
2. There is no constant interval of depth where the concentrations of elements are recorded except for stations 2, 3, 4, 5, and 6. What is the reason for the varying intervals?
3. What is the reason for terminating the recording at variable depths at different stations?
4. The variation of uranium for the studied stations is very less. Is there any major effect even with the very small increase in uranium concentration?
5. The term isotopy in figures 24 and 25 shall be changed to isotopic.
6. It is mentioned in Pg. 73 that high isotopic sulfur corresponds to oxidizing conditions in the Laptev Sea. But in the case of the black sea, it is written that positive values of isotopic sulfur reflect an increase in sulfate reduction intensity. Is it not contradictory?
7. The axes of the graph in figure 32 shall be interchanged because the deposition of thorium is dependent on clay minerals but the graph infers otherwise.
8. It is mentioned that uranium concentration was up to 35 ppm. But nowhere in the graph or figures, has the uranium content reached this value. Clarification is required.
9. More details on how thermodynamic modeling like governing equations shall be provided.

Chapter 4: Distribution of uranium (U) and uranium/TOC (U/TOC) ratios in the unconventional reservoir on the example of the Bazhenov Formation

1. What are the porosity and permeability values of BF rocks?
2. It is mentioned that 13 wells were studied in the Bazhenov Formation. But only data for 9 wells were provided. Clarification is required for the absence of data for 4 wells and a U/TOC diagram is presented for samples from 11 wells. Why this irregularity is occurring?
3. In figure 47, there is no isotopic sulfur variation presented. But in the figure description, it is included. It shall be removed.
4. It is given that at $U/TOC_{max}<U/TOC$, the deposition environment is anoxic. But subsequently, it is mentioned that sub-anoxic and anoxic environments characterize low uranium concentration. Is it not contradictory?
5. What is the significance of V/Mo and V/Cr ratios in studying redox conditions?

Dr. D N Singh FNAE, FASCE, FICE(UK)
Editor-in-Chief, Environmental Geotechnics, ICE, UK
D.L. Shah Chair Professor for Innovation
Department of Civil Engineering
dns@civil.iitb.ac.in
www.civil.iitb.ac.in/~dns

September 9, 2022

Provisional Recommendation

☒ *I recommend that the candidate should defend the thesis by means of a formal thesis defense*

☐ ~~*I recommend that the candidate should defend the thesis by means of a formal thesis defense only after appropriate changes would be introduced in candidate's thesis according to the recommendations of the present report*~~

☐ ~~*The thesis is not acceptable and I recommend that the candidate be exempt from the formal thesis defense*~~

Skolkovo Institute of Science and Technology

URANIUM ACCUMULATION IN MARINE SOURCE ROCKS: ROLE OF REDOX CONDITIONS AND CORRELATION WITH PRODUCTIVITY

Doctoral Thesis

by

NADEZHDA KHAUSTOVA

DOCTORAL PROGRAM IN PETROLEUM ENGINEERING

Supervisor
Professor Mikhail Spasennykh

Co-advisers Professor Yuri Popov and Doctor Elena Kozlova

Moscow – 2022

I hereby declare that the work presented in this thesis was carried out by myself at Skolkovo Institute of Science and Technology, Moscow, except where due acknowledgment is made and has not been submitted for any other degree.

Candidate (Nadezhda Khaustova)

Supervisor (Prof. Mikhail Spasennykh)

Abstract

Oil source rocks are characterized by increased uranium content, reaching values above 100 ppm. The uranium concentration variations are associated with a number of factors affecting the uranium accumulation during sedimentation and further geological history. Using uranium data for studies of unconventional reservoirs and source rock productivity remains limited and are mainly used for identification of source rock lithological boundaries, well-to-well log correlation, as well as for core-to-log data integration. One of the main reasons for such lack of application is insufficient knowledge of factors that determine uranium accumulation at the sedimentation stage and further geological history.

The purpose of the current study was to analyze factors influencing the uranium accumulation in oil source rocks and highlight the relationship between the uranium concentration and the U/TOC ratio with productivity.

The research includes the study of the uranium accumulation during modern marine sedimentation (Kandalaksha bay of the White Sea, the Seas of Russian Arctic shelf and in the Black Sea), the study of factors controlling uranium content in the Bazhenov source rock Formation, and the analysis of relationship between the uranium concentration and the oil rocks saturation using the data of gamma-ray spectrometry and Rock-Eval pyrolysis.

The research allows us to clarify the main factors affecting ~~on~~ uranium accumulation in marine source rocks, including concentration of uranium in sea water, accumulation of uranium in marine organisms, continental run-off and sedimentation rate, redox conditions, mineral composition of rocks and other. It was shown that the main factor controlling uranium content in marine sediments and source rocks in studied geological objects is redox conditions at the sedimentation stage. Analysis of relationship of uranium content with oil saturation shows that intervals with the maximum oil saturation index (promising for development using multi-stage hydraulic fracturing technologies) are characterized by uranium content in the range of 1–20 ppm. Intervals with intermediate uranium contents from 20 to 40 ppm should be considered conditionally productive. The intervals with uranium content above 40 ppm and high TOC are

usually characterized by low productivity index and low oil saturation index (except intervals enriched in phosphate minerals). These intervals may be promising for the production of hydrocarbons generated from kerogen using thermal methods of oil recovery, especially in case of low organic matter maturity. The obtained results provide the criteria for identifying the productive intervals and their classification in terms of the methods for oil production within the Bazhenov Formation.

Publications

1. **Khaustova, N.**; Tikhomirova, Y.; Korost, S.; Poludetkina, E.; Voropaev, A.; Mironenko, M.; Spasennykh, M. The Study of Uranium Accumulation in Marine Bottom Sediments: Effect of Redox Conditions at the Time of Sedimentation. Geosciences 2021, 11, 332. https://doi.org/10.3390/geosciences11080332
2. Patent for invention: METHOD AND DEVICE FOR PROFILING PROPERTIES OF ROCK SAMPLES OF OIL SHALE THICKNESS. Spasnykh Mikhail Yurievich, Chekhonin Evgeny Mikhailovich, Popov Yuri Anatolyevich, Popov Evgeny Yurievich, Kozlova Elena Vladimirovna, **Khaustova Nadezhda Alexandrovna**. / Патент на изобретение: СПОСОБ И УСТРОЙСТВО ДЛЯ ПРОФИЛИРОВАНИЯ СВОЙСТВ ОБРАЗЦОВ ПОРОД НЕФТЕМАТЕРИНСКИХ СЛАНЦЕВЫХ ТОЛЩ. Спасенных Михаил Юрьевич, Чехонин Евгений Михайлович, Попов Юрий Анатольевич, Попов Евгений Юрьевич, Козлова Елена Владимировна, **Хаустова Надежда Александровна**.
3. Chuvilin, B. Bukhanov, A. Yurchenko, D. Davletshina, N. Shakhova, E. Spivak, V. Rusakov, O. Dudarev, **N. Khaustova**, A. Tikhonova, O. Gustafsson, T. Tesi, J. Martens, M. Jakobsson, M. Spasennykh, I. Semiletov, In-situ temperatures and thermal properties of the East Siberian Arctic shelf sediments: Key input for understanding the dynamics of subsea permafrost, Marine and Petroleum Geology, 2022, https://doi.org/10.1016/j.marpetgeo.2022.105550

4. **Khaustova, N.**, Kozlova, E., Maglevannaia, P., Voropaev, A., Leushina, E., & Spasennykh, M. (2022). Uranium in Source Rocks: Role of Redox Conditions and Correlation with Productivity in the Example of the Bazhenov Formation. Minerals, 12(8), 976. https://doi.org/10.3390/min12080976

Extended abstracts in conference

1. Popov, E., **Khaustova, N.**, Popov, Y., Chekhonin, E., et al. The modern place of continuous thermophysical core profiling in the complex of methods for determining the content of organic matter. The international research to practice conference Geological exploration development strategy: Present and Future, 2018.
2. **N. Khaustova**, Y. Tikhomirova, M. Spasennykh, Y. Popov, E. Kozlova and A. Voropaev. U/Corg Ratio Within Unconventional Reservoirs: Indicator of Oil Generation Processes and Criteria for Productive Intervals Determination During the Bazhenov Formation Investigation. EAGE/SPE Workshop on Shale Science 2019.
3. **Khaustova N.A.**, Tikhomirova Yu.I., Poludetkina E.N., et al. The behavior of uranium in the system seawater-bottom sediments. VIII International Scientific and Practical Conference Marine Research and Education: MARESEDU – 2019.
4. **Khaustova N.A.**, Tikhomirova Yu.I., Poludetkina E.N., et al. The effect of redox conditions on the uranium behavior in source rocks (for example, the Bazhenov Formation). The International G&G Conference and Exhibition: Advanced Exploration and Development Technologies – 2020.

5. **Khaustova N.A.**, Tikhomirova Yu.I., Poludetkina E.N., et al. The effect of redox conditions on the uranium behavior in bottom sediments. V All-Russian Scientific Conference of Young Scientists "Integrated Research of the World Ocean: KIMO-2020.
6. **Nadezhda Khaustova**, Yulia Tikhomirova, Elena Poludetkina, Elena Kozlova, Andrew Voropaev, Mikhail Mironenko, Mikhail Spasennykh. The effect of redox conditions on the chemical behavior of uranium in the Bazhenov Formation. The 35th IAS Meeting of Sedimentology, 2021.

Acknowledgments

I am deeply indebted to say big thanks to all people who support and helped me during my PhD journey.

I would like to express my deepest appreciation to my scientific supervisor, Professor Mikhail Spasennykh, sincerely thank him for his loyalty and patience, interest and responsiveness, confidence and support.

I would like to express my deepest gratitude to my co-advisers, Professor Yuri Popov and Dr. Elena Kozlova, for their support, wise advice, and valuable knowledge.

This endeavor would not have been possible without Dr. Evgenia Leushina, Dr. Evgeny Bastrakov and Dr. Andrey Voropaev for their advice in discussing the topic and finding answers to the scientific questions posed in the geochemical aspects of my research.

Many thanks to Dr. Elena Poludentika, Dr. Svetalan Korost and Dr. Dmitry Korost for their assistance in the bottom sediments sampling.

I could not have undertaken this journey without my lab colleagues – Dr. Anna Yurchenko, Dr. Boris Bukhanov, Alina Bazhanova, and Timur Bulatov – for their complicated laboratory and field trip works and experimental measurements.

Special thanks to Dr. Natalia Bogdanovich and Dr. Evgeny Chekhonin for their valuable recommendations and comments and their constant support during the research.

I would like to extend my sincere thanks to all my colleagues and friends in the Center Hydrocarbon Recovery Skoltech for their support, humor and amazing attitude.

Words cannot express my gratitude to my close people, my family and husband–you are my main motivation and support.

The author is indebted to for the support in carrying out these studies the Ministry of Science and Higher Education of the Russian Federation under agreement No. 075-10-2022-011.

Table of contents

List of Figures

List of Tables

Table 37. The distribution of the uranium concentration (U), the organic carbon (TOC) and the ratio U/TOC for the wells 7, 8, 6. 172

Chapter 1. Introduction

Oil source rocks are characterized by increased uranium content, reaching values above 100 ppm. The patterns of the spatial and vertical variations of uranium concentration differ significantly for different formations and geological sections. These variations are associated with a number of factors affecting the accumulation of uranium during the formation of the deposits and further geological history. Despite the obvious connection between variations in the uranium content and the conditions of hydrocarbon formation processes, uranium concentration data are mainly used for identification of source rock lithological boundaries, well-to-well log correlation (in combination with other logging data), as well as for core-to-log data integration [Fertl, Rieke, 1980; Gudok N. S., Bogdanovich N. N., 2007; Parfenova, T. M., Melenevskij, V. N., Moskvin, 1999; Serra, 1964]. Using uranium data for studies of hydrocarbon formation and source rock productivity remains limited [Dudaev, 2011; Kulyapin, 2016; Mann, Müller, 1988]. One of the main reasons for such lack of application is insufficient knowledge of the factors that determine uranium accumulation at the sedimentation stage and subsequent changes in uranium concentration during rock catagenesis.

The purpose of the current study is to analyse the factors influencing the uranium accumulation in oil source rocks and highlight the relationship between the uranium concentration and the U/TOC ratio with productivity.

The research includes the analysis of published data on the matter of research, the study of uranium accumulation in the processes of modern marine sedimentation in different redox conditions, the study of factors controlling uranium content source rock formation, and the analysis of relationship between the uranium concentration and the oil saturation using the data of gamma-ray spectrometry and Rock-Eval pyrolysis on the example of the Bazhenov Formation. The literature review (Chapter 2) was carried out on more than 90 key publications describing factors, controlling the behavior of uranium in marine sediments and source rocks, including the Bazhenov Formation. The study of published results allow us to clarify the main factors affecting on uranium accumulation in marine source rocks, including uranium concentration in sea water, accumulation of uranium in marine organisms, continental run-off

and sedimentation rate, redox conditions, mineral composition of rocks and other. The conclusions made on results of literature review helped us to establish the main goals, select geological objects and methods of research.

The study of uranium accumulation in marine sedimentation are described in Chapter 3. We studied marine sediments in the Kandalaksha bay of the White Sea, the Laptev and East-Siberian Seas (oxidative conditions) and in the Black Sea (oxidative and reductive conditions) using different analytical methods, including optical microscopy, ICP-MS, CHNS, IRMS, XRD, Eh, pH and temperature measurements (sections 3.1 – 3.4). Interpreting results were carried out using thermodynamic modeling uranium forms in a water-sediment system under different conditions in the Chapter 3 (section 3.5).

The results of the uranium variations study, factors controlling behavior of uranium in source rocks and relationship of uranium content with oil saturation are considered using the data on core samples of the Bazhenov Formation (Chapter 4). We analyzed the data obtained on core samples from 13 wells, drilled in the Central and the North parts of the West Siberia Petroleum Basin (section 4.1). Analytical methods include Rock-Eval pyrolysis, gamma spectrometry on core, the thermal core logging, IRMS, XRF and other (section 4.2). The data on uranium content and TOC variations allowed us to obtain and analyze continues high-resolution profiles of U, TOC, and U/TOC for different geological sections of the Bazhenov Formation (section 4.3). The study of uranium content together with the other redox sensitive elements concentration, content and isotope composition of sulfur, the oxygen Rock-Eval pyrolysis index allowed us to establish the leading role of redox conditions in uranium accumulation in source rocks (section 4.4). The relationship of uranium content and oil productivity of intervals have been studied for 13 wells using the data of gamma spectroscopy of core and data of Rock-Eval pyrolysis (section 4.5). Main results are summarized in the Chapter 5. The detailed measurements results (uranim, TOC determining based on the thermal core logging results and U/TOC ratios) of the Bazhenov Formation rocks for 9 wells are presented in the Appendix A of this work.

Chapter 2. Review of the Literature

The uranium behavior in the earth's crust has been considered in a wide range of geochemical studies and has been studied in a huge number of works since the early 1960s. The most systematic uranium study was carried out in the research [Swanson, 1960; Swanson, 1961]. In this work, the main processes and factors influencing the uranium accumulation are analyzed. In the future, uranium research continued and is reflected in the following works [Bastrakov et al., 2018; Khaustova et al., 2019; Lüning, Kolonic, 2003; Zubkov, 2015]. To sum up, it is known at the moment that uranium is quite mobile during weathering, in contrast to thorium, and comes with suspension, included in the crystal lattice of biotite and apatite together with calcium. Some researchers noted uranium enrichment in carbonated fragments and in sulfide aggregates. Uranium is contained in minerals such as zircon and sphene [Hurley, Fairbairn, 1957] and interacts with organic matter, with iron hydroxides and clay minerals. In addition, uranium can be sorb by biogenic components (bone detritus, fish scales). During sedimentation, uranium is capable of coprecipitation with clay particles, and in a reducing environment, it can be extracted from water [Cumberland et al., 2016]. The transfer, accumulation processes and uranium behavior, described above, are schematically shown in Figure *1*.

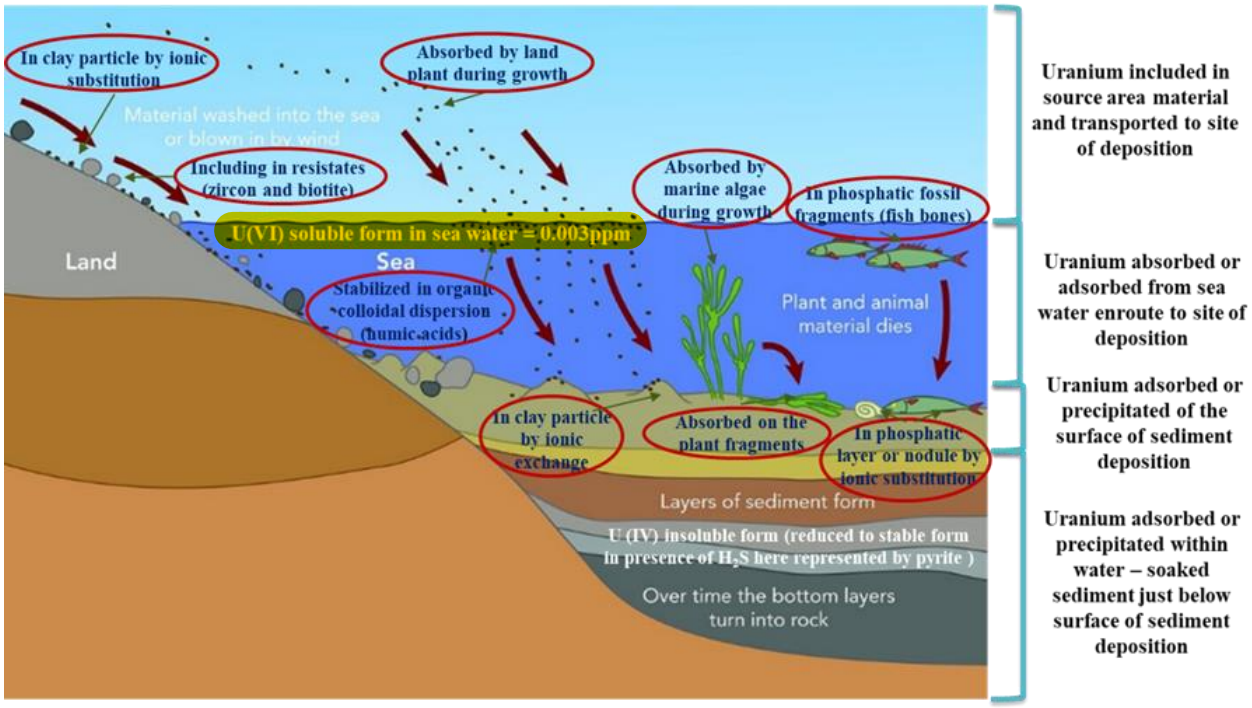

Figure 1. Diagrammatic sketch showing possible associations and time of uranium emplacement with common marine black shales constituents. Modified after [Swanson, 1960; https://intl.siyavula.com/read/science/grade-9/the-lithosphere/24-the-lithosphere?id=toc-id-3].

Factors defining U content and U/TOC ratios are shown in Figure *2*. And these factors include: initial urnium concentration and uranium accumulation by marine organisms, the uranium (U^{+6}) transition to insoluble forms (U_3O_8, UO_2) under anoxic conditions, uranium sorption (U^{+6}) by organic matter (depending on Eh, pH), the precipitated organic matter type (sapropelic, humic), sedimentation rate and lithological composition, presence of phosphates, also diagenetic and catagenetic processes.

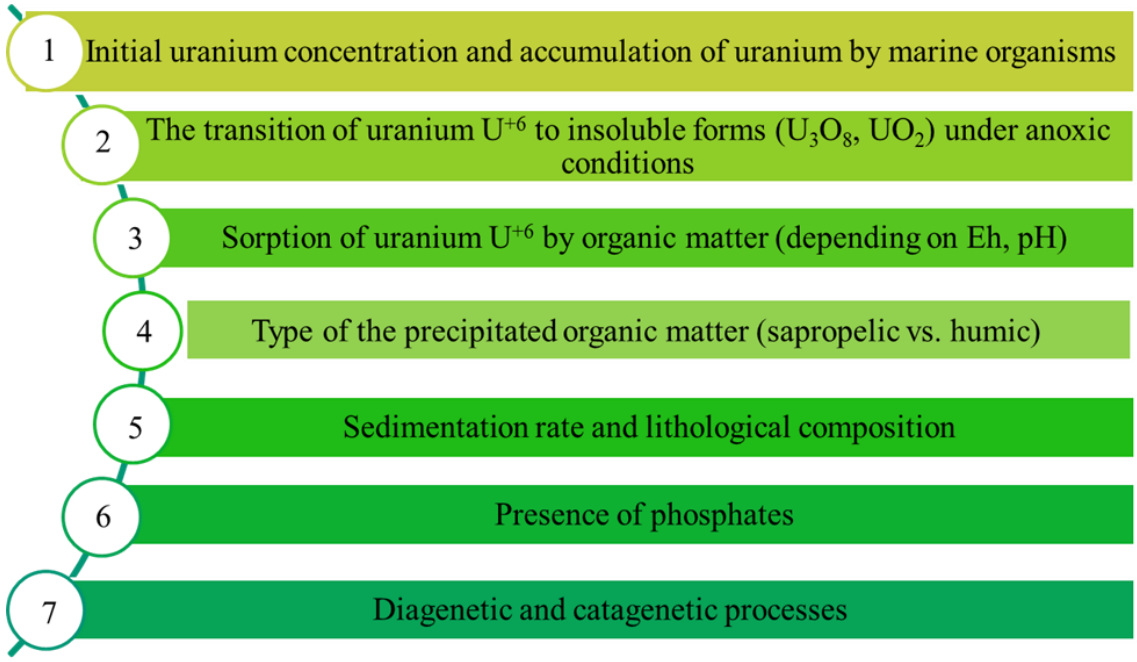

Figure 2. Factors controlling U content and U/TOC ratio in source rocks.

Before describing the factors controlling the uranium content, consider which increased uranium content characterized epochs in geological history Figure *3*.

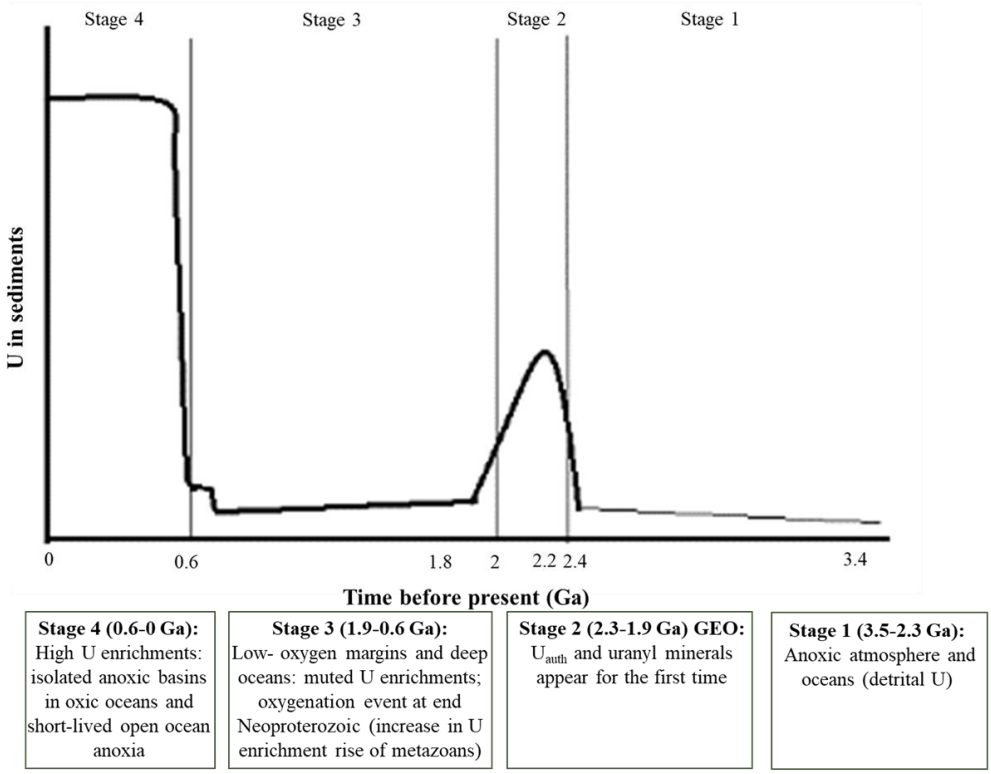

Figure 3. Variations in U concentrations in the sediments in geological history. Modified after [Partin et al., 2013].

During the geological history, U concentration in sediments was connected with oxygen concentration in the atmosphere and productivity in oceans, which depends on oxygen and CO_2 concentrations. This pattern of global view leads to a connection between U and deposition environment, diagenetic processes.

The factors controlling U content and U/TOC ratio include [Bastrakov et al., 2018; Cumberland et al., 2016; Khaustova et al., 2019; Kizil'shtejn, L. YA., CHernikov, 1999; Lüning, Kolonic, 2003; Partin et al., 2013; Swanson, 1960; Swanson, 1961; Zubkov, 2015]:

- **Precipitation of U with sinking particulate organic matter**

The first factor depends on the initial uranium concentration in the sea water, marine organisms' ability to accumulate uranium, and uranium sorption U(VI) by organic matter depending on Eh, pH.

The uranium concentration in natural waters varies mainly from $n \cdot 10^{-5}$ to $n \cdot 10^{-7}$ g/l. The uranium concentration in sea water is 0.0032-0.0033 ppm. The dissolved and suspended

uranium total amount carried from the continents by the globe's rivers is approximately 40 thousand tons per year [Baturin, 1975]. One half falls on solid run-off, the second on solutions ($5.5 \cdot 10^{-7}$ g/l) and suspensions ($1.5 \cdot 10^{-4}$%). Because of the differentiated uranium precipitation in different parts of the sea basins, these rather low contents create uranium concentrations in sediments that reach thousandths, hundredths, and in special cases, even tenths of a percent [Baturin, 1975]. River waters are characterized by a direct relationship between mineralization and dissolved uranium concentration, but such a relationship is absent in the seas.

Redox conditions are the most important physical and chemical characteristics that affect the uranium migration and accumulation in marine environments. The following conditions are distinguished – oxic, dysoxic, sub-oxic, and anoxic [Tyson, Pearson, 1991] (*Table 1*). The most common forms of uranium migration are uranyl-carbonate and uranyl-humate complexes; hydroxyl-uranyl and uranyl-sulfate complexes are less important (Figure *4*).

Table 1**.** Oxygen regime and marine environments.

Oxygen, ml/l	**Environments**	**Biofacies**	**Physiological regime**
8-2	Oxic	Aerobic	Normoxic
2-0.2	Dysoxic	Dysaerobic	Hypoxic
0.2-0	Suboxic	Quasi-anaerobic	
0 (H_2S)	Anoxic	Anaerobic	Anoxic

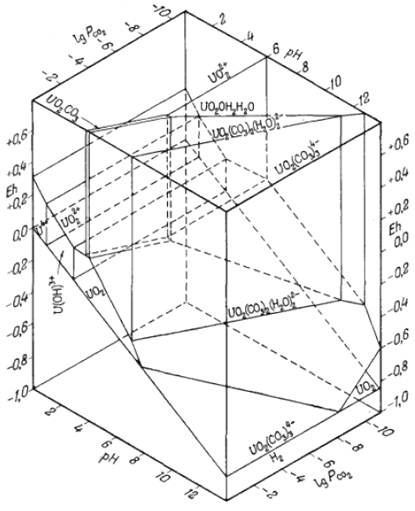

Figure 4. Solution chemistry and redox conditions of uranium species in seawater function of pH/Eh, t = 25°C, p = 1 atm as function pH, Eh and PCO_2 [Garrels, Christe, 1965]. The boundaries of the solid fields are drawn at a total uranium-containing components activity, equal to 10^{-6}.

The schemes of sedimentation condition under oxic and anoxic conditions [Demaison, Moore, 1980] are presented in Figure *5* and Figure *6*. According to Figure *5*, the main organic matter transformation direction is aerobic mineralization because of oxygen dissolved in water at high redox potential values (Eh) - about 400 mV. Starting in the water column, the most intensive process of organic matter aerobic destruction continues on the sediment's surface, as shown by a huge number of microorganisms. In the anaerobic scheme, the organic matter decomposition occurs at low Eh values, while the bacterial sulfate reduction process is the main one (Figure *6*). However, the organic matter anaerobic decomposition is always preceded by its aerobic mineralization; there is an area in sediments where both aerobic and anaerobic processes of organic matter decomposition are carried out simultaneously.

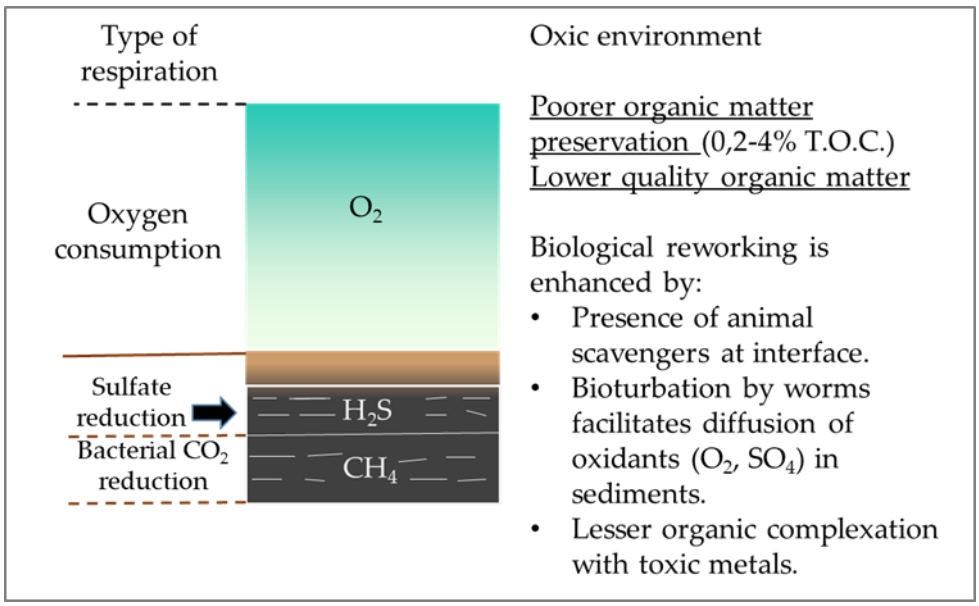

Figure 5. Degradation of organic matter under an oxygenated (oxic) water column. Modified after [Demaison, Moore, 1980].

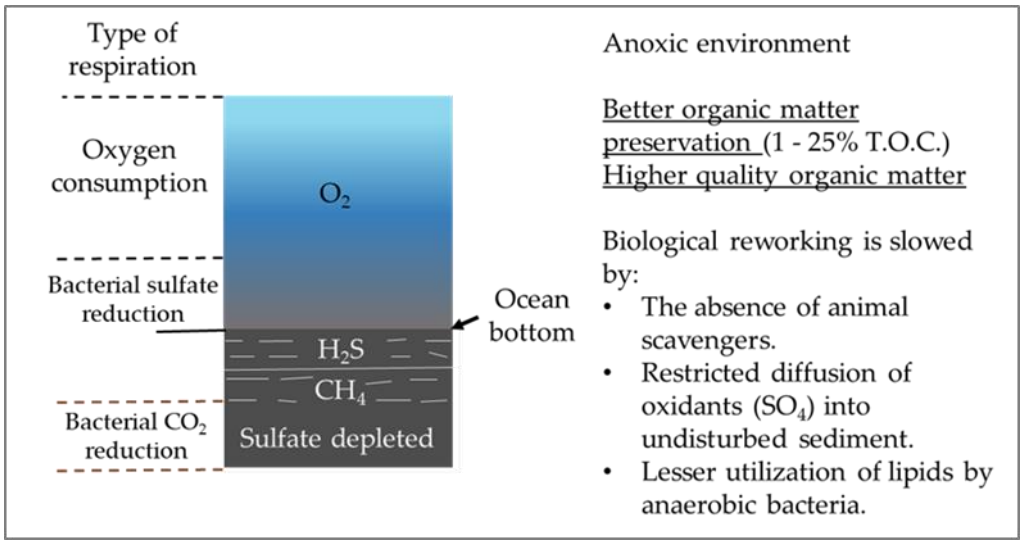

Figure 6. Degradation of organic matter under anoxic water column. Modified after [Demaison, Moore, 1980].

According to studies [Baturin, 1975; Neruchev, 2007], there are two main uranium accumulation mechanisms at the stage of sedimentation: the biological accumulation mechanism associated with the uranium accumulation by living organisms their vital activity, as well as the physicochemical factor when uranium is concentrated on the organisms surface, for example, on dead shells. Scientific work [Hlopkova and Asvarova, 2013] describes the uranium accumulation mechanisms in Caspian mollusks. According to this study, mollusks absorb uranium in seawater during their vital activity. In the digenesis process (with a change in the pH and Eh), uranium from seawater (U^{+6}) under reducing conditions precipitates (U^{+4}), and uranium adsorption occurs on the mollusk shells organic layer, the replacement of Ca^{+2} cations by U_{ions}^{+4} in shell aragonite and calcite.

The important factor is the uranium accumulation by marine organisms; the uranium accumulation study in fossil organisms makes it possible to understand the uranium accumulation mechanism in sedimentary rocks and deposition environment. The various studies have confirmed the V.I. Vernadsky assumption on the uranium accumulation by living organisms and explained the relationship between the organic matter and uranium concentrations in sediments and rocks [Neruchev, 2007]. The lifetime uranium accumulation by organisms occurs both in clarke uranium concentration and at a significantly increased

uranium concentration in water. Figure *7* shows the uranium accumulation factors (U/U_{water}). According to the diagram, $U_{phytoplankton}/U_{water}$ values characterize phytoplankton from 30-60 to 600-1600. Accumulation coefficients characterize some unicellular seaweed and freshwater algae from 800 to 3900. The accumulation coefficients range from 35-40 to 200-420 for various bottom algae species. Uranium accumulation coefficient in mollusk shells ranges from 24-33 to 130-190. The uranium accumulation coefficient ranges from 8-12 to 20 for fish. Uranium accumulation coefficients characterize corals from 490 to 1600. Microorganisms and phytoplankton actively accumulate uranium compared to zooplankton, mollusks, and fish.

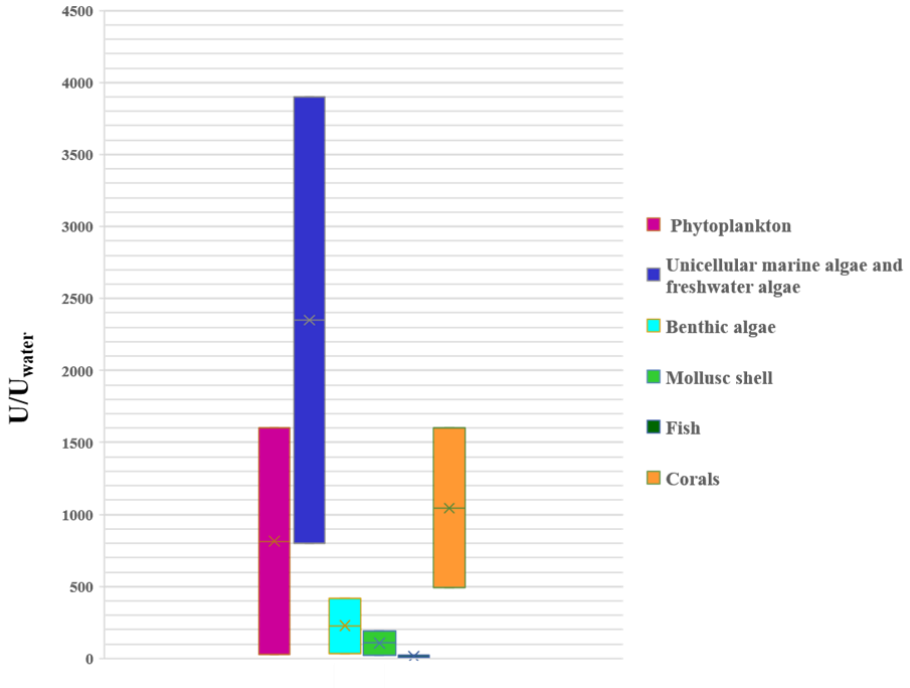

Figure 7. Uranium accumulation factor (U/U_{water}) by aquatic organisms and plants. Modified after [Neruchev, 2007].

All organisms accumulate uranium dissolved in water, increasing its concentration in the aquatic environment by tens, hundreds, and thousands of times. Organic matter has clarke uranium concentrations at a low average uranium concentration uranium in water (0.003 ppm). Moreover, organic matter has anomalously high uranium concentration in basins with an increased dissolved uranium concentration. There is a direct relationship between the uranium concentration in water and its accumulation in organisms. The uranium concentration in water increases by three orders of magnitude, also simultaneously, the organism's uranium

concentration increases by three orders of magnitude. Therefore, the U/TOC ratio increases with increased uranium concentration in organisms.

- **Diffusion of sea water U into sediment pore water and subsequent reduction of U(VI) to U(IV) with uranium fixation owithin the sediments**

Uranium dissolved in sea water is reduced to insoluble uranium oxide UO_2 and precipitates in the hydrogen sulfide presence. It is supported by the increased uranium concentrations in the hydrogen sulfide basins sediments. The results of the uranium form studying in the Black Sea water [Babinec, A. E., Bezborodov, A. A., Mitropol'skij, 1977] showed that the uranium reduction is starting from the uppermost hydrogen sulfide zone layer. And even the most difficult to reduce complex ion $UO_2(CO_3)_3^{-4}$ is capable of being reduced to UO_2 solid.

- **Type of the precipitated organic matter (sapropelic vs. humic)**

Theoretical distribution of humic and sapropelic materials, accumulating organic matter, estimated uranium and oil content in a shallow sea are presented in *Figure 8*. This scheme shows us that different combinations of humic and sapropelic organic matter and the organic matter content (TOC) influence the uranium concentrations.

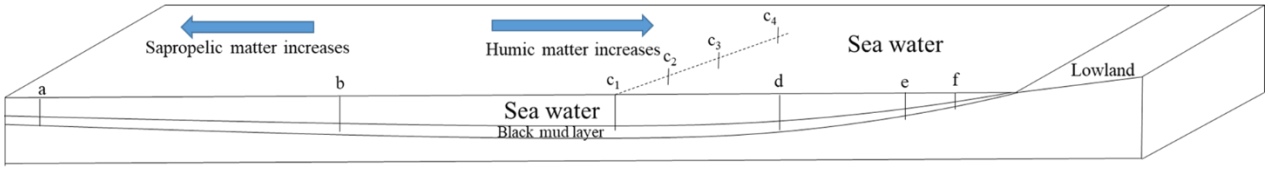

	a	b	c_1	c_2	c_3	c_4	d	e	f
Organic matter, %	30	25	20	17	15	10	15	10	5
Humic, %	15	25	50	50	50	50	75	85	95
Sapropelic, %	85	75	50	50	50	50	25	15	5
Uranium, ppm	30	41	63	64	48	31	70	54	31
Oil, gallons per ton	26.6	20.3	12.5	10.6	9.4	6.2	6.6	3.5	1.4

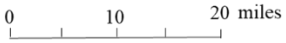

Figure 8**.** Theoretical humic and sapropelic materials distributions, accumulating organic matter, estimated uranium and oil content in a shallow sea. Modified after [Swanson, 1960].

For example, the U_{max} concentration = 70 ppm in the point «d» where TOC = 15%, and organic matter consists of 75% of the humic and 25% of the sapropelic. U_{min} concentration = 30 ppm

in point «a» where TOC = 30% organic matter consists of humic and sapropelic in the following ratio 15% to 85%. The points c_1, c_2, c_3, c_4 have characterized the same ratio of sapropel and humic (50% to 50%), and uranium concentrations in these points increase together with increasing the content of organic matter.

According to this theoretical distribution, we can conclude that the uranium concentration is affected to a greater extent by the ratio of sapropelic and humic components in organic matter, and the greater the humic component - the greater the organic matter concentration. Nevertheless, the uranium concentration will increase with an increase in organic matter content, provided that the sapropel and humic ratio is the same.

- **Sedimentation rates**

The relationship between U concentrations and sedimentation rates is presented in Figure *9*. The relationship shows us that the difference in accumulated uranium concentrations depends on the sedimentation rates.

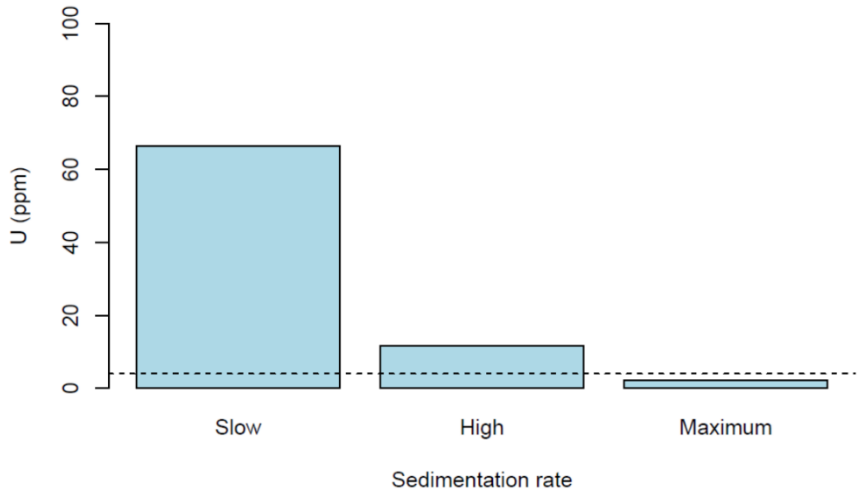

Figure 9**.** Relationship between U concentrations and sedimentation rates. Modified after [Zanin, Zamirajlova, Eder, 2016].

We can observe U_{max} concentration when slow sedimentation rate and U_{min} concentration is characterized for high and maximum sedimentation rates. The uranium concentration can increase at low sedimentation rates by more than ten times compared with high rates. Furthermore, this statement explains that the more uranium can be fixed, the longer organic

matter is in contact with sea water. The high sedimentation rates do not give these conditions for accumulating organic matter and uranium.

- **Presence of phosphates**

The relationship between the uranium content and organic carbon in bone phosphates is presented in Figure *10*.

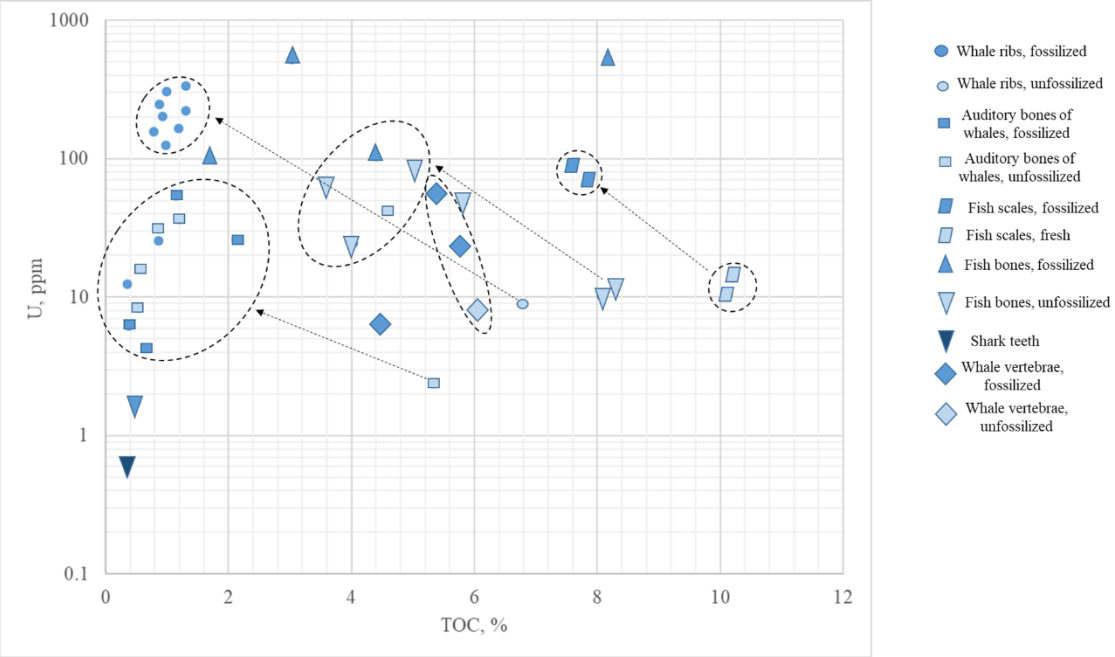

Figure 10**.** The relationship between the uranium content and organic carbon in bone phosphates. Modified after [Baturin, 2004].

According to Figure *10*, we can see that fresh (unfossilized) bone phosphate riched organic matter has a smaller uranium concentration than fossilized bone phosphate depleted in organic matter. It does not exclude the organic matter participation in the uranium accumulation in biogenic phosphates. It is known that as fossilization of organic matter is transformed into condensed compounds of the melanoidin type, which have the concentrating uranium and other heavy metals property [Manskaya, 1964]. Besides, experimental studies have shown that phosphate material enriched in organic matter extracts uranium from solution more actively than unenriched phosphate material [Savenko A. V., 2002]. However, in the case of the organic matter appearance, this is not the main event affecting the uranium content.

The uranium accumulation by phosphorus-containing minerals for Wallumbilla, Toolebuc, and Allaru Mudstone Formations is presented in Figure *11*. The organic matter riched layers are characterized by the low values of organic matter and high uranium concentrations.

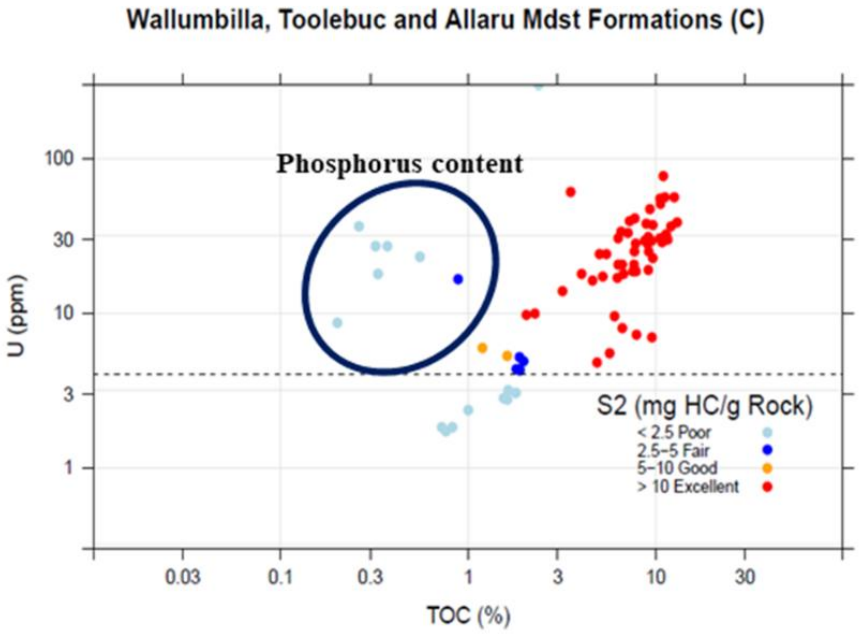

Figure 11**.** The uranium accumulation by phosphorus-containing minerals [Boreham C., 2012].

- **Diagenetic and catagenetic processes**

The relationships between the uranium content and organic carbon, U/TOC ratio and organic carbon, the bitumen content, and organic carbon for sediments and rocks are presented in Figure *12*. We can see that at the same TOC values, rocks formed millions of years ago contain about 30-40% more uranium than modern sediments; accordingly, already formed rocks are characterized by higher values of the U/TOC ratio. The explanation for this phenomenon is simple: in the formed rocks during catagenesis, due to the release and loss of volatile products, the organic matter mass decreased on average by 30–40%. With a partial loss of organic matter mass, an equivalent relative organic matter enrichment with uranium occurred. It is also important that the U/TOC ratio and bitumen content in organic matter increase significantly with a decrease in the organic matter concentration in sediments.

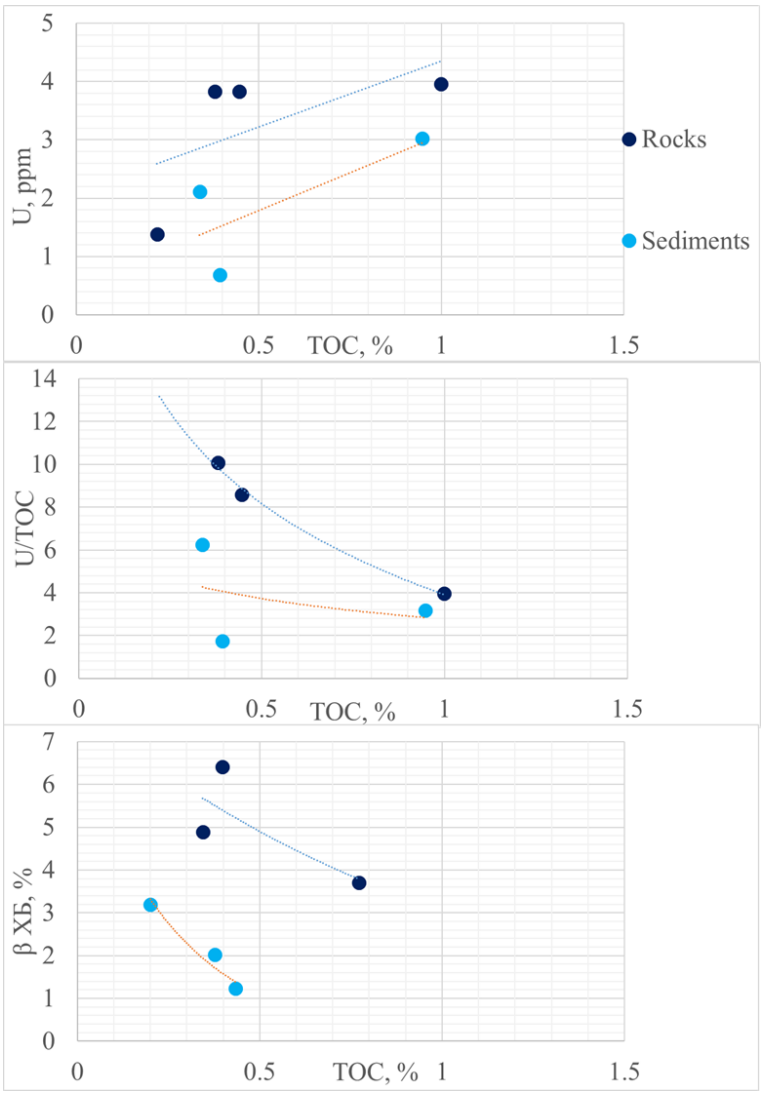

Figure 12. U vs. TOC, U/TOC vs. TOC, $\beta_{ХБ}$ vs. TOC for sediments with clarke content of organic matter and uranium. Modified after [Neruchev, 2007].

The TOC vs. Eh, U vs. Eh, P vs. Eh, U/TOC vs. Eh, P/TOC vs. Eh for Atlantic ocean sediments are presented in Figure *13*.

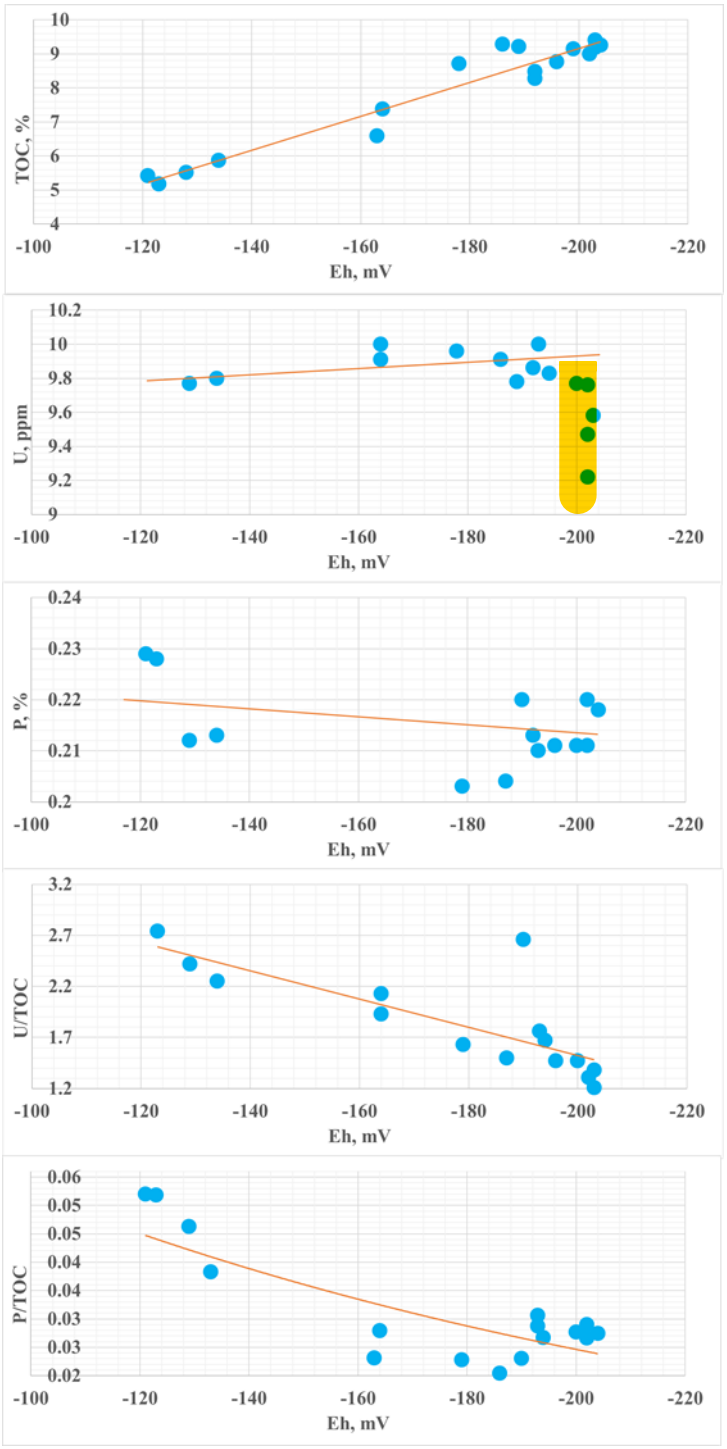

Figure 13. TOC vs. Eh, U vs. Eh, P vs. Eh, U/TOC vs. Eh, P/TOC vs. Eh for Atlantic ocean sediments. Modified after [Neruchev, 2007].

The average organic matter concentration is changed from 5 to 10%. When Eh changes from -200 to -120 mV, when moving from sharply reducing to less reducing conditions, the organic matter concentration decreases by half because of its bacterial oxidation. The uranium concentration in sediments almost does not change along with this facies profile and remains,

on average, constant; the uranium amount does not correspond to the uranium remaining amount after organic matter oxidation, but to its initial amount, which at the beginning of diagenesis was on average 10 ppm. When Eh changes from -200 to -120 mV and halves the organic matter mass, the U/TOC ratio also doubles. As can be seen, the increase in the U/TOC ratio occurs relative to the unexpected uranium accumulation during the organic matter oxidation. Phosphorus associated with organic matter behaves in precisely the same way in these sediments. Upon oxidation and a twofold decrease in the organic matter mass, the P/TOC ratio increases approximately twofold.

The above factors determine the high potential of informative data on the uranium content. When working on each geological object, the selection of factors determining the uranium content and assessment of their influence complicates interpretation.

Uranium almost entirely associated with solid organic matter, contributes to gamma-ray logging in the Bazhenov Formation rocks. The uranium content scattered in other rock components is negligible. Table *2* also shows the average values of the various chemical elements contents in the Bazhenov Formation compared with the clarke contents [Kasimov, Vlasov, 2015; Kuznetsov, 1984; Rihvanov, 2019; Zamirailova, Eder, 2016]. According to this table, the cadmium and uranium content in the BF is 18 and 15 times higher than the clarke values of these elements, respectively. Nickel, vanadium, and zinc are almost 3-6 times more in the Bazhenov Formation deposits, and the cobalt content is two times higher. The average chromium, iron and plumbum contents do not differ from their clarke values. Nevertheless, the average thorium content is lower in the Bazhenov Formation than these elements' clarke content.

Table 2. The average content in the Bazhenov Formation and bulk earth values of chemical elements according literature review [Kasimov, Vlasov, 2015; Rihvanov, 2019].

Chemical elements, ppm	Bulk earth values of the elements	Average content of elements in the Bazhenov Formation with standart deviation
Cd	0.64	11.45±7.07
Co	17	27.48±2.67
Cr	92	74.7±4.8
Fe	40600	39300±4600
Ni	50	162±68
Pb	17	15.04±4.18
Th	13	6.24±0.47
U	2.5	38.29±4.05
V	121	347±121
Zn	75	447±49

The weighted average uranium and thorium content in the Bazhenov Formation is 38 and 6 ppm, respectively, with the ratio Th/U = 0.16. The total uranium resources in the Bazhenov Formation are colossal and various from 1 to 3 billion tons [Nesterov, 2011]. Rocks type classification is presented in the Table *3* according to the uranium concentration in the Bazhenov Formation [Rihvanov, 2019].

Table 3. Rocks type according to the uranium concentration in the Bazhenov Formation [Rihvanov, 2019].

U concentration interval	Rocks association according to the uranium concentration
3÷6 ppm	Terrigenous mineral association
10÷30 ppm (with picks 10÷14 ppm and 20÷28 ppm)	Idiogenous uranium sorbed from sea water on the organic matter and the organisms
30÷120 ppm (with picks 50÷80 ppm)	Rocks were formed under epigenetic transformation and uranium were imported from outside

The native uranium mineral phases are confined to the calcium phosphate mineral phases. Uranium minerals have a spotty distribution and are represented by their own mineral species as coffinite and uranium oxide [Rihvanov, 2019].

The ratio between the parameters of the spectral gamma-ray logging modification and the organic matter concentration in oil source rocks was considered in the following works. Dudayev showed [Dudaev, 2011] application of the U/Th ratio and TOC organic matter concentration comparison based on the core studies results to determine the reservoirs layers in the Oligocene the Eastern Ciscaucasia oil source rocks. The reservoirs are characterized by low TOC values and elevated U/Th values and correspond to highly fractured intervals enriched in microfauna and fish detritus. Similarly, in Kulyapin's dissertation [Kulyapin, 2016], typification of the Bazhenov Formation rocks was carried out using a spectral gamma-ray logging modification.

The factors influencing the uranium content and variations in source rocks were identified in the literature review. These factors include initial uranium concentration and uranium accumulation by marine organisms, the uranium (U^{+6}) transition to insoluble forms (U_3O_8, UO_2) under anoxic conditions, uranium sorption (U^{+6}) by organic matter (depending on Eh, pH), the precipitated organic matter type (sapropelic, humic), sedimentation rate and lithological composition, presence of phosphates, also diagenetic and catagenetic processes. The role of these factors can be significantly different for different formations. Uranium data interpretation and the relationship uranium with productivity should be carried out taking into account the formations characteristics and the factors analysis affecting the uranium accumulation. The literature data analysis made it possible to select methods and refine the work tasks in the part of the redox conditions influence and the uranium behavior in the Bazhenov Formation. The redox conditions influence at the sedimentation stage revealed in the published works, motivated the author to study the uranium accumulation in sea bottom sediments formed under significantly different redox conditions of the Arctic and Black Seas. For redox conditions effects analyzing on the uranium accumulation in the Bazhenov Formation, a wide additional parameters range was used: the redox sensitive elements distribution and their ratios, the pyrolytic parameter oxygen index, and the isotopic sulfur composition.

The revealed relationship between the uranium content and phosphate minerals led to the inclusion in the measurement of these minerals content in the Bazhenov Formation and comparison with data on uranium.

Because of the uranium content and organic matter significant heterogeneity in the Bazhenov Formation rocks, it is necessary to use together the data of gamma-ray spectrometry on the core and thermal logging on the core. These methods make it possible to analyze the uranium, organic carbon (with a resolution of 1 mm) and the U/TOC ratio distributions of depth in the Bazhenov Formation.

Figure *12* showed that during catagenesis there is a decrease in the organic carbon content, while the uranium content does not change. And when comparing rocks and sediments with the same TOC values, the uranium content is higher in the formed rocks. Therefore, when analyzing the Bazhenov Formation, the uranium content and U/TOC ratio were analyzed depending on the maturity of the studied rocks.

In order to establish which factors affect the uranium content in the Bazhenov Formation rocks, the complex lithological, petrophysical, and isotope-geochemical studies results on the core were involved in the analysis.

Chapter 3. Uranium accumulation in marine sediments under different redox conditions on the example of the White, East Siberian and Black Seas, as well as the Laptev Sea

The study of modern marine deposits at the early diagenesis stage provides an opportunity to analyze in detail the processes and factors affecting the content and composition of organic matter and inorganic compounds in source rocks formed in marine conditions tens and hundreds of millions of years ago. In particular, the study of uranium concentrations in bottom sediments may provide valuable information on uranium accumulation in sedimentation and diagenesis processes, explaining high content and considerable variations (from 1 ppm to several hundred ppm) of uranium in source rocks. In this respect, uranium is one of the most interesting elements because the data on uranium content are available from gamma logging data for wells drilled at oil fields. Following existing knowledge, the uranium of marine source rocks accumulated in bottom sediments during marine sedimentation. The sources of uranium are continental run-off and uranium dissolved in seawater. Dissolved uranium can be accumulated by marine organisms, absorbed by organic matter, and included in minerals formed during sedimentations. Uranium concentration in bottom sediments (and in source rocks) depends on several factors, including the rate of sedimentation, uranium content in the seawater, content and the source of organic matter, redox conditions, and mineral composition sediments, and others [Bastrakov et al., 2018; Khaustova et al., 2019; Lüning, Kolonic, 2003; Swanson, 1961; Zubkov, 2015]. The interrelation of uranium content with the composition and genesis of source rock creates good opportunities for the characterization of oil shales. However, multiple factors affecting uranium content make interpretation difficult. In practical terms, the data on vertical variations of uranium are mainly used to delineate the oil source rock formations and cross-sections with other logging data [Fertl, Rieke, 1980].

The study of uranium variation is a valuable tool for the characterization of various geological objects and processes. For example, based on the dependence of uranium forms and concentrations in water and minerals on the system's composition and P, T, Eh, and pH conditions, the variations of uranium concentration are successfully applied in different

paleoclimatic reconstructions [Chappaz, Gobeil, Tessier, 2010; Mangini, Jung, Laukenmann, 2001; Rolison et al., 2017; Sklyarov, 2010; Vosel, 2016].

3.1 Regional Settings

To study the uranium concentration in marine sediments, the author of the thesis was directly involved in the White Sea field trip for sampling sediments in 2018, as well as in the sampling sediments from the Laptev and East Siberian Seas during the international Arctic expedition in 2020. Because of covid restrictions, the Black Sea sediments sampling was not carried out by the author. Therefore, data from a study of the Black Sea sediments, which were sampled by Moscow State University researchers, and literature data will be presented.

Coordinates and locations of the sampling stations and station from literature review are presented in Table 4, Table 5 and Figure 14, Figure 15, Figure 16, Figure 17.

Table 4. Coordinates of the sampling stations.

Station	Easting	Northing	Water depth, m	Column length, cm
1	510,868.13	7,379,725.5	82.9	285
2	516,170.33	7,377,367.5	80.0	173
3	130.3257	72.011.233	17	37
4	120.40085	77.186.97	350	24
5	150.493717	72.499.75	15	24
6	160.988433	74.990.300	45	22
7	E36 07.070	N44 43.100	253	380
8	E36 09.291	N44 44.394	100	240

Table 5. Coordinates of the Black Sea Deep Well. It was modified after [Neprochnov, 1980].

Station	Easting	Northing	Water depth, m	Column length, m
7	29°24'96"	41°40'25"	1750.5	503.5

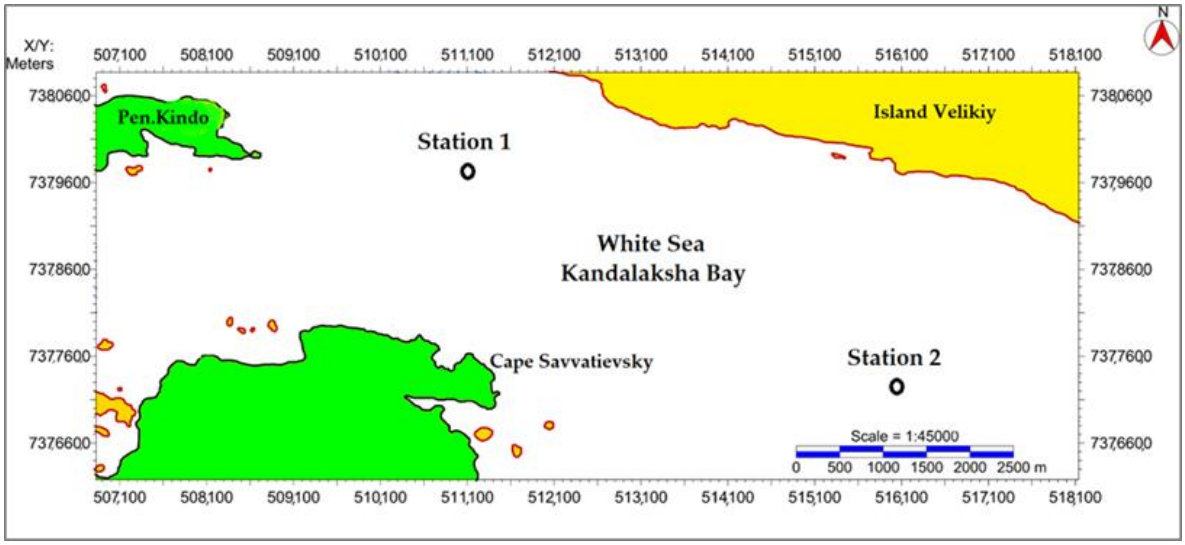

Figure 14. Location of the object of study. Stations 1 and 2 of the White Sea sampling.

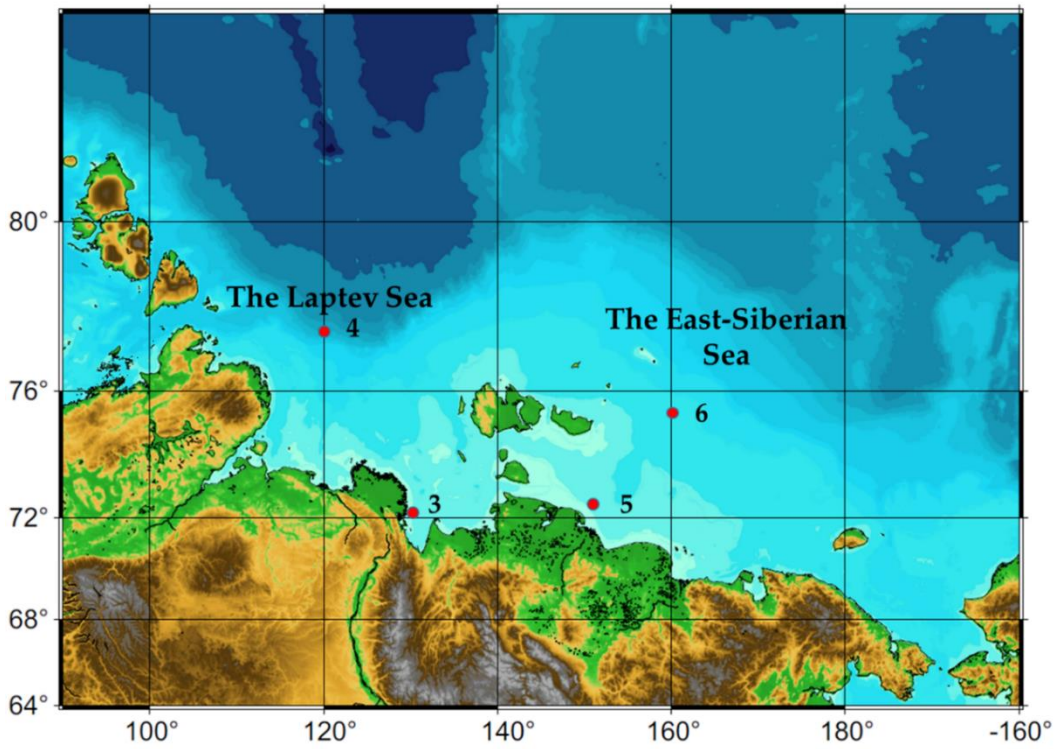

Figure 15. Location of the object of study. Stations 3, 4, and 5, 6 samplings the Laptev and the East-Siberian Seas.

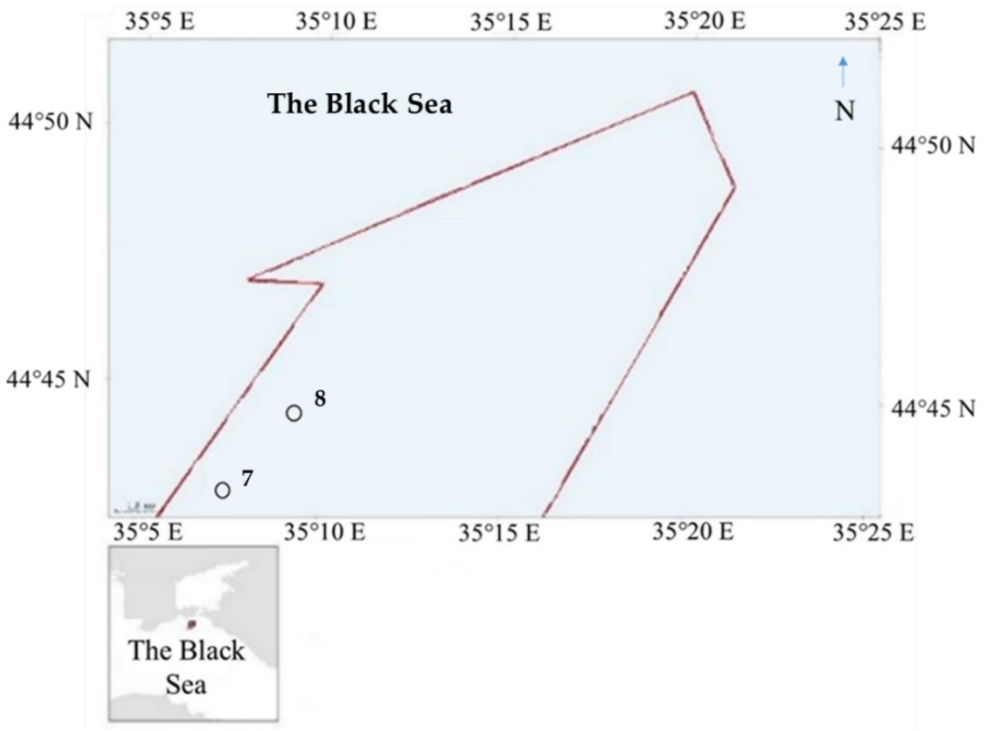

Figure 16. Location of the object of study. Stations 7 and 8 of the Black Sea sampling.

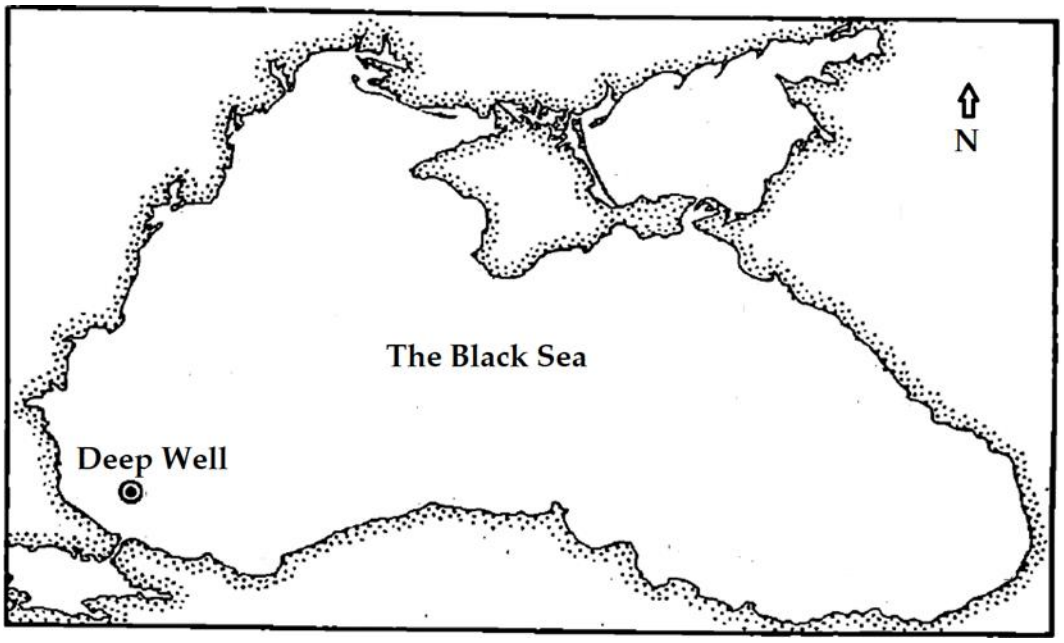

Figure 17. Location of the Black Sea Deep Well. Modified after [Neprochnov, 1980].

The objects of experimental studies were precipitation accumulated in oxidizing and sub-oxidizing conditions in the central part of the Kandalaksha Bay of the White Sea; sediments of the Laptev Sea and the East Siberian Sea, confined to the influence of the Lena River run-off,

the continental slope, and also to the zone of active methane degassing; sediments accumulated on the shelf of the northern part of the Black Sea under reducing conditions.

Literature data were used to study deep-sea hydrogen sulfide contamination. The data, which describe the geological and geophysical researches of the Black sea bottom sediments, were published in the monograph «The geological history of the Black Sea based on the results of deep-sea drilling» by Shirshov Institute of Oceanology of Russian Academy of Sciences [Neprochnov, 1980]. The deep well is located in the lower part of the continental slope in the southwestern part of the Black Sea at a depth of 1750.5 m (Table *6* and Figure 17).

3.2 Materials and Methods

Bottom sediments sampling from the White and Black Seas was carried out using a gravity steel pipe (Figure *18*). Bottom sediments of the Laptev Sea and the East Siberian Sea were sampled using a multicorer (Figure *19*). A twenty cm to four-meter-long core was lengthwise split.

Figure 18. A sampling of bottom sediments by a gravitational steel pipe.

Figure 19. A sampling of bottom sediments by multi-corer sediment.

The lithological description and sampling were performed immediately after core retrieval and temperature, pH, and Eh measurements. The pH and Eh measurements of pore water in the bottom sediments of the White Sea were performed by the pH testing tool (pH-150МИ). The redox potential's measurement results were reduced to a normal hydrogen electrode potential by the formula $Eh = E_{measured} + E_{reference\ electrode}$, where $E_{reference\ electrode}$ is reference electrode potential, which was 212 mV [http://www.izmteh.ru/esr/esr-10104/]. The pH and Eh measurements of pore water in the bottom sediments of the Laptev and East-Siberian Seas have been performed by the Ph-meter «Hanna» and the redox potential meter «ORP-200». Table *6* shows the samples numbers, a selection step, and research methods of marine bottom sediments.

Table 6. Stations, methods, and a sampling interval.

№ station	**Methods**					
	ICP-MS		**C, H, N, S Element Composition**		**C, N, S Isotope Composition**	
	Number of samples	**Sampling interval, cm**	**Number of samples**	**Sampling interval, cm**	**Number of samples**	**Sampling interval, cm**
1 (the White Sea)	10	18.5÷27.5	11	18.5÷29	4	66÷71.5
2 (the White Sea)	33	5	31	5	4	35÷50
3 (the Laptev Sea)	6	3÷6	6	3÷6		
4 (the Laptev Sea)	18	2	18	2	4	8÷12
5 (the East-Siberian Sea)	6	4	6	4		
6 (the East-Siberian Sea)	11	2	11	2		
7 (the Black Sea)			14	5÷85	8	30÷85
8 (the Black Sea)			8	30÷85	8	30÷85

Unfortunately, we could not conduct our own expedition to study the uranium behavior and other chemical elements in the Black Sea sediments because of covid restrictions. But in a separate part of this chapter, we will consider the uranium distribution in the Black Sea sediments according to the literature data. As well as the chemical C, H, N, S elements

distribution results and isotopic composition of C, N, S in the Black Sea bottom sediments stations 7 and 8 selected by colleagues from Moscow State University.

The bottom sediment samples under investigation were dried and crushed in laboratory conditions. After preparing the samples, the following measurements have been performed.

The concentrations of uranium, thorium, vanadium, cobalt, iron, and other metals were measured using the Agilent 7500c ICP-MS spectrometer (Agilent Technologies, USA).

Before ICP-MS measurements, the sample to be analyzed is brought into solution by autoclave digestion. The samples are placed in Teflon reaction vessels of autoclaves, and concentrated nitric acid (HNO_3) and concentrated hydrochloric acid (HCl) are added. The reaction vessels are capped and sealed in analytical autoclave jackets. The autoclaves are placed in an electric heater and incubated for 1 hour at 160°C, 1 hour at 180°C, and 2 hours at 200°C. After cooling, the contents of the autoclaves are transferred into polyethylene tubes diluted with deionized water.

The mineral composition of samples was determined by the XRD method using the DRON-3M X-ray diffraction meter for the White, the Laptev, and the East-Siberian Seas.

Isotopic compositions of sulfur, carbon, and nitrogen in bottom sediments were analyzed using Thermo Scientific DELTA V Plus mass spectrometer (Germany). The instrument is equipped with a Flash HT elemental analyzer. International standards [Coplen et al., 2002] used in the isotopic analyses of hydrogen, carbon, oxygen, and nitrogen are PDB for carbon, AIR for nitrogen, CDT for sulfur. The accuracy of isotopic composition determination defined by measurements on the reference samples was ±0.2‰ for carbon, ±0.5‰ for sulfur and nitrogen. The isotope measurements have been carried out on original dried and crushed samples. Before measuring the isotope composition of organic carbon, samples have been additionally treated, as described below, with orthophosphoric acid to remove carbonates.

For the measurements of oxygen, hydrogen, nitrogen, and sulfur element concentrations in the bottom sediment samples, dried samples were treated with orthophosphoric acid. The sediment weighing about 2 g was crushed in a porcelain pounder. 5 ml of 85 % phosphoric acid solution were added to 1 g of a crushed rock sample to remove calcite and dolomite from the rock and

obtain the correct concentration of organic carbon. After twenty-four hours of treatment in acid, the solution was filtered, the samples were washed with distillated water many times and then dried in a drying cabinet at 50°C. The carbon, hydrogen, nitrogen, and sulfur concentrations were performed on acid-treated homogenized samples using an elemental analyzer (LECO CHN628 Series w/Sulfur Add-On Module (S628)). Two or more technical replicates of each sample were measured; the sample amount is 80 mg. For calibration of the instrument standard samples SSS 9113-2008 (EDTA 502-896/502-896-250), SSS 10821-2016 (Coal 502-670), SSS 10822-2016 (Coal 502-671), SSS 10823-2016 (Coal 502-672), Phenilanine LECO (502-642) LOT 1017, BBOT 502-897 from the manufacturer of the elemental analyzer LECO have been used. The analytical uncertainty of the measurements is typically smaller than 0.08% for carbon, 0.02 % for nitrogen and sulfur, and 0.04% for hydrogen [Instrument: CHN628 Series w/Sulfur Add-On Module (S628), 2014; Instrument: CHN628, 2016].

3.3 Results of the Bottom Sediments Investigations

3.3.1 Lithology

In this part of the third chapter, a lithological description and lithological composition of the Arctic and Black Seas selected sediments will be presented. As well as a lithological description of the Black Sea sediment column according to the literature data will be shown.

The photographs of the sediments (2-4 meters long) sampled straight-flow gravitational steel sampler, and multicorer (20 – 40 cm) for stations are shown in Figure *20*.

Station 1, the White Sea | Station 2, the White Sea | Station 3, the Laptev Sea | Station 4, the Laptev Sea | Station 5, the East-Siberian Sea | Station 6, the East-Siberian Sea | The station of the Black Sea

Figure 20. The cores of bottom sediments.

Figure *21* and Figure *22* show a lithological description for stations 1 and 2 as examples. The deposits the Arctic Seas comprise sorted pelite/siltstone, siltstone/pelite, and pelite sediments.

Depth (cm)		Lithological description
top	bot	
0	5	Oxidized aleuropelitic silt, of flowing consistency, creamy, homogeneous.
5	15	Aleuropelitic silt of flowing consistency, creamy, homogeneous. Hydrotroilite content gradually increases downwards along the layer, which affects the change in color.
15	60	Aleuropelitic silt of flowing consistency, creamy, homogeneous. It is intensely saturated with hydrotroilite; due to this, the sediment is of black color. Texture is indistinct, horizontal, due to rare thin (h up to 1 mm) interlayers of silt, whose color is not changed by hydrotroilite. Multiple gas seepage textures are noted. A large whole bivalve shell is located at the depth of 40 cm.
60	285	Aleuropelitic silt of flowing/plastic consistency. It is intensely saturated with hydrotroilite; due to this, the sediment is of black color. The layer contains infrequent whole bivalve shells 1–1.3 cm in diameter, as well as fragments of unchanged flora (long, narrow algae). The interval is intensely saturated with gas and strongly smells of H_2S. There are multiple gas seepage textures, represented on the cleaned surface by bubbles and by small cracks

Figure 21. Lithological description and color photos of core from Station 1.

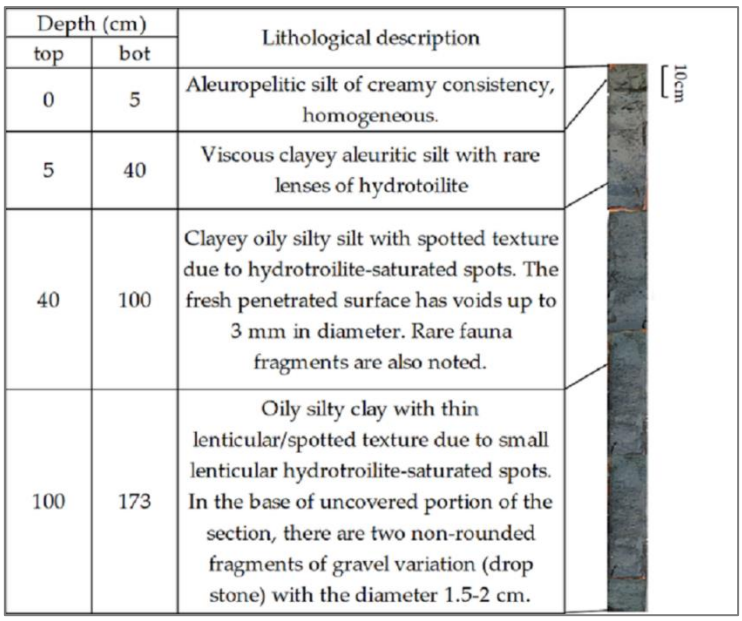

Figure 22. Lithological description and color photos of core from Station 2.

The color of sediments of the White, the Laptev and East-Siberian Seas in the top layer varies from brown to reddish-brown. The underlying greenish-grey sediments contain adhesions and balls of hydrotroilite. Quartz and plagioclases are the predominant minerals in the studied sediments of the Arctic Seas (Table *7*).

Table 7. The mineral composition measurements (the XRD method) of the bottom sediments.

Mineral, %	**The Laptev Sea**	**The East Siberian Sea**	**The White Sea**
Quartz	34	37	46.3
Plagioclase	23	21	37
Potassium feldspar	13.5	12	-
Montmorillonite	9	10	-
Kaolinite	6	8	2.2
Chlorite	3.5	4	-
Illit	4	4	11.3
Pyrite	-	-	1.8
Mica	-	-	1.3
Pyroxene	3	traces	-

Cristobalite	2	traces	-
Goethite	2	-	-
Amphibole	traces	traces	-

The upper part of the studied section of the bottom sediments of the Black Sea (stations 7 and 8) is represented by gray, light gray clayey silt with large shell material. The lower part of the section is a clay-aleurite layer with interlayers of finely dispersed crushed shell rock with a particle size of only 1-2 mm and dark gray clays with a large amount of hydrotroilite.

According literature review: the bottom sediments of the Black Sea are divided into modern, ancient Black Sea, and Novoeuxinian silt (Pleistocene) [Gursky, 2003]. Modern sediments are represented by microlaminated coccolith silt of white and grey color; the content of the hydrotroilite is 0.02–0.06%. Ancient Black Sea sediments (located under modern sediments) are represented by grey clayey silt and black sapropel silt, and the content of the hydrotroilite is 0.01–0.03%. Novoeuxinian sediments are represented by grey and black silt containing hydrotroilite and sulfides (the content of the hydrotroilite is 0.06%). The lithological slices in the bottom sediments of the Black Sea Deep Well are presented in the Table *8*.

Table 8. Lithological slices in the bottom sediments of the Black Sea Deep Well. Modified after [Neprochnov, 1980].

Slice	**Lithology**	**Thickness, m**	**Age**
1	Terrigenous silt	171	Holocene
1a	Aleurites and sands	9.5	Pleistocene
2	Carbonate sediments	2	Eopleistocene
3	Silt enriched with diatoms and coccoliths	112	Pleiocene
4	Carbonate sediments enriched with diatoms	38	Pleiocene
5	Clays enriched with diatoms	28.5	Pleiocene
6	Brecciated sediments and sand	85.5	Miocene
7	Black aleurolite	28	Miocene
8	Brecciated sediments	10	Miocene
9	Aleurolite	28.5	Miocene

3.3.2 Eh, pH, and Temperature Values

This section shows the measuring results of the redox environment potential (Eh, pH) as well as the temperature. These measurements were necessary to determine the oxidizing and reducing conditions in the studied sediments and were used in thermodynamic uranium forms modeling.

Measured Eh and pH of the pore water in the bottom sediments are shown in Table *9*, Table *10* and Table *11*.

Table 9. Station 1. Measurements of redox potential (Eh) reduced to the normal hydrogen electrode potential and pH on fresh bottom sediments.

Depth (cm)	Eh (mV)	pH
5	+392	8
42.5	−273	8.11
71.5	−243	7.95
91.5	−215	7.88
110.0	−145	7.81
136.5	−117	7.94
156.5	−138	7.92
181.5	−115	7.84
201.5	−150	7.82
220.0	−170	7.84
247.5	−73	7.76
267.5	−63	7.81

Table 10. Stations 2 and 3 of the Laptev Sea. Measurements of redox potential (Eh) and pH on fresh bottom sediments.

Station	Depth (cm)	Eh (mV)	pH
2	1	89	7.27
	3.5	88	7.17
	9.5	-70	7.47
	15.5	-33	7.44
	20.5	-42	7.13
	23.5	-85	7.41
3	1.5		6.62
	4		7.05
	6		7.05
	8		7.54
	10		7.13
	12		6.98

	14		7.45
	16		7.47
	18		7.82
	20		8.43
	22		8.55
	24		8.53
	26		8.66
	28		8.61
	30		8.36
	32		8.49
	34		8.54
	36		8.51

Table 11. Stations 4 and 5 of the East-Siberian Sea. Measurements of redox potential (Eh) and pH on fresh bottom sediments.

Station	**Depth (cm)**	**Eh (mV)**	**pH**
4	2	25	7.64
	6	-63	7.05
	10	-95	7.06
	14	-107	7.04
	18	-85	7.19
	22	-78	7.24
5	1	93	7.18
	3	70	8.06
	5	-65	8.39
	7	-130	8.07
	9	-172	8.18
	11	-191	8.2
	13	-223	8.26
	15	-184	7.63
	17	-167	8.14
	19	-105	8.32
	21	-188	8.26

Also, the Eh and pH of the pore water in the Black Sea bottom sediments are presented in the Table 12 and Table 13 according to the literature review [Gurskij, 2019; Lisitsyn, Gursky, 2003].

Table 12. Station of the Black Sea. The redox potential (Eh) potential and pH of the pore water. Modified after [Lisitsyn, Gursky, 2003].

Station	Easting	Northing	Water depth, m	Depth (cm)	Eh (mV)	pH
Black Sea station	38°44'6	43°18'0	2170	Bottom water	-160	7.8
				15	-185	7.68
				70	-200	7.68
				105	-205	7.68
				140	-210	7.68
				185	-195	7.74

Table 13. Station of the Black Sea. The redox potential (Eh) potential of the different ages bottom sediments along the profile in the southeast of the Kerch Strait. Modified after [Gurskij, 2019].

Parameter	Age									
	Modern sediments + Ancient sediments + Novoeuxinian sediments			Modern sediments			Ancient sediments			Novoeuxinian sediments
	average	*min*	*max*	*average*	*min*	*max*	*average*	*min*	*max*	*average*
Eh, mV	-142	-230	280	-103	-200	280	-185	-80	-220	-198

The measured temperature of the bottom sediments is presented in the Table *14*.

Table 14. Temperature of the fresh Arctic bottom sediments.

Location	№ station	Depth water (cm)	T (°C)
The East-Siberian Sea	6	41-45	-1.2...-1.0
The East-Siberian Sea, Dmitri Laptev Strait	5	12-15	+1.6…+1.9
The Laptev Sea, continental slope	4	350	+0.4
The White Sea, Kandalaksha Bay	1	80	+0.8...+1.0

The redox potential in the upper portion of the White Sea bottom sediments was positive (+392 mV), whereas Eh at the depth below 5 cm was negative and varied from −273 to −63 mV (Table *9*). The pH values decreased with depth from 8 to 7.8. The obtained data correspond to published data, which shows that Eh values in the bottom sediments may vary from −324 to +523 mV [Gursky, 2005]. According to [Lein, 2004], pH values in sediments fluctuate from 7.6 to 8.4; in our case, the bottom sediments' measuring pH varied from 7.76 to 8.11.

The Eh negative values in the underlying layers characterized by anoxic conditions at all stations (Table *10* and Table *11*). In addition, stations in areas of intense gas release from bottom sediments are characterized by lower values of the redox potential Eh in the lower part of the sediments. For example, for the core of the East Siberian Sea station 5, located in the active bottom methane degassing zone: the lowest Eh values are observed for the lower part of the sediment (from 4 cm), reaching -223 mV at a depth of 12–14 cm (Table *11*). The reduced values of the pore water redox potential in the sediment section lower part in the zones of active methane release from bottom sediments are associated with the anoxic conditions predominance. Anoxic conditions is accompanied by hydrogen sulfide H_2S (a characteristic hydrogen sulfide smell was observed during measurements and sediments sampling).

The measured pH values of the East Siberian Sea and the Laptev Sea pore waters (Table *10* and Table *11*) are characterized: lower pH values (about 7) for the upper part of the sediments (oxidized layer) compared to the underlying layers (reducing conditions) for which the pH values sometimes exceed 8.

The pore water in bottom sediments of the Black Sea station are characterized only negative Eh values in the range from -210 mV to -160 mV, the pH values varied from 7.68 to 7.8 (Table 12). Also, Eh analysis of the pore water in the Black Sea sediments (Table 13) is shown that the Eh avarege for different ages bottom sediments are characterized the negative values.

The temperature of the White Sea bottom sediments was positive and slightly less than 1 °C; at a depth of 5 cm, the temperature was 0.9 °C, and at a depth of 267.6 cm was 0.8 °C (Table 14). The highest bottom sediments temperatures in the Laptev Sea +0.4°C were found on the continental slope (the depth 350 m) station 4, which can be associated with the warm Atlantic water entry into this area. The upper part of the East Siberian Sea bottom sediments (station 6) is characterized by a temperature -1.2…-1.0°C. However, the temperature of the bottom sediments is positive and reaches +1.8°C in the East Siberian Sea, southern part (station 5), in the active thermal influence area of the river Indigirka [Chuvilin, B. Bukhanov, A. Yurchenko, D. Davletshina, N. Shakhova, E. Spivak, V. Rusakov, O. Dudarev, N. Khaustova, A. Tikhonova, O. Gustafsson, T. Tesi, J. Martens, M. Jakobsson, M. Spasennykh, 2022].

3.3.3 Uranium and Other Metals Concentrations

The ICP-MS method was used to study the uranium and other chemical elements distribution in the marine sediments. Unfortunately, it was not possible to measure the uranium and other chemical elements concentartions in the Black Sea sediments due to covid restrictions.

The uranium concentrations in the bottom sediments measured by ICP-MS for stations 1 and 2 are shown in Table *15* and Table *16*. For station 2, the concentrations of Cd, Co, Cr, Fe, Ni, Pb, Th, U, and V in the bottom sediments were also measured and shown in Table *16*. The uranium concentrations and other chemical elements in the bottom sediments measured by ICP-MS for stations 3 and 4 of the Laptev Sea; stations 5 and 6 of the East-Siberian Sea are shown in Table 17 and Table 18. The uranium distribution in the Black Sea sediments is presented in the Table 19 according to the deep sea drilling results [Neprochnov, 1980].

Table 15. The uranium concentration in the White Sea bottom sediments from station 1 (ppm).

Depth, cm	**U, ppm**
71.5	1.3
91.5	1.42
110	1.33
136.5	1.21
156.5	1.21
181.5	1.16
201.5	1.24
220	1.36
247.5	1.87
267.5	1.34

Table 16. The uranium and other metals concentration in the White Sea bottom sediments from station 2 (ppm).

Depth, cm	**U**	**Fe**	**Cr**	**V**	**Zn**	**Ni**	**Co**	**Pb**	**Th**	**Cd**	**Th/U**
2.5	1.89	35721	95	94	66	37	27	20	6.23	0.122	3.296
7.5	1.69	35078	97	95	66	39	15	13	6.08	0.119	3.598

12.5	1.79	35430	99	97	78	39	18	10	6.43	0.113	3.592
17.5	1.81	33801	102	93	66	38	15	11	6.62	0.106	3.657
22.5	1.9	32372	95	91	62	37	15	7	6.37	0.109	3.353
27.5	1.91	33269	92	88	62	37	15	7	6.88	0.114	3.602
32.5	1.76	33751	96	89	63	38	14	8	6.51	0.095	3.699
37.5	1.83	33153	96	89	65	37	14	6	6.49	0.092	3.546
42.5	1.88	33165	99	88	61	38	13	6	6.81	0.096	3.622
47.5	1.91	32839	98	87	65	37	14	6	6.86	0.107	3.592
52.5	1.91	32839	98	87	65	37	14	6	6.86	0.107	3.592
57.5	2.08	32551	92	84	59	35	13	6	7.03	0.098	3.380
62.5	2.12	32152	91	85	65	36	13	5	7.21	0.086	3.401
67.5	2.08	32100	94	84	57	36	13	5	7.07	0.085	3.399
72.5	2.06	31789	92	85	58	36	13	6	7.09	0.086	3.442
77.5	2.13	34040	97	87	61	37	14	6	7.94	0.078	3.728
82.5	2.3	33484	96	89	62	37	13	6	7.75	0.097	3.370
87.5	2.1	32074	92	84	58	36	13	6	7.58	0.071	3.610
92.5	2.16	31134	88	82	63	34	13	5	7.47	0.075	3.458
97.5	2.26	32848	90	85	60	36	14	6	8	0.088	3.540
102.5	2.27	33454	92	86	60	37	14	5	7.65	0.091	3.370
107.5	2.29	33027	91	85	63	37	13	6	8.18	0.092	3.572
112.5	2.34	33503	89	85	64	36	14	7	8.4	0.091	3.590
117.5	2.48	34274	90	89	65	37	14	6	8.89	0.097	3.585
122.5	2.38	33132	94	85	62	38	14	7	8.8	0.087	3.697
127.5	2.46	34200	94	83	66	38	14	6	9.02	0.097	3.667
132.5	2.44	31894	88	83	62	35	13	6	8.56	0.09	3.508
137.5	2.21	30840	87	76	57	34	13	8	8.29	0.081	3.751
142.5	2.42	33186	94	83	63	37	13	9	9.29	0.101	3.839
147.5	2.36	33411	92	84	65	36	13	13	9.06	0.092	3.839
152.5	2.29	32458	93	82	62	37	13	13	8.71	0.092	3.803
157.5	2.4	33932	98	83	64	37	13	9	8.9	0.087	3.708
162.5	2.52	33502	96	83	63	37	13	8	9.48	0.101	3.762
Instrumental detection limit	0.032	0.300	0.024	0,021	0.065	0.015	0.016	0.019	0.029	0.013	

Table 17. The uranium and other metals concentration in the Laptev Sea bottom sediments from stations 3 and 4 (ppm).

Station	Depth, cm	P	V	Cr	Mn	Fe	Co	Ni	Cu	Zn	Mo	Cd	Pb	Th	U	Al	Th/U
3	2.5	3208	112.9	87.9	337	34055	11.56	34.3	19.5	106	3.164	-	16.4	7.94	1.328	74754	5.979
	8.5	2302	117.6	88.9	302	36583	11.26	33.8	20.9	105	3.455	-	17.1	8.29	1.409	77317	5.884
	13.5	3820	111.8	84	320	38050	11.58	33.4	21	104	3.409	-	19.1	8.94	1.338	77781	6.682
	16.5	2622	108.3	86.9	298	35463	11.21	34.1	20.9	101	3.514	-	16.9	7.66	1.208	76564	6.341
	20	1832	95.7	81.3	281	31741	10.25	31.5	18	101	1.428	-	14.8	7.65	1.250	76348	6.12
	23	2301	104.7	80.6	268	32348	9.82	30.6	20	96	1.263	-	15.2	7.38	1.166	79091	6.329
4	1.5		165	107		59375	46	73	38	125		0.16	25	11.8	2.47	85118	4.777
	4		170	99		66107	26	57	35	113		0.13	22	10.1	1.97	83750	5.127
	6		185	1962		67694	28	64	47	127		0.24	24	11.4	2.11	85013	5.403
	8		181	114		59681	29	64	37	120		0.19	21	10.3	1.99	85492	5.176
	10		181	107		59002	27	62	160	113		0.15	17.3	8.3	1.56	82725	5.321
	12		183	107		66671	27	62	36	113		0.13	17.3	8.38	1.56	84551	5.372
	14		181	109		57181	24	59	42	112		0.21	16.8	8.46	2.29	89638	3.694
	16		181	109		57181	24	59	42	112		0.21	16.8	8.46	2.29	89638	3.694
	18		182	118		53052	26	62	42	118		0.24	17.8	9.02	2.4	85943	3.758
	20		179	113		55097	26	62	37	115		0.21	17.2	8.72	2.27	85191	3.841
	22		182	100		56518	24	56	33	103		0.19	15.6	8.06	1.85	87594	4.357
	24		180	97		54975	23	54	32	100		0.18	15.3	7.7	2.02	84619	3.812
	26		188	101		57627	24	55	32	100		0.16	15.7	8.03	2.21	85936	3.633
	28		186	97		58855	23	53	33	99		0.17	15.6	7.77	1.87	87168	4.155
	30		189	103		59020	24	55	33	101		0.21	16.4	8.45	2.08	86770	4.063
	32		191	96		58698	22	52	30	94		0.15	15.9	8.35	2.15	88995	3.884

	34		192	95		56892	22	52	30	92		0.17	15.7	8.16	2.27	81527	3.595
	36		194	90		56066	21	50	30	90		0.23	15.6	8.08	2.36	84782	3.424
Instrumental detection limit		0.41	0.268	0.299	0.312	0.344	0.213	0.286	0.321	0.316	0.131	0.061	0.146	0.014	0.011	0.324	

Table 18. The uranium and other metals concentration in the East-Siberian Sea bottom sediments from stations 5 and 6 (ppm).

Station	**Depth, cm**	**P**	**V**	**Cr**	**Mn**	**Fe**	**Co**	**Ni**	**Cu**	**Zn**	**Mo**	**Cd**	**Pb**	**Th**	**U**	**Al**	**Th/U**
5	2	895	70.3	52.2	268	23766	8.38	21.5	8.43	73	3.213	0.086	6.7	5.89	0.975	64917	6.041
	6	5685	90.4	72.4	323	29040	9.57	26.4	17.8	84	4.416	-	11.98	6.07	1.051	67899	5.775
	10	1801	89.9	65.8	294	27728	9.64	25.6	14.3	87	2.269	-	10.97	5.74	0.93	69276	6.172
	14	3102	95.8	72.2	284	31205	10.16	27.6	23.3	90	2.014	-	14.21	6.84	1.027	70179	6.660
	18	1710	94.7	73.4	277	25784	9.51	26.1	17.3	86	2.379	-	13.04	7.73	1.227	63019	6.300
	22	1091	78.1	62.8	245	23194	8.33	23.2	12.7	76	2.029	-	9.24	6.46	1.134	61830	5.697
6	1	1040	111.4	58.8	842	31066	11.79	24.3	10.5	96	3.419	-	12.36	5.45	0.766	69895	7.115
	3	1587	111.4	60.5	263	30627	10.77	24.2	12.8	93	1.459	-	9.69	5.53	0.877	69711	6.306
	5	534	115.8	64.2	282	31707	12.31	26.4	14.3	103	1.329	-	9.81	5.44	0.821	71050	6.626
	7	851	122	67.1	292	35027	28.14	30.5	15.1	103	96.932	-	11.91	6.11	0.943	78406	6.479
	9	694	120	66	292	32876	14.4	28.6	14.8	100	20.450	-	11.98	6.37	0.966	74124	6.594
	11	718	119.1	66	277	30555	13.13	26.4	15.8	102	13.419	0.067	9.84	5.44	0.872	70900	6.239
	13	1128	133.6	70.8	350	35135	15.26	28.7	17.4	108	6.142	0.077	14.27	6.75	1.093	75506	6.176
	15	1059	129.2	66.2	637	36859	13.61	26.4	15.3	107	4.287	-	13.43	6.16	0.878	73377	7.016
	17	949	142	71.7	620	37397	15.31	28.3	15.5	114	10.970	-	12.07	6.03	0.857	72126	7.036
	19	962	140	69.1	509	37443	13.51	26.3	15.1	108	1.850	-	12.74	5.92	0.866	73360	6.836
	21	864	134	69.7	362	35276	12.96	26.7	15.5	107	1.921	-	11	5.78	0.884	71628	6.538
Instrumental detection limit		0.41	0.268	0.299	0.312	0.344	0.213	0.286	0.321	0.316	0.131	0.061	0.146	0.014	0.011	0.324	

Table 19. The uranium and thorium concentration (ppm), the ratio Th/U in the Black Sea bottom sediments from station Deep Well [Neprochnov, 1980].

Depth, m	U, ppm	Th, ppm	Th/U
42.15	3.15	12.4	3.94
53.5	1.49	11.95	8.02
62.75	1.88	12.21	6.49
84.2	1.85	11.7	6.32
94.25	3.16	12.58	3.98
114	2.15	11.13	5.18
123.5	1.51	7.49	4.96
150	1.82	7.97	4.38
171	1.49	5.35	3.59
178.57	2.24	11.22	5.01
202.9	3.12	11.53	3.70
224.76	3.47	11.97	3.45
240.5	2.81	9.08	3.23
257.34	2.51	9.77	3.89
278	2.73	7.46	2.73
285.81	2.77	3.93	1.42
313.5	1.74	12.22	7.02
315.6	5.27	6.67	1.27
326.7	3.99	13.24	3.32
339.48	3.43	10.24	2.99
438.55	3.71	12.96	3.49
446.7	3.53	16.1	4.56
473.73	2.9	14.93	5.15
476.65	2.98	12.6	4.23
488.75	3.47	11.76	3.39
499.55	2.39	9.22	3.86

The uranium concentration in the White Sea bottom sediments for both studied stations did not exceed 2.6 ppm. For station 1, uranium concentrations varied from 1.16 ppm to 1.87 ppm at the depth interval 71.5 cm–267.5 cm, respectively. The difference in uranium concentration between the upper and lower parts of the sampled core was identified for station 2. In the upper part (0–50 cm), the concentration varied from 1.7 to 1.9 ppm; in the lower part, uranium concentration increased up to 2.52 ppm.

The sediments were enriched with iron (Fe) with concentrations up to 3.57%, which is explained by the presence of hydrotroilite and its high capacity for complexation with organic

matter even at low concentrations compared to other metals [Moiseenko, 2012]. The concentrations of Cr, V, Zn, Ni, Co, and Pb showed values in the range of 20–100 ppm, the concentrations of Cd were about 0.1 ppm. The concentrations of these metals in the upper layer were slightly higher and decreased with depth. The concentrations of Th varied from 6.2 ppm in the upper part to 9.5 ppm in the lower part of the column. The value of the Th/U ratio varied from 3.30 to 3.84 with an average value of 3.58, which corresponds to the marine sedimentation stage, according to Walter H. Fertl's research [Fertl, Rieke, 1980]. The following sources of accumulation of these metals in the bottom sediments of the White Sea are continental run-off, seawater, and anthropogenic impact (wastewater, smoke emissions). The character of Th/U variations showed that the source of these metals was continental run-off with a low income of autogenic uranium of marine genesis. No anthropogenic impact (another potential source of U) was identified.

According to the literature review, the main sources of enrichment of the Arctic bottom sediments with rare earth elements are terrigenous material brought by rivers [Astahov, 2018] and, with distance from the river delta, on the example of the Indigirka River in the East Siberian Sea, a decrease in the concentration of heavy metals and rare earth elements is observed [Sevast'yanov, 2020]. In [Novikov, ZHilin, 2016; Sevast'yanov, 2020], an emphasis is placed on the study of heavy metals in the sediments of the East Siberian Sea. In the East Siberian Sea, the average contents of heavy elements are Cu = 18.70 ppm, Zn = 109.5 ppm, Ni = 33.20 ppm, Cr = 69.81 ppm, Pb = 15.92 ppm. It also showed a rather significant relationship between the content of heavy metals and organic carbon, showing a stable contribution to the microelement composition of the biota on the entire Arctic shelf.

The study of the chemical elements distribution along the profile from south to north from Billings Cape to the Mendeleev submerged ridge in the East Siberian Sea sediments [Novikov, 2017; SHakirov, R. V. Sorochinskaya, A. V. Obzhirov, 2012; SHakirov, 2010], and in [Miroshnikov, 2020] showed:

- the surface layer of sediments is depleted in most chemical elements, but elevated concentrations of Mn (4-10 times), Cu (8 times), Zn (2 times) are observed;
- the contents of Mg, Sc, V, Pb in sediments are close to the average content of these elements in the sedimentary rocks of the continents;
- for elements such as Rb, Cs, Li, K, Ca, Sr, Ba, U, Th, Ti, Hf concentration factors are less than 1;
- the content of Fe, V, Zn along the studied profile is 1.5-2 times higher than the average content of these elements in the sedimentary rocks of the continents;
- the content of U, Th and Hf in the surface layer of sediments along the profile is lower than the average contents of these elements in the sedimentary rocks of the continents, while the minimum concentrations of these elements were found at stations with a minimum amount of pelite and organic matter content;
- elements of the iron and heavy metals group have a high correlation with the content of organic carbon in the sediments of this profile.

The uranium concentration in the bottom sediments for both studied seas (Laptev and East-Siberian Seas) did not exceed 2.5 ppm. For station 3, uranium concentrations varied from 1.17 ppm to 1.41 ppm at the depth interval 2.5 cm–23 cm. For station 4, uranium concentrations varied from 1.56 ppm to 2.47 ppm at 1.5 cm–36 cm depth. For station 5, uranium concentrations varied from 0.93 ppm to 1.23 ppm at 2 cm–22 cm depth. For station 6, uranium concentrations varied from 0.77 ppm to 1.09 ppm at the depth interval 1 cm–21 cm.

The characteristic of the Laptev Sea bottom sediments (stations 3 and 4):

- Sediments were enriched iron concentrations (Fe) up to 3.81% for station 3 and 6.77% for station 4. According to the material-genetic typification [Ruban, 2017], the sediments of station 3 are classified as non-ferrous (Fe <5%), and the sediments at station 4 are low iron (Fe = 5 ÷ 10%). The maxima of the iron content in the sediments of station 4 are due to reducing conditions (black sediment due to hydrotroilite, formed due to biogenic sulfate reduction).

- In sedimentary rocks of the continents, the clarke content of Mn is 0.073%, the Mn content in sediments of station 3 reaches 0.034%, which is two times less than the clarke content of this element. Therefore, the sediments of station 3 are classified as non-manganese.
- Sediments were enriched nickel concentrations (Ni) up to 34.3 ppm for station 3 and 73 ppm for station 4.
- Sediments were enriched zinc concentrations (Zn) up to 106 ppm for station 3 and 125 ppm for station 4. The clarke content of zinc in sedimentary rocks is approximately ≈ 70 ppm; the zinc content in the sediments of the stations under study exceeds the clarke content of this element.
- Sediments were enriched chromium concentrations (Cr) up to 88.9 ppm for station 3 and up to 1962 ppm for station 4. Station 4 is characterized by a sharp peak in the chromium concentration at a depth of 6 cm.
- Sediments were enriched with cobalt concentrations (Co) up to 11.58 ppm for station 3 and 46 ppm for station 4. The clarke content of cobalt in sedimentary rocks is approximately ≈ 13 ppm, the cobalt content in the sediments of station 3 is comparable to the clarke content of this element, and the cobalt in sediments from station 4 exceeds its clarke value by more than 1.5 times.
- Sediments were enriched thorium concentrations (Th) up to 8.94 ppm for station 3 and 11.8 ppm for station 4. The clarke content of thorium in sedimentary rocks is approximately ≈ 10 ppm; the thorium in the studied sediments is comparable to the clarke content of this element.
- Sediments were enriched phosphorus concentrations (P) up to 0.38% for station 3. Phosphorus oxide varies from 0.42% to 0.87% in the studied sediments. The phosphorus content in Arctic sediments [Baturin, 2004] ranges from 0.1-0.9%. In enclosed and semi-enclosed seas, phosphorus is concentrated in the sediments of deep-sea depressions and the open seas - mainly in sediments of the continental zones, while the overall distribution of phosphorus is generally similar to organic carbon.

- Sediments were enriched:
  - vanadium concentrations (V) up to 117.6 ppm for station 3 and 194 ppm for station 4.
  - aluminum concentrations (Al) up to 7.91% for station 3 and 8.96% for station 4.
  - Copper copper concentrations (Cu) up to 21 ppm for station 3 and 160 ppm for station 4.
  - molybdenum concentrations (Mo) up to 3.514 ppm for station 3.
  - cadmium concentrations (Cd) up to 0.24 ppm for station 4.
  - plumbum concentrations (Pb) up to 19.07 ppm for station 3 and 25 ppm for station 4.
- The value of the Th/U ratio varied from 5.88 to 6.68 (average value is 5.2) for station 3, and for station 4, the Th/U ratio varied from 3.42 to 5.40 with an average value of 4.28 corresponding to the marine sedimentation stage. Also, the Th/U ratio is very close to the Th/U=7 that corresponds to the oxic continental conditions for station 3.

The characteristic of the East-Siberian Sea bottom sediments (stations 5 and 6):

- Sediments were enriched iron concentrations (Fe) up to 4% for stations 5 and 6. Following the material-genetic typing, the sediments of the studied stations are classified as non-ferrous (Fe <5%).
- In sedimentary rocks of continents, the clarke content of Mn is 0.073%, the content of Mn in sediments from station 5 reaches 0.032%, which is two times less than the clarke content of this element. In the sediments of station 6, the Mn content reaches 0.084%, which is comparable to the clarke content of this element.
- Sediments were enriched nickel concentrations (Ni) up to 31 ppm for both stations.
- Sediments were enriched zinc concentrations (Zn) up to 90 ppm for station 5 and 114 ppm for station 6. The zinc content in the sediments of the stations under study exceeds the clarke content of this element.

- Sediments were enriched chromium concentrations (Cr) up to 75 ppm for both stations.
- Sediments were enriched with cobalt concentrations (Co) up to 10.16 ppm for station 5 and 28.14 ppm for station 6. The cobalt content in the sediments of station 5 is comparable to the clarke content of this element, and the cobalt content in the sediments of station 6 exceeds its clarke value by more than two times.
- Sediments were enriched thorium concentrations (Th) up to 7.73 ppm for station 5 and up to 6.75 ppm for station 6. The thorium content in the studied sediments is lower than its clarke content.Sediments were enriched phosphorus concentrations (P) up to 0.57% for station 5 and up to 0.16% for station 6.
- Sediments were enriched:
  - vanadium concentrations (V) up to 95.8 ppm for station 5 and 142 ppm for station 6.
  - aluminum concentrations (Al) up to 8% for both stations.
  - Copper copper concentrations (Cu) up to 23.3 ppm for station 5 and 17.4 ppm for station 6.
  - molybdenum concentrations (Mo) up to 4.416 ppm for station 5 and up to 96.932 ppm for station 6.
  - cadmium concentrations (Cd) up to 0.09 ppm for both stations.
  - plumbum concentrations (Pb) up to 15 ppm for both stations.

The value of the Th/U ratio varied from 5.68 to 6.66 (average value is 6.11) for station 5, and for station 6, the Th/U ratio varied from 6.18 to 7.12 (average value is 6.63), which corresponds to the marine sedimentation stage. Also, the Th/U ratio is close to the Th/U=7 corresponding to the oxic continental conditions.

The main research idea is to investigate the uranium concentration in marine sediments under various redox conditions. With the uranium concentration determination, the ICP-MS method makes it possible to determine the other chemical elements concentration such as P, V, Cr, Mn, Fe, Co, Ni, Cu, Zn, Mo, Cd, Pb, Th and Al. These elements' distribution and concentration were taken into account because the sediments of the intensive planktonogenic sapropelic

organic matter accumulation periods are characterized not only by a unique saturation with organic matter but also by an increased concentration of a wide chemical elements range [Neruchev, 2007]. The study of each chemical element concentration and distribution requires a more detailed analysis of the factors affecting their concentration. Since the work is devoted to the uranium study, the other chemical elements' distribution and concentration analysis in marine sediments is of a general and descriptive nature. Unfortunately, it was not possible to measure the uranium concentration in the Black Sea sediments due to the conducting of our own expedition impossibility to collect marine sediments. But in this subtopic, the uranium concentration distribution for one of the deep-water drilling stations carried out in the Black Sea was shown [Neprochnov, 1980]. A more detailed uranium concentration analysis of the Black Sea sediments will be shown in subtopic 3.4 of Chapter 3.

3.3.4 C, H, N, S Element Composition

This section shows the elemental composition of marine sediments. The study of the elemental composition made it possible to analyze the organic carbon, nitrogen, sulfur and hydrogen concentration, as well as to determine the organic matter source by the C/N ratio.

The results of C, H, N, S element composition in the bottom sediments samples of stations are shown in *Table 20*,

Table 21,

Table 22 and

Table *23*. The carbonate concentartion was also determined in the bottom sediments (*Table 20*, *Table 21* and

Table 23).

Table 20. Stations 1 and 2. Results of elemental composition (CHNS) measurements of bottom sediments.

Station	**Depth, cm**	**Elemental composition**						
		N, %	**TOC, %**	**Ccarb, %**	**H, %**	**S, %**	**C/N**	**U/TOC**
1	42.5	0.35	2.77	0.07	0.79	0.72	7.91	
	71.5	0.33	2.68		0.75	0.76	8.12	0.49
	91.5	0.36	2.76		1.19	0.72	7.67	0.51
	110	0.38	2.89	0.11	0.8	0.86	7.61	0.46
	136.5	0.34	2.58		0.71	0.67	7.59	0.47
	156.5	0.3	2.36		0.71	0.55	7.87	0.51
	181.5	0.29	2.29	0.03	0.76	0.55	7.9	0.51
	201.5	0.29	2.3		0.46	0.56	7.93	0.54
	220	0.28	2.17		0.68	0.56	7.75	0.63
	247.5	0.33	2.56	0.05	0.36	0.21	7.76	0.73
	267.5	0.3	2.29		0.65	0.63	7.63	0.59
2	2.5	0.31	2.31		0.4	0.15	7.45	0.82

	7.5	0.3	2.21		0.5	0.18	7.37	0.76
	12.5	0.25	1.9		0.46	0.26	7.6	0.94
	17.5	0.24	1.76		0.42	0.26	7.33	1.03
	22.5	0.23	1.68		0.42	0.2	7.3	1.13
	27.5	0.24	1.79		0.45	0.21	7.46	1.07
	32.5	0.24	1.77		0.44	0.29	7.38	0.99
	37.5	0.23	1.7		0.44	0.26	7.39	1.08
	47.5	0.18	1.45		0.38	0.33	8.06	1.32
	52.5	0.15	1.22		0.3	0.28	8.13	1.57
	57.5	0.21	1.6		0.38	0.27	7.62	1.30
	62.5	0.19	1.39		0.33	0.32	7.32	1.53
	67.5	0.22	1.57		0.37	0.33	7.14	1.32
	72.5	0.2	1.55		0.37	0.4	7.75	1.33
	77.5	0.21	1.59		0.38	0.41	7.57	1.34
	82.5	0.19	1.69		0.48	0.41	8.89	1.36
	87.5	0.21	1.61		0.36	0.44	7.67	1.30
	92.5	0.22	1.68		0.44	0.42	7.64	1.29
	97.5	0.22	1.63		0.42	0.39	7.41	1.39
	102.5	0.21	1.66		0.4	0.4	7.9	1.37
	107.5	0.18	1.6		0.41	0.44	8.89	1.43
	112.5	0.23	1.79		0.44	0.44	7.78	1.31
	117.5	0.23	1.66		0.43	0.51	7.22	1.49
	122.5	0.2	1.54		0.4	0.61	7.7	1.55
	127.5	0.25	1.84		0.46	0.56	7.36	1.34
	132.5	0.21	1.62		0.43	0.67	7.71	1.51
	137.5	0.22	1.65		0.44	0.51	7.5	1.34
	142.5	0.2	1.53		0.4	0.65	7.65	1.58
	147.5	0.21	1.68		0.46	0.84	8	1.40
	152.5	0.22	1.69		0.29	0.84	7.68	1.36
	157.5	0.22	1.86		0.5	0.61	8.45	1.29

Table 21. Stations 3 and 4 of the Laptev Sea. Results of elemental composition (CHNS) measurements of bottom sediments.

Station	**Depth, cm**	**Elemental composition**						
		N, %	**TOC, %**	**Ccarb, %**	**H, %**	**S, %**	**C/N**	**U/TOC**
3	3	0.19	2.19		0.49	0.03	11.44	0.61
	8.5	0.18	2.21		0.52	0.03	12.07	0.64
	13.5	0.18	2.18		0.51	0.03	12.10	0.61
	16.5	0.18	2.05		0.50	0.03	11.32	0.59
	20	0.15	1.66		0.42	0.03	11.11	0.75

	23.5	0.17	1.98		0.46	0.04	11.45	0.59
4	1.5	0.20	1.32	0.09	0.75	0.03	6.54	1.87
	4	0.19	1.23		0.70	0.03	6.31	1.60
	6	0.21	1.22		0.86	0.03	5.76	1.73
	8	0.19	1.14		0.86	0.02	5.91	1.75
	10	0.20	1.13		0.86	0.03	5.67	1.38
	12	0.17	1.11		0.86	0.03	6.40	1.41
	14	0.19	1.12	0.1	0.79	0.03	5.79	2.04
	16	0.19	1.13		0.83	0.02	5.83	2.03
	18	0.20	1.20		0.75	0.03	5.97	2.00
	20	0.21	1.17		0.77	0.03	5.51	1.94
	22	0.19	1.13	0.05	0.81	0.02	5.86	1.64
	24	0.19	1.16		0.81	0.02	5.99	1.74
	26	0.19	1.12		0.79	0.03	5.92	1.97
	28	0.22	1.07		0.79	0.02	4.89	1.75
	30	0.23	1.05	0.07	0.81	0.03	4.53	1.98
	32	0.24	1.08		0.81	0.04	4.56	1.99
	34	0.20	1.08		0.82	0.03	5.50	2.10
	36	0.19	1.04		0.82	0.04	5.55	2.27

Table 22. Stations 5 and 6 of the East-Siberian Sea. Results of elemental composition (CHNS) measurements of bottom sediments.

Station	**Depth, cm**	**Elemental composition**					
		N, %	**TOC, %**	**H, %**	**S, %**	**C/N**	**U/TOC**
5	2	0.12	0.85	0.19	0.01	4.54	1.15
	6	0.18	1.84	0.42	0.03	4.35	0.57
	10	0.15	1.18	0.29	0.02	4.07	0.79
	14	0.21	2.21	0.51	0.04	4.31	0.46
	18	0.14	1.21	0.36	0.02	3.38	1.01
	22	0.10	1.03	0.23	0.01	4.40	1.10
6	1	0.12	0.87	0.24	0.02	3.67	0.88
	3	0.10	0.67	0.20	0.02	3.37	1.31
	5	0.10	0.72	0.18	0.03	4.00	1.14

	7	0.10	0.74	0.19	0.03	3.86	1.27
	9	0.11	0.73	0.16	0.04	4.41	1.32
	11	0.10	0.77	0.20	0.03	3.85	1.13
	13	0.11	0.83	0.22	0.05	3.76	1.32
	15	0.14	0.83	0.25	0.03	3.31	1.06
	17	0.14	0.88	0.27	0.02	3.31	0.97
	19	0.14	0.88	0.27	0.02	3.27	0.98
	21	0.11	0.81	0.23	0.02	3.58	1.09

Table 23. Stations 7 and 8 of the Black Sea. Results of elemental composition (CHNS) measurements of bottom sediments.

Station	**Depth, cm**	**Elemental composition**						
		N, %	**C,%**	**TOC, %**	**Carbonates, %**	**H, %**	**S, %**	**C/N**
7	2.5	0.30	4.53	2.34	2.19	1.18	1.15	7.70
	52.5	0.27	4.20	2.17	2.03	1.14	1.38	7.88
	82.5	0.27	5.21	2.22	2.98	0.90	1.29	8.28
	142.5	0.19	4.44	1.69	2.75	0.83	1.33	8.76
	212.5	0.27	4.36	2.11	2.25	1.11	1.41	7.93
	242.5	0.28	4.45	2.28	2.16	1.10	1.39	8.12
	272.5	0.26	3.46	2.11	1.34	1.13	1.49	8.27
	302.5	0.29	3.66	2.54	1.12	1.13	1.32	8.88
	322.5	0.27	3.48	2.36	1.13	1.11	1.37	8.72
	347.5	0.40	4.51	3.70	0.81	1.27	1.58	9.19
	352.5	0.48	5.20	4.61	0.59	1.39	1.50	9.61
	357.5	0.53	5.74	5.32	0.42	1.51	1.55	10.08
	362.5	0.46	4.91	4.51	0.40	1.42	1.42	9.90
	367.5	0.44	4.77	4.41	0.36	1.37	1.38	10.06
8	2.5	0.26		2.29	2,95	0.79	0.33	8.96
	41.5	0.22		1.36	2,73	0.43	1.51	6.20
	64	0.10		0.68	2,52	0.21	1.10	6.54

	84	0.43		4.03	2,58	0.96	1.91	9.32
	119	0.47		4.25	4,09	1.02	1.27	9.08
	141	0.05		0.26	1,10	0.25	0.87	5.22
	176	0.07		0.45	1,04	0.43	0.78	6.51
	216	0.03		0.34	2,76	0.15	0.98	10.14

The lowest contents of organic carbon, about 1%, are observed in the upper horizons of the sediments of the East Siberian Sea, the highest ones, up to 2.8%, in all samples of the sediments of station 1 of the White Sea, and in individual horizons of the Black Sea both stations sediments with higher variations of this parameter in the depth.

The positive correlation between nitrogen contents with organic carbon contents (Figure *23*) shows the organic nature of nitrogen in the studied sediment samples. This correlation is less pronounced in the northern seas sediments than in the Black Sea sediments.

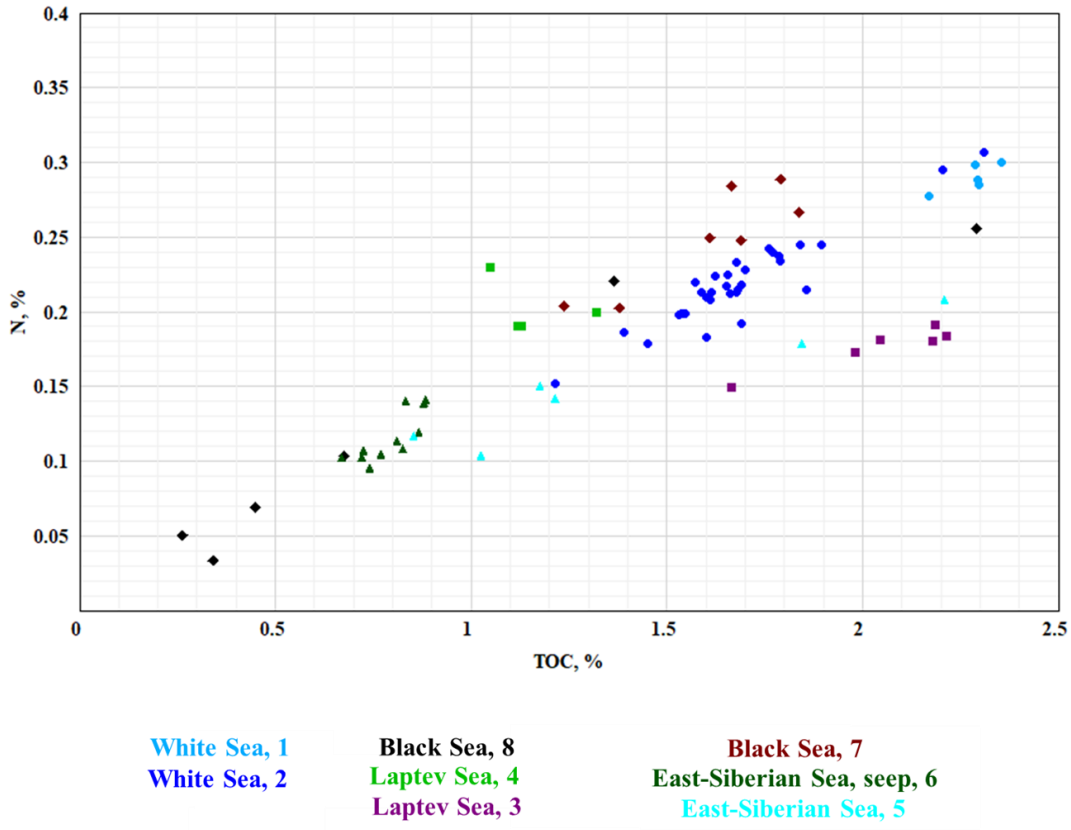

Figure 23. The correlation between organic carbon content and nitrogen content in the bottom sediments.

C/N ratio in organic matter is an important characteristic that makes it possible to distinguish the organic matter of terrestrial plants from marine ones. Algae have a C/N ratio of 4-10, while terrestrial plants have a C/N ratio of over 20 because of nitrogen-free cellulose. The organic matter of the studied samples corresponds to a mixture of marine and freshwater algae with a small admixture of organic matter from land plants. The most "marine" is the White Sea station 1 organic matter, but the station 2 sediments contain an admixture of organic matter from land plants. Compared to the White Sea, the Laptev Sea sediments contain more freshwater algae organic matter. The widest variations of the parameters under consideration are observed in the Black Sea sediments, organic matter from marine to freshwater, with a higher admixture of organic matter from terrestrial plants than in the Laptev and White Seas sediments.

The hydrogen content in the White Sea sediments varies from 0.29% to 1.19%, higher values are typical for station 1. The hydrogen content in the Laptev Sea sediments varies from 0.42% to 0.86%; higher values are typical for station 4. The hydrogen content varies from 0.16% to 0.51% in the East Siberian Sea sediments. The minimum hydrogen content values characterized these sediments in comparison with the other studied seas sediments. The maximum hydrogen content reaching 1.51% characterizes the Black Sea sediments.

The sulfur content is less than 1% in the White, East Siberian and Laptev Seas sediments. The sulfur content is higher (in some horizons reach 2%) in the Black Sea sediments than in the White, East Siberian and Laptev Seas sediments.

Low carbonate carbon content (0.05-0.1 %) characterizes the Laptev and White Seas sediments. The highest carbonates concentrations in the Black Sea sediments - from 1.04 to 4.09 %.

The carbon, hydrogen, nitrogen and sulfur concentrations comprehensive comparison analysis was carried out for all studied objects of marine sediments in this subtopic.

3.3.5 C, N, S Isotope Composition

The modern bottom sediments geochemistry studies make it possible to reconstruct changes in the recent geological reservoirs history, to develop geochemical tools for studying the conditions for the sediments formation, including oil source rocks, in the geological past. The light elements of carbon, nitrogen, oxygen and sulfur isotopic composition study is an important part of these studies. The bottom sediments samples isotopic compositions results are discussed in this section of the report which were taken without disturbing the stratigraphic sequence from the Laptev, White and Black Seas. Samples were taken from the board during expeditions of the last 5 years. Despite the limited number of samples and the geodistance, an attempt was made to generalize the obtained results and establish general patterns in the light elements' isotope ratios distribution, reflecting with the formation processes. Since the White and Black Seas sediments have been studied by numerous researchers, the obtained data analysis was carried out in comparison with the published results. The most detailed previous studies include the next works [Belyaev, 2015; Lein, 2004; Lisitsyn, Gursky, 2003; Rozanov, A.G.; Kokratskaya, N.M.; Gursky, 2017] and a number of other researchers.

Bulk isotope compositions of organic carbon, carbonate carbon, sulfur, and nitrogen in the bottom sediments were measured in selected samples from different depths (Table 24, Table 25 and Table 26).

Table 24. Station 1 of the White Sea. Results of isotopic composition measurements of bottom sediments.

Station	Depth, cm	$\delta^{15}N_{Air}$, ‰	$\delta^{13}C_{PDB}$ org., ‰	$\delta^{13}C_{PDB}$ carb.,‰	$\delta^{34}S_{CDT}$, ‰
1	42.5	5.8	−23.7	−9.1	−5.3
	110	6.1	−23.3	−5.7	−10.8
	181.5	6.7	−23.2	−4.2	−5.8
	247.5	5.0	−23.5	−4.1	−23.2
2	12.5	5.4	−24.5		−4.2
	52.5	6.1	−24.6		−34.2
	102.5	4.4	−23.7		−36.9
	137.5	5.0	−24.6		−34.9

Table 25. Station 4 of the Laptev Sea. Results of isotopic composition measurements of bottom sediments.

Station	Depth, cm	$\delta^{15}N_{Air}$, ‰	$\delta^{13}C_{PDB}$ org., ‰	$\delta^{13}C_{PDB}$ carb.,‰	$\delta^{18}O_{PDB}$ carb.,‰	$\delta^{34}S_{CDT}$, ‰	C/N
4	1.5	12.6	-25.2	-6.2	-8.9	17.5	6.54
	14	5.7	-25.6	-1.6	-4.4	16.9	5.79
	22	6.1	-24.8	-1.7	-5.6	17.5	5.86
	30	7.2	-25.0	-1.9	-6.2	16.0	4.53

Table 26. Station 7 and 8 of the Black Sea. Results of isotopic composition measurements of bottom sediments.

Station	Depth, cm	$\delta^{15}N_{Air}$, ‰	$\delta^{13}C_{PDB}$ org., ‰	$\delta^{13}C_{PDB}$ carb.,‰	$\delta^{18}O_{PDB}$ carb.,‰	$\delta^{34}S_{CDT}$, ‰
7	2.5	5.8	-25.6	2.0	0.8	-21.5
	52.5	4.8	-25.6	1.7	0.2	-21.1
	82.5	6.3	-23.7	0.8	0.0	6.6
	142.5	7.3	-25.9	0.9	0.1	3.8
	212.5	4.4	-25.7	1.4	0.1	-21.1
	242.5	4.2	-25.6	1.3	0.1	-19.1
	272.5	4.0	-26.0	0.6	-1.5	-6.1
	357.5	4.0	-24.3	0.2	-1.8	10.3
8	2.5	5.1	-25.4	1.9	0.9	-20.6
	41.5	3.9	-26.1	0.3	-1.2	-35.8
	64	6.2	-27.2	0.7	-3.2	-29.1
	84	5.4	-26.0	1.1	-1.3	-29.1
	119	4.2	-24.2	0.1	0.9	-23.1
	141	9.8	-27.2	-2.8	-5.3	31.2
	176	9.0	-27.2	-3.5	-5.4	23.6
	216	12.8	-27.6	-0.8	-3.7	5.2

The organic carbon isotopic composition shows a stable relationship with the organic carbon concentration, and lower contents correspond to lower values of $\delta^{13}C$, higher - to more positive

$\delta^{13}C$ values. The trend between $\delta^{13}C$ and TOC is more stable for the Black Sea sediments (Figure *24*).

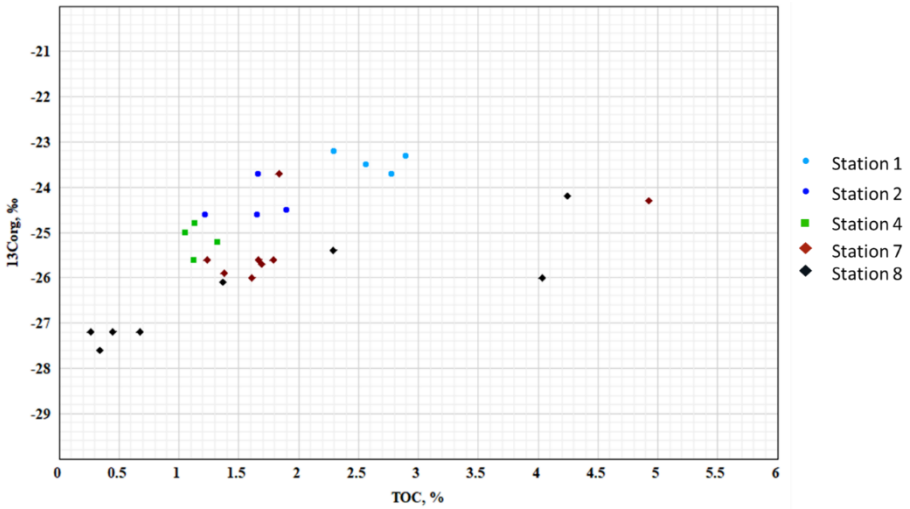

Figure 24. The correlation between isotopy organic carbon composition and organic matter concentration in the bottom sediments.

Based on the example of suspended organic matter and organic matter from the Kara Sea bottom sediments [Galimov et al., 2006], it was shown that a lighter isotopic composition is characteristic of continental origin organic matter brought into the Kara Sea water by the Ob and Yenisei rivers. The marine plankton is characterized a heavier organic carbon isotopic composition. The average isotopic composition of organic matter, which is a product of terrestrial photosynthesis $\delta^{13}C_{PDB}$ = –25‰. Aquatic plants absorb carbon directly from dissolved bicarbonate and carbonate. The carbon of bicarbonate and carbonate is noticeably heavier than atmospheric carbon CO_2. As a result, TOC in aquatic plants should theoretically be approximately 10‰ isotopically heavier than in terrestrial plants [Udovich, Ketris, 2010]. In the waters of the shelf and epeiric seas, a mixture of continental and marine organic matter occurs, obviously the observed distribution of $\delta^{13}C$ values in the studied sediments of the Laptev Sea, White and Black Seas is associated with this, while high contents of organic matter are associated with marine bio-productivity. Only allochthonous organic matter of continental origin accumulates in sediments with a low reservoir bio-productivity, as it is observed in the sediments of the Laptev Sea (station 4).

The isotopic composition of nitrogen shows significant variations with $\delta^{15}N$ values from + 3.9 to + 12.8 ‰. Samples with the lowest contents of nitrogen and organic matter are characterized

by high values of $\delta^{15}N$. The correlation between $\delta^{15}N$ and nitrogen content for northern seas sediments is less stable than for the Black Sea sediments (Figure *25*).

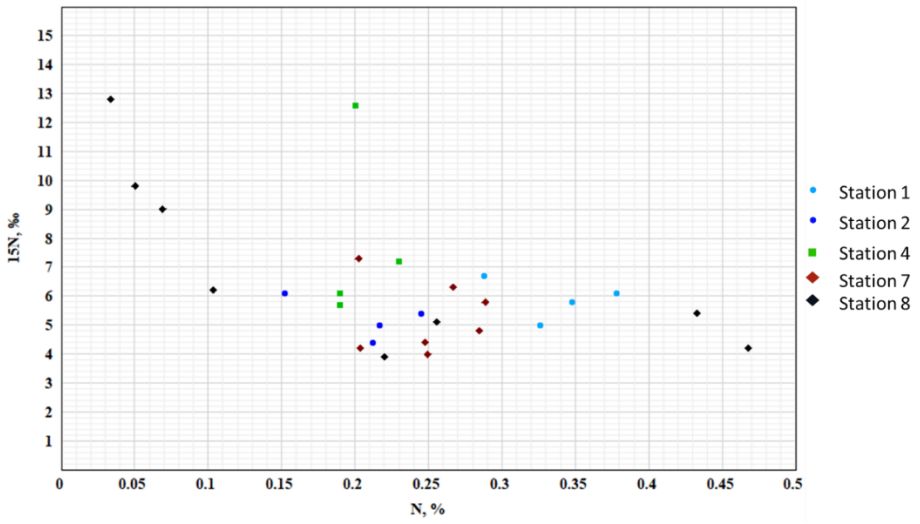

Figure 25. The correlation between isotopy nitrogen composition and nitrogen content in the bottom sediments.

The marine component of the organic matter of the bottom sediments differs from the freshwater component in a “lighter” isotopic composition of nitrogen and a “heavier” isotopic composition of carbon for the northern seas and the Black Sea based on the analysis of the carbon and nitrogen isotopic compositions (Figure *26*).

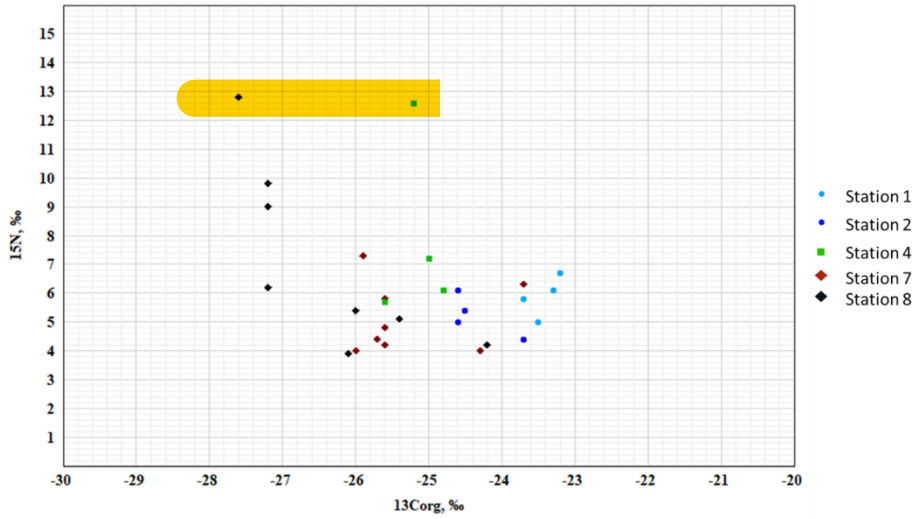

Figure 26. The correlation between $\delta^{15}N$ and $\delta^{13}Corg$ in the bottom sediments.

The sulfur isotopic composition varies widely, $\delta^{34}S$ values vary from -36,9 to +31,2 ‰. Variations in the sulfur isotope composition in sedimentary rocks are associated with varying degrees of marine sulfate bacterial reduction, which is associated with variations in redox

conditions at the stages of sedimentation and diagenesis. The total sulfur was analyzed in the studied sediments, which is significantly difficult for interpretation, because it is necessary to analyze separately reduced and oxidized sulfur for a correct redox conditions reconstruction. The high $\delta^{34}S$ values and low sulfur contents in the upper layers of the Laptev Sea sediments show an oxidizing environment of sedimentation. The analyzed sediments station 1 of the White Sea at sediment depths of 60 cm and below, sulfate reduction occurs at constant redox conditions. Sulfur content increasing together with the $\delta^{34}S$ decreasing with depth in the bottom sediments of station 2 show the development of reducing conditions. The upper part of the Black Sea bottom sediments is characterized negative $\delta^{34}S$ values. The bottom part of the Black Sea sediments is characterized positive $\delta^{34}S$ values with depth reflecting an increase in the sulfate reduction intensity from the initial stages – "light" values to a significant depletion of pore water sulfate at values higher than the values of the initial sulfate $\delta^{34}S$ +20 ‰. The cyclicity of changes in redox conditions is shown in the Black Sea sediments (station 7), since below 200 cm the $\delta^{34}S$ values are the same as for the upper part of the sediment: "lightening" and again "heavier" isotopic composition.According to the results of sulfur studies, the Black Sea sediments accumulated in a more reducing environment with more significant variations in redox conditions and the sulfate reduction intensity than the White and the Laptev Seas sediments.

The carbonate material isotopic composition of the northern water basins at low carbonate contents is characterized by low values of $\delta^{13}C$ = -9,1 to -1,6 ‰ and $\delta^{18}O$ = -8,9 to -4,4 ‰, which is unusual for marine carbonates, usually characterized by values close to 0 ‰. The isotope composition of carbonates in the Black Sea sediments (station 7) is typical for marine carbonates with values of $\delta^{13}C$ = 0,2 to 2,0 ‰ and $\delta^{18}O$ = -1,8 to 0,8 ‰. Four samples from the Black Sea sediments (station 8) show $\delta^{13}C$ and $\delta^{18}O$ values close to marine carbonates - $\delta^{13}C$ = 0,1 to 1,9 ‰ and $\delta^{18}O$ =-1,2 to 0,9 ‰, but four samples have relatively "light" isotopic composition - $\delta^{13}C$ = -3,5 to 0,7 ‰ and $\delta^{18}O$ = -5,4 to -3,2 ‰ which is closer to carbonates of the northern water basins sediments.

The results of the White, Laptev and Black Seas bottom sediments isotopic composition studies were analyzed. It has been established that variations in the carbon and nitrogen isotopic composition in the sediments of the studied Seas are associated with mixing in different proportions of continental and marine origin organic matter. The sediments are richer in organic carbon, where marine origin organic matter dominates. Variations in sulfur content and $\delta^{34}S$ values reflect differences in the bacterial sulfate reduction intensity, which depends on redox conditions. More oxidizing conditions are typical for the northern seas bottom sediments and more reducing conditions are typical for the Black Sea sediments. The increasing in $\delta^{34}S$ values with the depth in the Black Sea bottom sediments is observed, and this behavior is indicating the sulfate reduction intensity with the reducing conditions development. The carbon and oxygen isotope composition of carbonates indicates the presence of carbonates with low $\delta^{18}O$ and $\delta^{13}C$ values in addition to normal marine carbonates. These carbonates are allochtonous origin, brought in the suspension form of river runoff and dominate in the Laptev and White Sea bottom sediments and the individual Black Sea sediments layers.

3.4 Behaviour of Uranium in Bottom Sediments under Reducing Conditions in the Example of Black Sea

In contrast with the White Sea, the sedimentation process in the Black Sea is mostly carried out in typically reducing conditions due to high hydrogen sulfide content in the water below 90–160 m. The study of Black Sea sediments is an appropriate way to analyze sedimentation processes in oxygen-free conditions [Rozanov, A.G.; Kokratskaya, N.M.; Gursky, 2017]. Comparing the Arctic Seas and Black Sea cases provides an opportunity to analyze the difference between uranium accumulation in oxidizing and reducing conditions.

Following [Baturin, 1975], uranium concentration in the Black Sea's water varies from 0.0013 ppm to 0.0051 ppm, typical for seawater and close to the White Sea's water (0.0014–0.0018 ppm) for example.

The bottom sediments of the Black Sea are divided into modern, ancient Black Sea, and Novoeuxinian silt (Pleistocene) [Gursky, 2003]. Modern sediments are represented by microlaminated coccolith silt of white and grey color; the content of the hydrotroilite is 0.02–0.06%. According to [Baturin, 1975; Gursky, 2003; Gursky, 2019; Rozanov, A.G.; Kokratskaya, N.M.; Gursky, 2017], the organic substance content in modern sediments varies from 0.83% to 4.72% (Figure *27*), uranium concentration varies from 1.7 ppm to 20 ppm (Figure *28*), the average values of the U / TOC ratio vary from 1.89 to 3.62 ppmU /% TOC, and Eh values vary from −230 mV to +280 mV. The low values of the uranium concentration correspond to the shelf area and high values in deep-sea bottom sediments; additionally, the highest uranium concentration values correspond to the highest organic carbon content. Positive values of Eh = +280 mV are found on the shelf conditions only, whereas the other regions are characterized by negative values of Eh −80 to −230 mV.

Figure 27. TOC concentration in the modern sediments of the Black Sea (%). Modified after [Shnyukov, E.F.; Bezborodov, A.A.; Melnik, V.I.; Mitropolsky, 1979].

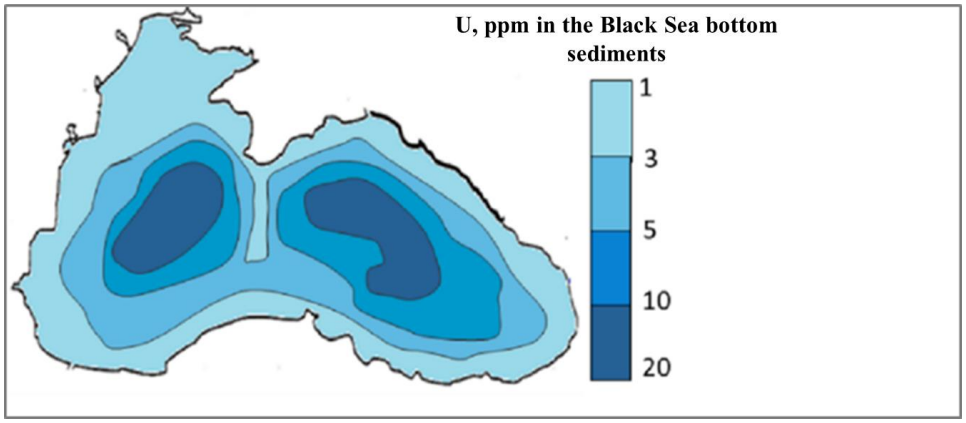

Figure 28. U concentration in the modern sediments of the Black Sea (ppm). Modified after [Shnyukov, E.F.; Bezborodov, A.A.; Melnik, V.I.; Mitropolsky, 1979].

Ancient Black Sea sediments (located under modern sediments) are represented by grey clayey silt and black sapropel silt, and the content of the hydrotroilite is 0.01–0.03%. Organic matter concentration is in the range of 0.22%–8.95%, uranium concentration is 1.1 ppm–35 ppm, the average values of the U/TOC ratio vary from 0.96 to 2.83 ppmU/% TOC, and Eh values vary from −220 mV to −80 mV.

Novoeuxinian sediments are represented by grey and black silt containing hydrotroilite and sulfides (the content of the hydrotroilite is 0.06%). The organic carbon content is 0.97%, uranium concentrations vary from 0.3 ppm to 4 ppm, the average value of the U/TOC ratio is 2.31 ppmU/% TOC, and the average value of Eh is -198 mV. The concentrations of Th in the Black Sea sediments reach 16.1 ppm, Th/U ratio varies from 1 to 4 [Neprochnov, 1980].

The summary of the uranium compounds and concentration of physicochemical characteristics in the water and bottom sediments developed in [Anderson, Fleisher, LeHuray, 1989; Barnes, Cochran, 1991; Baturin, 1975; Gursky, 2003; Gursky, 2019; Neprochnov, 1980; Rozanov, A.G.; Gursky, 2016; Rozanov, A.G.; Kokratskaya, N.M.; Gursky, 2017; Shnyukov, E.F.; Bezborodov, A.A.; Melnik, V.I.; Mitropolsky, 1979] is shown in Table *27*.

Table 27. The physicochemical characteristics (pH, Eh, and H_2S), compounds, and uranium concentration in the Black Sea water and bottom sediments. Modified after [Shnyukov, E.F.; Bezborodov, A.A.; Melnik, V.I.; Mitropolsky, 1979].

		Depth, m	pH	Eh, mV	H_2S, mg/l	Compounds and concentration of uranium
Seawater		0–200	7.85–7.95	−140...−160	0.08–0.83	$UO_2(CO_3)_2^{2-}$, $UO_2(CO_3)_3^{4-}$, $U_{concentration\ in\ seawater}$= 0.00093–0.00324 ppm

		200–1500	7.74–7.8	−176…−194	2.39–10.18	$[UO_2(CO_3)_3]^{4-}$, $U_{concentration\ in\ seawater}$ = 0.00095–0.00261 ppm
		1500–2000	7.64–7.73	−200…−203	10.40–11.66	$[UO_2(CO_3)_3]^{4-}$, $U(OH)_4$, UO_{2cr}, the concentration of uranium in water decreases $U_{concentration\ in\ seawater}$= 0.00029–0.00299 ppm
Sediments		Modern	6.4–8.5	−80...−230	0–121.24	$U(OH)_4$, UO_{2cr}, $U_{concentration}$ = 1.7–20 ppm
		Ancient	6.2–8.2	−80...−220	50–60	Maximum uranium concentration in sapropel, $U_{concentration}$ = 1.1–35 ppm
		Novoeuxinian	6.2–8.0	−198	0	Minimum uranium concentration, $U_{concentration}$ = 0.3–4 ppm

The distribution of the uranium (U), the thorium (Th), the ratio Th/U, the content of organic matter (TOC), and clay minerals in the bottom sediments of the Black Sea deep well at the depth are shown in *Table 28* and *Figure 29*. The obtained results of CHNS, and isotopic analysis of the Black Sea bottom sediments for stations 7 and 8 are given in Figure 30 and Figure 31.

Table 28. Uranium, thorium concentrations, organic carbon and clay minerals contens, as well as Th/U and U/TOC ratios for the Black Sea Deep Well [Neprochnov, 1980].

Depth, m	**U, ppm**	**Th, ppm**	**Th/U**	**Clay, %**	**TOC, %**	**U/TOC**
42.15	3.15	12.4	3.94	68.51	0.80	3.95
53.5	1.49	11.95	8.02	54.63		
62.75	1.88	12.21	6.49	64.13	0.40	4.68
84.2	1.85	11.7	6.32	59.76	0.56	3.29
94.25	3.16	12.58	3.98	63.10	0.17	18.75
114	2.15	11.13	5.18	46.28	0.30	7.11
123.5	1.51	7.49	4.96	46.85	0.33	4.61
150	1.82	7.97	4.38	45.25	0.35	5.21
171	1.49	5.35	3.59	17.42	0.37	4.02
178.57	2.24	11.22	5.01	53.89	0.79	2.84
202.9	3.12	11.53	3.70	75.73	1.84	1.69
224.76	3.47	11.97	3.45	77.57	1.00	3.47
240.5	2.81	9.08	3.23	75.29	1.50	1.88
257.34	2.51	9.77	3.89	51.62	1.13	2.22
278	2.73	7.46	2.73	41.08	2.13	1.28
285.81	2.77	3.93	1.42	45.13	1.65	1.68
313.5	1.74	12.22	7.02	61.36	1.17	1.49
315.6	5.27	6.67	1.27	61.36	1.23	4.30
326.7	3.99	13.24	3.32	50.96	5.80	0.69
339.48	3.43	10.24	2.99	38.37	1.64	2.09
438.55	3.71	12.96	3.49	73.12	0.72	5.18
446.7	3.53	16.1	4.56	70.97	1.16	3.04

473.73	2.9	14.93	5.15	72.05	0.48	6.00
476.65	2.98	12.6	4.23	80.28	0.45	6.56
488.75	3.47	11.76	3.39	69.81	1.32	2.64
499.55	2.39	9.22	3.86	71.08	1.54	1.55

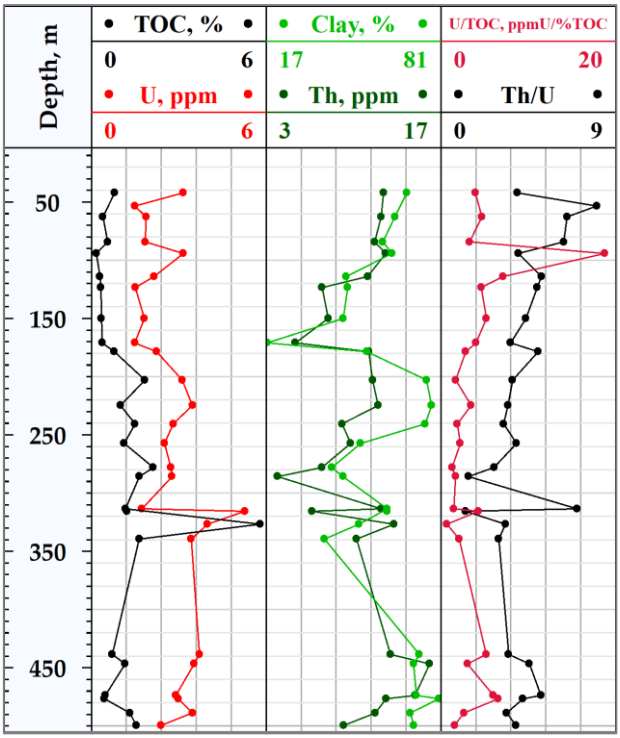

Figure 29. The Black Sea Deep Well. The distributions of the uranium concentration U (natural gamma-ray spectrometry), thorium concentration Th (natural gamma-ray spectrometry), the ratio Th/U, the content of organic matter, and the content of the clay minerals. It was modified after [Neprochnov, 1980].

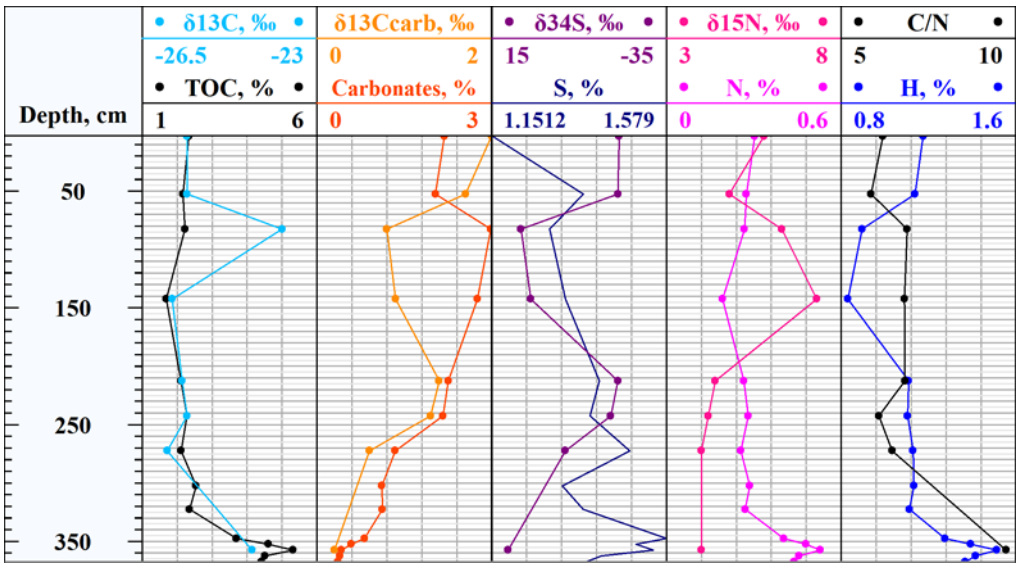

Figure 30. The bottom sediments of station 7. The distributions: H, N, S elements and TOC (analyzer CHN628); isotopy data: $\delta^{34}S$, $\delta^{13}C$, δ13Ccarb, $\delta^{15}N$; the ratio C/N.

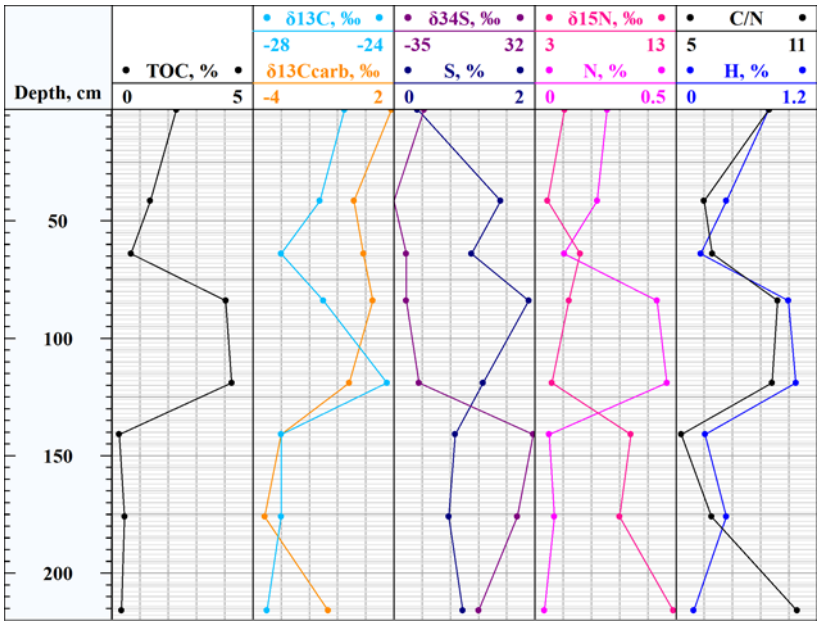

Figure 31. The bottom sediments of station 8. The distributions: H, N, S elements and TOC (analyzer CHN628); isotopy data: $\delta^{34}S$, $\delta^{13}C$, and δ^{13}Ccarb, $\delta^{15}N$; the ratio C/N.

The uranium concentration in the bottom sediments for the Deep Well varies from 1 to 6 ppm, the thorium concentration varies from 3.93 to 16.1 ppm, the content of organic matter varies from 0.1 to 6.47 %, and the ratio Th/U varies from 1.27 to 8.02.

Station 7 of the Black Sea is characterized by:

- The organic carbon content is stable up to a depth of 350 cm reaching 2%, below 350 cm - the organic carbon content reaches values above 5%. The carbonates content decreases with depth.
- The nitrogen, hydrogen content distribution is like the organic carbon distribution in depth.
- The upper part of the Black Sea bottom sediments is characterized by negative values of $\delta^{34}S$. Sediments are characterized by positive $\delta^{34}S$ values at depths from 80 to 140 cm. There is a cyclical change in redox conditions in the Black Sea sediments.

Station 8 of the Black Sea is characterized by:

- The organic carbon content reaches its maximum values (TOC=4%) at depths from 80 to 140 cm. The organic carbon content in the upper part decreases with

depth. The organic carbon content does not reach 1% at lower depths (140-220 cm).

- The nitrogen, hydrogen content distribution is like the organic carbon distribution in depth.
- The upper part of the Black Sea bottom sediments is characterized by negative values of $\delta^{34}S$. Sediments are characterized by positive $\delta^{34}S$ values at depths from 140 to 220 cm.

The following trends are visible: the organic carbom distribution has similar behavior with the uranium concentration distribution, and the distribution of thorium changes following the content of clay minerals (Figure *29*), because thorium is insoluble in water, and concentrates on clay minerals. The average value of the ratio Th/U = 4.21, which corresponds to the stage of marine sedimentation, according to the Fertl research [Fertl, Rieke, 1980].

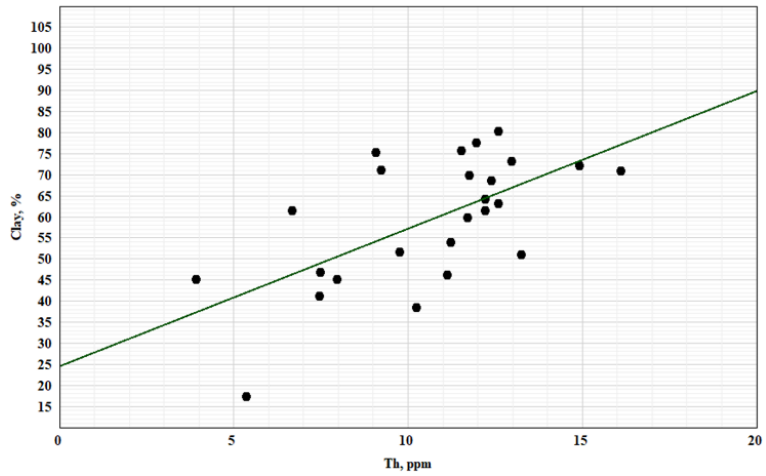

Figure 32. The correlation between the content of clay minerals and thorium concentration for bottom sediments of the Black Sea deep well. Green line corresponds to the equation Clay = 3.26*Th+ 24.52, where the R = 0.61. Modified after [Neprochnov, 1980].

Thus, in the case of Black Sea sediments, the upper oxidized layer is absent, hydrogen sulfide is present not only in sediments but also in the water; only negative Eh values characterize bottom sediment–water. Organic carbon concentration is comparable with the Arctic Seas; the uranium concentrations are much higher and achieve values up to 35 ppm. The next chapter considers the possible reasons for uranium behavior in oxidizing and reducing conditions using thermodynamic modeling methods.

3.5 Discussion

3.5.1 The results comprehensive analysis of the bottom sediments studies

In this section 3.5, we will analyze the results of the Arctic and the Black Seas marine sediments study, as shown in the previous sections.

The obtained results of ICP-MS, CHNS, and isotopic analysis of the bottom sediments for stations are given in Figure *33*, Figure *34*, Figure *35*, Figure *36*, Figure *37*, Figure *38*, Figure 30, Figure 31.

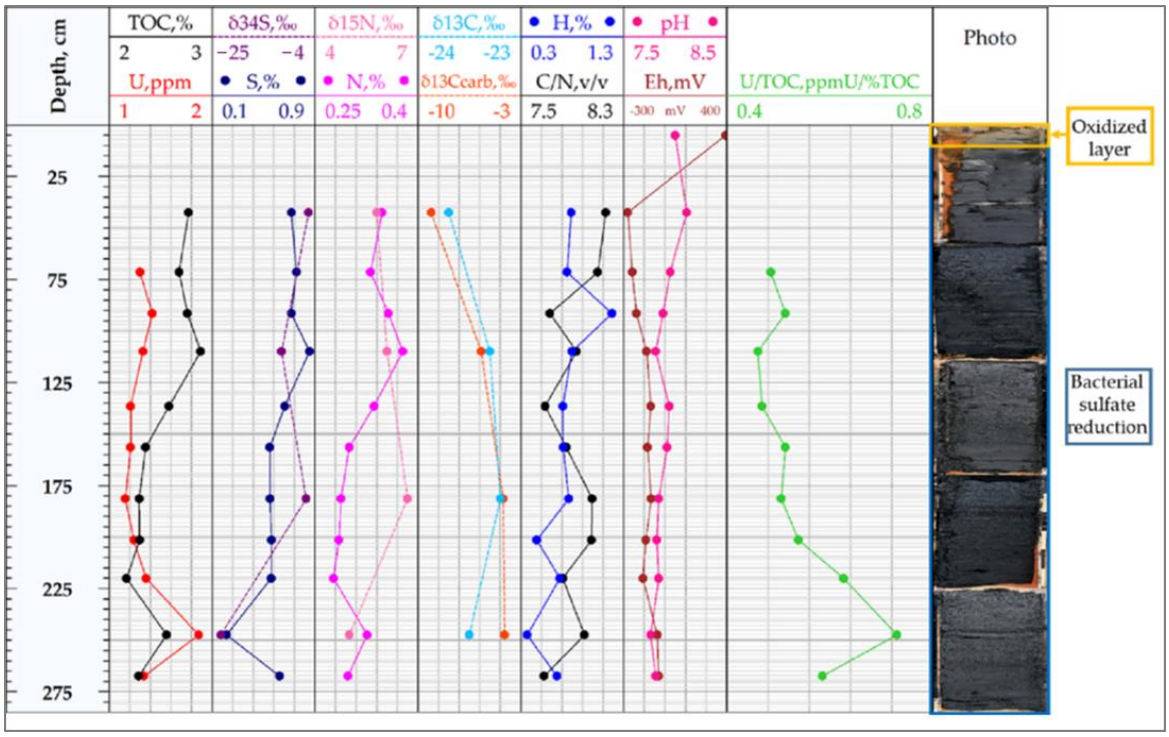

Figure 33. The bottom sediments of station 1. The distributions: H, N, S elements, and TOC (analyzer CHN628); uranium concentration U (ICP-MS); isotopy data: $\delta^{34}S$, $\delta^{13}C$, $\delta^{13}C_{carb}$, $\delta^{15}N$; the ratios C/N, U/TOC, also pH and Eh.

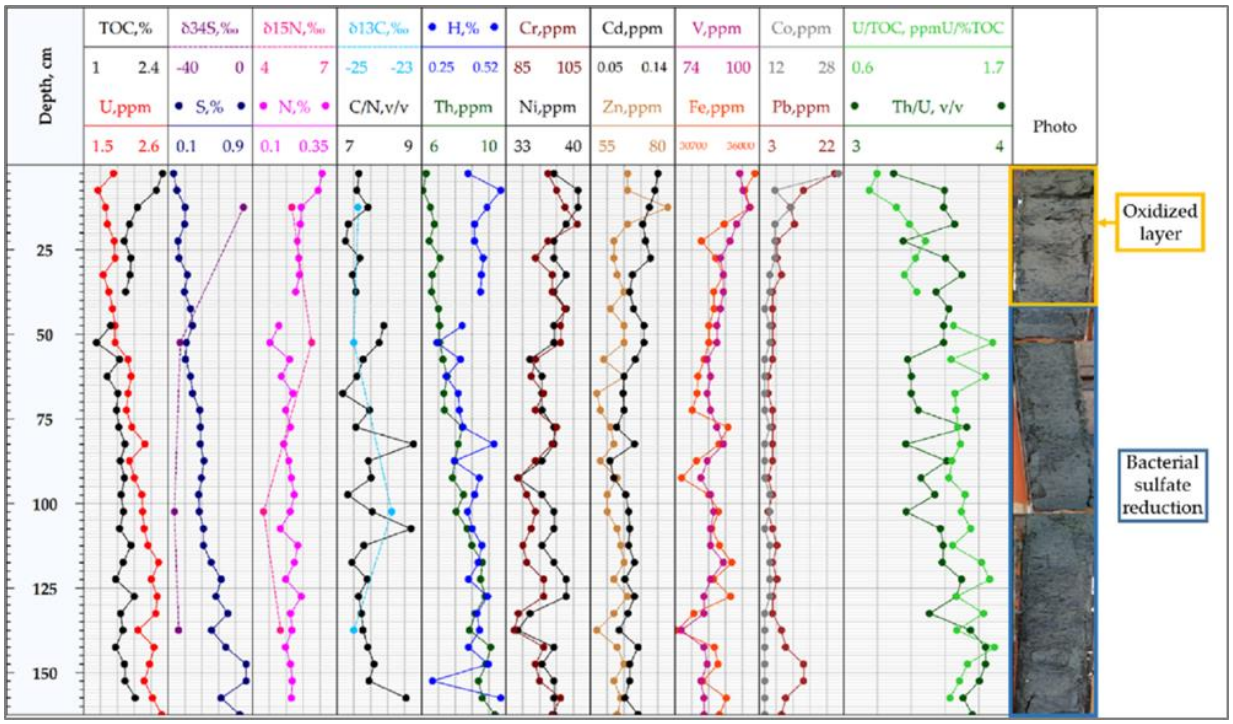

Figure 34. The bottom sediments of station 2. The distributions: H, N, S elements and TOC (analyzer CHN628); U, Th, Cr, Ni, Cd, Zn, V, Fe, Co, Pb concentrations (ICP-MS); isotopy data: $\delta^{34}S$, $\delta^{13}C$, $\delta^{15}N$; the ratios C/N, U/TOC, and Th/U.

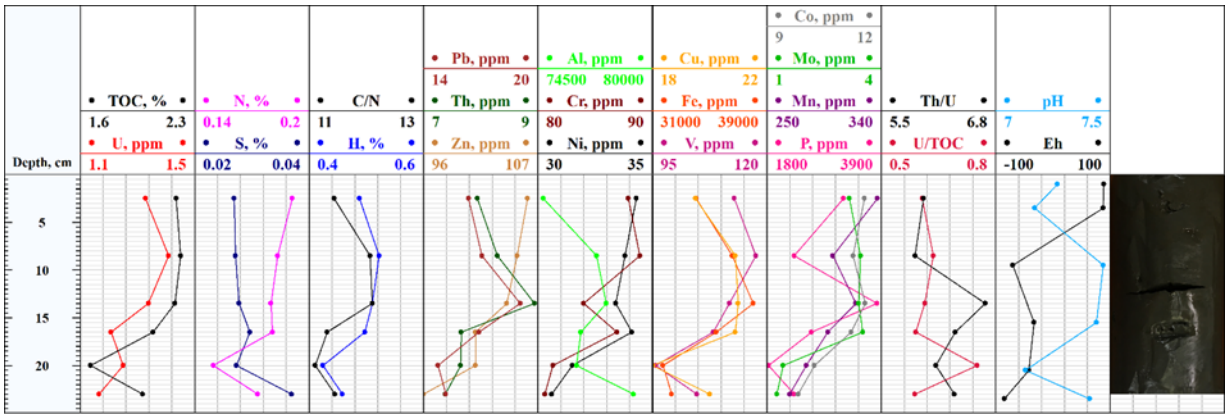

Figure 35. The bottom sediments of station 3. The distributions: H, N, S elements and TOC (analyzer CHN628); U, Pb, Th, Zn, Al, Cr, Ni, Cu, Fe, V, Co, Mo, Mn, P concentrations (ICP-MS); the ratio C/N, U/TOC, and Th/U; also pH and Eh.

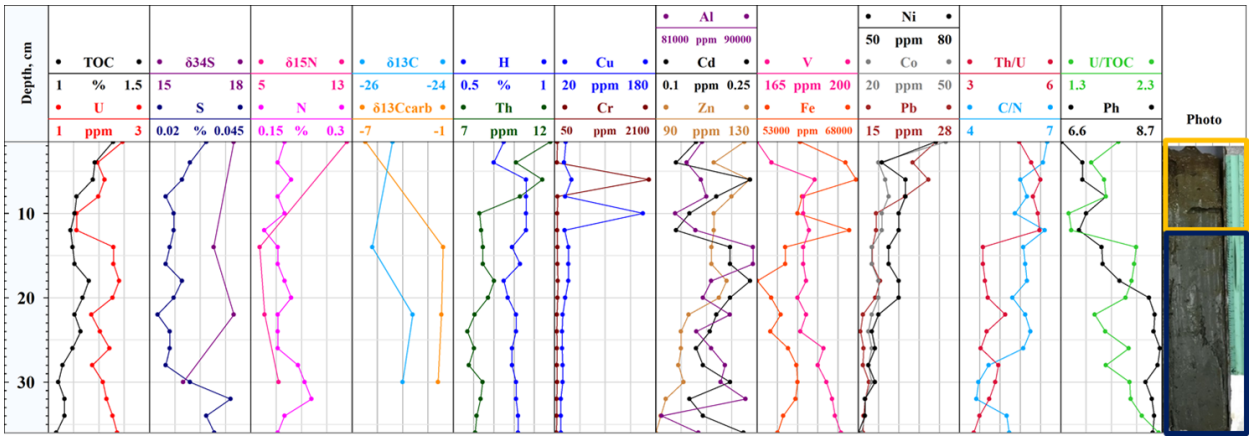

Figure 36. The bottom sediments of station 4. The distributions: H, N, S elements and TOC (analyzer CHN628); U, Th, Cu, Cr, Al, Cd, Zn, V, Fe, Ni, Co, Pb concentrations (ICP-MS); isotopy data: $\delta^{34}S$, $\delta^{13}C$, and $\delta^{13}C_{carb}$, $\delta^{15}N$; the ratios C/N, U/TOC, and Th/U; also pH.

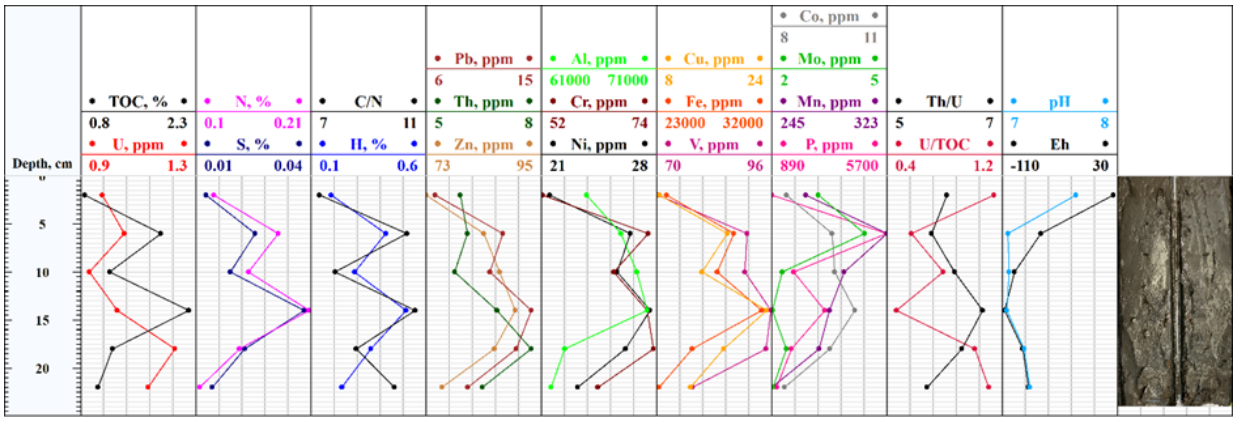

Figure 37. The bottom sediments of station 5. The distributions: H, N, S elements and TOC (analyzer CHN628); U, Pb, Th, Zn, Al, Cr, Ni, Cu, Fe, V, Co, Mo, Mn, P concentrations (ICP-MS); the ratios C/N, U/TOC, and Th/U; also pH and Eh.

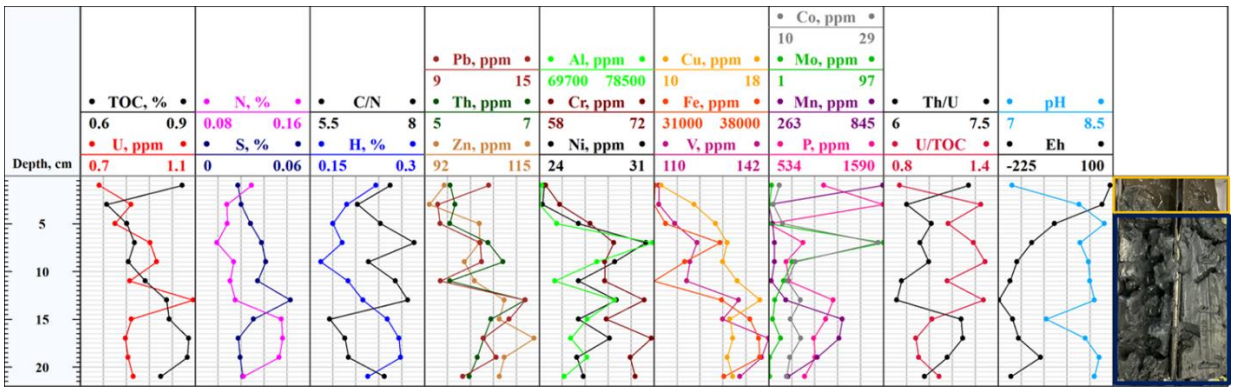

Figure 38. The bottom sediments of station 6. The distributions: H, N, S elements and TOC (analyzer CHN628); U, Pb, Th, Zn, Al, Cr, Ni, Cu, Fe, V, Co, Mo, Mn, P concentrations (ICP-MS); the ratio C/N; also pH and Eh.

The Arctic Seas bottom sediment study provided an opportunity to analyze uranium accumulation in the bottom sediments as a part of marine sedimentation processes in oxidizing conditions. Additionally, the sediments had a high involvement of organic and inorganic matter from continental run-off. The Arctic Seas bottom sediment study results show that the upper part of sediments, which is in contact with the seawater, is characterized by an oxidizing environment with positive Eh values. This layer is visually distinguished by a brown-gray color with traces of bioturbation and is characterized by the highest organic carbon values (up to 2.5%) and the correspondently highest concentration of nitrogen and hydrogen-containing inorganic matter.

On the example of the White Sea, the upper part of the sediments is characterized:

- the sulfur concentration in the upper interval is varied from 0.15% to 0.3%, which was several times less than for the deeper layers;
- the measured value of sulfur isotope composition $\delta^{34}S = -4.2‰$ confirms the marine genesis of sulfur due to sulfate reduction in oxidizing conditions;
- the uranium concentration in the upper oxidized layer was lowest for the bottom sediment column and did not exceed 1.5 ppm;
- the genesis of uranium in the bottom sediments is close to uranium concentration in the continental run-off; however, we suggest that some uranium parts can also come with organic matter (the U/TOC ratio for the upper layer varied from 0.8 to 1.1 ppmU/%TOC).

The bottom sediments were characterized by reduced conditions, with negative Eh values. This layer was denser and visually distinguished by a dark color due to increased hydrotroilite content. Hydrotroilite has been identified in the current study in black dots and patches against the greenish-grey background of sediments and described more in detail in [Rozanov, Volkov, Emelyanov, 2012]. The identified decrease of organic matter content could be explained by the activity of anaerobic microorganisms, which is confirmed by the results of [Belyaev, 2015; Demaison, Moore, 1980] that show that the oxic environment is characterized by lower organic matter preservation due to microbial activity.

On the example of the White Sea, the lower part of the sediments is characterized:

- sulfur concentration increased with depth by up to 0.8%;
- the isotope compositions of sulfur for lower layers of station 1 varied from −23.2‰ to −5.3‰ and from −36.9‰ to −34.2‰ for station 2; the observed values show that hydrotroilite and other sulfur-containing minerals in the sediments at station 2 were formed in typically reduced conditions, whereas for station 1 these minerals were formed in more oxidizing conditions;
- the U/TOC ratio increased with depth, reaching a value of 1.4 ppmU/%TOC;
- one reason that could explain an increase in uranium concentration is the reducing conditions that facilitate uranium accumulation in sediments due to the formation of insoluble uranium-containing compounds.

The trends discussed above are illustrated in (Figure *39*) in the U-TOC diagram. Ellipses select two areas corresponding to different redox conditions.

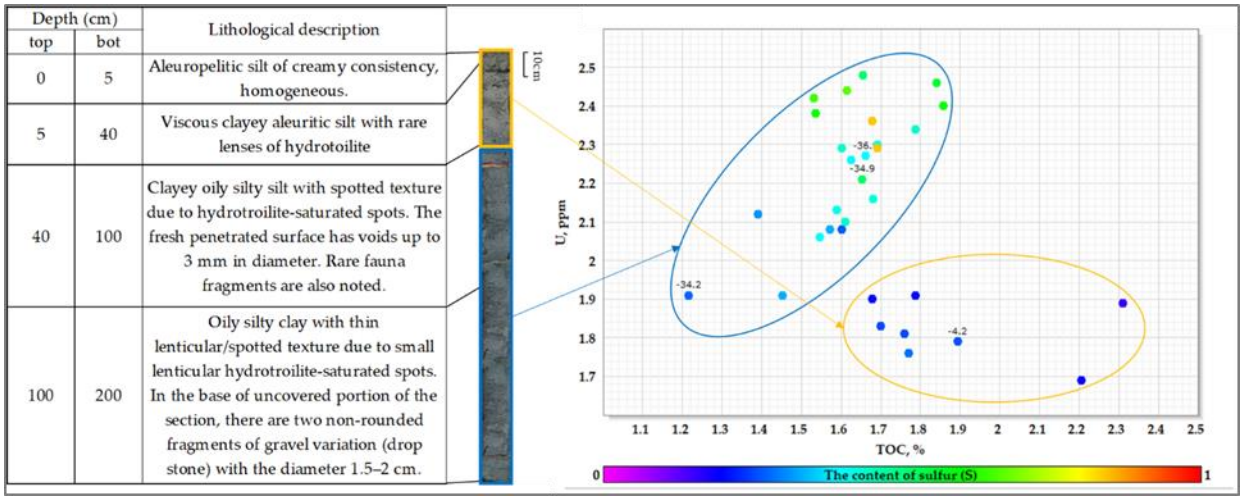

Figure 39. Correlation between the uranium concentration and organic matter content in the bottom sediments of the White Sea for station 2. Above the points, the sulfur isotopic composition ($\delta^{34}S$) is indicated. Dot color change is due to sulfur content (S).

Also, the U-TOC diagram is illustrated in Figure *40*, where we can see all studied Arctic stations.

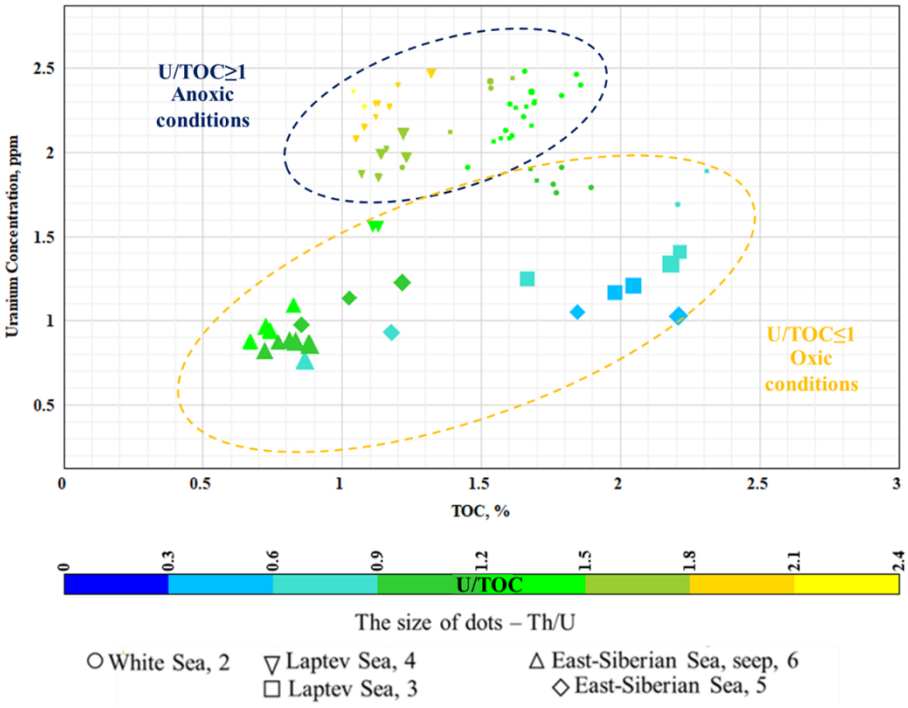

Figure 40. Correlation between the uranium concentration and organic matter content in the bottom sediments. The size of dots is the Th/U ratio value. Dot color change is due to the U/TOC ratio. The form of dots is the station.

The stations near the coast are characterized by lower uranium concentration and the ratio U/TOC, higher organic matter concentrations, and the highest Th/U ratio than the stations located further from the coast. For example, station 3 of the Laptev Sea and station 5 of the East-Siberian Sea, characterized by more oxidized conditions (absence of hydrotroilite balls and brown color of sediments), are also near cost. These stations have maximum values of Th/U ratio and minimal U/TOC values. It can be explained that active environments near the coast bring more organic matter from the land; also, these active conditions influence the uranium sorption process.

The sediments' dots, which have an upper oxic layer, are divided into two parts on the diagram U-TOC (Figure *40*). For example, station 4 of the Laptev Sea: the upper oxic layer has minimal values of the U/TOC ratio, and the other part of the sediments with anoxic conditions has a maximum U/TOC ratio. So the dots of the station are divided into two parts, like the station 2 sediments (Figure *39*).

To sum up, the sedimentation process in the Arctic Seas is carried out in oxidizing conditions (oxygen in the bottom layer of water) and does not lead to considerable uranium

accumulation in bottom sediments. Typical values of about 1.5 ppm correspond to uranium content in the continental run-off. Increased uranium concentration up to 2.5 ppm was identified for the lower part of the bottom sediments, which could be explained by changing redox conditions from oxidizing to reducing. The U/TOC ratio values were about 0.25 to 1.1 ppmU/%TOC for the upper part of the sediments and reached 2.3 ppmU/%TOC for the lower part. Also, the Th/U ratio shows that most of the uranium source was a continental run-off for stations near cost, stations located further cost with not so active hydrodynamics characterize more uranium concentration and reducing conditions influence on uranium accumulation process.

3.5.2 Behavior of Uranium in the Aqueous Solution at Different Eh and pH Conditions: Results of Thermodynamic Modeling

In order to simulate the distribution of the uranium between bottom sediments and pore waters, and predict uranium speciation as a function of redox and pH, we calculated equilibrium phase compositions in the system «seawater–bottom sediment». Calculations were completed for multiple pairs of Eh and pH measured in the bottom sediments of the White and Black Seas. To constrain the redox conditions, the chemical system was considered open with respect to the oxygen pressure, measured pH values, and atmospheric pressure of carbon dioxide. Values of partial pressures of oxygen were calculated from the measured values of Eh and pH [Garrels, Christe, 1965]. Calculations were completed using the Geocheq software, including the thermodynamic database [Mironenko, Akinfiev, Melikhova, 2000; Wignall, Myers, 1988] by the free energy minimization technique.

The chemical equilibria were calculated for a simplified 7-component (U, C, H, Na, Cl, O, S) system for the temperature of 273.15K, which approximates to bottom sediment conditions. Fifteen possible minerals (U_2S_3(cr), U_3O_7(beta), U_4O_9(beta), UO_2(am), UO_2(cr), $UO_{2,25}$(cr), $UO_{2.6667}$(cr), UO_2CO_3(cr), UO_2SO_4(cr), γUO_3(cr), $UO_3 \cdot 2H_2O$(cr), US(cr), $US_{1.90}$(cr), US_2(cr), α-$UO_{2.3333}$), 46 aqueous species (H_2O,aq, H_2,aq, UO_3,aq, $UO_4^{2-}UOH^{2+}$, $UO_2(CO_3)_2^{2-}$, H_2S,aq, Cl, CO,aq, CO_2,aq, CO_3^{2-}, NaCl,aq, UO_2OH^+, $(UO_2)_2OH^{3+}$, HCO^{3-}, HS^-, HSO^{3-}, HSO^{4-}, HUO_2,aq, HUO^{2+}, HUO^{3-}, HUO^{4-}, H^+, UO^+, UOH^{3+}, NaOH,aq, $NaSO^{4-}$, O_2,aq, OH^-, SO_2,aq, SO_3^{2-}, SO_4^2, UO^{3-}, U^{4+}, UO_2SO_4(aq), UO^{2+}, Na^+, $UO_2(CO_3)_3^{4-}$, $UO_2(OH)_4^{2-}$, UO_2,aq, UO^{2+}, UO_2^{2+}, UO_2CO_3(aq), UO_2OH,aq, $UO_2(OH)^{3-}$, U^{3+}), and 6 gaseous species (CO, CO_2, H_2, H_2O, O_2, SO_2) were taken into account. Processes of uranium sorption on organic matter were not considered in the model. The system was modeled for different values of Eh (from 273 mV to

392 mV), pH (from 7.68 to 8.11), partial pressure of oxygen from 4.28×10^{-79} to 7.45×10^{-65} bar and the initial uranium concentration in pore water of 1×10^{-5} mol/l in our calculation. The calculated uranium speciation and the distribution of uranium between the aqueous phases and solid uranium phases (minerals) along the bottom sediment column are shown in Table *29*, Table *30*, and Figure *41*, Figure *42*.

Table 29. The calculated uranium concentration in the pore water and the solid phase of the White Sea bottom sediments for station 1.

Depth, cm	**pH**	**Eh, mV**	**pO_2**	**The Calculated Concentration of Uranium in Pore Water, mol/L**	**The Proportion of the Total Uranium Contained by Pore Water, %**	**The Calculated Concentration of Uranium in the Solid Phase UO_2 (cr), mol/L**	**The Proportion of the Total Uranium Contained by the Solid Phase, %**	**The Total Amount of Uranium, mol/L**
5	8	392	1.23×10^{-30}	1.00×10^{-5}	$1.00\times 10^{+2}$	0	0	1.00×10^{-5}
42.5	8.11	−273	4.28×10^{-79}	3.99×10^{-10}	3.99×10^{-3}	1.00×10^{-5}	1.00×10^{2}	1.00×10^{-5}
71.5	7.95	−243	1.57×10^{-77}	3.99×10^{-10}	3.99×10^{-3}	1.00×10^{-5}	1.00×10^{2}	1.00×10^{-5}
91.5	7.88	−215	9.46×10^{-76}	3.97×10^{-10}	3.97×10^{-3}	1.00×10^{-5}	1.00×10^{2}	1.00×10^{-5}
110	7.81	−145	6.97×10^{-71}	3.97×10^{-10}	3.97×10^{-3}	1.00×10^{-5}	1.00×10^{2}	1.00×10^{-5}
136.5	7.94	−117	2.64×10^{-68}	3.97×10^{-10}	3.97×10^{-3}	1.00×10^{-5}	1.00×10^{2}	1.00×10^{-5}
156.5	7.92	−138	6.28×10^{-70}	3.97×10^{-10}	3.97×10^{-3}	1.00×10^{-5}	1.00×10^{2}	1.00×10^{-5}
181.5	7.84	−115	1.48×10^{-68}	3.97×10^{-10}	3.97×10^{-3}	1.00×10^{-5}	1.00×10^{2}	1.00×10^{-5}
201.5	7.82	−150	3.28×10^{-71}	3.97×10^{-10}	3.97×10^{-3}	1.00×10^{-5}	1.00×10^{2}	1.00×10^{-5}
220	7.84	−170	1.33×10^{-72}	3.97×10^{-10}	3.97×10^{-3}	1.00×10^{-5}	1.00×10^{2}	1.00×10^{-5}
247.5	7.76	−73	8.65×10^{-66}	3.97×10^{-10}	3.97×10^{-3}	1.00×10^{-5}	1.00×10^{2}	1.00×10^{-5}
267.5	7.81	−63	7.45×10^{-65}	3.98×10^{-10}	3.98×10^{-3}	1.00×10^{-5}	1.00×10^{2}	1.00×10^{-5}

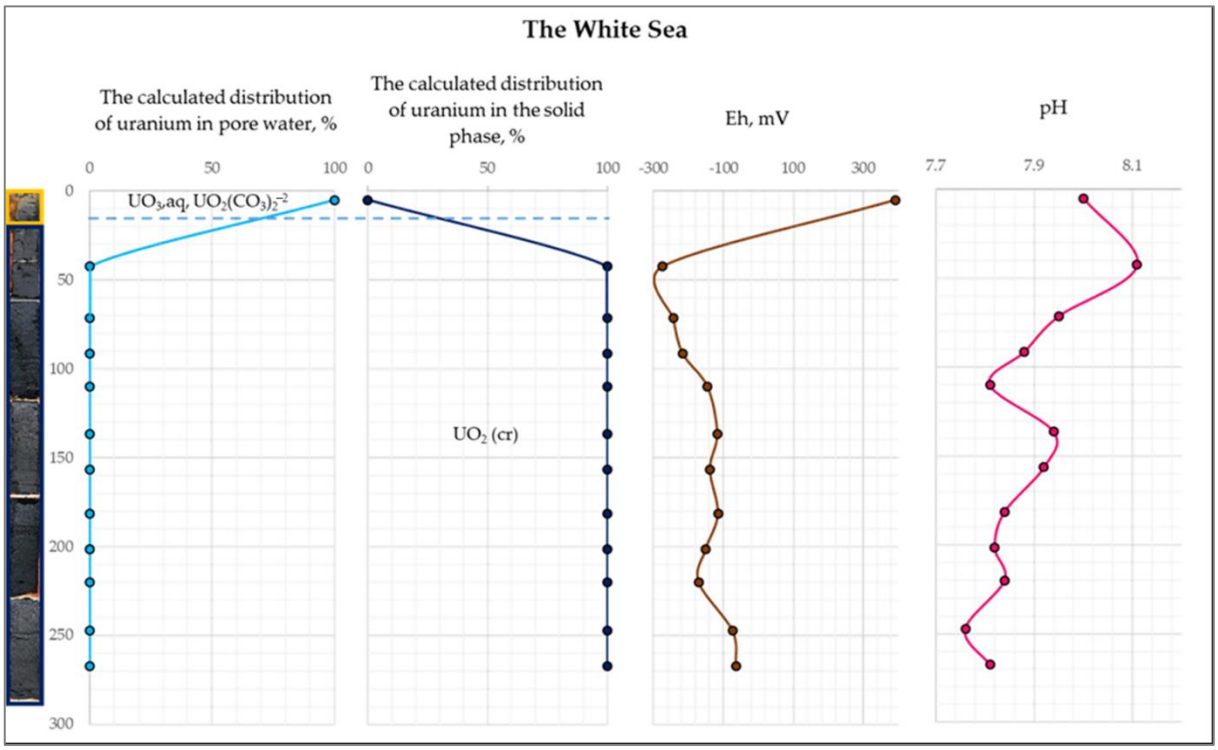

Figure 41. The distribution of the calculated uranium concentration in the pore water and the solid phase of the White Sea bottom sediments for station 1.

It is to be noted that we did not obtain solid uranium oxides of intermediate (between VI and IV) uranium oxidation state. The only stable uranium mineral was uraninite UO_2(cr).

Table 30. The calculated uranium concentration in the pore water and the solid phase of the Black Sea bottom sediments (the Eh and pH data distribution from [Gursky, 2003].

Depth, cm	**pH**	**Eh, mV**	**pO_2**	**The Calculated Concentration of Uranium in Pore Water, mol/L**	**The Proportion of Uranium in the Pore Water, %**	**The Calculated Concentration of Uranium in the Solid Phase UO_2 (cr), mol/L**	**The Proportion of Uranium in the Solid Phase, %**	**The Total Amount of Uranium, mol/L**
15	7.68	−185	2.41×10^{-74}	3.97×10^{-10}	3.97×10^{-3}	1.00×10^{-5}	1.00×10^{2}	1.00×10^{-5}
70	7.68	−200	1.90×10^{-75}	3.97×10^{-10}	3.97×10^{-3}	1.00×10^{-5}	1.00×10^{2}	1.00×10^{-5}
105	7.68	−205	8.15×10^{-76}	3.97×10^{-10}	3.97×10^{-3}	1.00×10^{-5}	1.00×10^{2}	1.00×10^{-5}
140	7.68	−210	3.50×10^{-76}	3.97×10^{-10}	3.97×10^{-3}	1.00×10^{-5}	1.00×10^{2}	1.00×10^{-5}
185	7.74	−195	7.70×10^{-75}	3.97×10^{-10}	3.97×10^{-3}	1.00×10^{-5}	1.00×10^{2}	1.00×10^{-5}

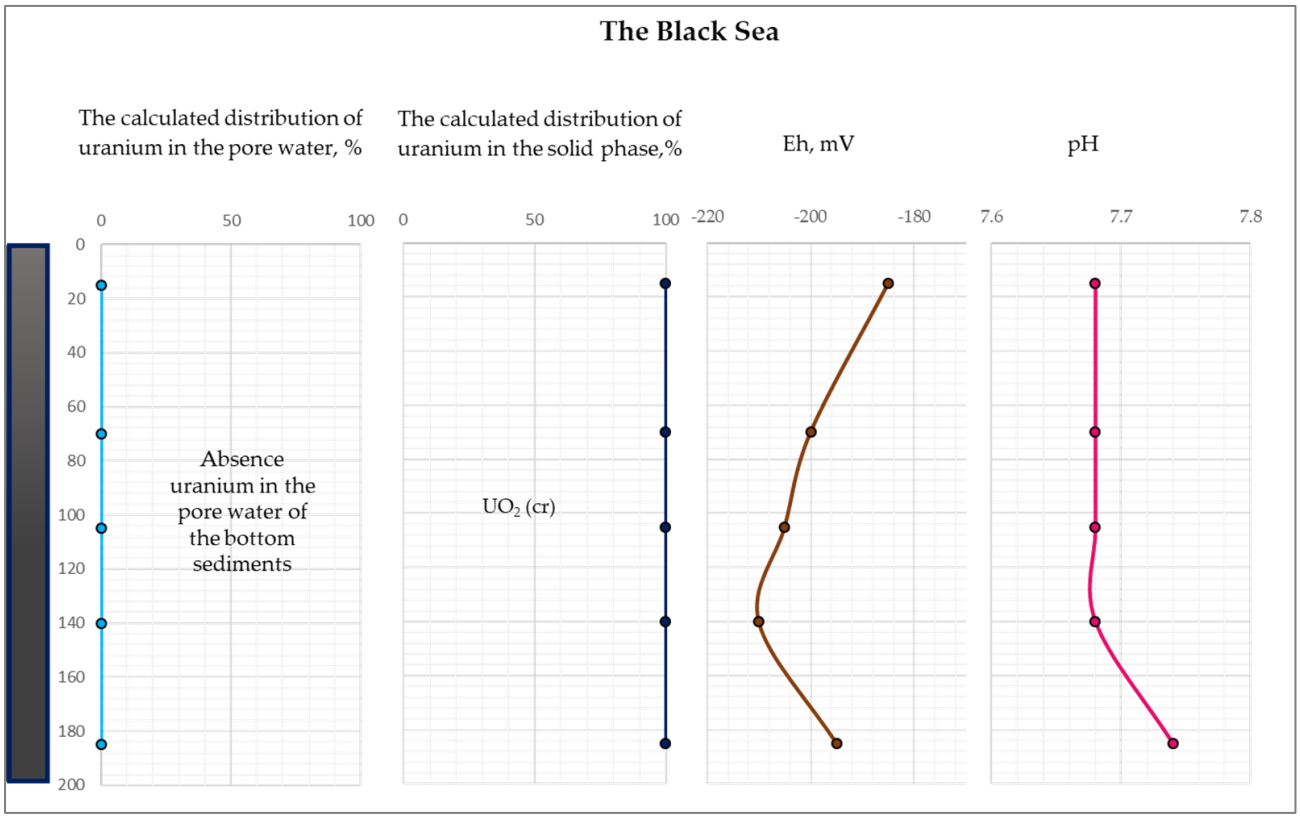

Figure 42. The distribution of the calculated uranium concentration in the pore water and the solid phase of the Black Sea bottom sediments (the Eh and pH data distribution from [Gursky, 2003].

As follows from Figure *41*, at the oxidizing conditions (upper part of the bottom sediments) of the White Sea, uranium is completely retained in the aqueous phase as U^{+6} aqueous species (the dominant species are UO_3, aq and $UO_2(CO_3)_2^{-2}$) and does not have the potential to

accumulate in the sediments. In contrast, within the rest of the sediment column (reducing conditions), uranium precipitates as uraninite (UO_2cr). At the reducing conditions of the Black Sea, most of the uranium is predicted to occur as U^{+4} in the form of uraninite (Figure *42*). These results explain the different accumulations of uranium in the White Sea and the Black Sea bottom sediments. The obtained results are also consistent with [Bone and et.al., 2017], which shows that the amount of uranium absorbed by organic matter is much higher under reducing conditions compared to oxidizing conditions.

3.5.3 Comparison of Uranium Accumulation in Oxidizing and Reducing Conditions

Obtained experimental data and thermodynamic modeling results explain the difference in uranium accumulation in bottom sediments in oxic and anoxic environments in the examples of the Arctic Seas and the Black Sea (Figure *43*).

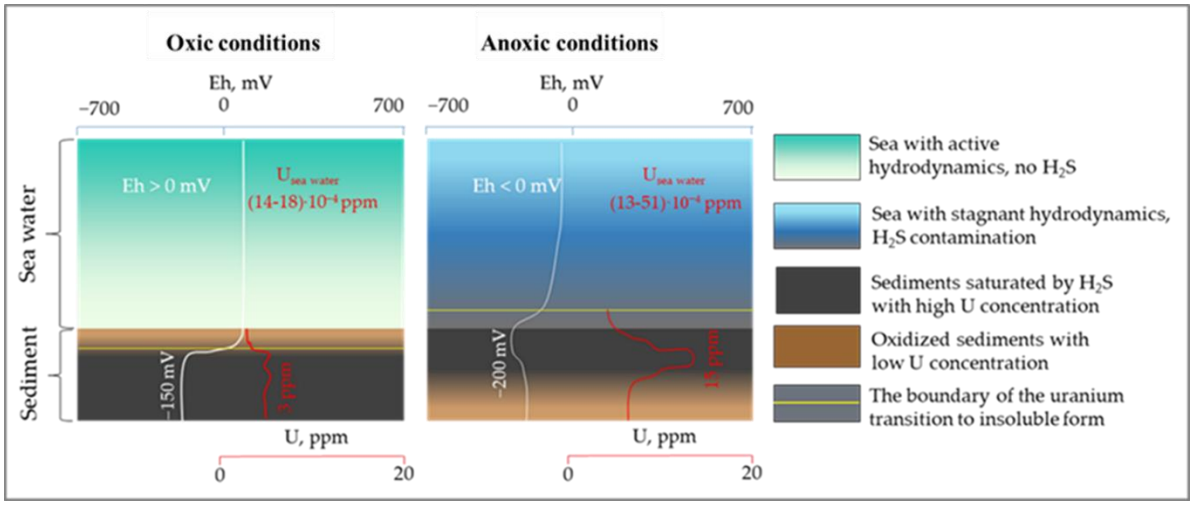

Figure 43. The behavior of uranium in the different redox conditions in the water sea and the bottom sediments (the Arctic Sea (**left**) and the Black Sea (**right**)).

In oxidizing conditions, the seawater contains uranium (VI) in soluble forms; typical concentrations vary in the range of 0.002–0.003 ppm. In such conditions, part of the uranium is accumulated in marine organisms and absorbed in the organic matter of sediments; however, the total content of uranium in oxidizing layers of sediments does not exceed 1–1.5 ppm, including uranium contained in the inorganic matter of continental run-off and uranium accumulated in organic matter. The content of uranium in deeper layers of sediments may be slightly (up to 2.5–3 ppm) higher than in upper oxidizing layers due to the change of redox conditions from oxidizing to reducing, which results in the fixation of uranium contained in sludge water in organic and inorganic particles of the bottom sediments. This uranium behavior

has been observed in the Arctic Seas and is typical for water reservoirs characterizing oxygen in the bottom layer.

In the case of reducing conditions in the bottom layer, if thermodynamic equilibria are reached, most of the uranium in the water–bottom sediment system is accumulated in the forms of insoluble compounds in the solid phase. A considerable part of uranium could also be absorbed by organic matter, e.g., following [Bone and et. al., 2017], uranium sorption is increased in reducing conditions. In this case, the concentrations of uranium in bottom sediments could be at least one order of magnitude higher, depending on sedimentation conditions, including the concentration of uranium in water, redox conditions, sedimentation rate, the content of organic matter, and other factors. This behavior has been found in the Black Sea and is typical for reducing conditions in a water reservoir's bottom layer. Following the study results, we propose that considerable variations of uranium content in marine source rocks could be explained by the variations in redox conditions at the sedimentation stage; however, other factors affecting uranium accumulation could also be taken into account.

3.5.4 Summary

The lithological and geochemical study of the bottom sediments at eight stations of Arctic Seas and the Black Sea was performed. The uranium concentrations distribution and contents, and compositions of organic and inorganic components, along with the bottom sediment columns were studied. This study showed that, in the Arctic Seas oxidizing conditions, the concentration of uranium in the bottom sediments varies from 1 to 1.5 ppm in the upper oxidizing part of the sediments and slightly increases up to 2.5 ppm in deeper layers characterized by reducing conditions. The U/TOC ratio varies from 0.8 ppm U/%TOC in the upper part to 1.5 ppm U/%TOC in deeper layers. The results have been compared with the behavior of uranium in the bottom sediments, accumulated in anoxic conditions of the Black Sea, where the concentration of uranium achieves 35 ppm according literature review, and the U/TOC ratio increases up to 3.6 ppm U/%TOC, while uranium content in water and composition of the bottom sediments are close to values observed for the Arctic Seas. Considerable differences in uranium content and U/TOC ratio were analyzed using thermodynamic models of the water–sediment system for different redox conditions. It was shown that an increase in uranium accumulation in sediments in reducing conditions by comparison with oxidizing conditions could be explained by the difference in solubility of uranium in the water–bottom layers contacting with sediments and in the water saturating the upper part of sediments. However, reducing conditions observed in sediments located deeper than 0.5 m in the White Sea, for

example, did not lead to an increase in the accumulation of uranium because the amount of uranium that can be precipitated from the pore water of sediments is much less by comparison with uranium content in the inorganic part of sediments that originated from continental run-off.

The obtained results revealed that the redox condition in the bottom layer of seawater during sedimentation is one of the most important factors controlling the concentration of uranium in the bottom sediments and source rocks of marine genesis. The obtained experimental data and results of thermodynamic modeling provide additional information that can help to understand the behavior of uranium during sedimentation and improve the methods of unconventional reservoir characterization using data on uranium content from gamma logging.

Chapter 4. Distribution of uranium (U) and uranium/TOC (U/TOC) ratios in the unconventional reservoir on the example of the Bazhenov Formation

The Bazhenov Formation (BF) is one of the largest oil source formations in the world in terms of its area and hydrocarbon resources. The Upper Jurassic-Lower Cretaceous deposits of the Formation (J3-K1) are distributed throughout the West Siberian oil and gas Basin, covering over 1 million km^2. They lie at depths of 2500÷3500 m at Upper Jurassic terrigenous rocks and are overlain by Lower Cretaceous mudstones [Braduchan и др., 1986; Ulmishek, 2003; Zanin, Zamirajlova, Eder, 2005]. The thickness of the formation varies from 25 to 80 meters, with an average of 30÷40 m. The rocks are represented by siliceous, clayey-siliceous, carbonate, and clayey-carbonate-siliceous varieties with high organic matter (OM) content [Kontorovich et al., 2016; Nemova V.D., 2017]. The BF rocks are characterized by low porosity and permeability and thus are classified as oil shale. The total initial OM of the Formation reaches 30 wt. % with average values of 10–15 wt.% and is represented by solid kerogen and free or bound light and heavy hydrocarbons [Goncharov et al., 2021; Kontorovich et al., 2019]. OM content of the upper BF subformation (strata) is several percent higher than in the lower one, which allows us to distinguish between the upper and lower subformations in logging diagrams. In the vast area of the West Siberian Basin, the nature of OM remains the same and is represented by type II kerogen. Its phase composition depends on OM maturity [Goncharov et al., 2021; Kozlova et al., 2015]. The main BF feature is increased gamma-ray logging values associated with an increased uranium content. The lower strata of the BF is characterized by lower values of uranium content (up to 25 ppm), while the upper strata are characterized by higher concentrations of uranium, reaching 150 ppm. The lower strata are mainly composed of kerogenic-clayey/clayey-kerogenic silicites. In the upper part of the lower strata, we distinguish an interval of “radiolarites” (radiolarite-rich silicites) and developed secondary dolomites and limestones. The upper strata are represented by kerogenic-clayey-carbonate/clayey-carbonate-kerogenic silicites and contain a large amount of biogenic carbonate associated with remains of the shell debris (bivalve) and coccolithophorids [Panchenko et al., 2016; Zanin, Zamirajlova, Eder, 2016]. Due to poor reservoir properties, two main technologies are used for hydrocarbon production from BF. The first is multi-stage hydraulic fracturing, which is applicable for the intervals containing the largest free hydrocarbons with smaller amounts of solid kerogen and demonstrating increased permeability. The second includes thermal and thermogas reservoir stimulation resulting in the partial conversion of kerogen and heavy fractions into mobile hydrocarbons.

4.1 Objects of research

In the current study, we analyzed uranium concentration and the content and composition of organic matter in the Bazhenov Formation rocks from 13 wells located in the Central (Salymsky arch, Krasnoleninsky arch, Nizhnevartovsk arch), Eastern and Northern of the Basin (Figure 44). The BF deposits of the studied wells are identical in terms of lithological composition and initial OM content but demonstrate different degrees of maturation (catagenetic transformation) [Spasennykh et al., 2021].

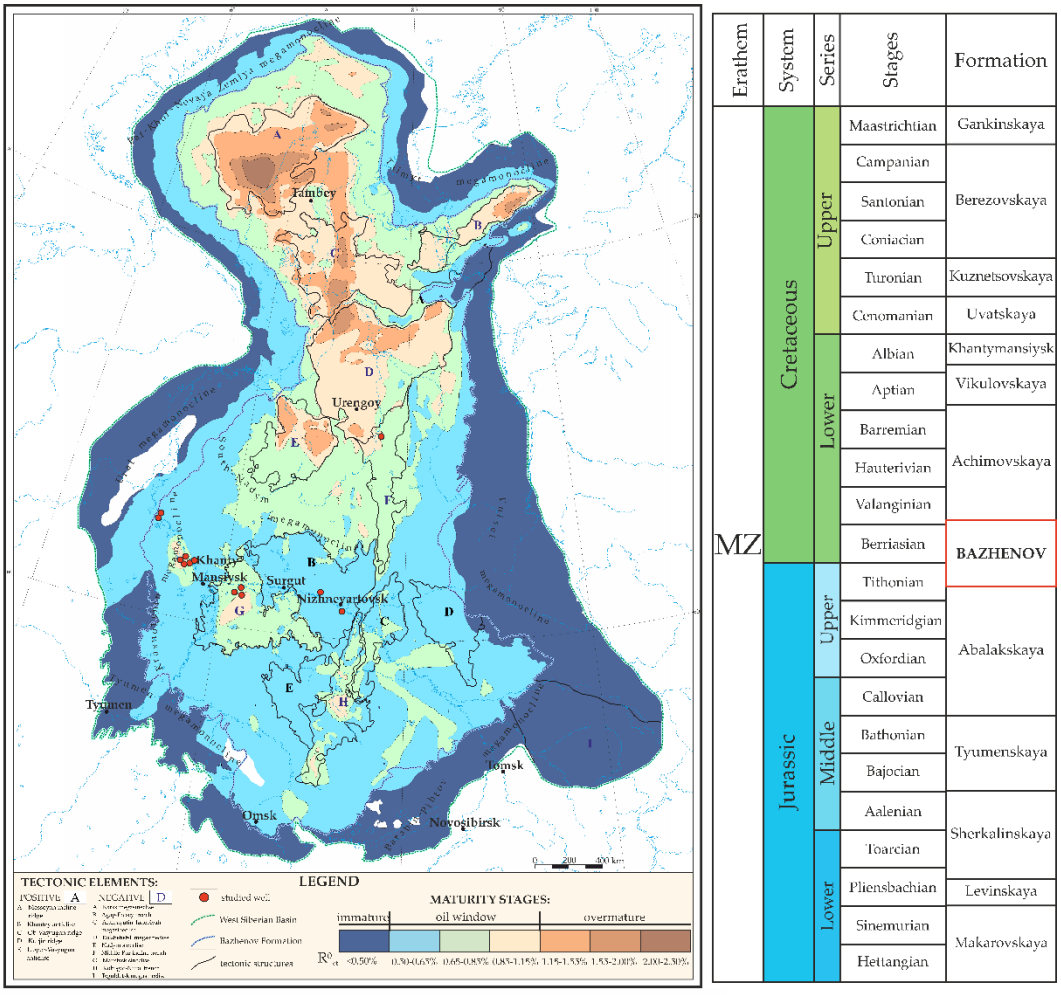

Figure 44. The geological map (modified after [Fomin et al., 2004]) with location of studied wells and stratigraphic column.

4.2. Methods of research

We report data on the uranium concentration, the content and composition of organic matter. We have conducted extended lithological-petrophysical and isotopic-geochemical studies for several sections within the Bazhenov Formation interval, including determining the lithological composition, reservoir properties, sulfur isotopic composition, and elemental composition rocks, including selected micro-elements.

The distribution of uranium content in the rocks was determined by spectral gamma-ray analyser. The principle of gamma spectrometers operation is based on the intensity of the registered spectra of rocks' natural radioactivity on the mass fraction of potassium, uranium, and thorium in the studied rocks [Coretest Systems, 2012].

The Total Organic Carbon and petroleum generation characteristics were measured by the Rock-Eval pyrolysis using pyrolyser HAWK Resource Workstation (Wildcat technology) [Emec T.P., 1987; Espitalie, Marquis, Barsony, 1984; Langford, Blanc-Valleron, 1990; Maende, David Weldon, 2013]. Pyrolytic analysis includes two cycles - pyrolysis in an inert gas flow and subsequent oxidation (Figure *45*).

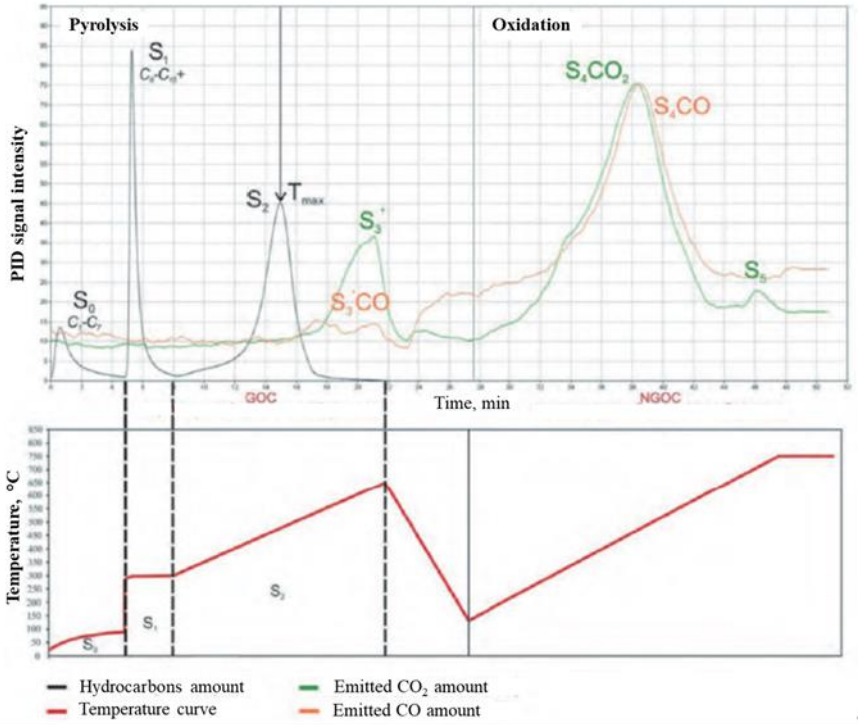

Figure 45. A rock sample pyrogram. Modified after [Vtorushina, Bulatov, 2018].

Following the procedure of measurements the amounts of thermally desorbed hydrocarbon gases (S_0, mg HC/g rock), liquid hydrocarbons (S_1, mg HC/g rock), the amounts of kerogen cracking hydrocarbon products (S_2, mg HC/g rock) and oxygen containig products (S_3, mg CO_2/g rock) were measured during pyrolysis in inert gas at increasing temparature. Amount of nonpyrolyzed kerogen (S_4, mg CO_2/g rock) was measured separately at oxydazing stage of analysis. Total organic carbon (TOC, %) is calculated using the data on all the carbon-containing compounds. Following the procedure described in [Kozlova et al., 2015] the pyrolysis procedure was performed twice: for the original sample and the same sample after extraction with chloroform (the measured values of S_0, S_1, S_2, S_3 and TOC obtained for samples after extraction are marked by index "ex"). Double analysis of the samples allowed us to determine the corrected amount of kerogen decomposition products S_{2ex} and corrected indices T_{maxex} [Kozlova et al., 2015]. The

following indices were used to determine the OM quality: hydrogen index HI (mg HC/g TOC) given by a ratio of the among of organic carbon S_2 to TOC content ($HI = S_2/TOC \cdot 100\%$), oxygen index OI (mg CO_2/g TOC) given by a ratio of S_3 to TOC content ($OI = S_3/TOC \cdot 100\%$). During data interpretation and estimation of the OM maturity, the following indices were also taken into account: oil saturation index ($OSI = S_1/TOC \cdot 100\%$, mg HC/g TOC), PI - productivity index ($PI = S_1/(S_1+S_2)$), and coefficient $Kgoc_{ex}=GOC_{ex}/TOC_{ex} \cdot 100\%$, reflecting the percent of the residual generative organic carbon (GOC) in $TOC_{ex} = GOC_{ex} + NGOC_{ex}$ [Behar, Beaumont, B. Penteado De, 2001; Jarvie, 2012; Kozlova et al., 2015; Spasennykh et al., 2021]. Generative organic carbon content GOC (wt.%) = $(S_0+S_1+S_2) \cdot 0.085 + S_3 \cdot 12/440 + (S_3CO + S_3'CO) \cdot 12/280$, non-generative organic carbon content NGOC (wt.%) = $S_4CO \cdot 12/280 + S_4CO_2 \cdot 12/440$.

Determining continuous variations of organic carbon based on results of thermal core logging [Popov at al., 2016]. The method is non-contact and non-destructive, the profiling spatial resolution is ~1 mm. Measurements can be carried out on the whole core cylindrical surface or on a flat surface of its small-sized duplicates. The basis for determining TOC from data on the low-permeability reservoir rocks thermal conductivity is a significant difference in the thermal conductivity of the mineral matrix rocks and organic matter. Also, the spatial resolution during TOC profiling is determined by the spatial resolution during thermal conductivity profiling.

The content of uranium, vanadium, phosphorus oxide (P_2O_5), and manganese oxide (MnO) was determined during chemical elemental analysis using X-ray fluorescence analysis (XRF). It was used a X-ray fluorescence spectrometer AXIOS. The X-ray fluorescence spectrometer AXIOS characteristics:

- the determined elements range from Be to U;
- the detection elements limits at the level from 0.5 to 5 ppm.

The sulfur isotope composition in rock samples was analyzed using Thermo Scientific DELTA V Plus mass spectrometer equipped by Flash HT elemental analyzer [Coplen et al., 2002]. The instrument is equipped with peripherals of the same manufacturer: ISQ quadrupole mass spectrometer, TRACE GC Ultra gas chromatographer, and Flash HT elemental analyzer. International standards used in the isotopic analyses of sulfur is CDT (Table *31*).

Table 31.International standard used in sulfur isotopic analysis.

Standard	**Abbreviated name**	**Isotopes**	**Ratio (average ±1s)**
Troilite (FeS) from the Diabolo Canyon iron meteorite	CDT	$^{34}S/^{32}S$	0,0454

A static mass spectrometer with a sector magnet (known as IRMS, Isotope Ratio Mass-Spectrometer) was used for the determination of masses and relative abundance of light element isotopes. The accuracy of isotopic composition determination defined by measurements on the reference sample was ±0.5‰ for sulfur.

4.3 The high-resolution analysis results of variations TOC and uranium concentrations in the Bazhenov Formation

Analyzing the results of studying the uranium and organic carbon distributions and concentrations, it must be emphasized that the U/TOC ratio is an important parameter indicating the deposition environment. Many researches have been devoted to the study of the relationship between the uranium and organic carbon concentrations [Dudaev, 2011; Lüning, Kolonic, 2003; Parfenova, T. M., Melenevskij, V. N., Moskvin, 1999].

The problem of analyzing the relationship between uranium and TOC is the high Bazhenov Formation heterogeneity which affects the uranium and TOC distributions. The organic carbon concentration is getting by applying the pyrolysis method with the selection of 2-3 samples per meter. Analysis of the uranium content is carried out using gamma spectrometry on a core with a resolution not higher than 10 cm. With the Bazhenov Formation high heterogeneity (on a scale of millimeters to a few centimeters) it is impossible to get reliable data on variations in the U/TOC ratio with these measuring instruments.

The thermal core logging is used to determine TOC, which makes it possible to get a TOC profile (with a resolution of 1–2 mm) for the Bazhenov Formation to increase the data reliability. Thus, to study the U/TOC ratio, the thermal core logging was applied and the U/TOC ratio profiles were constructed for the first time.

The results of studies for 9 wells belonging to different geological structures are shown in the Figure *46* and Figure *47*.

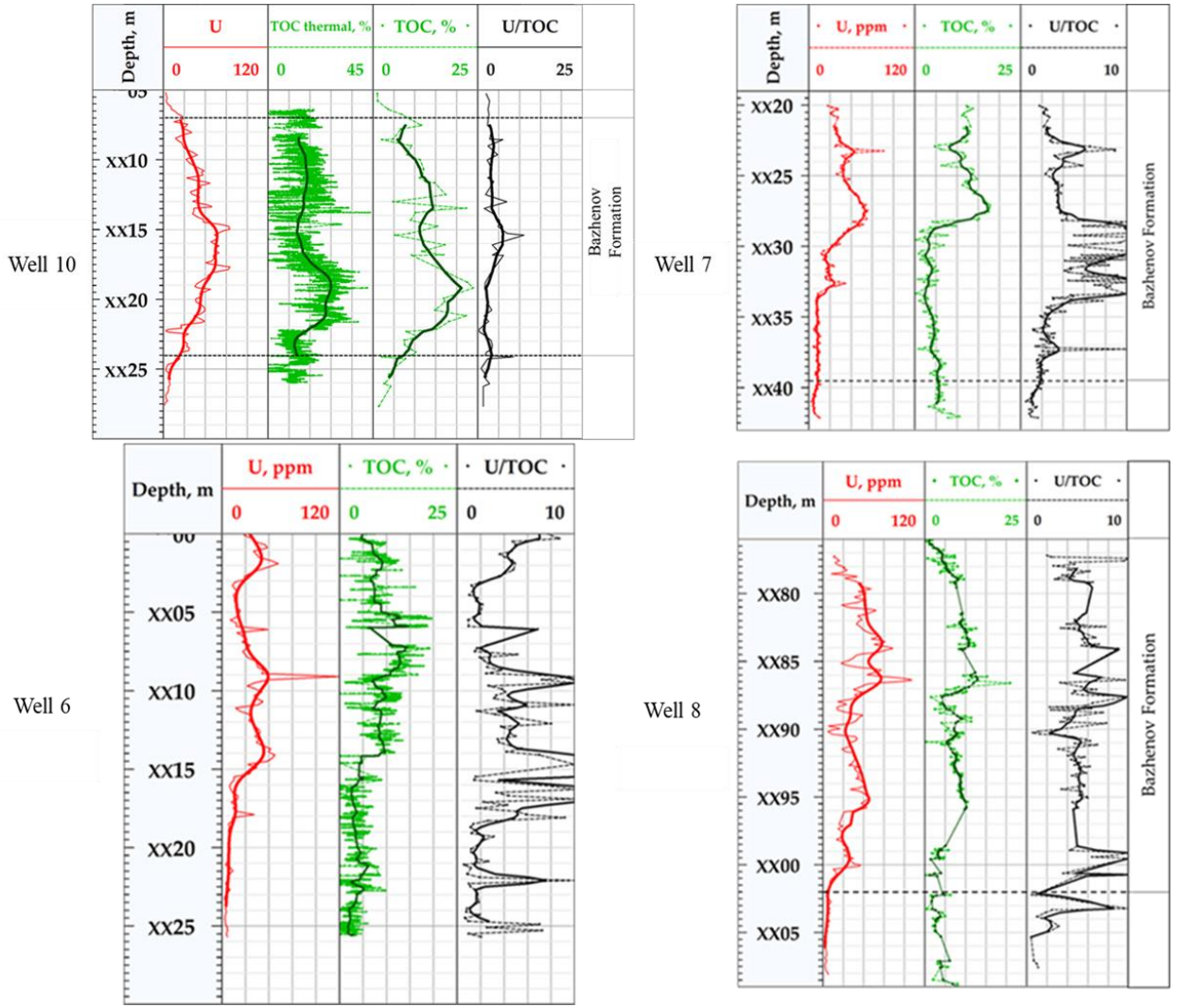

Figure 46. Logviews BF: U-core (gamma spectrometry); TOC – organic matter profile with 1 mm resolution (TOC thermal was determined by the thermal core logging, TOC was determined by the Pyrolysis for Well 10).

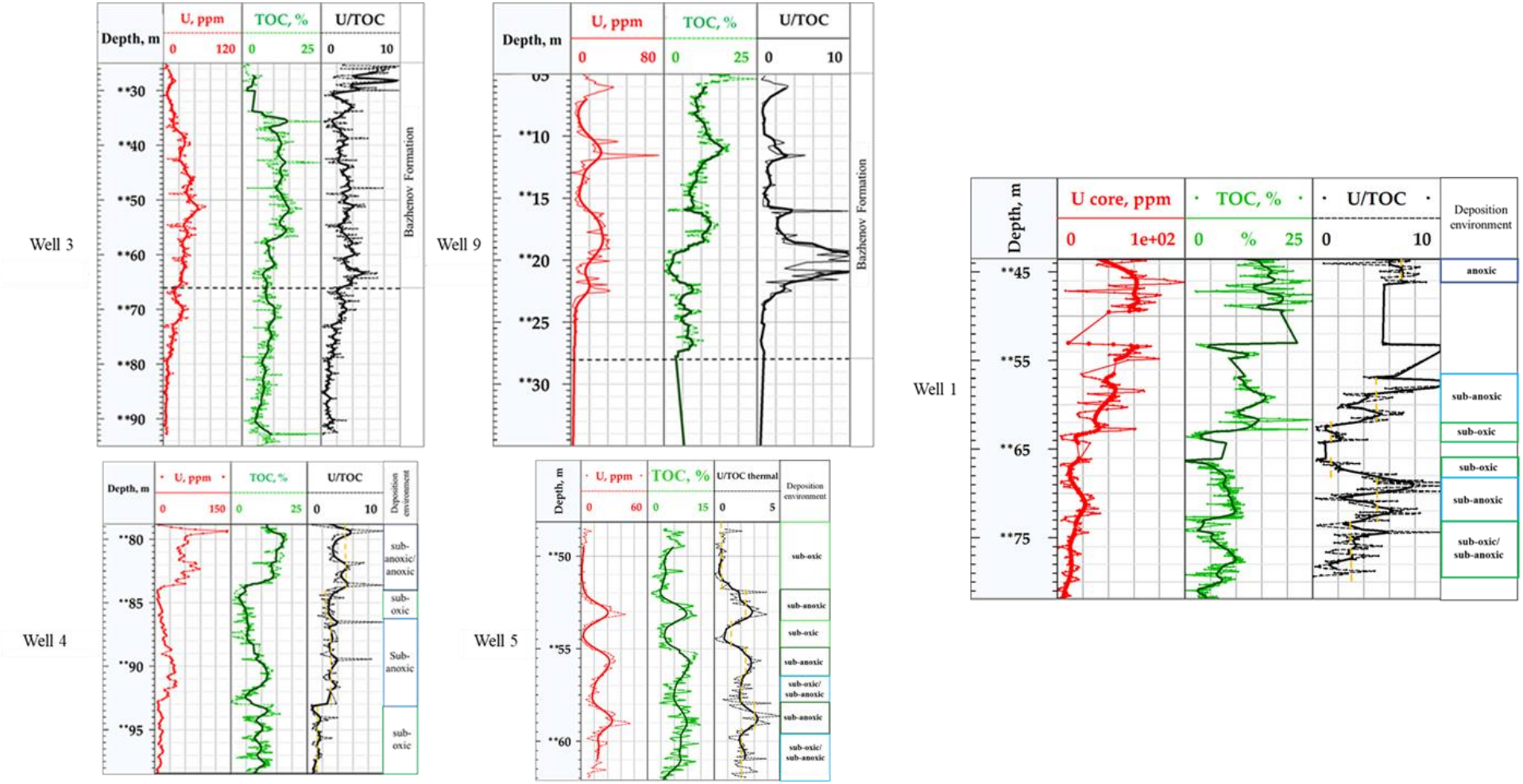

Figure 47. Logviews BF: U-core (gamma spectrometry); TOC – organic matter profile with 1 mm resolution (TCP); ratio U/TOC; sulphur isotopy $\delta^{34}S$; deposition environment: sub-anoxic, anoxic, sub-oxic.

The uranium content ranges from 0 to 150 ppm, TOC ranges from 0 to 25 wt%, U/TOC ratios are also not constant, the range of variation is 0−10 according to the data of the 9 studies wells.

The variations nature in these parameters is different for the objects considered. In particular, the uranium content in the well 3 varies from 0 to 60 ppm (Figure *47*). The maximum uranium concentration values characterize the central part of the section (at a depth of **45 - **55 m). Organic matter content varies from 0 to 25%, with a higher TOC content also in the middle part of the section. The average TOC values for the upper part of the section are higher than for the lower part. The U/TOC ratio varies from 4 to 10 in the uppermost part, from 2 to 4 for most of the section in the middle part and between 0-2 for the lower third of the section.

The uranium concentration for the well 9 has a distribution with three maxima in the upper and middle parts, reaching mean values up to 40 ppm at the maxima with peaks up to 75 ppm (Figure *47*). The TOC distribution is more complex, with higher values for the upper part of the section. U/TOC ratio has a maximum values (U/TOC ≈10) in the lower part of the section (U and TOC have minimum values). The other intervals characterize the U/TOC ratio in the range from 0 to 4, reaching maximum values synchronously with the maximum uranium.

Uranium content and TOC for the well 4 change synchronously in the upper and middle parts of the section, reaching maximum values for the upper quarter of the section (Figure *47*). A local minimum of uranium concentration and TOC follows the uranium concentration and TOC maximum. The uranium concentration decreases to minimum values and TOC content varies around 10 wt% in the lower quarter of the section. The U/TOC ratio decreases naturally from top to bottom of the section in the range between 6 and 1, with variations around the trend line.

The uranium content, TOC, as well as U/TOC ratios profiles for the well 5 are synchronous throughout the depth (Figure *47*). The maximum U/TOC ratio reaches 6, and the minimum U/TOC ratio is 1-2.

Figure *46* shows the distributions of uranium content (U core), TOC (Rock-Eval pyrolysis), as well as the TOC thermal organic matter content profile (position resolution 1 mm) calculated from the thermal core logging, U/TOC ratio for the well 10. The uranium content for well 10 varies from 0 to 75 ppm. The middle part of the section is characterized by the maximum uranium concentration values. The organic matter content for this section varies from 0 to 45%. Pyrolytic organic carbon (TOC) profile and organic carbon profile (TOC thermal) have similar behavior: the organic carbon values reach 25% in the lower part, decreasing up to 5% in the Bazhenov Formation upper part. The U/TOC ratio varies from 0 to 10, the average U/TOC ratio is less than 5. The lowest U/TOC values (up to 2.5) are the lower part characteristic of the section, the

maximum values (up to 10) are the central part characteristic of the section. The upper part of the section is characterized by U/TOC values ranging from 2 to 5.

As follows from published data, variations in uranium and U/TOC ratios are primarily related to deposition environment. Minimum uranium concentrations are characteristic of sedimentation under sub-oxidative conditions at shallow sea depths (marginal marine depositional environment), where uranium is contained in continental runoff minerals. Maximum uranium values are reached in marine conditions, in a reducing environment, where uranium is accumulated through deposition from seawater. The U/TOC ratio changes between 2 and 6 for the intervals formed in marine conditions, reaching a maximum in zones of maximum organic matter catagenetic transformation. The U/TOC ratio varies in a wide range in the zones of uranium and TOC content minimum values. And it's not being informative because of measurement error. The results of measurements are presented in the Tables (Appendix 1).

Conducted research started the development of a method for assessing deposition environment and productivity of deposits by uranium and TOC, which was protected by a patent [Spasennykh, M.Yu., Chekhonin, E. M., Popov, Yu. A., Popov, E. Yu., Kozlova, E. V., Khaustova, N.A., 2021]. The approach for determining the deposition environment and identifing the natural reservoirs by U/TOC ratio described in the patent "METHOD AND DEVICE FOR PROFILING THE PROPERTIES OF ROCK SAMPLES OF OIL SHALE Source Rocks".

In order to determine the deposition environment and natural reservoirs, it is necessary:

1. The total organic carbon content profile with a 1 mm resolution, which was calculated from the results of the thermal core logging, is brought to a position resolution that characterizes the detail of profiling the uranium concentration by averaging the thermal conductivity values profile in 100 mm window.
2. The U/TOC ratio profile is calculated using obtained uranium concentrations and organic matter contents.
3. The redox conditions of sedimentation are determined by comparing predetermined boundary values - U/TOC_{min} and U/TOC_{max}: at U/TOC < $\mathbf{U/TOC_{min}}$ the deposition environment is sub-oxidative, at $\mathbf{U/TOC_{min}}$ < U/TOC < $\mathbf{U/TOC_{max}}$ the deposition environment is sub-anoxic, at $\mathbf{U/TOC_{max}}$ < U/TOC the deposition environment is anoxic [Khaustova et.al., 2019]. The boundary U/TOC_{min} and U/TOC_{max} values are determined using published research results, where

U/TOC_{min} = 2, U/TOC_{max} = 5. The intervals with the sub-oxic deposition environment correspond to the natural reservoirs intervals in the BF.

The deposition environment was determined and intervals of natural reservoirs were identified along the U/TOC ratio profile for wells 4 and 5 of the Priobskoye and the Salmanovskoye fields (Figure *47*).

The Figure *47* shows the uranium concentration, organic matter and U/TOC ratio distributions for well 4. Sub-oxic conditions of sedimentation U/TOC < 2 correspond to the intervals in the well section at depths of XX84-XX87 m and XX93-XX98 m. We characterized these intervals as natural reservoirs. The interval in the central part of the section is characterized by sub-anoxic deposition environment with U/TOC in the range between 2 and 5. There are intervals with U/TOC>5 in the upper part of the section, which corresponds to the anoxic deposition environment.

The Figure *47* shows the uranium content, organic matter and U/TOC ratio distributions for the well 5. The ratio U/TOC < 2 corresponds to the sub-oxic deposition environment for two intervals: XX48–XX52 m and XX53.5–XX55 m. Also, these intervals can be called natural reservoirs. The ratio U/TOC in the range between 2 and 5 is typical for the sub-anoxic deposition environment for three intervals. The ratio U/TOC ≈ 2 is for the two intervals with uranium concentration and organic matter content average values. These intervals may have been formed under transitional deposition environment (from oxic to anoxic). The promising for development using reservoir stimulation intervals with immobile oil or heavy hydrocarbons can be identified based on the relationship between uranium concentration and total organic carbon content analysis. Intervals with sub-anoxic and anoxic deposition environment characterize low uranium concentration or a high organic carbon content relative to the general changes trend in the uranium concentration and the organic carbon content. Therefore, the intervals with U/TOC ≈ 2 can be called promising for development using reservoir stimulation intervals.

A new approach to the Bazhenov Formation sections characterization was shown in the joint analysis of the uranium, organic carbon (with a resolution of 1-2 mm) and the U/TOC ratio results distribution for 9 wells. Combined uranium, TOC and U/TOC ratios analysis makes it possible to determine deposition environment and natural reservoirs intervals. This approach is described in the patent, which shows the evaluation and calculation procedure in more detail.

4.4 Role of redox conditions in uranium accumulation in source rocks

In order to identify the most important factors affecting uranium accumulation in Bazhenov Formation rocks, we compared data on uranium distribution with the results of lithological and isotopic-geochemical studies for two wells (1 and 2) located in the central part of the Basin, attributed to the Frolovskaya megadepression (Salym region). The identified uranium and organic matter content, pyrolysis indexes, sulfur isotopic composition, chemical elemental composition, and U/TOC ratio of the Bazhenov Formation section are shown in Figure *48* and Figure *49*.

Figure *48* shows the distribution of uranium (U core), vanadium (V), sulfur isotopic composition ($\delta^{34}S$), pyrolytic indicators (TOC, OI, OSI), and ratios (U/TOC, Th/U, Mo/(Mo+Mn), Mo/Al, V/Mo, V/Cr) for well 1. Figure *49* shows the distribution of uranium content (U core), pyrolytic indexes (TOC, OI, OSI), and ratios (U/TOC, Th/U, Mo/(Mo+Mn), Mo/Al) for well 2.

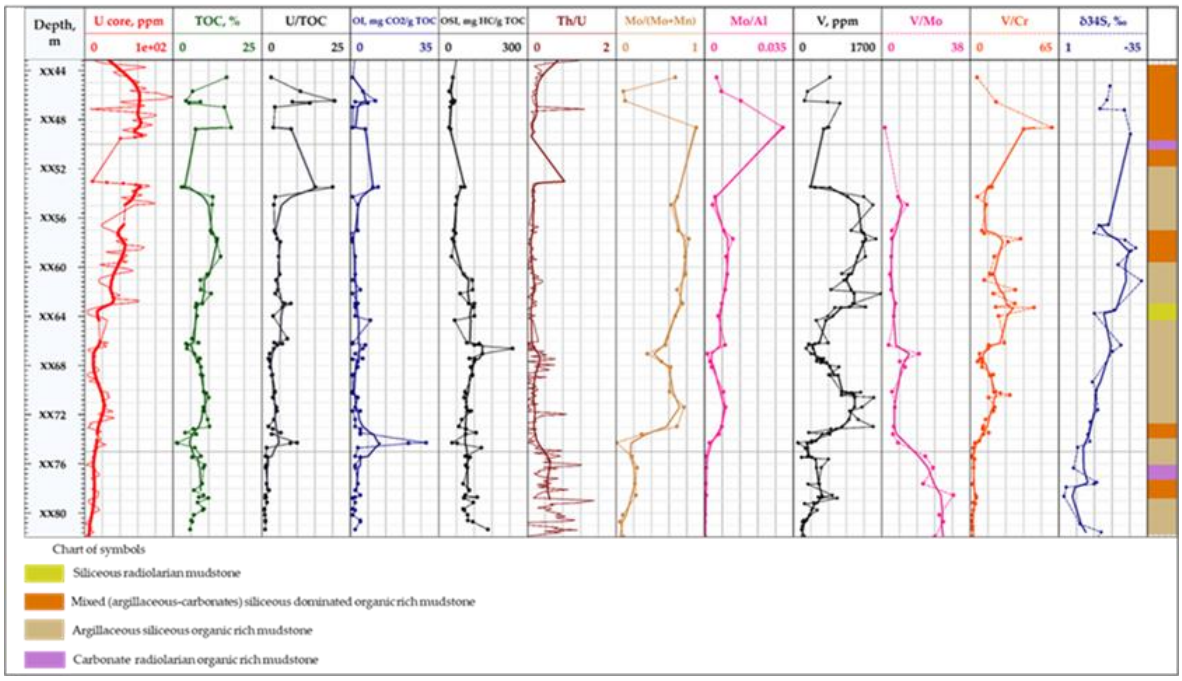

Figure 48. Logview well 1: U and Th/U ratio (gamma-ray spectrometry); TOC is the content of organic matter, OI is the oxygen index, and OSI is the oil saturation index; U/TOC ratio; V, V/Mo, V/Cr, Mo/Al, and Mo/(Mo+Mn) ratios (X-ray fluorescence XRF, ICP-MS); δ34S sulfur isotopic composition.

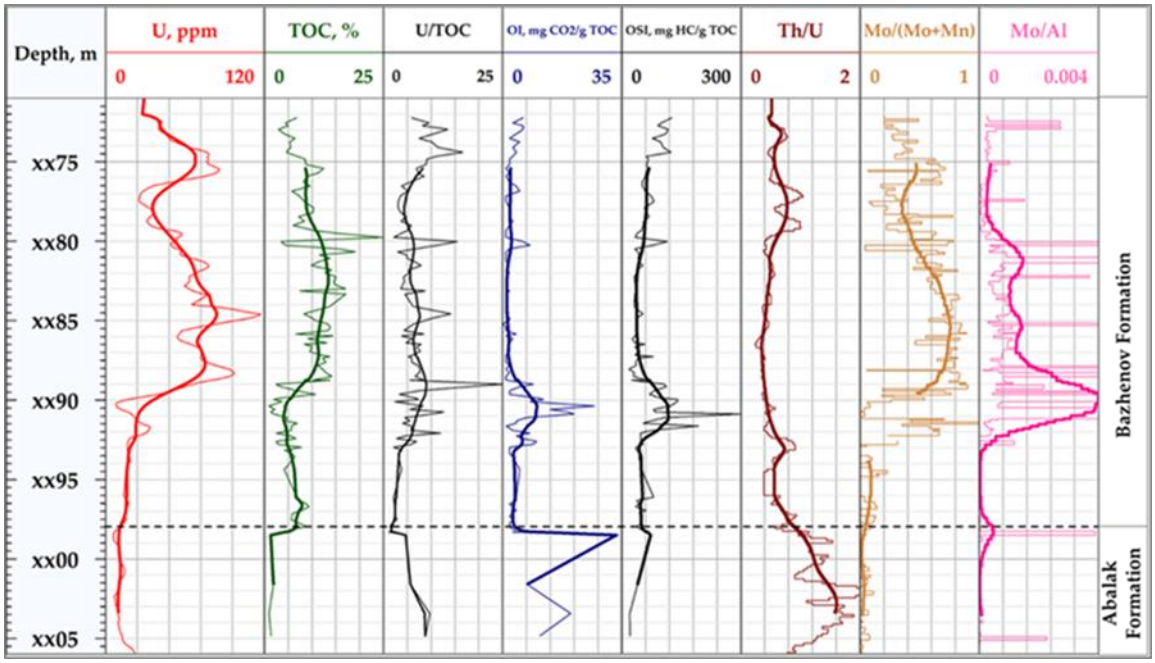

Figure 49. Logview well 2: U and Th/U ratio (gamma-ray spectrometry); TOC is organic matter content, OI is oxygen index, and OSI is oil saturation index (Rock-Eval pyrolysis); U/TOC ratio; Mo/Al and Mo/(Mo+Mn) ratios (XRF analysis).

According to the obtained results, uranium content variations strongly correlate with parameters indicating redox conditions at the sedimentation stage, such as oxygen index, vanadium, molybdenum, Mo/Al, Mo/(Mo+Mn), V/Mo, V/Cr ratios (Figure *48*). We also observe a correlation with the Mo/(Mn+Mo) ratio, one of the most sensitive indicators of redox conditions for the Bazhenov Formation rocks [Baioumy, Lehmann, 2017; Elbaz-Poulichet et al., 2005; Leushina [Baioumy, Lehmann, 2017; Elbaz-Poulichet et al., 2021; Zanin, Zamirajlova, Eder, 2017].

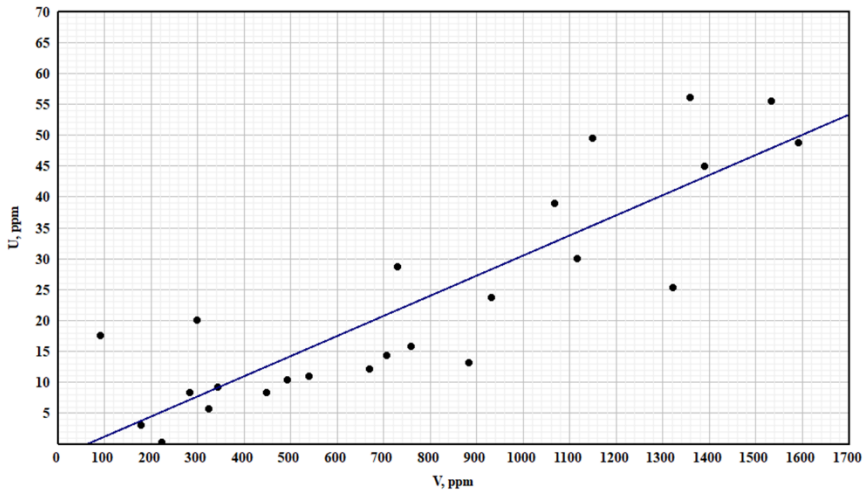

Figure 50. Cross-plot of uranium and vanadium concentrations for well 1, Bazhenov Formation. Blue line corresponds to equation U = 0.03·V-2.05, where the correlation coefficient R = 0.87.

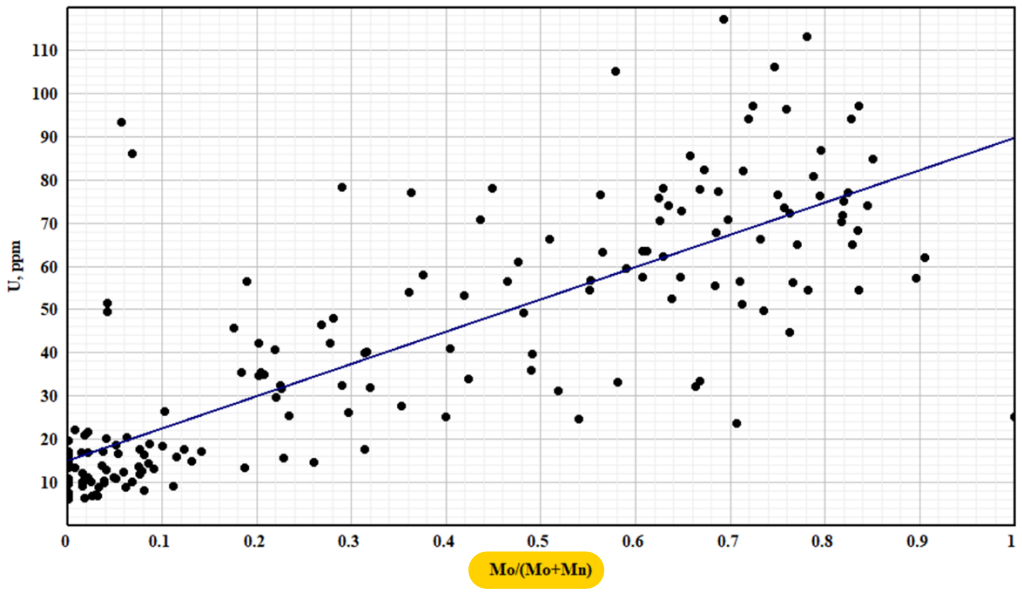

Figure 51. Cross-plot of uranium concentration and Mo/(Mo+Mn) ratio for well 2, Bazhenov Formation. Blue line corresponds to equation U = 74.81·Mo/(Mo+Mn)+14.95, where the correlation coefficient R = 0.81.

The distributions of these ratios are given in Figure *48* and Figure *49*, indicating a change in redox environments: from slightly oxidizing conditions in the lower part of the BF to reducing in the middle and upper parts of the BF. For example (Figure *49*), the lower part of the BF cross-section of well **30 is characterized by low uranium content and low Mo/(Mn + Mo) ratio, while the upper part is characterized by increased uranium content and high Mo/(Mn + Mo) ratio. Figure *51* demonstrates the correlation between U and the Mo/(Mn + Mo) ratio.

Figure *48* represents the distribution of the sulfur isotopic composition $\delta^{34}S$. Comparison of the uranium content, the U/TOC ratio, and the sulfur isotopic composition (Figure *52* and Figure *53*) demonstrates that rocks with a high content of uranium and organic matter are characterized by a high sulfide sulfur content and low content of the heavy sulfur isotope ($\delta^{34}S$ varies from -40 to -30‰CDT). According to the data of [Idrisova et al., 2021] and the results of other studies [Newton, Bottrell, 2007], a high pyrite content with low isotope composition values indicates reducing conditions and the presence of hydrogen sulfide at the sedimentation stage.

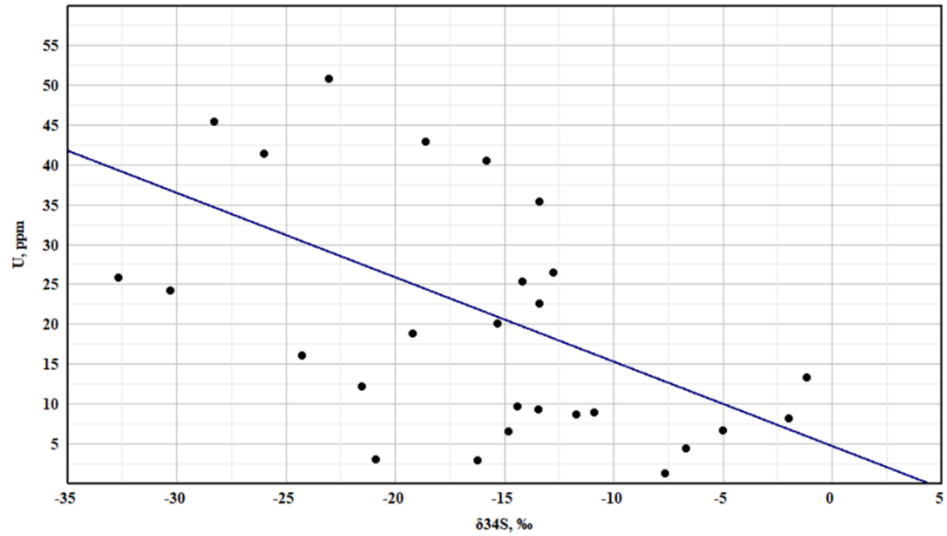

Figure 52. Cross-plot of uranium concentration and sulfur isotopic composition for well 1, Bazhenov Formation. Blue line corresponds to equation $U = -1.06 \cdot \delta^{34}S + 4.69$, where the correlation coefficient R = 0.46.

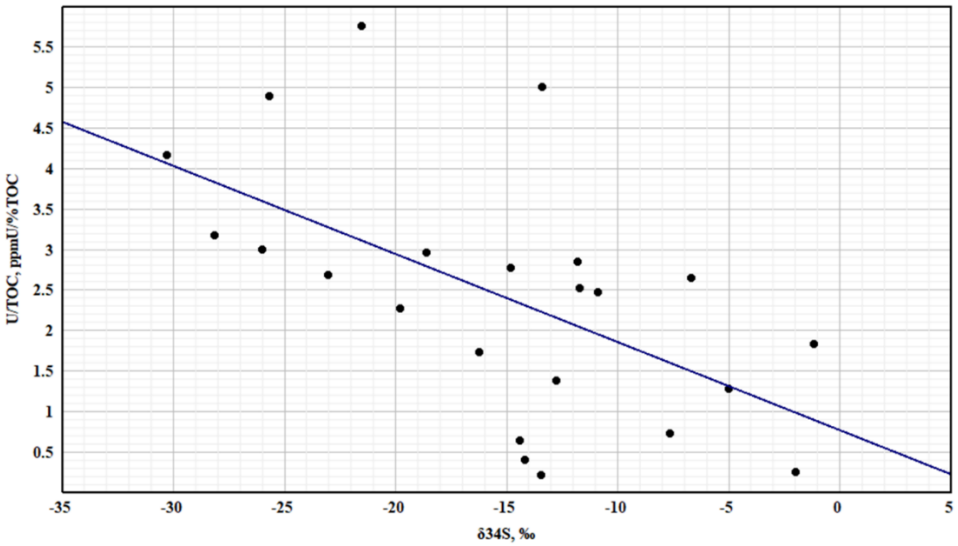

Figure 53. Cross-plot of U/TOC and sulfur isotopic composition for well 1, Bazhenov Formation. Blue line corresponds to equation $U/TOC = -0.11 \cdot \delta^{34}S + 0.77$, where the correlation coefficient R = 0.57.

In Figure *54*, we report a U-TOC diagram for the samples from 11 wells. The colors of dots represent oxygen index values (OI), which characterizes the oxygen content in the Bazhenov Formation organic matter. Increased values of OI correspond to more oxidizing conditions while low values of OI correspond to reductive conditions of marine sedimentation [Melenevsky, Klimin, Tolstokorov, 2019]. In Figure *54*, points are falling into low organic matter (TOC < 5 wt.%), and low uranium values (uranium concentration < 20 ppm) intervals are characterized by increased oxygen index values. In contrast, lower oxygen index values are typical for intervals with high uranium and organic matter contents.

Figure 55 shows diagrams of the uranium concentration distribution at fixed oxygen index values: OI = 4-10 (left), OI > 10 (right). The higher oxygen indexes, the lower the percentage of intervals with a uranium content > 20 ppm, and vice versa.

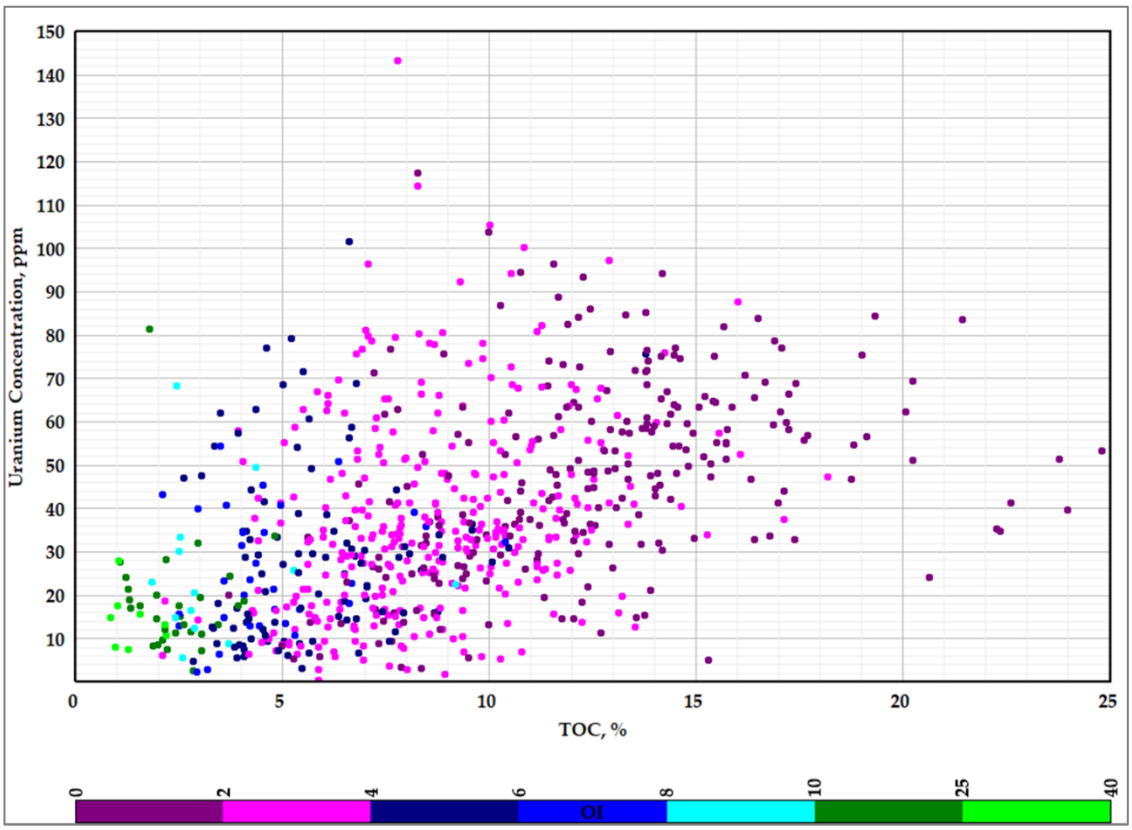

Figure 54. Cross-plot of uranium concentration (measured by gamma-ray spectrometry) and organic matter content (TOC, determined by Rock-Eval pyrolysis) according to the study of 11 wells. Dot color corresponds to oxygen index (determined by Rock-Eval pyrolysis).

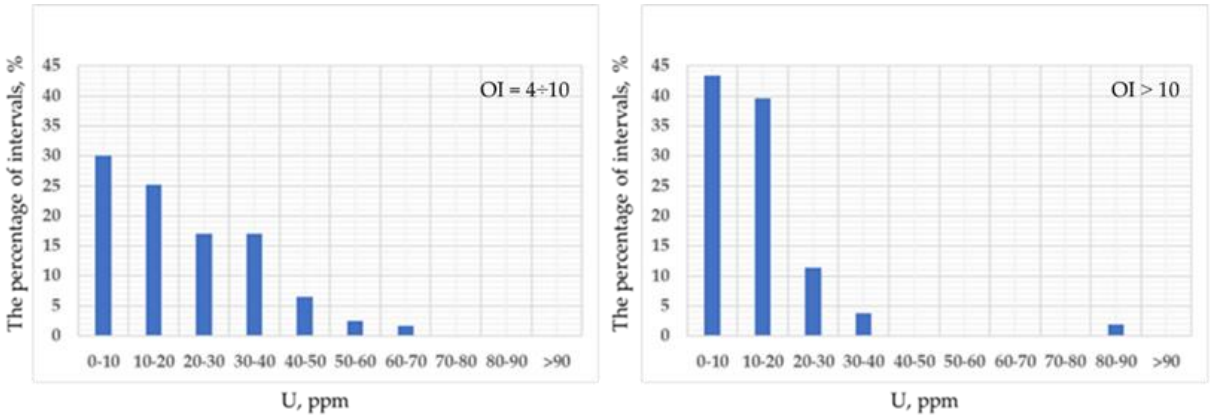

Figure 55. The proportion of intervals with values of OI = 4 ÷ 10 mg CO_2/g TOC, OI > 10 mg CO_2/g TOC (vertical axis, %) as a function of uranium content (horizontal axis, ppm).

Thus, we conclude that low uranium concentration and TOC values characterize the intervals formed in relatively more intensive oxidizing conditions. The intervals formed in reducing conditions show significantly higher uranium concentration and TOC values. The observed pattern of the uranium behavior in BF rocks is similar to that observed for the modern marine sediments [Khaustova et al., 2021].

4.5 Relationship of uranium content, total organic carbon, mineral composition and productivity of source rocks

In order to study the relationship between the uranium content with productivity, we used gamma-ray spectrometry on core and pyrolysis data on more than 900 core samples from 13 wells of the Bazhenov Formation. The U-TOC diagram values integrating the data form these wells is shown in Figure *56*. The color of points show oil saturation index.

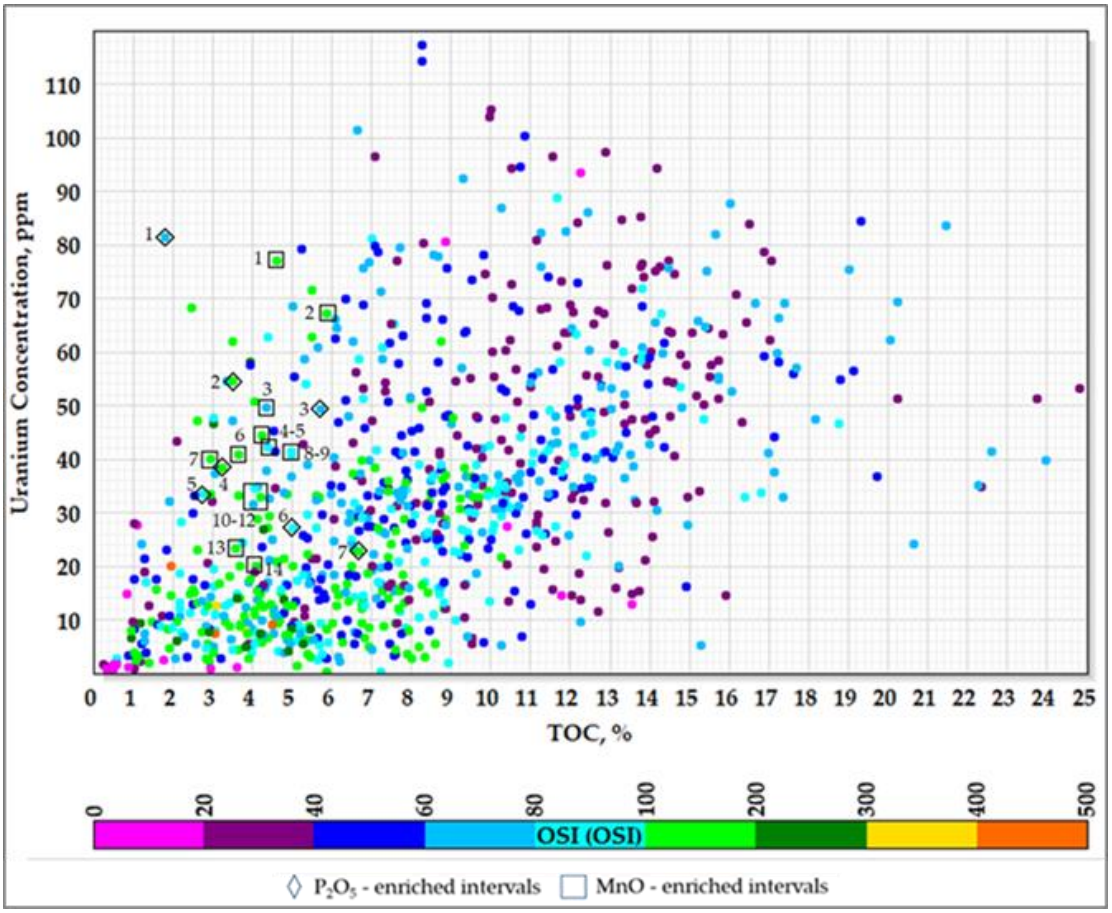

Figure 56. Cross-plot of the uranium concentration and total orgaic carbon (TOC) according to the study of 12 wells penetrating the BF. The color of the dots reflects the oil saturation index (OSI) values.

The data in Figure *56* does not reveal a clear correlation between OSI, TOC, and U. Nevertheless, it indicates that most of the points with increased oil saturation indices (> 100)

[Dakhnova, M.V.; Mozhegova, S.V.; Nazarova, E.S.; Paizanskaya, 2015] are located in the quadrant with low uranium (< 20 ppm) and TOC contents (< 10 wt.%). Intervals with higher uranium values predominantly show lower oil saturation index values. The results of data processing are shown in Figure *57*. According to these data, at OSI > 100, only 35% of the intervals are characterized by more than 30 ppm of uranium content. Therefore, the remaining 65% is characterized by less than 30 ppm uranium concentrations.

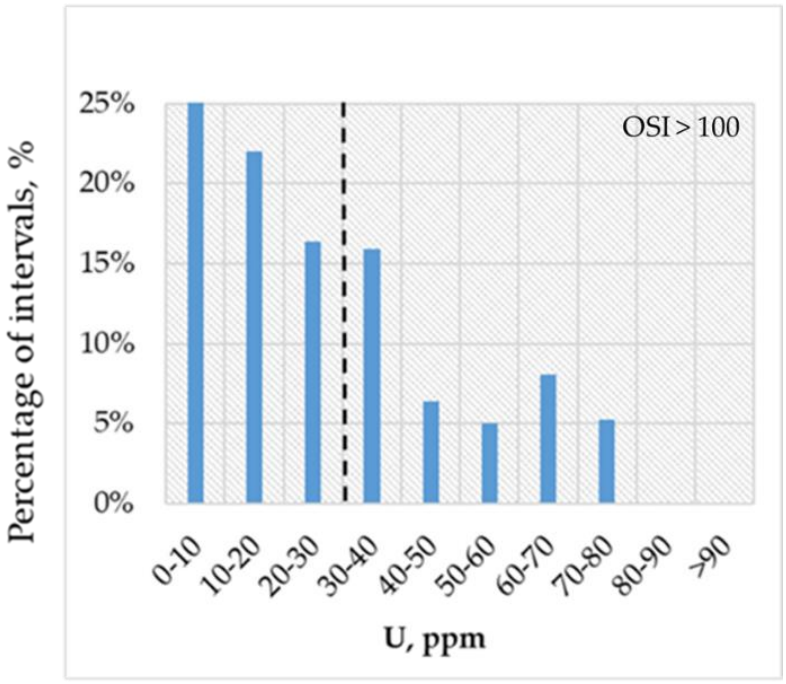

Figure 57. The number of intervals with OSI > 100 for different uranium concentrations.

Figure *58* shows the relationship between uranium concentration and OSI for 3 wells located within one oilfield and characterized by the same catagenetic maturity of OM (Kgoc≈55). As follows from Figure *58*, OSI values > 200 are achieved for uranium content below 10 ppm. For higher uranium content, the oil saturation index decreases.

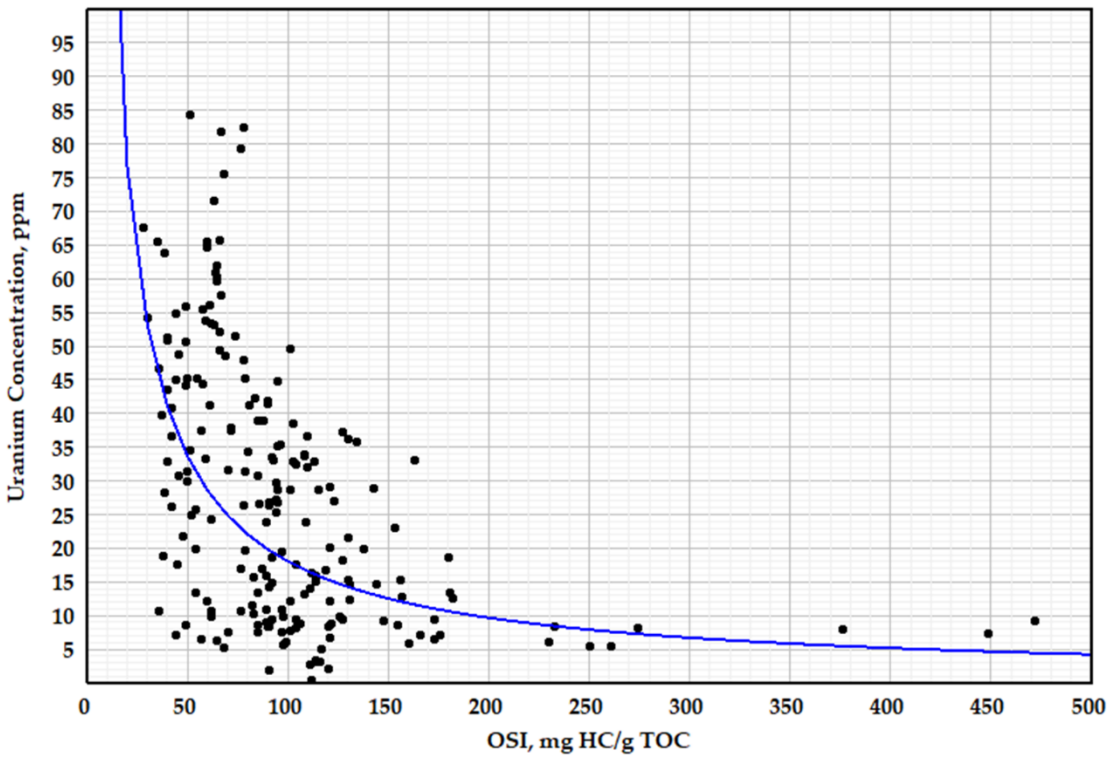

Figure 58**.** Uranium concentration as a function of oil saturation index (OSI) according to the study of 3 wells drilled at oil fields [Spasennykh и др., 2021] characterized by low maturity kerogen (Kgoc≈55). Blue line corresponds to the equation $U = 1133*OSI^{-0.9}$, where the determination coefficien $R^2 = 0.25$.

In Figure *59* , we present U/TOC – $Kgoc_{ex}$ diagrams, where the dot color reflects TOC (Figure *59*, A) and PI (Figure *59*, B), the size of the dots reflects the uranium concentration. According to the diagrams the values of U/TOC ratio and PI are increase with incerase of maturity (decrease of $Kgoc_{ex}$). In the range $20 < Kgoc_{ex} < 65$ we observe a gradual increase in the U/TOC ratio from 0 to 10 with decrease of $Kgoc_{ex}$. In this range the productivity index PI varies from 0.1 to 0.2 (light blue and blue colors, Figure *59*, B) with few exceptions. In the range $Kgoc_{ex} < 20$ we observe a sharp increase in the U/TOC ratio from 5 to 45 with decrease of $Kgoc_{ex}$. The productivity index in this range varies from 0.2 to 0.6 (green, yellow and orange dots, Figure *59*, B).

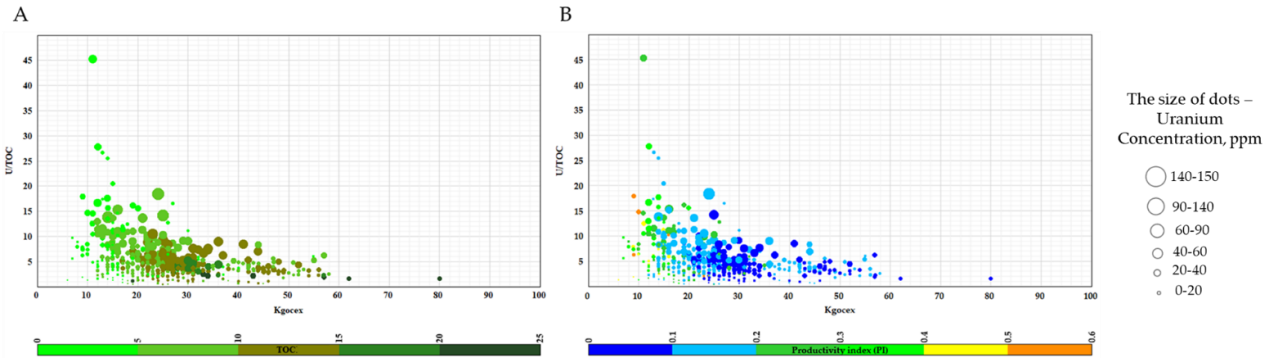

Figure 59. U/TOC - $Kgoc_{ex}$ diagram based on pyrolysis studies of 11 wells. The dot color corresponds to the total organic carbon TOC (A) and the productivity index PI (B), the dot size reflects the uranium concentration.

The increase in U/TOC ratio with increase of maturity (decrease of $Kgoc_{ex}$) can be explained by decrease of TOC during catagenesis. Increase of PI values with maturation is a result of the additional porosity formation during the kerogen transformation into mobile hydrocarbons [Kalmykov, A. G., Karpov, YU. A., Topchij, M. S., Fomina, M. M., Manuilova, E. A., SHeremet'eva, E. V., ... & Kalmykov, 2019; Karpov et al., 2019].

The relationship between uranium content, TOC, and oil saturation is illustrated by the diagram S_0+S_1 - TOC, where the color corresponds to OSI values and the dot size reflects uranium concentration (Figure *60*). The dotted line corresponds to OSI = 100. According to [Dakhnova, M.V.; Mozhegova, S.V.; Nazarova, E.S.; Paizanskaya, 2015], this line distingwishes accumulating (reservoir rocks) and non productive intervals. As it follows from diagram collector intervals are characterized by lower content of uranium (0-20 ppm).

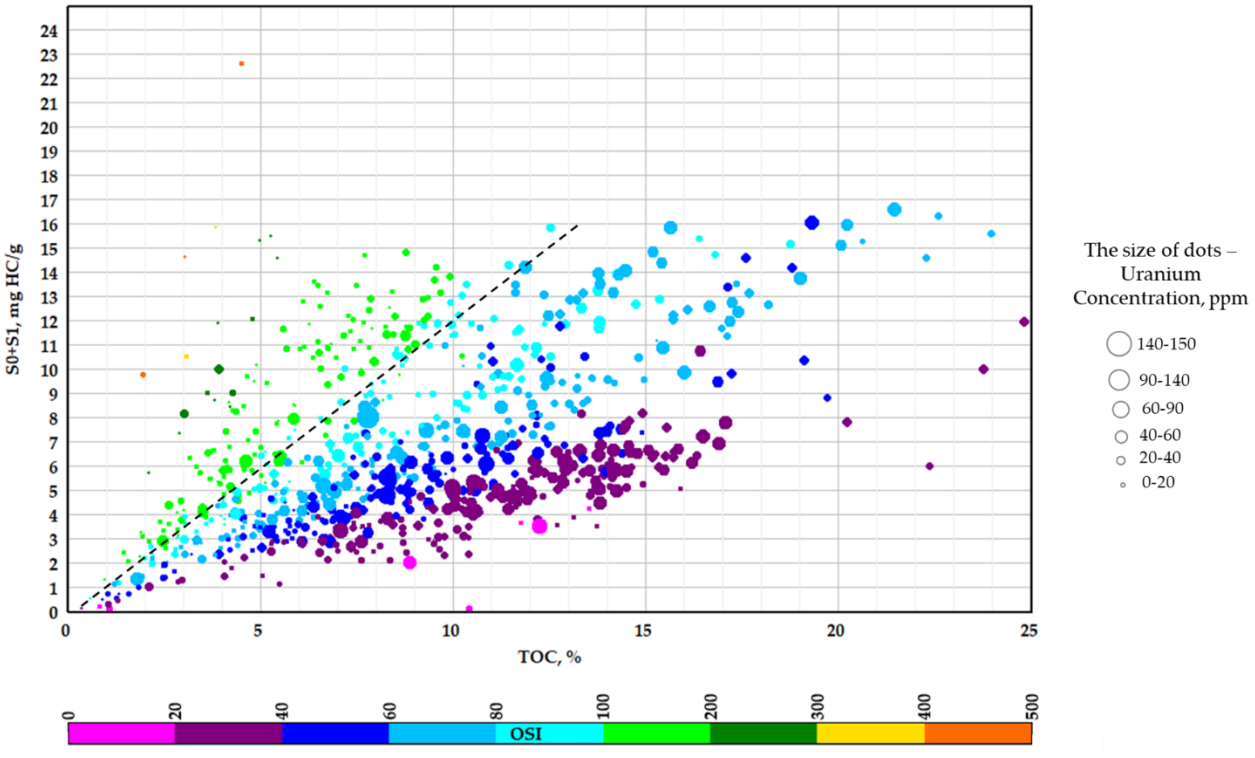

Figure 60. S_0+S_1 - TOC diagram from pyrolysis studies of 11 wells, where color indicates OSI value and dot size reflects uranium concentration. The dotted line separates dots with OSI > 100 from other dots for which OSI < 100 (see color fill).

Following the results discussed above, increased values of the productivity index PI and increased mobile hydrocarbon content are associated with intervals formed in the presence of

oxygen in the water and having lower uranium concentrations. Such conditions mainly appear at shallow depths, when the vital activity of marine organisms develops in bottom sediments. Intervals with a high uranium content are formed during sedimentation under reducing conditions and sulfidic environments. These intervals are source rocks characterized by the highest TOC values. However, their reservoir properties are reduced due to the small volume of void space and ultra-low permeability associated with the presence of solid organic matter kerogen and semi-solid heavy hydrocarbon fractions.

It is particularly important to note that the points obtained from samples with increased P_2O_5 and MnO content (up to 9% and up to 1%, respectively) fall out of the described pattern. In Figure *56*, these points are marked with rhombuses and squares. According to the lithological and petrophysical studies, these points in the upper left corner of the diagram (Figure *56*) correspond to the increased porosity and permeability intervals, which provide higher oil saturation values. Data on uranium, P_2O_5, MnO content, and pyrolytic indices are shown in Table *32* and Table *33*. Increased uranium content is associated with uranium concentration by phosphate minerals (P_2O_5) and pyrolusite (MnO). High uranium content in phosphate minerals is explained by incorporating uranium into the crystal structure of fluorapatite [Kalmykov et al., 2016; Zubkov, 2015]. Rocks enriched in pyrolusite (MnO) exhibit increased uranium contents due to the reducing properties of manganese oxide, which transform water-soluble U^{+6} into insoluble U^{+4}.

Table 32. Pyrolytic characteristics, the concentration of uranium and phosphates (P_2O_5) for the intervals with a high uranium content and a low organic matter content (Figure 56).

№ layer with phosphate	**U, ppm**	**TOC, %**	**U/TOC**	**PI**	**OSI**	**S_0+S_1, mg HC/g rock**	**HI, mg HC/g TOC**	**P_2O_5, %**
1	82	1.8	46	0.27	70	1.3	188	9.37
2	55	3.5	16	0.3	115	4.3	271	0.28
3	50	5.7	9	0.17	66	6.1	329	0.25
4	40	3.2	12	0.32	196	6.4	379	8.33
5	34	2.5	13	0.24	59	1.9	185	0.3
6	28	5.0	6	0.24	94	6.4	297	0.32

7	24	6.6	4	0.3	153	12.6	358	1.4

Table 33. Pyrolytic characteristics, the concentration of uranium and MnO for the intervals with a high uranium content and a low organic matter content (Figure 56).

№ layer with pyrolusite	**U, ppm**	**TOC, %**	**U/TOC**	**PI**	**OSI**	**S_0+S_1, mg HC/g rock**	**HI, mg HC/g TOC**	**MnO, %**
1	77	4.6	17	0.35	124	6.2	235	0.19-0.22
2	68	5.9	12	0.36	130	8.0	233	1.05
3	50	4.4	12	0.24	79	4.1	252	0.84
4	44	4.2	10	0.35	111	5.1	211	0.24-0.33
5	42	4.4	10	0.31	99	4.9	219	0.24-0.33
6	40	3.6	11	0.38	102	3.9	170	0.17
7	40	3.0	14	0.36	117	3.8	209	0.23
8	40	5.0	8	0.28	91	5.1	232	0.33
9	38	5.0	8	0.33	74	4.1	153	0.24
10	31	4.0	8	0.39	69	3.0	110	0.24-0.29
11	34	4.4	8	0.55	178	8.3	146	0.24-0.29
12	32	4.4	7	0.29	64	3.0	156	0.24-0.29
13	23	3.6	6	0.42	161	6.6	225	0.29
14	22	4.2	5	0.16	54	2.5	293	0.24

Figure *61* shows an example of the depth distribution of MnO and P_2O_5 content, uranium content, productivity index, and organic carbon content for one of the studied wells. It is important to emphasize that the uranium peaks are directly related to the increasing P_2O_5, and MnO concentration, the maximum uranium peak equal to 150 ppm corresponds to the maximum P_2O_5 peak. According to Figure *61*, the maximum P_2O_5 and MnO content reach 9.4% and 0.2%, respectively, while the minimum values are 0.06% and 0.01%, respectively.

At the same time, maxima are characterized by reduced organic carbon content and increased PI compared to the background values.

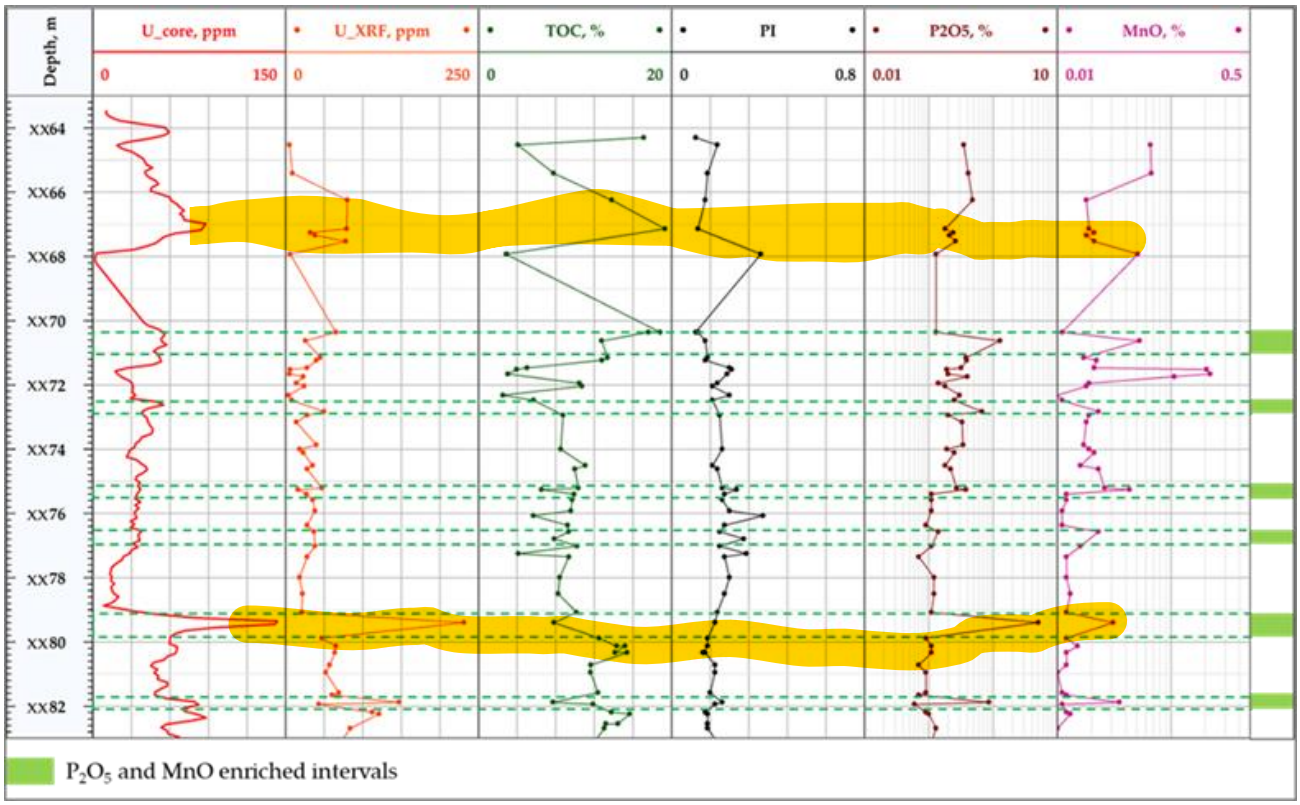

Figure 61. Example of depth distributions of MnO, P_2O_5, and uranium concentration (from gamma-ray spectrometry on core samples and XRF), as well as pyrolytic productivity indices (PI) and total organic carbon (TOC).

Thus, intervals with increased phosphate and pyrolusite content are exceptions to the identified pattern of low uranium content and increased oil saturation. However, these intervals can be identified by higher U/TOC ratios, which can reach the highest values within the Bazhenov interval.

4.6 Classification of productive intervals by uranium content and U/TOC ratio

To classify productive intervals by uranium content, we used the diagram (S_0+S_1) – S_2 (Figure *62*), which was previously used in [Spasennykh et al., 2021] to analyze productive intervals using the pyrolysis data. The maturity values expressed in units of pyrolyzable organic carbon share (K_{goc}) are highlighted in color.

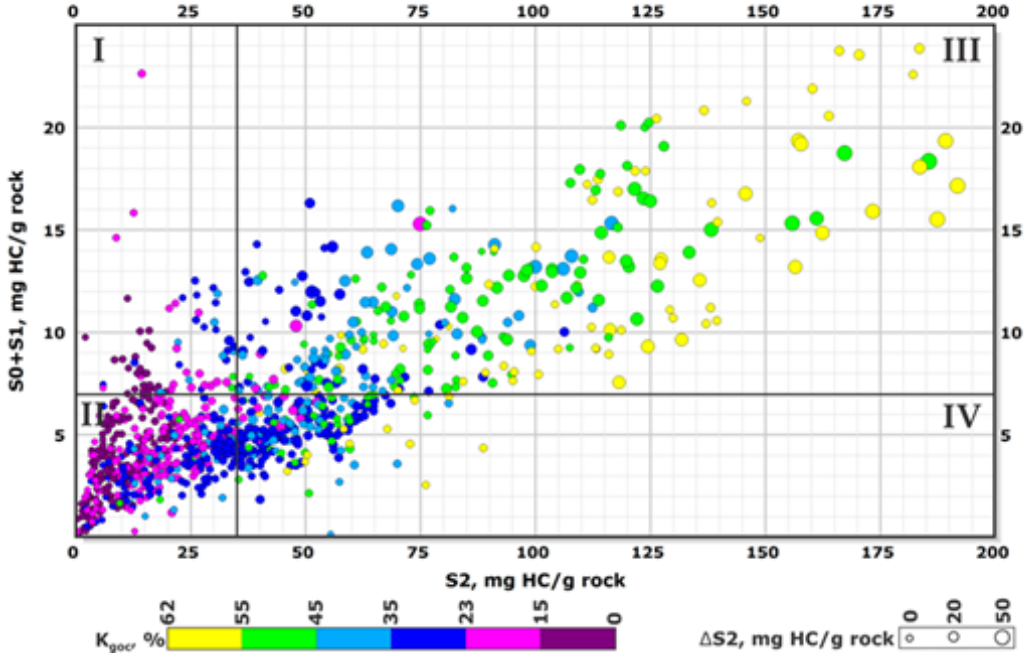

Figure 62. Diagram S_0 + S_1 vs. S_2 [Spasennykh et al., 2021], Quadrants I - IV. The color indicates K_{goc} the proportion of generative organic carbon in TOC wt.%, and the size of dots reflect ΔS_2, mg HC/g TOC.

The authors of [Spasennykh et al., 2021] have identified four quadrants in Figure *62*. Quadrant I includes rock samples with increased reservoir properties and oil saturation (natural reservoirs) intervals. Quadrant II corresponds to the conditional productive reservoirs with low oil saturation that may result from a fluid loss during core recovery and storage. Promising intervals of Quadrant II are characterized by higher values of S_1, OSI, and lower S_2. Quadrant III includes promising intervals for thermal treatment, and Quadrant IV includes intervals unsuitable for oil production. For the analysis, this diagram (Figure *62*) has been supplemented with data on uranium concentration (dot size) and OSI (shown in color).

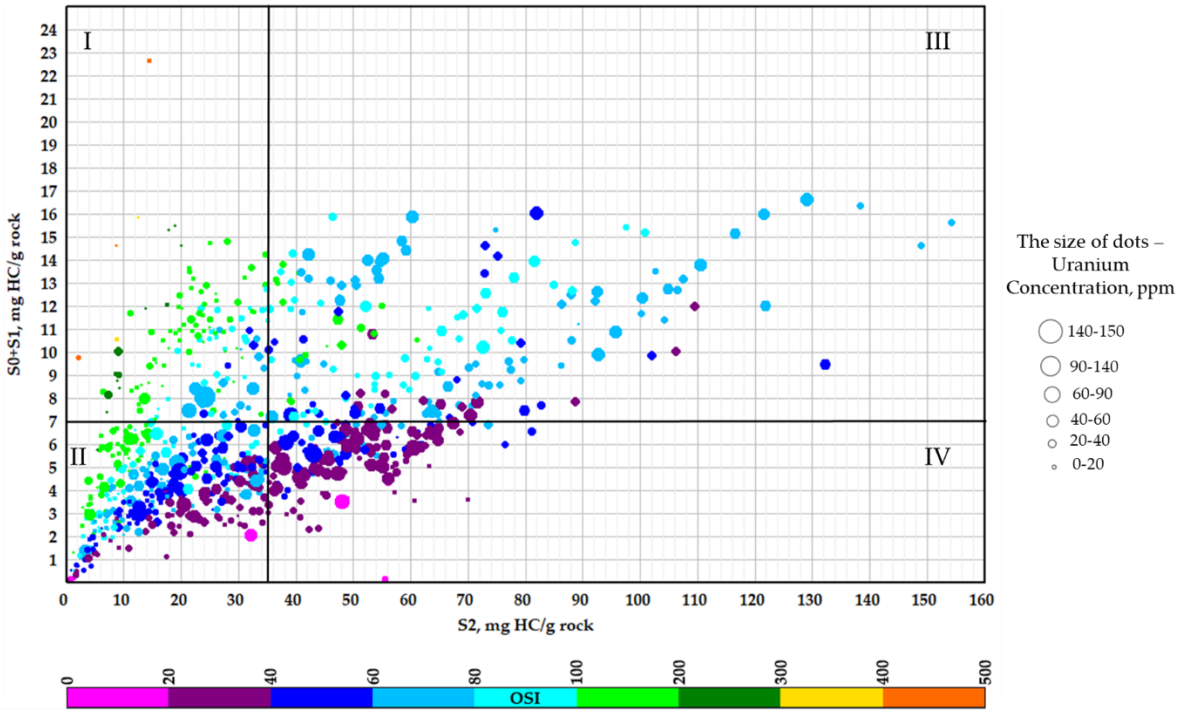

Figure 63. Diagram $S_0+S_1 – S_2$ from core studies of 11 wells. Dot color reflects oil saturation index (OSI), dot size corresponds to the uranium concentration.

Figure *63* illustrates that Quadrants I and II (productive and conditionally productive intervals) are characterized by low uranium content and high OSI values. In contrast, Quadrants III and IV (S_2 > 35 mg HC/g rock) are characterized by higher uranium content and lower OSI. The uranium distributions in these intervals are shown in the diagrams (Figure *64*). Also, box plots for uranium and pyrolytic indices are presented in Figure *65*. Box plots make it possible to consider the distribution of the studied parameters.

For example, the box plot of OSI values is illustrated that the values median: Quadrants I – 110 mg HC/g TOC, Quadrants II - ≈55 mg HC/g TOC, Quadrants III - ≈75 mg HC/g TOC, Quadrants IV - ≈35 mg HC/g TOC. And the box plot of PI values is illustrated that the values median: Quadrants I – 0.26, Quadrants II – 0.18, Quadrants III - ≈0.11, Quadrants IV – 0.08. Moreover, the box plot of U values is shown that the values median: Quadrants I – 16 ppm, Quadrants II – ≈18 ppm, respectively Quadrants III and IV – ≈42 и ≈38 ppm. Also, the box plot of TOC values is shown that the values median: Quadrants I – ≈7 %, Quadrants II – 5 %, respectively Quadrants III and IV – ≈12.5 и ≈11.5 %.

The selected zones differ in all 4 presented parameters (OSI, PI, TOC, U). And these parameters are different not only in median values, but also in the minimum and maximum values.

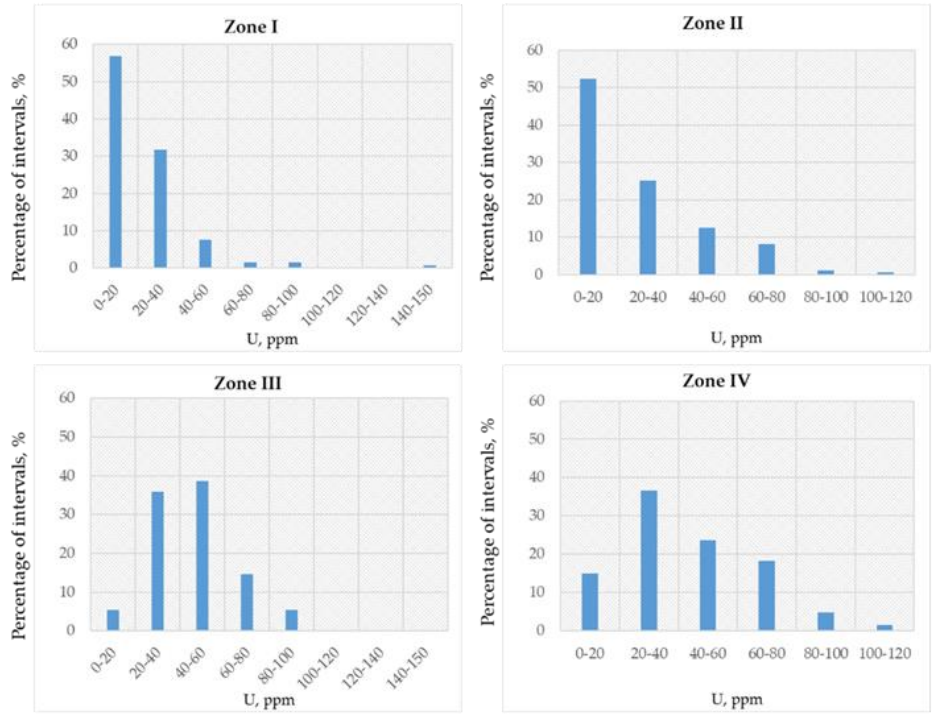

Figure 64. Diagrams of uranium distribution for Quadrants I - IV.

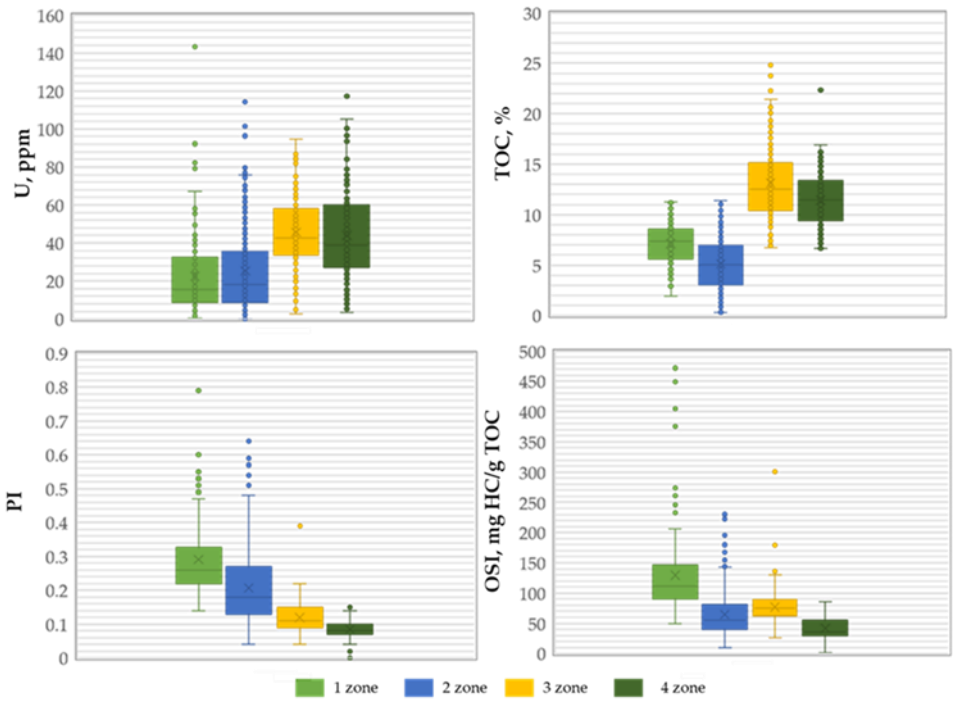

Figure 65. Box-plots for 4 productivity types. Uranium content, TOC, oil saturation, and productivity indices are shown.

From the data presented in Figure *63*, Figure *64*, Figure *65*, we have established the types of productive intervals in terms of the uranium content. The results are summarized in Table *34*.

Table 34. Types of productive intervals as a function of uranium and total organic carbon, U/TOC ratio.

№	Interval type	Average values of U, TOC, U/TOC with standard deviations			Comments
I	Intervals with increased oil saturation and improved reservoir properties. In terms of productivity, they are similar to titght oil reservoirs, for which hydraulic fracturing and multi-stage hydraulic fracturing technologies can be efficiently applied.	U = 23±20 ppm	TOC = 7±2 %	U/TOC = 3±3 ppm U/%TOC	U < 25 ppm for the more than 60% of intervals.
II	Conditionally productive intervals. Differ from the intervals of Quadrant I by lower oil saturation (S_1), which may be associated with partial loss of fluid during sample extraction and storage.	U = 27±22 ppm	TOC = 5±3 %	U/TOC = 6±5 ppm U/%TOC	U < 20 ppm for the more than 50% of intervals. Phosphorite intervals.
III	Oil-saturated source rocks with high potential for developing using thermal EOR, promoting the conversion of kerogen and high-viscosity hydrocarbons into mobile hydrocarbons. The closer the point is to the upright position, the more promising the interval is under thermal treatment.	U = 46±18 ppm	TOC = 13±4 %	U/TOC = 4±1 ppm U/%TOC	20 < U < 60 ppm for the 75% of intervals.
IV	Non-productive intervals, including low maturity rocks, which may be promising for thermal EOR when TOC > 9 %.	U = 45±24 ppm	TOC = 11±3 %	U/TOC = 4±2 ppm U/%TOC	20 < U < 60 ppm for the ≈60% of intervals.

The reported diagrams allow us to establish the relationship between productivity and uranium content of the Bazhenov Formation intervals. U *vs.* TOC, S_0+S_1 *vs.* TOC, and S_0+S_1 *vs.* S_2 plots demonstrate a pronounced difference in the uranium concentration and the organic matter content for productive and non-productive intervals. The U - TOC diagram is a working tool for differentiation of the Bazhenov Formation section. It allows us to distinguish between productive intervals (radiolarians), intervals enrihed in phosphates (P_2O_5), and pyrolusite (MnO), as well as the non-productive part of the section, which differ in uranium and organic matter content. The S_0+S_1 - TOC diagram demonstrates clear differences between the upper, middle, and lower parts of the Bazhenov Formation cross-section [Kozlova, E.V.; Spasennykh, M.YU.; Kalmykov, G.A.; Gutman, I.S.; Potemkin, G.N.; Alekseev, 2017] and can also be applied for the subdivision into members.

4.7 Summary

The analysis of data for 13 wells of the Bazhenov Formation (Western Siberia, Russia) was carried out. The uranium content of the rocks was measured by gamma-ray spectrometry on core samples. In order to analyse factors affecting uranium accumulation in source rocks, we studied content and characteristics of organic matter (Rock-Eval pyrolysis), and mineral, element and isotope composition of rocks. The relationship between the uranium content and the potential productivity of rocks was studied by comparing the data on uranium concentration with the organic matter content and oil saturation index using diagrams S_0+S_1 – TOC and S_0+S_1 – S_2. We have shown that the intervals with the maximum oil saturation index are characterized by uranium content in the range of 1-20 ppm. These intervals should be considered promising for development using multi-stage hydraulic fracturing technologies applied to the low-permeability reservoirs. Intervals with intermediate uranium contents from 20 to 40 ppm should be considered conditionally productive. Greater maturity of organic matter and higher U/TOC ratios can be considered as factors enhancing oil recovery potential.

The intervals with uranium content above 40 ppm and high TOC are characterized by low productivity index and low oil saturation index. For this reason these intervals can be classified as non-promising for oil production. Nevertheless, these intervals may be promising for the production of hydrocarbon generating from kerogen using thermal methods of oil recovery, especially in case of low maturirity of organic matter.

However, the discussed above uranium-based productivity criteria cannot be directly applied to the classification of the phosphorite intervals, which can have high oil saturation for high uranium concentrations (from 20 to 100 ppm).

The obtained results provide the criteria for identifying the productive intervals within the Bazhenov Formation cross-section according to logging data on the uranium content in rocks and neutron logging data (using Lithoscanner) and their classification in terms of the methods for oil production.

Chapter 5. Conclusion

The purpose of the current study was to analyse the factors influencing the uranium accumulation in oil source rocks and highlight the relationship between the uranium concentration and the U/TOC ratio with productivity. The research included the analysis of published data in the area of research, the study of uranium accumulation in the processes of modern marine sedimentation in different redox conditions, the study of factors controlling uranium content source rock formation, and the analysis of relationship between the uranium concentration and the oil saturation on the example the Bazhenov shale oil Formation. Results of the study are summarized below.

Oil source rocks are characterized by increased uranium content, reaching values above 100 ppm. The patterns of the spatial and vertical uranium concentration variations differ significantly for different formations and geological sections. These variations are associated with a number of factors affecting the uranium accumulation during the deposits formation and further geological history.

Following literature review, the main factors affecting on uranium accumulation in marine source rocks include concentration of uranium in seawater, uranium accumulation in marine organisms, continental runoff and sedimentation rate, redox conditions, mineral composition of rocks, organic matter maturity and other. In each particular source rocks formation and even in each particular geological section of formation the abovementioned factors effect and processes on uranium content and the U/TOC ratio could be different. The understanding of these factors provide real opportunity to extract valuable geological information on conditions of source rocks formation, oil generation processes and oil productivity from gamma ray logging data for studied geological objects.

The study of uranium content in modern marine sediments provides an opportunity to analyze the processes and factors affecting uranium accumulation during sedimentation and early diagenesis stages. Main sources of uranium in bottom sediments are continental runoff and uranium dissolved in seawater. Dissolved uranium can be accumulated by marine organisms, absorbed by organic matter and included in mineral phases, formed during sedimentations. We studied marine sediments accumulated in the Kandalaksha bay of the White Sea, the Laptev and East-Siberian Seas (oxidative conditions) and in the Black Sea (oxidative and reductive conditions) using optical microscopy, ICP-MS, CHNS, IRMS, XRD, Eh, pH and temperature measurements. Interpreting results was carried out using thermodynamic modelling uranium

forms in a water-sediment system under different conditions. Sediments in Arctic Seas and shallow shelf of the Black Sea show low uranium (1-3 ppm) and TOC (1-3%) concentrations. Low uranium concentration and correlation between U and TOC show that uranium in studied samples represents uranium in continental runoff and uranium accumulated by marine organisms (or sorbed by organic matter). Not a considerable increase of uranium concentration with depth, where Eh values are considerably decreased by comparison with seawater, shows that some small amount of uranium could be accumulated in sediments due to formation of insoluble uranium phases. Increase in uranium concentrations (up to 35 ppm) is a typical for marine sediments formed in reducing conditions of the Black Sea at the depth more 200 m where bottom water contents high concentration of H_2S and Eh values are negative (~-200 mV). Under reducing conditions and presence of H_2S in the bottom water, increased uranium accumulation is associated with its transition from soluble to an insoluble form and sorption of uranium by organic matter. Thus, the main factor affecting on accumulation of uranium accumulation in marine sedimentation processes is redox conditions in bottom water. In reducing conditions uranium content increases due to formation of insoluble uranium containing phases and sorption at organic matter. In the case of the presence of oxygen in the water (shallow sea depth, intense water exchange), the uranium content in sediments is related to its concentration in the mineral components of continental runoff and to the uranium concentration in marine organisms since some species can accumulate uranium from seawater. In both cases, higher uranium content in seawater and higher organic carbon concentration lead to an increase in uranium accumulation in sediments. Decrease of Eh with depth may also lead to uranium accumulation in sediments, but this is not a considerable effect because of the limited uranium amount in pore water.

The study of uranium content in the Bazhenov Formation provides an opportunity to analyze the factors affecting uranium accumulation in the source rocks and studying the relationship between uranium content and productivity. We have explored almost 1000 core samples from 13 wells of the Bazhenov Formation and we used the next methods for analysing: gamma spectrometry on core, pyrolysis, thermal core logging, XRF analysis, IRMS, also lithological description. The study of uranium content in 13 wells of the Bazhenov source rock Formation also indicate the considerable role of redox conditions. First, we found a positive correlation of uranium content with the concentration of other redox sensitive elements (for example, the positive correlation between uranim and vanadium concentrations) and element ratios, which are also sensitive to the redox conditions (for example, the positive correlation between uranim

and the ratio Mo/(Mo+Mn)). The other evidences are positive correlations of uranium with content sulfur (in pyrite form) and negative correlation with isotope composition of sulfur in rocks, which are depends on redox conditions. One more evidence is negative correlation of uranium content with Rock-Eval oxygen index, which is increasing at oxidative conditions. The study of the Bazhenov Formation demonstrate, that the mineral composition is also an important factor for uranium content in rocks. We found, that presence of phosphate minerals may considerably increase uranium content in rocks due to highn uranium concentration in these mineral phases. It was also found, that increase in organic matter maturation leads to an increase of uranium content. The maturation causes a decrease of the organic carbon in rocks due to conversion of kerogen to mobile hydrocarbons. The considerable part of mobile hydrocarbons is usually migrate from source rocks to other formations. Amount of kerogen in the end of oil window could be in 2-3 times less by comparison with its initial content. In these conditions the uranium concentration in the rock is increasing proportionally decrease of the kerogen content, because the uranium concentration in oil and gas is negligible by comparison with concentration in solid kerogen. Thus, redox conditions at sedimentations stage play a leading role in uranium accumulation in rocks, however the presence of phosphate minerals and high maturation of organic matter may considerably increase uranium content in source rocks. These factors should be taken into account for interpretation of the data on uranium content.

According literature review and experimental data, we can compare uranium concentrations in the different conditons: sea water, marine organisms, the bottom sediments (on the sedimentation stage) and in the unconventional reservoirs rocks on the example of the Bazhenov Formation (Figure *66*).

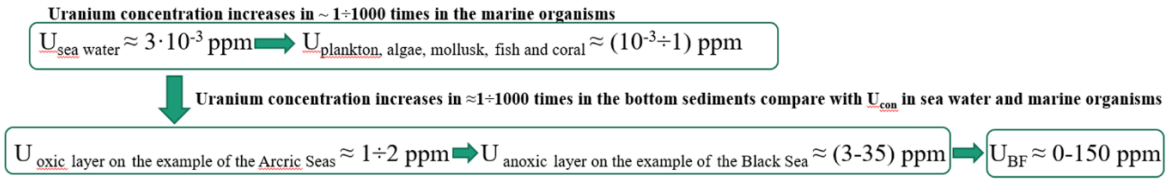

Figure 66. The scheme of the uranium concentrations difference in the sea water, marine organisms, bottom sediments in different redox conditions (on the example of the Arctic Seas and the Black Sea) and in the Bazhenov Formation.

Initial uranium concentration in the sea water is 0.003 ppm, marine organisms in the process of life accumulate uranium and uranium concentration varies approximately $U_{plankton,\ algae,\ mollusk,\ fish\ and\ coral}$=0.001÷1 ppm. It can be seen that the uranium concentration in marine organisms can

be 1000 times greater than the uranium concentration in sea water. If we look at the uranium content in marine sediments, we will see that in the oxidizing layer based on experimental data from the study of the Arctic Seas marine sediments, the uranium concentration reaches 2 ppm, increasing by 10÷1000 times compared to the uranium concentration in marine organisms. Uranium concentrations increase in bottom sediments with anoxic conditions up to 10 times compared to sediments formed under oxidizing conditions. Similarly, the uranium concentration increases almost 10 times in the Bazhenov Formation rocks in comparison with the uranium concentration in the Black Sea sediments under reducing conditions. Generalizing the described scheme, we can say that in the process of the sediments formation, and then their transformation into rocks, we see a constant accumulation and an increase in the uranium concentration.

The study of relationship between uranium content and productivity shows that higher oil saturation is associated with intervals characterizing by low uranium content. It could be explained by better collector properties of the rocks formed in oxidative conditions. These intervals, formed in the presence of oxygen are usually bioturbated, contains remains shells and skeletons of marine organisms, which form void space saturating with hydrocarbons during oil forming processes. It should be also considered, that formation of pores in kerogen during maturation leads to a considerable increase of secondary porosity, which also may contain mobile hydrocarbons. However, the permeability of such kerogen containing and potentially productive intervals formed in reducing conditions are usually considerably lower by comparison with abovementioned intervals formed in oxidizing conditions and should be considered as a different type of productive intervals. Joint analysis of data on uranium content and the Rock-Eval pyrolysis data with considering conditions of sedimentation allowed us to formulate criteria for the selection and typification of productive intervals in source rocks formation based on the data on uranium content.

We have shown that the intervals with the maximum oil saturation index are characterized by uranium content in the range of 1-20 ppm. These intervals should be considered promising for development using multi-stage hydraulic fracturing technologies applied to the low-permeability reservoirs. Intervals with intermediate uranium contents from 20 to 40 ppm should be considered conditionally productive. Greater maturity of organic matter and higher U/TOC ratios can be considered as factors enhancing oil recovery potential. The intervals with uranium content above 40 ppm and high TOC are characterized by low productivity index and low oil saturation index. For this reason, these intervals can be classified as non-promising for oil

production. Nevertheless, these intervals may be promising for the production of hydrocarbon generating from kerogen using thermal methods of oil recovery, especially in case of low maturity of organic matter. The discussed above uranium-based productivity criteria cannot be directly applied to the classification of the phosphate intervals, which can have high oil saturation for high uranium concentrations (from 20 to 100 ppm). However, these intervals could be identified by increased value of U/TOC ratio.

A new approach to the Bazhenov Formation sections characterization was shown in the joint analysis of the uranium, organic carbon with a resolution of 1-2 mm (the thermal core logging is used to determine TOC) and the U/TOC ratio results distribution for 9 wells. Combined uranium, TOC and U/TOC ratios analysis makes it possible to determine deposition environment and natural reservoirs intervals. This approach is described in the patent, which shows the evaluation and calculation procedure in more detail.

Following abovementioned conclusions, we also may formulate criteria for geological sections of oil shale formations, which could be considered as the most promising for oil production based on uranium content data. Considering, that (1) the intervals with the highest values of uranium content should contain high concentrations of organic matter of high maturity (which means a high amount of produced hydrocarbons) and (2) the intervals with lowest uranium content are characterized by better collector properties (which means better conditions for accumulation), the sections, containing intervals with high and low uranium content should be considered as the most promising for oil production. Geological sections analysis with the uranium and organic carbon concentrations distribution in the depth in order to classify well sections into productive, low-yield and unproductive can be recommended for further research.

The obtained results provide the criteria for identifying the productive intervals within the Bazhenov Formation cross-section according to logging data on the uranium content in rocks and neutron logging data (using Lithoscanner) and their classification in terms of the methods for oil production.

Bibliography

1. Anderson R. F., Fleisher M. Q., LeHuray A. P. Concentration, oxidation state, and particulate flux of uranium in the Black Sea // Geochim. Cosmochim. Acta. 1989. V. 53. № 9.

2. Babinec, A. E., Bezborodov, A. A., Mitropol'skij A. Y. Formy nahozhdeniya urana v chernomorskoj vode // Geol. zhurn. 1977. V. 37. № 5.

3. Baioumy H., Lehmann B. Anomalous enrichment of redox-sensitive trace elements in the marine black shales from the Duwi Formation, Egypt: Evidence for the late Cretaceous Tethys anoxia // J. African Earth Sci. 2017. P. 133.

4. Barnes C. E., Cochran J. K. Geochemistry of uranium in Black Sea sediments // Deep. Res. Part A. 1991. V. 38. № Suppl. 2A.

5. Bastrakov E. и др. Uranium in organic-rich shales as a tool for predicting hydrocarbon potential: Proterozoic to Cretaceous examples from Australia // Org. Geochemistry Conf. Orig. Oil, Old Org. Org. Progr. Abstr. 2018. № August. P. 39–40.

6. Baturin G. N. Uran v sovremennom morskom osadkoobrazovanii // Atomizdat. 1975.

7. Baturin G. N. Fosfatonakoplenie v okeane. Moscow: Nauka, 2004.

8. Behar F., Beaumont V., B. Penteado H. L. De. Rock-Eval 6 Technology: Performances and Developments // Oil Gas Sci. Technol. 2001. V. 56. № 2.

9. Belyaev N. A. Organic Matter and Hydrocarbon Markers of the White Sea // 2015.

10. Bone S. E. и др. Uranium(IV) adsorption by natural organic matter in anoxic sediments // Proc. Natl. Acad. Sci. U. S. A. 2017. V. 114. № 4. P. 711–716.

11. Boreham C. H. K. Vertical Geochemical Profling of the Marine Toolebuc Formation, Eromanga Basin-Implications for Shale Gas/oil Potential, 2012.

12. Braduchan Y. V. и др. Bazhenovskij Gorizont Zapadnoj Sibiri (Stratigrafiya, Paleogeografiya, Ekosistema, Neftenosnost') // 1986. P. 217.

13. Chappaz A., Gobeil C., Tessier A. Controls on uranium distribution in lake sediments // Geochim. Cosmochim. Acta. 2010. V. 74. № 1.

14. Chuvilin, B. Bukhanov, A. Yurchenko, D. Davletshina, N. Shakhova, E. Spivak, V. Rusakov, O. Dudarev, N. Khaustova, A. Tikhonova, O. Gustafsson, T. Tesi, J. Martens, M. Jakobsson, M. Spasennykh I. S. In-situ temperatures and thermal properties of the East Siberian Arctic shelf sediments: Key input for understanding the dynamics of subsea permafrost // Mar. Pet. Geol. 2022.

15. Coplen T. B. и др. Compilation of minimum and maximum isotope ratios of selected elements in naturally occurring terrestrial materials and reagents // Usgs. 2002.

16. Coretest Systems I. EGL-255 Profil'nyj gamma-registrator (spektral'nyj) Rukovodstvo pol'zovatelya // 2012.

17. Cumberland S. A. и др. Uranium mobility in organic matter-rich sediments: A review of geological and geochemical processes // Earth-Science Rev. 2016. V. 159.

18. Dakhnova, M.V.; Mozhegova, S.V.; Nazarova, E.S.; Paizanskaya I. L. Evaluation of reserves of shale oil using geochemical parameters // Geol. Neft. i gaza. 2015. V. 4. P. 55–61.

19. Demaison G. J., Moore G. T. Anoxic environments and oil source bed genesis // Org. Geochem. 1980. V. 2. № 1.

20. Dudaev S. A. Izuchenie estestvennoj radioaktivnosti glinistyh kollektorov po rezul'tatam gamma-spektrometrii kerna // Karotazhnik. 2011. № 6. P. 12–25.

21. Dudaev S. A. PETROFIZICHESKIE PREDPOSYLKI IZUCHENIYA GLINISTYH KOLLEKTOROV PREDKAVKAZ'YA PO DANNYM GAMMA-SPEKTROMETRII // Karotazhnik. 2011. P. 12–25.

22. Elbaz-Poulichet F. и др. Sedimentary record of redox-sensitive elements (U, Mn, Mo) in a transitory anoxic basin (the Thau lagoon, France) // Mar. Chem. 2005. V. 95. № 3–4.

23. Emec T.P. L. N. V. Piroliz V Neftegazovoj Geohimii, 1987. 144 p.

24. Espitalie J., Marquis F., Barsony I. GEOCHEMICAL LOGGING, 1984.

25. Fertl W. H., Rieke H. H. GAMMA RAY SPECTRAL EVALUATION TECHNIQUES IDENTIFY FRACTURED SHALE RESERVOIRS AND SOURCE-ROCK CHARACTERISTICS. // JPT, J. Pet. Technol. 1980. V. 32. № 11.

26. Fomin A. N. и др. Scheme of organic matter catagenesis in the top of the Upper Jurassic deposits of the West Siberian basin // 2004.

27. Galimov E. M. и др. Carbon isotope and biogeochemical studies of the Kara Sea—Yenisei and Ob river systems // Geochim. Cosmochim. Acta. 2006. V. 70. № 18.

28. Garrels R., Christe C. L. Solutions, Minerals, and Equilibria. New York: Harper & Row: New York, 1965.

29. Goncharov I. V. и др. Petroleum generation and migration in the southern Tyumen region, Western Siberia Basin, Russia // Org. Geochem. 2021. V. 152.

30. Gudok N. S., Bogdanovich N. N. M. V. G. OPREDELENIE FIZICHESKIH SVOJSTV NEFTEVODOSODERZHASHCHIH POROD. Moskva: Izdatel'stvo «Nedra», 2007. 592 p.

31. Gurskij Y. N. RASPREDELENIE MIKROELEMENTOV V ILOVOJ VODE I DONNYH OSADKAH CHERNOGO MORYA // Vestn. Mosk. Univ. 2019. V. 4. № 1. P. 14–25.

32. Gursky Y. N. Metody izucheniya i processy formirovaniya himicheskogo sostava ilovyh vod otlozhenij Chernogo, Azovskogo, Kaspijskogo, Belogo i Baltijskogo morej // Geohim. Litogidrosfery Vnutr. Morej. 2003. V. 1.

33. Gursky Y. N. Zakonomernosti povedeniya mikroelementov v sisteme ilovye vody-osadki Chernogo morya // XXIII MEZHDUNARODNAYA NAUCHNAYA KONFERENCIYA (SHKOLA) PO MORSKOJ GEOLOGII «GEOLOGIYA MOREJ I OKEANOV». Moscow, 2019. P. 18–22.

34. Idrisova E. и др. Pyrite morphology and δ34S as indicators of deposition environment in organic-rich shales // Geosci. 2021. V. 11. № 9.

35. Jarvie D. M. Shale resource systems for oil and gas: Part 2—shale-oil resource systems // AAPG Memoir, 2012.

36. Kalmykov, A. G., Karpov, YU. A., Topchij, M. S., Fomina, M. M., Manuilova, E. A., SHeremet'eva, E. V., ... & Kalmykov G. A. Vliyanie katageneticheskoj zrelosti na formirovanie kollektorov s organicheskoj poristost'yu v bazhenovskoj svite i osobennosti ih

rasprostraneniya // GEORESURSY. 2019. V. 21. № 2. P. 159–171.

37. Kalmykov A. G. и др. Fosfatsoderzhashchie prosloi bazhenovskoj svity kak vozmozhnyj kollektor // Vestn. Mosk. Univ. 2016. V. 4. № 5. P. 60–66.

38. Karpov Y. A. и др. Kriterii rasprostraneniya nefteproduktivnyh porod bazhenovskoj vysokouglerodistoj formacii s razvitoj sistemoj porovoj emkosti v kerogene // Vestn. Mosk. Univ. 2019. V. 4. № 2. P. 58–71.

39. Kasimov N. S., Vlasov D. V. Clarkes of chemical elements as comparison standards in ecogeochemistry // Vestn. Mosk. un-ta. Ser. 5. Geolografiya. 2015. V. 2. P. 7–17.

40. Khaustova N. и др. U/Corg ratio within unconventional reservoirs: Indicator of oil generation processes and criteria for productive intervals determination during the Bazhenov formation investigation // EAGE/SPE Workshop on Shale Science 2019 - Shale Sciences: Theory and Practice, 2019.

41. Khaustova N. и др. The study of uranium accumulation in marine bottom sediments: Effect of redox conditions at the time of sedimentation // Geosci. 2021. V. 11. № 8.

42. Kizil'shtejn, L. YA., CHernikov B. A. Rol' organicheskogo veshchestva zemnoj kory v obrazovanii mestorozhdenij urana. Rostov-na-Donu: Izd-vo Rostovskogo universiteta, 1999.

43. Kontorovich A. E. и др. Classification of Rocks of the Bazhenov Formation // Geologiya I Geofizika. 2016. № 11.

44. Kontorovich A. E. и др. Geochemistry and catagenetic transformation of kerogen from the bazhenov horizon // Geohimiya. 2019. V. 64. № 6. P. 585–593.

45. Kozlova, E.V.; Spasennyh, M.YU.; Kalmykov, G.A.; Gutman, I.S.; Potemkin, G.N.; Alekseev A. D. Balans uglevodorodnyh soedinenij neftyanogo ryada v pirolizuemom organicheskom veshchestve bazhenovskoj svity // Neft. hozyajstvo. 2017. V. 3. P. 18–21.

46. Kozlova E. V и др. Tekhnologiya izucheniya geohimicheskih parametrov organicheskogo veshchestva v kerogenonasyshchennyh otlozheniyah (na primere bazhenovskoj svity, Zapadnaya Sibir') // Vestn. Mosk. Univ. 2015. V. 8. P. 44–53.

47. Kulyapin P. S. Razrabotka interpretacionnoj i petrouprugoj modelej porod-kollektorov mnogokomponentnogo sostava i slozhnoj struktury emkostnogo prostranstva // 2016.

48. Kuznetsov V. A. Associaciya mikroelementov s organicheskim veshchestvom v osadochnyh tolshchah Sibiri. Novosibirsk: Institute of Geology and Geophysics SB AS USSR, 1984. 157 p.

49. Langford F. F., Blanc-Valleron M. M. Interpreting Rock-Eval pyrolysis data using graphs of pyrolizable hydrocarbons vs. total organic carbon // Am. Assoc. Pet. Geol. Bull. 1990. V. 74. № 6. P. 799–804.

50. Lein A. Y. Izuchenie morej rossijskoj Arktiki: myslitel'nye processy // Priroda. 2004. P. 11–19.

51. Leushina E. и др. Upper jurassic–lower cretaceous source rocks in the north of western siberia: Comprehensive geochemical characterization and reconstruction of paleo-sedimentation conditions // Geosci. 2021. V. 11. № 8.

52. Lisitsyn A. P., Gursky Y. N. Geohimiya litogidrosfery vnutrennih morej. Tom 1 [Электронный ресурс]. URL: https://www.rfbr.ru/rffi/ru/books/o_64276#1.

53. Lüning S., Kolonic S. Uranium spectral gamma-ray response as a proxy for organic richness in black shales: Applicability and limitations // J. Pet. Geol. 2003. V. 26. № 2.

54. Maende A., David Weldon W. Pyrolysis and TOC identification of tight oil sweet spots // Unconventional Resources Technology Conference 2013, URTC 2013, 2013.

55. Mangini A., Jung M., Laukenmann S. What do we learn from peaks of uranium and of manganese in deep sea sediments? // Mar. Geol. 2001. V. 177. № 1–2.

56. Mann U., Müller P. J. Source rock evaluation by well log analysis (Lower Toarcian, Hils syncline) // Org. Geochem. 1988. V. 13. № 1–3.

57. Manskaya S. M. Geohimiya organicheskogo veshchestva, 1964.

58. Melenevsky V. N., Klimin M. A., Tolstokorov S. V. A study of the diagenesis of organic matter of peat using Rock Eval pyrolysis // Geohimiya. 2019. V. 64. № 2. P. 206–211.

59. Mironenko M. V., Akinfiev N. N., Melikhova T. Y. GEOCHEQ—The complex for thermodynamic modeling of geochemical systems // Vestn. OGGGN RAN. 2000. V. 5. № 15. P. 96–97.

60. Miroshnikov A. Y. et al. Ekologicheskoe sostoyanie i mineralogo-geohimicheskie harakteristiki donnyh osadkov Vostochno-Sibirskogo morya // Okeanologiya. 2020. V. 60. № 4. P. 595–610.

61. Nemova V.D. P. I. V. Faktory produktivnosti bazhenovskogo gorizonta vo Frolovskoj megavpadine // Neftegazov. Geol. Teor. i Prakt. 2017. V. 12. № 4. P. 16.

62. Neprochnov Y. P. Geological history of the Black Sea: On the results of deep-water drilling (in Russian). : Nauka, 1980. 212 p.

63. Neruchev S. G. Uran i zhizn’ v istorii Zemli. Sankt-Peterburg: VNIGRI, 2007. 328 p.

64. Nesterov I. I. BITUMINOUS CLAY AND SILICEOUS-CLAY ROCKS – A NEW GLOBAL SOURCE OF FUEL-AND-ENERGY RAW MATERIALS // Geol. poiski i Razved. mestorozhdenij Neft. i gaza. 2011. № 6. P. 8–34.

65. Newton R., Bottrell S. Stable isotopes of carbon and sulphur as indicators of environmental change: Past and present // J. Geol. Soc. London. 2007. V. 164. № 4.

66. Novikov M. A. K voprosu o fonovyh znacheniyah urovnej soderzhaniya tyazhelyh metallov v donnyh otlozheniyah Barenceva morya // Vestn. Murm. Gos. tekhnicheskogo Univ. 2017. V. 20.

67. Panchenko I. V. и др. Stratification and detailed correlation of Bazhenov Horizon in the central part of the Wetern Siberia according to lithological and paleontological core analysis and well logging // Oil gas Geol. 2016. V. 6. P. 22–34.

68. Parfenova, T. M., Melenevskij, V. N., Moskvin V. I. Ispol’zovanie gamma-karotazha dlya opredeleniya soderzhaniya organicheskogo veshchestva v vysokouglerodistyh osadochnyh formaciyah (na primere Bazhenovskoj svity) // Neft. i Gazov. promyshlennost’. Geol. Geofiz. i Razrab. Neft. mestorozhdenij. 1999. № 11. P. 29–34.

69. Partin C. A. и др. Large-scale fluctuations in Precambrian atmospheric and oceanic oxygen levels from the record of U in shales // Earth Planet. Sci. Lett. 2013. V. 369–370.

70. Popov Y. и др. ISRM Suggested methods for determining thermal properties of rocks from

laboratory tests at atmospheric pressure. // Rock Mech. Rock Eng. 2016. V. 49. № 10.

71. Rihvanov L. P. et al. CHernye slancy bazhenovskoj svity // Neftegaz. 2019. № 6. P. 32–39.

72. Rolison J. M. и др. Uranium stable isotope fractionation in the Black Sea: Modern calibration of the 238U/235U paleo-redox proxy // Geochim. Cosmochim. Acta. 2017. V. 203.

73. Rozanov, A.G.; Gursky Y. N. Geohimicheskie osobennosti osadkov v severo-vostochnoj chasti Chernogo morya // Okeanologiya. 2016. P. 919–934.

74. Rozanov, A.G.; Kokratskaya, N.M.; Gursky Y. N. Sostav ilovyh vod i formy soedinenij sery v donnyh otlozheniyah severo-vostochnoj chasti Chernogo morya. // Litol. Polezn. Iskop. 2017. P. 291–305.

75. Rozanov A. G., Volkov I. I., Emelyanov E. M. Redoks-sistema donnyh otlozhenij Belogo morya: Zhelezo, marganec, sera // White Sea Syst. Process. Sedimentation, Geol. Hist. 2012. V. 4. P. 639–661.

76. Ruban A. S. Geohimicheskie Osobennosti Sovremennyh Donnyh Osadkov Vostochnoj CHasti Morya Laptevyh (Na Primere Guby Buor-Haya) // 2017.

77. Savenko A. V. B. G. N. Eksperimental’noe izuchenie pogloshcheniya uranil-ionov okeanskimi fosforitami // Radiohimiya. 2002. V. 44. № 5. P. 443–444.

78. Serra O. Petroleum Engineering: The Fundamentals of Well Log Interpretation 1.the acquisition of logging data, 1964. 560 p.

79. SHakirov, R. V. Sorochinskaya, A. V. Obzhirov A. I. Nekotorye gazogeohimicheskie osobennosti osadkov Vostochno-Sibirskogo morya // Reg. Probl. 2012. V. 15. № 1.

80. SHakirov R. B. et al. Gazogeohimicheskie osobennosti osadkov Vostochno-Sibirskogo morya // Vestn. Dal’nevostochnogo Otd. Ross. Akad. Nauk. 2010. № 6.

81. Shnyukov, E.F.; Bezborodov, A.A.; Melnik, V.I.; Mitropolsky A. Y. Geohimicheskaya evolyuciya urana v Chernom more // Geol. Zhurn. 1979. P. 1–9.

82. Sklyarov E. V. Klimaticheskaya istoriya golocena Zapadnogo Pribajkal’ya v karbonatnoj osadochnoj letopisi ozera Holbo-Nur // Dokl. Akad. Nauk. 2010. V. 431. № 5. P. 668–674.

83. SPASENNYKH, M.YU., CHEKHONIN, E. M., POPOV, YU. A., POPOV, E. YU., KOZLOVA, E. V., HAUSTOVA N. A. SPOSOB I USTROJSTVO DLYA PROFILIROVANIYA SVOJSTV OBRAZCOV POROD NEFTEMATERINSKIH SLANCEVYH TOLSHCH // 2021.

84. Spasennykh M. и др. Geochemical trends reflecting hydrocarbon generation, migration and accumulation in unconventional reservoirs based on pyrolysis data (On the example of the bazhenov formation) // Geosci. 2021. V. 11. № 8.

85. Swanson V. E. Oil yield and uranium content of black shales: uranium in carbonaceous rocks // USGS Prof. Pap. 1960.

86. Swanson V. E. Geology and geochemistry of uranium in marine black shales. A review. Uranium in Carbonaceous rocks // 1961. P. 356.

87. Tyson R. V., Pearson T. H. Modern and ancient continental shelf anoxia // Mod. Anc. Cont. shelf anoxia. 1991. № 58. P. 1–24.

88. Udovich Y. E., Ketris M. P. Sootnosheniya izotopov ugleroda v stratisfere i biosfere: chetyre scenariya // Biosfera. 2010.

89. Ulmishek G. F. Petroleum Geology and Resources of the West Siberian Basin, Russia // U.S. Geol. Surv. Bull. 2003.

90. Vosel J. S. Geohimiya Urana v Sovremennyh Karbonatnyh Otlozheniyah Malyh Ozer (Formy Nahozhdeniya i Izotopnye Otnosheniya 234U/238U) // 2016.

91. Vtorushina E. A., Bulatov T. D. HARAKTERISTIKA ORGANICHESKOGO VESHCHESTVA PORODDLYA BASSEJNOVOGO. MODELIROVANIYA NA OSNOVE DANNYH PIROLIZATORA HA WK // Modelirovanie geologicheskogo stroeniya i processov razrabotki - osnova uspeshnogo osvoeniya neftegazovyh mestorozhdenij. Kazan': Izdatel'stvo «Slovo», 2018. P. 167–169.

92. Wignall P. B., Myers K. J. Interpreting benthic oxygen levels in mudrocks: A new approach // Geology. 1988. V. 16. № 5.

93. Zamirailova A. G., Eder V. G. Chalcophile Elements in Black Shales of the Bazhenov Formation, West Siberian Sea Basin // Geologiya I Geofizika. 2016. V. 57. № 4. P. 771–781.

94. Zanin Y. N., Zamirajlova A. G., Eder V. G. Nekotorye Aspekty Formirovaniya Bazhenovskoj Svity V Central'nyh Rajonah Zapadno-Sibirskogo Osadochnogo Bassejna // Litosfera. 2005. № 4. P. 118–135.

95. Zanin Y. N., Zamirajlova A. G., Eder V. G. Uran, Torij I Kalij V CHernyh Slancah Bazhenovskoj Svity Zapadno-Sibirskogo Morskogo Bassejna // Litol. I Polezn. Iskop. 2016. V. 2016. № 1. P. 82–94.

96. Zanin Y. N., Zamirajlova A. G., Eder V. G. Nikel', Molibden, Kobal't V CHernyh Slancah Bazhenovskoj Svity Zapadno-Sibirskogo Morskogo Bassejna, «Geohimiya» // Geohimiya. 2017. № 2. P. 161–170.

97. Zubkov M. Y. Osobennosti raspredeleniya urana v bituminoznyh otlozheniyah bazhenovskoj svity (Zapadnaya Sibir') // Karotazhnik. 2015. № 5. P. 3–32.

98. https://intl.siyavula.com/read/science/grade-9/the-lithosphere/24-the-lithosphere?id=toc-id-3.

99. http://www.izmteh.ru/esr/esr-10104/.

100. Instrument: CHN628 Series w/Sulfur Add-On Module (S628), 2014.

101. Instrument: CHN628, 2016.

Appendix A

Table 35. The distribution of the uranium concentration (U), the organic carbon (TOC) and the ratio U/TOC for the wells 3, 4, 5.

Depth, m	TOC thermal, %	U, ppm	U/TOC thermal	Depth, m	TOC thermal, %	U, ppm	U/TOC thermal	Depth, m	TOC thermal, %	U, ppm	U/TOC thermal
Well 3				Well 4				Well 5			
2825.31	1.81	5.40	3.0	3163.57	5.59	10.57	1.9	3448.55	3.80	3.21	0.8
2825.41	1.97	5.40	2.7	3163.67	5.61	14.36	2.6	3448.65	4.51	9.26	2.1
2825.51	0.73	8.20	11.3	3163.77	5.71	20.39	3.6	3448.75	7.15	3.07	0.4
2825.61	0.64	5.90	9.2	3163.88	9.20	38.19	4.1	3448.85	6.65	5.11	0.8
2825.71	0.59	3.90	6.6	3163.98	15.74	55.99	3.6	3448.95	4.43	2.80	0.6
2825.81	0.68	6.40	9.4	3164.13	18.68	59.55	3.2	3449.05	5.27	4.19	0.8
2825.91	0.77	5.50	7.1	3164.23	29.50	55.71	1.9	3449.15	6.51	4.36	0.7
2826.01	0.86	2.20	2.5	3164.33	18.52	44.15	2.4	3449.25	6.88	5.06	0.7
2826.11	0.96	8.20	8.6	3164.44	18.67	26.90	1.4	3449.35	7.08	0.95	0.1
2826.26	1.09	8.50	7.8	3164.54	9.75	18.79	1.9	3449.45	8.25	3.16	0.4
2826.36	1.19	9.50	8.0	3164.64	7.04	22.62	3.2	3449.55	6.70	1.32	0.2
2826.46	1.28	9.90	7.7	3164.74	9.53	30.48	3.2	3449.65	4.28	2.84	0.7
2826.56	1.37	9.10	6.6	3164.84	11.81	34.39	2.9	3449.75	3.46	3.04	0.9
2826.66	1.46	9.00	6.2	3164.95	12.67	39.15	3.1	3449.85	4.75	2.00	0.4

2826.76	1.40	11.80	8.4	3165.14	16.12	41.86	2.6	3449.95	3.73	1.34	0.4
2826.86	1.43	11.30	7.9	3165.24	20.27	46.58	2.3	3450.05	2.71	2.12	0.8
2826.96	1.62	10.50	6.5	3165.35	19.84	40.86	2.1	3450.25	3.69	2.30	0.6
2827.06	1.81	10.50	5.8	3165.45	14.73	41.20	2.8	3450.35	3.89	1.87	0.5
2827.16	2.63	13.50	5.1	3165.55	16.33	44.22	2.7	3450.45	2.90	1.00	0.3
2827.26	4.93	13.30	2.7	3165.65	18.83	49.28	2.6	3450.65	2.85	1.06	0.4
2827.36	6.26	13.40	2.1	3165.75	15.22	50.98	3.3	3450.85	7.30	3.14	0.4
2827.46	5.98	10.90	1.8	3165.86	15.18	45.75	3.0	3450.95	3.97	0.26	0.1
2827.58	5.64	9.20	1.6	3165.96	19.59	45.02	2.3	3451.15	2.19	0.43	0.2
2827.68	5.36	8.80	1.6	3166.16	16.22	60.18	3.7	3451.35	2.84	1.49	0.5
2827.78	4.00	13.90	3.5	3166.26	15.29	60.89	4.0	3451.45	3.45	3.91	1.1
2827.88	3.18	16.20	5.1	3166.36	16.83	65.11	3.9	3451.75	4.46	2.33	0.5
2827.98	2.22	17.10	7.7	3166.47	23.59	67.84	2.9	3451.85	2.75	5.00	1.8
2828.08	1.56	16.70	10.7	3166.57	20.32	71.06	3.5	3451.95	1.28	5.00	3.9
2828.38	2.59	17.60	6.8	3166.67	22.09	67.92	3.1	3452.05	1.10	1.37	1.2
2828.48	3.88	17.20	4.4	3166.77	22.59	70.61	3.1	3452.25	2.90	4.87	1.7
2828.58	3.89	16.10	4.1	3166.87	16.99	71.07	4.2	3452.35	3.26	4.07	1.2
2828.68	3.89	15.40	4.0	3166.98	21.86	87.89	4.0	3452.45	3.41	9.10	2.7
2828.78	3.90	11.10	2.8	3167.18	27.70	84.32	3.0	3452.55	6.12	8.75	1.4
2828.88	4.29	10.80	2.5	3167.28	30.55	64.37	2.1	3452.65	9.07	20.35	2.2
2828.98	4.49	9.00	2.0	3167.38	21.61	56.14	2.6	3452.75	9.31	26.76	2.9

2829.08	3.86	9.70	2.5	3167.48	22.15	52.39	2.4	3452.85	8.17	27.14	3.3
2829.18	3.30	8.90	2.7	3167.59	26.96	48.78	1.8	3452.95	9.11	26.20	2.9
2829.28	2.73	8.40	3.1	3167.69	24.42	41.22	1.7	3453.05	9.73	33.36	3.4
2829.38	1.92	8.60	4.5	3167.79	18.91	31.52	1.7	3453.15	10.16	39.79	3.9
2829.48	1.62	11.30	7.0	3167.91	22.81	2.66	0.1	3453.25	9.73	30.80	3.2
2829.58	1.74	6.80	3.9	3168.01	6.26	2.16	0.3	3453.35	9.28	19.28	2.1
2829.68	1.86	7.00	3.8	3168.11	6.16	1.89	0.3	3453.45	8.22	15.05	1.8
2829.78	1.67	8.70	5.2	3168.21	5.57	2.83	0.5	3453.55	6.39	10.30	1.6
2829.88	1.28	8.80	6.9	3170.05	27.68	39.55	1.4	3453.65	4.53	8.80	1.9
2829.98	0.88	9.10	10.4	3170.15	26.84	43.05	1.6	3453.75	3.45	3.46	1.0
2830.08	4.14	6.60	1.6	3170.25	26.32	50.22	1.9	3453.85	3.24	3.67	1.1
2830.18	4.11	8.40	2.0	3170.35	26.24	54.77	2.1	3453.95	2.86	2.63	0.9
2830.28	4.09	5.00	1.2	3170.45	23.10	55.82	2.4	3454.35	2.80	1.59	0.6
2830.38	4.06	6.50	1.6	3170.55	20.33	53.37	2.6	3454.45	5.02	0.46	0.1
2830.58	4.02	5.60	1.4	3170.65	20.89	53.68	2.6	3454.55	5.23	1.11	0.2
2830.68	3.99	5.70	1.4	3170.75	20.93	57.57	2.8	3454.65	4.31	2.85	0.7
2830.78	3.97	5.10	1.3	3170.85	19.98	50.79	2.5	3454.75	3.12	4.42	1.4
2830.88	3.95	2.00	0.5	3170.95	18.51	47.31	2.6	3454.85	3.55	6.03	1.7
2830.98	3.92	2.30	0.6	3171.05	20.85	50.74	2.4	3454.95	3.64	8.98	2.5
2831.05	3.90	7.20	1.8	3171.15	19.39	52.08	2.7	3455.05	5.27	10.20	1.9
2831.15	3.88	8.30	2.1	3171.27	18.94	53.31	2.8	3455.25	10.81	24.99	2.3

2831.25	3.86	6.90	1.8	3171.37	17.76	46.55	2.6	3455.35	11.25	27.45	2.4
2831.35	3.83	8.40	2.2	3171.47	13.95	27.16	1.9	3455.45	10.52	29.66	2.8
2831.45	3.81	9.20	2.4	3171.57	1.81	17.58	9.7	3455.55	10.52	28.16	2.7
2831.55	3.79	7.20	1.9	3171.77	13.19	23.36	1.8	3455.65	8.86	30.89	3.5
2831.65	3.76	9.60	2.6	3171.87	12.34	28.66	2.3	3455.75	10.09	29.81	3.0
2831.75	3.74	11.90	3.2	3171.97	13.94	30.83	2.2	3455.85	9.19	23.11	2.5
2831.85	3.71	12.80	3.4	3172.07	15.62	31.31	2.0	3455.95	7.80	21.11	2.7
2831.95	3.69	11.70	3.2	3172.22	10.72	30.70	2.9	3456.05	9.21	27.77	3.0
2832.05	3.67	9.60	2.6	3172.32	14.58	33.26	2.3	3456.15	9.11	23.97	2.6
2832.15	3.64	9.90	2.7	3172.42	15.72	29.31	1.9	3456.25	8.08	22.34	2.8
2832.28	3.61	10.00	2.8	3172.52	16.87	49.31	2.9	3456.35	8.07	20.19	2.5
2832.38	3.59	11.50	3.2	3172.62	17.09	55.15	3.2	3456.45	9.34	20.11	2.2
2832.48	3.56	13.70	3.8	3172.72	18.31	44.02	2.4	3456.55	8.76	15.32	1.7
2832.58	3.54	15.00	4.2	3172.82	15.33	38.67	2.5	3456.65	6.94	10.51	1.5
2832.68	3.52	14.90	4.2	3172.92	12.75	38.99	3.1	3456.75	6.44	13.81	2.1
2832.78	3.49	13.50	3.9	3173.02	14.99	42.09	2.8	3456.85	8.13	12.49	1.5
2832.88	3.47	13.70	3.9	3173.12	14.75	42.80	2.9	3456.95	3.71	9.96	2.7
2832.98	3.45	12.80	3.7	3173.23	13.57	43.95	3.2	3457.05	4.95	8.67	1.8
2833.08	3.42	14.40	4.2	3173.33	14.59	46.01	3.2	3457.15	4.90	13.85	2.8
2833.18	3.40	13.80	4.1	3173.43	15.74	46.89	3.0	3457.25	8.12	11.21	1.4
2833.28	3.37	11.80	3.5	3173.53	12.50	45.36	3.6	3457.35	8.93	16.13	1.8

2833.38	3.35	12.00	3.6	3173.63	11.00	37.93	3.4	3457.45	4.11	9.84	2.4
2833.48	3.33	12.50	3.8	3173.73	8.55	36.74	4.3	3457.55	6.25	7.35	1.2
2833.58	3.30	12.20	3.7	3173.83	13.39	33.26	2.5	3457.65	4.19	10.44	2.5
2833.68	3.28	10.00	3.0	3173.93	12.83	32.85	2.6	3457.75	7.03	4.85	0.7
2833.78	2.44	12.80	5.3	3174.03	10.76	28.66	2.7	3457.85	5.81	7.48	1.3
2833.88	4.74	16.70	3.5	3174.13	11.20	27.98	2.5	3457.95	2.79	11.74	4.2
2833.98	8.64	14.60	1.7	3174.24	9.53	26.41	2.8	3458.05	6.28	7.42	1.2
2834.08	8.83	18.20	2.1	3174.34	10.65	34.53	3.2	3458.15	9.48	13.66	1.4
2834.18	8.10	16.30	2.0	3174.44	11.02	37.33	3.4	3458.25	7.48	14.59	2.0
2834.29	7.29	20.30	2.8	3174.54	11.97	41.22	3.4	3458.35	9.18	22.12	2.4
2834.39	6.55	18.30	2.8	3174.64	12.00	42.33	3.5	3458.45	9.08	28.62	3.2
2834.49	6.17	17.10	2.8	3174.74	11.05	39.09	3.5	3458.55	7.21	30.82	4.3
2834.59	6.62	15.80	2.4	3174.84	11.90	34.37	2.9	3458.65	5.54	28.08	5.1
2834.69	7.55	18.60	2.5	3174.94	9.69	33.20	3.4	3458.75	10.37	22.57	2.2
2834.79	8.27	21.70	2.6	3175.04	11.71	36.81	3.1	3458.85	8.12	25.78	3.2
2834.89	7.61	21.40	2.8	3175.14	12.80	35.05	2.7	3458.95	10.94	39.79	3.6
2834.99	6.95	21.30	3.1	3175.24	11.07	37.20	3.4	3459.05	10.63	44.07	4.1
2835.09	7.99	16.80	2.1	3175.34	9.05	35.61	3.9	3459.15	11.64	32.27	2.8
2835.19	9.23	9.50	1.0	3175.44	13.19	33.97	2.6	3459.25	6.43	16.92	2.6
2835.3	11.38	12.80	1.1	3175.54	9.07	32.89	3.6	3459.35	7.29	20.91	2.9
2835.4	13.60	14.70	1.1	3175.64	12.88	37.10	2.9	3459.45	9.33	16.19	1.7

2835.5	15.83	13.30	0.8	3175.74	12.10	33.03	2.7	3459.55	6.33	10.95	1.7
2835.6	22.07	12.10	0.5	3175.84	10.62	35.90	3.4	3459.65	7.23	18.45	2.6
2835.7	30.66	12.50	0.4	3175.94	10.78	32.86	3.0	3459.75	8.78	10.02	1.1
2835.8	25.36	15.60	0.6	3176.04	7.86	32.95	4.2	3459.85	5.18	5.99	1.2
2835.9	7.10	20.90	2.9	3176.14	12.49	34.28	2.7	3459.95	5.71	10.40	1.8
2836	7.23	23.30	3.2	3176.24	11.92	29.49	2.5	3460.15	10.72	23.23	2.2
2836.1	8.41	20.10	2.4	3176.34	11.92	32.52	2.7	3460.25	7.92	17.90	2.3
2836.2	9.59	17.30	1.8	3176.44	10.27	29.35	2.9	3460.35	8.53	16.07	1.9
2836.32	10.73	10.40	1.0	3176.54	14.65	38.43	2.6	3460.45	6.11	14.96	2.4
2836.42	10.46	8.60	0.8	3176.64	15.45	35.67	2.3	3460.55	7.42	13.26	1.8
2836.52	8.53	17.00	2.0	3176.74	15.37	35.67	2.3	3460.65	5.52	16.49	3.0
2836.64	7.34	6.40	0.9	3176.84	14.43	36.68	2.5	3460.75	6.08	14.92	2.5
2836.74	8.08	5.60	0.7	3176.94	14.48	31.21	2.2	3460.85	8.73	15.09	1.7
2836.84	5.83	15.10	2.6	3177.04	10.89	35.30	3.2	3460.95	3.94	15.27	3.9
2836.94	7.36	20.80	2.8	3177.14	13.66	30.07	2.2	3461.05	8.78	13.61	1.6
2837.04	7.51	21.10	2.8	3177.24	14.46	28.85	2.0	3461.15	9.49	18.71	2.0
2837.14	4.62	18.30	4.0	3177.34	12.19	23.90	2.0	3461.25	8.75	14.08	1.6
2837.24	6.04	18.40	3.0	3177.44	13.00	22.83	1.8	3461.35	7.15	12.66	1.8
2837.34	7.52	17.60	2.3	3177.59	12.94	17.20	1.3	3461.45	3.73	10.02	2.7
2837.44	9.57	15.00	1.6	3177.69	11.87	14.77	1.2	3461.55	8.06	22.27	2.8
2837.6	11.91	25.60	2.1	3177.79	12.81	14.07	1.1	3461.65	3.37	10.87	3.2

2837.7	12.42	27.10	2.2	3177.89	13.78	13.50	1.0	3461.75	4.57	6.21	1.4
2837.8	11.54	32.30	2.8	3177.99	12.69	14.96	1.2	3461.85	5.17	8.20	1.6
2837.9	14.73	36.80	2.5	3178.09	12.05	14.19	1.2	3461.95	2.95	6.94	2.3
2838	14.73	36.00	2.4	3178.19	12.62	16.74	1.3				
2838.1	13.14	36.00	2.7	3178.29	13.55	14.39	1.1				
2838.2	11.56	32.90	2.8	3178.39	13.39	15.12	1.1				
2838.36	12.78	31.20	2.4	3178.49	12.78	16.34	1.3				
2838.46	13.10	33.50	2.6	3178.59	11.54	20.26	1.8				
2838.56	11.46	34.10	3.0	3178.69	9.74	17.81	1.8				
2838.66	7.06	35.80	5.1	3178.79	10.23	14.67	1.4				
2838.76	5.83	34.60	5.9	3178.87	11.62	8.39	0.7				
2838.86	7.76	26.90	3.5	3179.05	11.99	33.50	2.8				
2838.96	10.35	26.50	2.6	3179.15	12.23	52.06	4.3				
2839.06	9.86	22.40	2.3	3179.25	13.47	80.18	6.0				
2839.16	8.53	24.30	2.8	3179.35	11.58	143.41	12.4				
2839.26	13.22	27.60	2.1	3179.45	12.64	141.77	11.2				
2839.37	16.03	33.70	2.1	3179.55	16.95	95.40	5.6				
2839.47	14.60	41.00	2.8	3179.65	18.05	71.62	4.0				
2839.57	14.24	39.90	2.8	3179.75	17.97	63.86	3.6				
2839.67	13.72	40.20	2.9	3179.85	16.89	60.20	3.6				
2839.77	13.22	40.10	3.0	3179.95	17.94	60.33	3.4				

2839.87	12.10	41.40	3.4	3180.05	18.24	59.59	3.3
2839.97	12.32	40.80	3.3	3180.15	17.82	65.74	3.7
2840.07	12.45	38.00	3.1	3180.25	17.28	65.38	3.8
2840.17	11.49	32.80	2.9	3180.35	16.24	64.63	4.0
2840.27	11.40	26.70	2.3	3180.45	16.30	58.06	3.6
2840.38	11.42	24.80	2.2	3180.55	16.66	55.71	3.3
2840.48	11.80	27.10	2.3	3180.65	17.20	46.97	2.7
2840.58	11.42	26.20	2.3	3180.75	15.22	45.29	3.0
2840.68	11.30	23.70	2.1	3180.85	15.01	50.31	3.4
2840.78	12.92	24.70	1.9	3180.96	12.91	47.84	3.7
2840.88	11.85	27.60	2.3	3181.06	12.98	51.17	3.9
2840.98	11.12	30.20	2.7	3181.16	16.81	50.41	3.0
2841.08	11.31	25.70	2.3	3181.26	17.24	58.18	3.4
2841.18	10.67	25.40	2.4	3181.36	17.16	58.31	3.4
2841.28	10.94	24.80	2.3	3181.46	16.51	53.06	3.2
2841.38	11.68	25.00	2.1	3181.56	16.14	48.50	3.0
2841.48	10.85	27.10	2.5	3181.66	15.90	48.38	3.0
2841.58	11.11	25.80	2.3	3181.76	16.00	57.59	3.6
2841.68	11.56	26.90	2.3	3181.86	10.72	79.34	7.4
2841.83	11.95	33.50	2.8	3181.96	12.15	82.38	6.8
2841.93	10.82	34.80	3.2	3182.06	14.08	70.52	5.0

2842.03	11.26	34.00	3.0	3182.16	12.92	71.51	5.5
2842.13	11.29	26.30	2.3	3182.26	15.47	81.81	5.3
2842.23	11.04	25.20	2.3	3182.36	15.86	88.28	5.6
2842.4	10.61	20.80	2.0	3182.46	14.65	75.48	5.2
2842.5	11.05	6.90	0.6	3182.56	13.23	57.58	4.4
2842.55	10.20	16.30	1.6	3182.66	13.27	53.20	4.0
2842.65	7.57	24.10	3.2	3182.76	15.25	58.05	3.8
2842.75	4.93	22.10	4.5	3182.86	15.37	58.66	3.8
2842.85	7.61	15.40	2.0	3182.96	14.62	67.33	4.6
2842.95	14.75	23.30	1.6	3183.06	14.53	59.29	4.1
2843.05	17.55	30.00	1.7	3183.16	12.63	46.17	3.7
2843.15	27.21	28.30	1.0	3183.26	11.01	41.74	3.8
2843.25	19.37	29.30	1.5	3183.36	12.65	44.86	3.5
2843.34	10.86	30.00	2.8	3183.52	8.17	60.32	7.4
2843.44	11.08	35.00	3.2	3183.62	3.05	36.80	12.1
2843.54	10.97	35.20	3.2	3183.72	3.49	18.70	5.4
2843.64	9.57	31.70	3.3	3183.82	3.57	13.27	3.7
2843.74	8.46	33.30	3.9	3183.92	2.94	10.70	3.6
2843.84	8.51	33.20	3.9	3184.02	2.30	5.98	2.6
2843.94	8.55	35.00	4.1	3184.12	1.69	6.01	3.6
2844.04	9.30	38.60	4.2	3184.22	1.35	5.38	4.0

2844.14	9.59	35.50	3.7	3184.32	2.51	7.43	3.0
2844.24	9.82	32.60	3.3	3184.42	4.64	7.90	1.7
2844.39	10.80	30.70	2.8	3184.52	2.03	7.29	3.6
2844.49	13.22	32.20	2.4	3184.62	1.92	9.12	4.8
2844.59	10.94	34.80	3.2	3184.72	2.50	4.85	1.9
2844.69	14.01	36.30	2.6	3184.82	2.47	6.73	2.7
2844.79	14.12	36.50	2.6	3184.92	3.54	8.24	2.3
2844.89	12.47	34.50	2.8	3185.02	3.15	8.32	2.6
2844.98	11.10	28.30	2.5	3185.12	2.90	10.20	3.5
2845.08	10.20	27.50	2.7	3185.22	3.74	10.68	2.9
2845.18	11.01	31.50	2.9	3185.32	4.32	11.97	2.8
2845.28	11.57	32.40	2.8	3185.42	6.01	12.59	2.1
2845.38	13.38	36.00	2.7	3185.52	4.90	14.27	2.9
2845.48	12.32	36.30	2.9	3185.63	4.51	14.52	3.2
2845.58	14.59	40.90	2.8	3185.73	4.28	15.23	3.6
2845.74	12.72	46.10	3.6	3185.83	6.41	13.39	2.1
2845.84	13.03	48.70	3.7	3185.93	2.78	9.51	3.4
2845.94	13.21	43.20	3.3	3186.03	6.03	8.72	1.4
2846.04	13.33	44.80	3.4	3186.13	6.61	15.10	2.3
2846.14	13.45	45.60	3.4	3186.23	4.83	13.07	2.7
2846.24	13.58	46.90	3.5	3186.33	5.04	12.85	2.6

2846.34	13.58	44.00	3.2	3186.43	3.43	12.58	3.7
2846.43	12.61	44.50	3.5	3186.53	1.07	11.94	11.1
2846.53	11.45	46.20	4.0	3186.63	6.49	15.13	2.3
2846.63	10.70	38.60	3.6	3186.73	6.63	17.72	2.7
2846.73	12.25	43.40	3.5	3186.83	5.84	17.52	3.0
2846.83	12.58	43.40	3.4	3186.93	6.22	14.33	2.3
2846.93	12.39	41.50	3.4	3187.03	5.42	15.38	2.8
2847.03	12.23	44.30	3.6	3187.13	7.02	21.64	3.1
2847.13	12.42	40.10	3.2	3187.73	1.43	18.53	12.9
2847.23	12.50	44.00	3.5	3187.83	4.23	16.80	4.0
2847.33	11.27	35.20	3.1	3187.93	7.54	16.87	2.2
2847.43	10.22	31.80	3.1	3188.03	4.94	19.77	4.0
2847.52	10.97	32.50	3.0	3188.13	6.27	19.70	3.1
2847.62	11.34	30.40	2.7	3188.27	7.22	20.13	2.8
2847.74	11.51	28.90	2.5	3188.37	9.58	21.30	2.2
2847.84	4.04	31.60	7.8	3188.47	9.54	25.75	2.7
2847.94	11.52	42.70	3.7	3188.57	9.50	29.57	3.1
2848.06	12.29	45.00	3.7	3188.67	9.46	32.95	3.5
2848.16	11.64	43.10	3.7	3188.77	9.43	31.89	3.4
2848.26	11.16	38.20	3.4	3189.05	8.30	14.93	1.8
2848.35	10.78	36.50	3.4	3189.15	10.00	22.57	2.3

2848.45	11.32	34.20	3.0	3189.25	10.03	29.74	3.0
2848.55	12.05	31.90	2.6	3189.35	9.21	33.08	3.6
2848.65	12.41	36.50	2.9	3189.45	3.99	33.50	8.4
2848.75	12.61	33.50	2.7	3189.55	9.59	36.22	3.8
2848.85	13.10	9.90	0.8	3189.65	9.29	33.60	3.6
2848.95	13.44	18.40	1.4	3189.75	10.25	32.73	3.2
2849.05	14.43	42.50	2.9	3189.85	11.25	36.39	3.2
2849.15	13.28	50.30	3.8	3189.95	11.17	39.30	3.5
2849.25	10.67	46.70	4.4	3190.05	11.41	37.42	3.3
2849.35	8.91	42.00	4.7	3190.15	11.78	36.65	3.1
2849.45	13.69	37.60	2.7	3190.25	12.02	38.83	3.2
2849.54	12.68	44.40	3.5	3190.35	13.63	37.74	2.8
2849.64	13.97	46.00	3.3	3190.45	12.85	40.81	3.2
2849.76	13.16	41.40	3.1	3190.55	10.11	38.08	3.8
2849.86	11.60	38.20	3.3	3190.65	12.74	32.87	2.6
2849.96	15.81	40.90	2.6	3190.75	11.95	28.18	2.4
2850.06	12.73	39.90	3.1	3190.85	11.76	25.22	2.1
2850.16	14.07	41.30	2.9	3190.95	12.40	27.73	2.2
2850.26	14.98	36.40	2.4	3191.05	12.34	30.18	2.4
2850.35	16.05	39.30	2.4	3191.15	11.75	40.52	3.4
2850.45	16.39	35.90	2.2	3191.25	10.77	42.86	4.0

2850.55	16.74	40.20	2.4	3191.35	10.14	39.74	3.9
2850.65	16.13	45.40	2.8	3191.45	10.52	38.66	3.7
2850.76	13.99	46.80	3.3	3191.55	10.99	42.80	3.9
2850.85	9.27	50.40	5.4	3191.65	8.82	37.75	4.3
2850.95	12.89	53.90	4.2	3191.75	7.59	27.05	3.6
2851.05	14.19	60.20	4.2	3191.95	3.78	20.06	5.3
2851.15	13.44	64.50	4.8	3192.05	8.15	25.65	3.1
2851.25	11.58	64.60	5.6	3192.95	1.89	7.26	3.8
2851.35	15.30	62.80	4.1	3193.05	13.86	8.21	0.6
2851.45	17.45	59.10	3.4	3193.15	13.47	7.84	0.6
2851.55	18.40	51.90	2.8	3193.25	12.52	8.06	0.6
2851.65	17.24	54.30	3.1	3193.35	11.49	7.52	0.7
2851.76	15.68	56.70	3.6	3193.45	12.57	6.59	0.5
2851.85	14.79	54.30	3.7	3193.55	11.97	9.43	0.8
2851.95	13.98	51.60	3.7	3193.65	12.77	11.40	0.9
2852.05	15.26	43.00	2.8	3193.75	15.72	12.65	0.8
2852.15	16.54	49.20	3.0	3193.85	13.56	13.29	1.0
2852.25	15.11	47.60	3.2	3193.95	9.64	13.33	1.4
2852.35	15.63	47.70	3.1	3194.05	4.10	16.27	4.0
2852.45	13.90	47.60	3.4	3194.15	6.84	15.08	2.2
2852.55	14.43	42.80	3.0	3194.25	4.60	12.43	2.7

2852.65	13.95	47.10	3.4	3194.35	7.92	12.40	1.6
2852.77	13.83	43.40	3.1	3194.45	7.90	9.84	1.2
2852.87	12.70	42.10	3.3	3194.55	10.82	8.45	0.8
2852.97	12.08	43.10	3.6	3194.65	10.28	10.97	1.1
2853.07	12.61	45.10	3.6	3194.75	10.96	10.06	0.9
2853.16	12.28	42.90	3.5	3194.85	11.81	9.36	0.8
2853.26	12.40	38.30	3.1	3194.95	13.47	9.87	0.7
2853.36	12.72	39.00	3.1	3195.05	12.94	14.89	1.2
2853.46	11.85	34.10	2.9	3195.15	8.81	16.21	1.8
2853.56	10.27	36.10	3.5	3195.26	8.77	14.82	1.7
2853.66	11.39	32.00	2.8	3195.36	8.56	13.05	1.5
2853.76	12.22	35.30	2.9	3195.46	9.00	12.43	1.4
2853.86	12.96	36.40	2.8	3195.56	5.44	10.84	2.0
2853.96	12.87	38.80	3.0	3195.66	3.84	12.29	3.2
2854.08	11.66	42.70	3.7	3195.76	8.35	12.76	1.5
2854.18	11.14	42.30	3.8	3195.86	6.88	12.17	1.8
2854.28	10.68	32.30	3.0	3195.96	12.03	10.50	0.9
2854.38	9.51	21.90	2.3	3196.06	9.61	8.11	0.8
2854.48	9.70	21.10	2.2	3196.16	11.65	8.09	0.7
2854.58	10.51	6.90	0.7	3196.26	11.54	14.05	1.2
2854.77	13.52	37.00	2.7	3196.36	9.30	11.51	1.2

2854.87	10.66	11.00	1.0	3196.46	11.26	14.53	1.3
2854.97	13.33	13.10	1.0	3196.56	8.84	14.47	1.6
2855.07	14.41	40.80	2.8	3196.66	10.64	16.78	1.6
2855.16	15.08	48.00	3.2	3196.76	11.43	15.92	1.4
2855.26	10.73	49.60	4.6	3196.86	8.92	15.28	1.7
2855.36	15.91	48.40	3.0	3196.96	5.60	10.82	1.9
2855.46	13.23	37.50	2.8	3197.06	7.84	9.32	1.2
2855.56	12.81	25.90	2.0	3197.16	3.97	7.21	1.8
2855.66	14.06	27.90	2.0	3197.26	6.72	10.58	1.6
2855.77	16.28	32.20	2.0	3197.36	13.14	11.67	0.9
2855.87	15.61	38.40	2.5	3197.46	11.99	11.80	1.0
2855.97	14.66	39.00	2.7	3197.56	11.36	12.18	1.1
2856.07	13.75	34.90	2.5	3197.66	12.64	12.88	1.0
2856.17	12.86	37.50	2.9	3197.76	11.33	11.17	1.0
2856.27	11.98	42.60	3.6	3197.86	10.66	11.14	1.0
2856.36	11.18	50.00	4.5	3197.96	11.10	8.83	0.8
2856.46	12.33	44.70	3.6	3198.06	8.14	6.39	0.8
2856.56	16.85	42.20	2.5	3198.16	6.44	4.60	0.7
2856.66	16.48	34.50	2.1	3198.27	5.15	6.50	1.3
2856.78	14.24	40.20	2.8	3198.37	8.59	6.10	0.7
2856.88	12.90	39.70	3.1	3198.47	8.84	6.46	0.7

2856.98	7.66	39.90	5.2	3198.57	8.29	5.24	0.6
2857.08	7.70	31.20	4.1	3198.67	8.01	5.86	0.7
2857.18	7.16	22.50	3.1	3198.77	6.28	8.63	1.4
2857.28	7.90	25.10	3.2	3198.87	8.77	9.63	1.1
2857.38	8.33	25.00	3.0	3198.97	9.14	5.71	0.6
2857.48	7.30	29.10	4.0	3199.24	5.70	4.23	0.7
2857.58	6.93	27.00	3.9	3199.34	5.01	6.03	1.2
2857.68	7.64	25.80	3.4	3199.44	5.11	11.42	2.2
2857.8	5.15	25.90	5.0	3199.53	12.45	27.85	2.2
2857.9	7.38	29.50	4.0	3199.63	12.34	48.77	4.0
2857.99	6.17	29.10	4.7	3199.73	12.94	59.07	4.6
2858.09	7.10	30.80	4.3	3199.83	12.75	45.96	3.6
2858.19	8.20	28.30	3.5	3199.93	8.15	30.11	3.7
2858.29	8.83	26.20	3.0	3200.02	7.70	14.01	1.8
2858.39	8.47	26.80	3.2	3200.12	6.28	5.81	0.9
2858.49	9.00	31.30	3.5				
2858.59	9.22	28.50	3.1				
2858.76	10.14	33.60	3.3				
2858.86	10.00	39.30	3.9				
2858.96	9.61	35.90	3.7				
2859.06	8.62	35.70	4.1				
2859.15	7.83	30.60	3.9				
2859.25	7.85	31.90	4.1				

2859.35	7.99	30.70	3.8
2859.45	8.20	31.20	3.8
2859.55	7.55	30.10	4.0
2859.65	7.50	32.70	4.4
2859.81	7.42	36.30	4.9
2859.9	7.97	36.90	4.6
2860	8.58	36.80	4.3
2860.1	8.86	40.90	4.6
2860.2	9.08	41.80	4.6
2860.3	9.42	33.80	3.6
2860.4	9.75	35.70	3.7
2860.5	8.83	28.10	3.2
2860.6	9.21	15.00	1.6
2860.7	8.80	15.30	1.7
2860.75	9.23	23.40	2.5
2860.85	9.52	31.50	3.3
2860.95	8.95	28.50	3.2
2861.05	8.37	17.60	2.1
2861.15	7.80	23.80	3.1
2861.25	10.36	34.20	3.3
2861.35	10.13	36.00	3.6
2861.45	10.46	32.90	3.1
2861.55	10.75	29.30	2.7
2861.65	10.85	28.00	2.6
2861.75	10.79	33.20	3.1
2861.85	11.12	35.50	3.2
2861.95	10.52	34.70	3.3
2862.05	10.60	35.10	3.3
2862.15	10.36	33.20	3.2

2862.26	10.82	34.40	3.2
2862.36	10.47	37.00	3.5
2862.46	7.33	33.50	4.6
2862.56	10.33	33.50	3.2
2862.66	6.55	31.10	4.8
2862.76	8.58	29.80	3.5
2862.86	8.87	30.30	3.4
2862.97	8.28	30.90	3.7
2863.07	4.77	29.10	6.1
2863.17	5.47	27.00	4.9
2863.27	5.18	29.20	5.6
2863.37	3.99	28.30	7.1
2863.47	3.81	26.20	6.9
2863.57	4.94	27.30	5.5
2863.67	5.78	29.50	5.1
2863.77	6.70	28.50	4.3
2863.87	8.28	28.20	3.4
2863.97	8.63	28.50	3.3
2864.07	8.99	26.20	2.9
2864.17	7.31	27.90	3.8
2864.27	3.55	25.40	7.2
2864.37	8.35	27.80	3.3
2864.47	7.77	26.60	3.4
2864.57	7.36	25.90	3.5
2864.67	7.22	27.30	3.8
2864.77	7.35	24.70	3.4
2864.87	6.85	27.10	4.0
2864.99	7.93	30.70	3.9
2865.09	9.01	32.90	3.7

2865.19	8.33	37.20	4.5
2865.29	7.89	35.30	4.5
2865.39	9.23	35.20	3.8
2865.49	9.33	35.60	3.8
2865.59	9.15	31.30	3.4
2865.69	7.25	28.70	4.0
2865.79	6.52	19.30	3.0
2865.89	6.81	16.40	2.4
2866	8.01	13.60	1.7
2866.1	7.04	15.50	2.2
2866.2	6.78	14.80	2.2
2866.3	7.12	14.30	2.0
2866.4	7.55	15.50	2.1
2866.5	7.84	18.30	2.3
2866.6	7.74	16.60	2.1
2866.7	7.59	14.20	1.9
2866.8	7.66	6.60	0.9
2866.9	7.25	15.30	2.1
2867	6.71	20.20	3.0
2867.1	6.83	7.30	1.1
2867.2	7.99	11.00	1.4
2867.3	9.19	21.90	2.4
2867.4	8.47	27.30	3.2
2867.5	6.22	25.50	4.1
2867.6	8.47	23.30	2.8
2867.7	10.25	21.80	2.1
2867.8	8.59	18.60	2.2
2867.9	7.52	18.30	2.4
2868	7.89	13.60	1.7

2868.1	7.18	15.00	2.1
2868.2	6.47	16.00	2.5
2868.3	5.77	15.30	2.6
2868.4	5.14	18.70	3.6
2868.5	3.84	18.40	4.8
2868.6	6.92	24.20	3.5
2868.7	6.43	20.30	3.2
2868.8	7.13	18.70	2.6
2868.9	8.16	19.00	2.3
2869.04	9.43	22.40	2.4
2869.14	9.02	26.40	2.9
2869.24	11.22	29.50	2.6
2869.34	12.33	34.50	2.8
2869.44	12.23	34.20	2.8
2869.54	11.66	30.80	2.6
2869.64	10.04	30.70	3.1
2869.74	10.68	27.50	2.6
2869.84	11.94	31.00	2.6
2869.94	11.43	38.40	3.4
2870.04	8.49	37.50	4.4
2870.14	7.87	33.50	4.3
2870.24	9.61	31.60	3.3
2870.34	9.55	27.30	2.9
2870.44	10.51	28.00	2.7
2870.54	11.48	29.90	2.6
2870.64	10.13	28.70	2.8
2870.74	9.73	29.70	3.1
2870.84	10.49	24.20	2.3
2870.94	9.98	25.90	2.6

2871.05	10.55	25.20	2.4
2871.15	10.84	25.00	2.3
2871.25	11.13	25.10	2.3
2871.35	11.56	27.20	2.4
2871.45	11.75	30.30	2.6
2871.55	12.33	37.80	3.1
2871.65	11.30	35.40	3.1
2871.75	10.23	26.80	2.6
2871.85	10.39	22.50	2.2
2871.95	10.33	22.90	2.2
2872.07	9.23	28.20	3.1
2872.17	9.36	23.00	2.5
2872.27	9.89	20.80	2.1
2872.37	8.36	21.50	2.6
2872.47	8.55	21.20	2.5
2872.57	8.13	21.10	2.6
2872.67	8.36	14.40	1.7
2872.77	8.46	14.10	1.7
2872.87	9.31	3.90	0.4
2872.97	8.87	7.20	0.8
2873.09	8.29	8.40	1.0
2873.19	8.58	2.00	0.2
2873.29	9.85	4.50	0.5
2873.39	8.81	15.30	1.7
2873.49	7.96	20.70	2.6
2873.59	8.02	17.10	2.1
2873.69	7.55	15.90	2.1
2873.79	8.11	14.40	1.8
2873.89	7.44	15.00	2.0

2873.99	9.81	16.00	1.6
2874.11	10.07	20.30	2.0
2874.21	9.87	19.10	1.9
2874.31	8.61	21.40	2.5
2874.41	9.40	21.80	2.3
2874.51	10.20	18.10	1.8
2874.61	9.68	17.50	1.8
2874.71	10.76	16.80	1.6
2874.81	9.63	13.10	1.4
2874.91	9.56	10.30	1.1
2875.01	10.06	9.90	1.0
2875.12	9.82	11.60	1.2
2875.22	9.50	13.10	1.4
2875.32	9.63	14.90	1.5
2875.42	9.32	14.30	1.5
2875.52	10.03	20.20	2.0
2875.62	8.51	20.20	2.4
2875.72	7.80	17.70	2.3
2875.82	7.16	12.60	1.8
2875.92	6.53	12.90	2.0
2876.02	8.29	14.60	1.8
2876.13	7.19	14.10	2.0
2876.23	6.33	14.80	2.3
2876.33	5.48	10.70	2.0
2876.43	6.14	7.70	1.3
2876.53	8.76	6.40	0.7
2876.63	6.49	7.00	1.1
2876.73	9.28	7.60	0.8
2876.83	9.26	8.20	0.9

2876.93	8.25	10.60	1.3
2877.03	5.73	11.80	2.1
2877.14	9.67	15.80	1.6
2877.24	8.54	14.90	1.7
2877.34	8.50	14.90	1.8
2877.44	8.90	16.10	1.8
2877.54	9.25	15.10	1.6
2877.64	9.19	12.50	1.4
2877.74	8.95	10.40	1.2
2877.84	8.98	11.40	1.3
2877.94	9.01	8.40	0.9
2878.04	8.19	11.30	1.4
2878.15	5.86	14.50	2.5
2878.25	6.04	13.20	2.2
2878.35	7.17	13.00	1.8
2878.45	8.30	10.80	1.3
2878.55	9.15	11.80	1.3
2878.65	7.41	12.30	1.7
2878.75	4.39	12.40	2.8
2878.85	9.91	7.90	0.8
2878.95	7.18	1.70	0.2
2879.01	6.15	4.90	0.8
2879.11	5.85	6.80	1.2
2879.21	5.55	7.30	1.3
2879.31	5.72	2.30	0.4
2879.43	6.45	4.20	0.7
2879.53	6.85	2.60	0.4
2879.63	5.72	5.90	1.0
2879.73	5.31	6.20	1.2

2879.82	5.37	6.20	1.2
2879.92	5.20	5.00	1.0
2880.02	6.83	7.10	1.0
2880.12	6.48	5.80	0.9
2880.22	7.10	6.70	0.9
2880.32	6.58	6.30	1.0
2880.42	5.74	8.60	1.5
2880.51	8.20	8.10	1.0
2880.61	7.15	7.80	1.1
2880.71	7.06	7.10	1.0
2880.81	6.75	6.10	0.9
2880.91	6.43	5.10	0.8
2881	8.40	5.00	0.6
2881.1	7.95	7.40	0.9
2881.2	7.10	5.80	0.8
2881.3	7.58	6.60	0.9
2881.4	7.29	7.80	1.1
2881.5	5.89	8.10	1.4
2881.6	6.33	10.50	1.7
2881.69	7.01	15.50	2.2
2881.79	7.92	14.70	1.9
2881.96	12.06	9.70	0.8
2882.05	9.31	9.70	1.0
2882.2	7.23	5.80	0.8
2882.29	5.98	4.50	0.8
2882.39	4.60	3.70	0.8
2882.49	6.09	5.40	0.9
2882.59	6.61	6.10	0.9
2882.69	5.22	6.60	1.3

2882.79	3.82	4.00	1.0
2882.88	2.89	4.70	1.6
2882.98	6.11	4.70	0.8
2883.08	7.51	5.20	0.7
2883.2	8.57	5.40	0.6
2883.3	8.61	7.60	0.9
2883.4	7.34	6.80	0.9
2883.5	8.23	8.50	1.0
2883.59	7.64	8.80	1.2
2883.69	5.73	5.90	1.0
2883.79	9.08	5.80	0.6
2883.89	7.25	5.50	0.8
2883.99	5.46	3.20	0.6
2884.08	6.48	5.20	0.8
2884.2	7.98	4.90	0.6
2884.3	6.59	5.40	0.8
2884.4	6.91	7.40	1.1
2884.5	8.32	6.10	0.7
2884.59	7.49	6.30	0.8
2884.69	4.76	4.30	0.9
2884.79	7.06	5.60	0.8
2884.89	9.05	3.40	0.4
2884.99	6.39	0.00	0.0
2885.08	5.79	3.20	0.6
2885.19	6.51	2.70	0.4
2885.29	8.13	1.40	0.2
2885.39	6.99	1.90	0.3
2885.49	6.24	3.10	0.5
2885.59	8.87	5.00	0.6

2885.68	7.77	6.50	0.8
2885.78	6.59	5.40	0.8
2885.88	5.74	5.10	0.9
2885.98	4.96	4.50	0.9
2886.08	4.82	5.00	1.0
2886.19	4.88	6.40	1.3
2886.28	3.22	6.30	2.0
2886.38	5.02	7.40	1.5
2886.48	5.89	6.70	1.1
2886.58	6.76	7.00	1.0
2886.68	7.10	5.60	0.8
2886.78	7.07	5.40	0.8
2886.87	7.06	5.70	0.8
2886.97	7.05	5.10	0.7
2887.07	6.86	5.60	0.8
2887.22	7.87	2.60	0.3
2887.31	7.45	4.30	0.6
2887.41	6.29	4.20	0.7
2887.51	5.66	3.80	0.7
2887.61	6.27	5.00	0.8
2887.71	5.98	4.50	0.8
2887.81	5.30	3.80	0.7
2887.9	4.13	4.30	1.0
2888	3.95	3.50	0.9
2888.1	5.38	5.00	0.9
2888.21	4.38	4.20	1.0
2888.31	5.77	4.80	0.8
2888.41	6.29	4.20	0.7
2888.51	5.26	3.00	0.6

2888.61	3.95	4.70	1.2
2888.7	3.50	3.10	0.9
2888.8	3.74	3.30	0.9
2888.9	3.98	3.20	0.8
2889	4.22	4.30	1.0
2889.1	5.61	3.60	0.6
2889.21	4.83	3.20	0.7
2889.31	4.64	5.70	1.2
2889.4	5.27	5.80	1.1
2889.5	5.96	6.00	1.0
2889.6	4.15	4.90	1.2
2889.7	5.54	5.90	1.1
2889.8	3.67	4.00	1.1
2889.89	4.99	4.30	0.9
2889.99	4.57	3.80	0.8
2890.09	3.38	5.50	1.6
2890.2	2.85	5.00	1.8
2890.3	1.54	4.90	3.2
2890.39	1.63	2.50	1.5
2890.49	3.73	4.00	1.1
2890.59	4.07	4.60	1.1
2890.69	5.13	5.50	1.1
2890.79	2.74	4.60	1.7
2890.89	2.85	4.30	1.5
2890.98	4.40	1.80	0.4
2891.08	6.52	3.80	0.6
2891.18	6.57	5.10	0.8
2891.28	7.31	1.70	0.2
2891.38	7.56	2.20	0.3

2891.48	7.08	4.20	0.6
2891.58	5.10	7.30	1.4
2891.67	4.77	7.40	1.5
2891.77	4.94	5.30	1.1
2891.87	4.97	4.30	0.9
2891.97	3.86	4.60	1.2
2892.07	3.11	5.10	1.6
2892.19	3.52	6.20	1.8
2892.29	4.70	7.20	1.5
2892.39	3.73	6.90	1.8
2892.49	2.77	5.80	2.1
2892.59	7.77	3.80	0.5
2892.69	20.09	5.10	0.3
2892.78	21.49	6.90	0.3
2892.88	17.07	5.00	0.3

Table 36. The distribution of the uranium concentration (U), the organic carbon (TOC) and the ratio U/TOC for the wells 9, 1, 10.

epth, m	TOC thermal, %	U, ppm	U/TOC thermal	Depth, m	TOC thermal, %	U, ppm	U/TOC thermal	Depth, m	TOC thermal, %	U, ppm	U/TOC thermal
Well 10				Well 1				Well 9			
2606.43	14.369	9.110	0.63400	3040.35	2.93	23.57	8.0	3005.05	14.69	10.94	0.7
2606.48	12.327	12.690	1.02945	3040.55	6.98	60.90	8.7	3005.15	15.14	12.90	0.9
2606.58	2.546	13.380	5.25451	3040.65	9.21	69.38	7.5	3005.25	17.94	14.98	0.8
2606.67	0.000	15.980	35.36204	3040.75	9.20	58.50	6.4	3005.35	28.25	12.67	0.4
2606.78	4.342	18.580	4.27888	3040.85	7.18	50.58	7.0	3005.45	26.57	12.29	0.5
2606.88	12.099	22.130	1.82914	3041.05	7.06	32.55	4.6	3005.55	16.18	19.72	1.2
2606.98	7.235	22.280	3.07949	3041.15	5.78	31.18	5.4	3005.65	14.16	21.81	1.5
2607.08	19.665	22.640	1.15129	3041.27	6.45	38.65	6.0	3005.75	11.25	20.21	1.8
2607.164	17.378	21.210	1.22054	3041.37	8.42	45.38	5.4	3005.85	8.88	23.87	2.7
2607.258	15.229	12.300	0.80765	3041.47	9.69	48.78	5.0	3005.95	9.27	30.55	3.3
2607.45	17.754	27.770	1.56415	3041.57	9.90	51.02	5.2	3006.05	11.55	37.05	3.2
2607.55	20.162	27.460	1.36199	3041.67	6.11	51.41	8.4	3006.15	10.61	33.97	3.2
2607.65	17.150	24.780	1.44493	3041.77	4.45	58.20	13.1	3006.25	10.90	34.65	3.2
2607.715	4.712	22.660	4.80936	3041.87	8.62	61.83	7.2	3006.45	10.57	23.16	2.2
2608.15	14.539	26.580	1.82816	3041.97	8.18	58.98	7.2	3006.55	11.18	21.00	1.9
2608.25	4.739	21.620	4.56197	3042.07	7.99	54.69	6.8	3006.65	11.00	16.71	1.5
2608.35	6.599	19.730	2.98982	3042.25	7.28	61.52	8.5	3006.85	7.51	11.20	1.5

2608.46	17.129	13.790	0.80507	3042.35	8.11	69.36	8.6	3006.95	7.92	10.33	1.3
2608.56	9.838	13.100	1.33161	3042.45	8.14	67.18	8.3	3007.05	9.47	14.62	1.5
2608.66	10.595	17.550	1.65641	3042.55	4.59	50.78	11.1	3007.15	9.47	11.40	1.2
2608.78	15.385	20.650	1.34222	3042.65	8.24	60.11	7.3	3007.35	7.25	4.00	0.6
2608.86	13.827	21.050	1.52236	3042.75	6.83	83.86	12.3	3007.45	7.79	4.34	0.6
2608.96	14.806	22.360	1.51022	3042.85	11.30	86.15	7.6	3007.55	8.59	5.47	0.6
2609.06	15.424	24.290	1.57483	3042.95	7.16	92.76	13.0	3007.65	10.37	6.75	0.7
2609.17	16.923	23.550	1.39157	3043.05	10.91	100.52	9.2	3008.05	9.43	5.11	0.5
2609.26	10.083	25.660	2.54495	3043.25	8.29	88.35	10.7	3008.15	7.12	3.92	0.6
2609.341	11.924	30.040	2.51930	3043.35	7.85	62.12	7.9	3008.25	7.97	4.25	0.5
2609.46	10.897	33.770	3.09908	3043.45	7.95	40.78	5.1	3008.35	7.69	4.84	0.6
2609.56	19.575	36.260	1.85233	3043.55	8.01	45.27	5.6	3008.45	9.27	6.37	0.7
2609.66	20.230	39.030	1.92930	3043.65	10.71	53.84	5.0	3008.55	9.18	8.22	0.9
2609.76	16.985	37.440	2.20431	3043.75	8.94	67.94	7.6	3008.65	10.84	7.51	0.7
2609.86	10.214	30.750	3.01053	3043.85	8.70	63.86	7.3	3008.75	9.85	7.85	0.8
2609.96	20.344	25.870	1.27160	3044.05	7.45	6.44	0.9	3008.85	10.71	8.95	0.8
2610.06	20.436	27.690	1.35495	3044.25	7.44	44.89	6.0	3008.95	11.95	6.06	0.5
2610.16	15.738	28.900	1.83635	3044.35	9.08	63.74	7.0	3009.05	11.10	8.41	0.8
2610.28	18.435	31.050	1.68427	3044.45	9.35	78.26	8.4	3009.25	10.42	6.32	0.6
2610.38	18.695	29.050	1.55392	3044.55	10.02	80.94	8.1	3009.35	12.21	9.72	0.8
2610.434	16.115	36.140	2.24269	3044.65	10.02	77.14	7.7	3009.45	12.21	11.47	0.9

2610.58	9.740	40.050	4.11178	3044.75	9.99	69.11	6.9	3009.55	12.38	8.68	0.7
2610.7	19.176	41.130	2.14488	3044.85	9.11	62.18	6.8	3009.65	9.45	5.36	0.6
2610.793	20.736	46.710	2.25257	3044.95	10.21	54.07	5.3	3009.75	9.45	6.97	0.7
2610.9	19.553	43.590	2.22932	3045.05	8.82	59.95	6.8	3009.85	10.93	8.48	0.8
2611	18.825	43.340	2.30224	3045.15	8.46	63.02	7.4	3009.95	12.65	8.24	0.7
2611.1	18.543	45.520	2.45483	3045.25	8.69	71.99	8.3	3010.05	9.25	13.49	1.5
2611.2	18.738	37.450	1.99861	3045.45	8.66	68.46	7.9	3010.25	11.97	18.89	1.6
2611.31	22.700	26.680	1.17532	3045.55	9.87	65.46	6.6	3010.35	15.23	34.06	2.2
2611.48	11.049	37.650	3.40764	3045.65	9.39	50.84	5.4	3010.45	14.53	40.66	2.8
2611.58	19.110	48.130	2.51860	3045.95	9.90	57.32	5.8	3010.55	10.82	31.48	2.9
2611.68	20.829	53.430	2.56514	3046.05	7.94	63.33	8.0	3010.65	17.53	18.59	1.1
2611.765	21.512	47.080	2.18859	3046.15	7.91	70.39	8.9	3010.75	17.53	17.72	1.0
2611.88	19.442	40.180	2.06670	3046.25	10.10	68.10	6.7	3010.85	17.03	20.66	1.2
2611.97	28.659	43.580	1.52062	3046.35	9.82	58.57	6.0	3010.95	16.39	21.82	1.3
2612.1	17.026	38.840	2.28122	3046.45	7.27	40.60	5.6	3011.05	16.18	21.12	1.3
2612.2	12.861	35.700	2.77587	3052.99	10.66	58.44	5.5	3011.15	16.87	20.07	1.2
2612.3	21.583	30.990	1.43585	3053.16	10.78	65.04	6.0	3011.25	16.60	19.39	1.2
2612.468	0.000	32.840	125.91400	3053.25	10.16	56.04	5.5	3011.35	14.02	19.55	1.4
2612.57	10.662	37.440	3.51154	3056.77	7.91	48.74	6.2	3011.45	15.54	33.96	2.2
2612.66	17.649	41.340	2.34234	3056.87	8.86	35.67	4.0	3011.55	14.73	75.90	5.2
2612.77	21.607	42.560	1.96974	3056.97	7.76	34.58	4.5	3011.65	12.80	53.10	4.1

2612.87	18.114	40.450	2.23307	3057.07	7.03	41.43	5.9	3011.75	13.29	41.50	3.1
2612.97	1.661	33.650	20.25352	3057.17	4.65	43.72	9.4	3011.85	12.28	28.00	2.3
2613.07	4.725	38.630	8.17495	3057.27	4.74	60.02	12.6	3011.95	10.62	14.86	1.4
2613.17	26.014	40.070	1.54034	3057.37	5.52	67.09	12.2	3012.05	10.08	8.81	0.9
2613.3	19.044	52.970	2.78147	3057.47	5.20	68.20	13.1	3012.15	9.56	7.98	0.8
2613.377	21.227	55.660	2.62208	3057.57	5.22	63.80	12.2	3012.25	10.79	10.76	1.0
2613.48	16.557	34.800	2.10186	3057.77	2.13	24.21	11.4	3012.35	9.25	12.40	1.3
2613.58	9.562	32.920	3.44263	3057.87	1.97	32.22	16.4	3012.45	9.41	9.58	1.0
2613.68	30.999	35.110	1.13263	3057.97	3.53	45.47	12.9	3012.55	10.01	9.89	1.0
2613.78	27.452	34.340	1.25091	3058.07	7.43	48.63	6.5	3012.65	10.41	12.27	1.2
2613.86	12.064	33.420	2.77033	3058.17	7.89	45.02	5.7	3012.75	9.51	11.99	1.3
2613.98	19.309	34.270	1.77487	3058.27	6.56	45.82	7.0	3012.85	8.41	7.49	0.9
2614.08	8.346	38.530	4.61677	3058.37	5.88	43.90	7.5	3012.95	10.53	0.40	0.0
2614.18	7.235	42.110	5.82034	3058.47	5.51	41.37	7.5	3013.05	6.83	7.23	1.1
2614.278	16.699	45.670	2.73492	3058.57	6.26	48.87	7.8	3013.15	7.30	11.29	1.5
2614.38	8.626	47.590	5.51716	3058.67	5.74	33.55	5.8	3013.35	11.38	13.46	1.2
2614.48	13.477	46.150	3.42429	3058.79	6.76	16.79	2.5	3013.45	11.26	16.29	1.4
2614.62	27.859	59.700	2.14293	3058.89	8.47	22.82	2.7	3013.55	9.10	15.45	1.7
2614.663	26.710	69.330	2.59562	3058.99	8.84	36.34	4.1	3013.65	8.21	12.04	1.5
2614.83	18.221	75.110	4.12222	3059.19	8.17	50.87	6.2	3013.75	9.51	14.07	1.5
2614.861	11.561	76.640	6.62945	3059.49	8.03	39.40	4.9	3013.85	7.22	10.74	1.5

2614.98	6.790	76.140	11.21367	3059.79	6.81	22.08	3.2	3013.95	4.71	9.31	2.0
2614.984	9.083	69.130	7.61123	3059.99	7.21	16.54	2.3	3014.05	6.40	8.37	1.3
2615.19	21.607	68.650	3.17722	3060.09	7.09	15.85	2.2	3014.15	8.78	5.48	0.6
2615.28	6.497	61.960	9.53704	3060.19	7.13	16.70	2.3	3014.25	7.54	8.02	1.1
2615.38	13.846	58.650	4.23597	3060.29	8.22	17.35	2.1	3014.35	6.84	6.89	1.0
2615.48	17.817	59.380	3.33271	3060.39	8.72	17.29	2.0	3014.45	5.78	5.28	0.9
2615.58	16.537	62.630	3.78737	3060.69	5.57	30.47	5.5	3014.55	7.28	5.36	0.7
2615.68	17.088	63.070	3.69095	3060.90	4.04	28.74	7.1	3014.65	8.23	4.48	0.5
2615.78	15.385	58.020	3.77122	3061.00	4.70	28.70	6.1	3014.75	5.88	6.93	1.2
2615.89	10.579	54.430	5.14532	3061.10	4.70	32.95	7.0	3014.85	7.74	5.68	0.7
2615.98	13.994	55.490	3.96518	3061.20	7.73	37.36	4.8	3014.95	7.70	5.06	0.7
2616.07	16.195	59.740	3.68891	3061.30	7.81	39.84	5.1	3015.15	7.12	3.79	0.5
2616.18	9.338	63.870	6.84008	3061.40	8.31	35.88	4.3	3015.25	8.26	5.26	0.6
2616.28	18.008	60.310	3.34911	3061.50	9.64	29.67	3.1	3015.65	11.97	7.61	0.6
2616.38	17.232	58.600	3.40059	3061.70	10.53	61.35	5.8	3015.75	6.47	13.29	2.1
2616.48	18.178	59.970	3.29904	3061.93	10.74	49.48	4.6	3015.85	9.50	12.66	1.3
2616.58	7.220	58.100	8.04706	3062.03	9.99	29.14	2.9	3015.95	3.00	11.21	3.7
2616.68	17.503	63.690	3.63890	3062.13	8.71	20.18	2.3	3016.05	1.34	13.07	9.8
2616.78	19.044	59.270	3.11228	3062.23	8.79	16.65	1.9	3016.15	11.56	17.84	1.5
2616.88	15.757	57.040	3.61987	3062.33	9.88	11.08	1.1	3016.25	11.50	28.69	2.5
2616.98	16.862	57.780	3.42664	3062.43	9.02	6.21	0.7	3016.45	10.94	26.45	2.4

2617.072	21.275	58.180	2.73472	3062.53	9.98	2.96	0.3	3016.55	12.42	25.22	2.0
2617.196	0.000	59.580	200.90980	3062.63	10.01	4.06	0.4	3016.75	11.13	23.84	2.1
2617.28	27.022	54.880	2.03094	3062.83	9.93	3.71	0.4	3016.85	12.37	26.26	2.1
2617.38	25.767	48.410	1.87877	3062.93	8.87	4.56	0.5	3016.95	11.53	26.63	2.3
2617.48	12.169	54.110	4.44666	3063.03	8.37	12.12	1.4	3017.05	14.32	27.36	1.9
2617.58	26.263	65.480	2.49326	3063.13	11.06	20.73	1.9	3017.15	14.46	27.03	1.9
2617.664	28.510	76.340	2.67770	3063.23	11.04	22.62	2.0	3017.25	13.72	29.87	2.2
2617.78	11.133	76.270	6.85055	3063.33	10.04	25.64	2.6	3017.45	13.54	26.22	1.9
2617.873	22.577	74.170	3.28524	3063.55	11.43	17.92	1.6	3017.65	10.38	23.73	2.3
2617.98	15.659	64.480	4.11776	3063.65	11.30	26.69	2.4	3017.75	5.88	13.86	2.4
2618.08	23.808	56.850	2.38784	3063.75	10.69	19.90	1.9	3017.88	12.54	25.70	2.0
2618.18	25.767	57.770	2.24203	3063.85	9.63	20.09	2.1	3017.98	7.46	32.06	4.3
2618.28	29.205	51.350	1.75828	3063.95	5.81	24.90	4.3	3018.08	6.54	26.90	4.1
2618.49	23.073	49.860	2.16093	3064.05	7.13	15.74	2.2	3018.18	11.52	27.74	2.4
2618.58	27.684	46.020	1.66233	3064.15	5.82	5.49	0.9	3018.28	10.95	28.96	2.6
2618.68	27.452	47.410	1.72701	3064.25	7.32	3.41	0.5	3018.38	11.47	33.58	2.9
2618.78	34.064	41.400	1.21537	3064.35	4.80	2.78	0.6	3018.48	12.14	30.29	2.5
2618.91	28.450	38.340	1.34763	3064.45	9.05	8.92	1.0	3018.58	11.81	32.65	2.8
2618.98	26.069	37.540	1.44003	3066.05	9.05	9.35	1.0	3018.68	9.52	32.77	3.4
2619.08	30.548	36.040	1.17977	3066.15	9.35	3.55	0.4	3018.78	8.97	30.25	3.4
2619.18	23.680	39.760	1.67904	3066.25	9.46	3.43	0.4	3018.88	8.97	31.55	3.5

2619.244	34.135	54.170	1.58691	3066.35	10.39	3.06	0.3	3019.18	4.81	22.15	4.6
2619.38	25.225	55.240	2.18989	3066.45	8.76	5.60	0.6	3019.28	1.56	17.63	11.3
2619.48	28.901	46.780	1.61865	3066.55	4.70	12.88	2.7	3019.38	1.26	15.02	11.9
2619.58	28.361	41.660	1.46894	3066.65	3.82	13.99	3.7	3019.58	3.01	19.28	6.4
2619.68	26.767	45.080	1.68417	3066.75	6.22	5.36	0.9	3019.68	2.72	26.73	9.8
2619.78	25.333	43.300	1.70926	3066.85	6.76	10.05	1.5	3019.98	1.96	15.03	7.7
2619.88	28.539	41.180	1.44291	3066.95	8.15	17.52	2.1	3020.18	4.48	23.80	5.3
2619.98	11.941	36.800	3.08172	3067.05	8.03	16.27	2.0	3020.28	4.00	10.87	2.7
2620.09	22.429	35.640	1.58899	3067.15	9.52	17.13	1.8	3020.38	0.78	7.48	9.6
2620.18	26.994	37.560	1.39144	3067.25	8.71	15.64	1.8	3020.48	1.27	9.67	7.6
2620.24	24.958	39.860	1.59711	3067.35	8.38	17.32	2.1	3020.58	1.89	5.04	2.7
2620.38	19.531	38.890	1.99122	3067.45	7.76	15.88	2.0	3020.68	1.25	3.66	2.9
2620.479	23.274	45.430	1.95193	3067.55	8.02	16.32	2.0	3020.78	1.36	5.31	3.9
2620.574	27.568	45.470	1.64939	3067.65	6.18	23.79	3.9	3020.98	0.94	5.85	6.2
2620.7	26.823	47.830	1.78315	3067.75	6.87	26.84	3.9	3021.08	1.25	8.95	7.1
2620.78	25.091	49.660	1.97919	3067.85	4.03	26.43	6.6	3021.18	1.47	12.49	8.5
2620.88	17.503	46.860	2.67733	3067.95	4.77	25.43	5.3	3021.28	3.55	13.26	3.7
2620.98	26.965	45.560	1.68959	3068.05	5.86	28.43	4.9	3021.38	3.96	13.93	3.5
2621.08	31.654	41.790	1.32022	3068.15	6.76	26.50	3.9	3021.58	2.32	20.13	8.7
2621.18	28.599	35.160	1.22940	3068.25	5.99	24.73	4.1	3021.68	2.66	7.61	2.9
2621.28	28.212	38.580	1.36750	3068.35	3.97	18.60	4.7	3021.78	4.82	4.57	0.9

2621.47	31.096	44.690	1.43716	3068.45	3.69	20.52	5.6	3021.88	4.35	12.57	2.9
2621.58	30.389	47.330	1.55747	3068.55	2.47	21.23	8.6	3021.98	9.83	31.57	3.2
2621.67	26.014	43.350	1.66642	3068.65	4.61	22.27	4.8	3022.08	6.69	16.18	2.4
2621.77	23.224	29.080	1.25215	3068.75	1.81	25.04	13.8	3022.18	6.39	15.31	2.4
2621.87	25.414	19.780	0.77833	3068.85	4.87	25.32	5.2	3022.28	6.65	21.21	3.2
2621.97	21.512	21.620	1.00504	3068.95	4.19	21.37	5.1	3022.38	8.94	30.40	3.4
2622.066	24.299	21.120	0.86916	3069.05	2.72	22.70	8.4	3022.48	9.14	33.88	3.7
2622.17	24.404	5.080	0.20817	3069.15	2.16	28.75	13.3	3022.58	9.89	29.38	3.0
2622.27	5.691	2.730	0.47974	3069.25	2.83	32.03	11.3	3022.68	8.53	12.69	1.5
2622.37	8.037	6.960	0.86596	3069.35	3.03	17.61	5.8	3022.78	1.87	10.99	5.9
2622.49	16.075	28.890	1.79724	3069.47	4.03	15.52	3.8	3022.88	1.87	8.43	4.5
2622.58	13.222	28.120	2.12677	3069.57	4.90	17.21	3.5	3022.98	3.52	5.46	1.6
2622.68	7.611	23.100	3.03515	3069.67	3.59	27.91	7.8	3023.08	3.35	4.65	1.4
2622.78	8.548	24.110	2.82063	3069.77	2.70	33.65	12.4	3023.18	3.98	3.81	1.0
2622.88	10.148	22.980	2.26441	3069.87	3.88	26.41	6.8	3023.28	4.34	3.55	0.8
2622.98	15.777	23.990	1.52055	3069.97	4.90	24.01	4.9	3023.38	4.66	3.34	0.7
2623.08	6.908	25.400	3.67691	3070.07	5.22	14.17	2.7	3023.48	4.06	2.49	0.6
2623.18	14.863	27.690	1.86299	3070.17	4.23	6.46	1.5	3023.58	4.20	1.97	0.5
2623.28	5.225	26.610	5.09266	3070.27	4.24	7.50	1.8	3023.68	3.06	1.47	0.5
2623.38	8.579	26.660	3.10761	3070.37	2.96	6.51	2.2	3023.98	4.83	4.60	1.0
2623.48	10.629	29.890	2.81223	3070.47	1.68	5.21	3.1	3024.08	9.40	6.13	0.7

2623.59	12.451	30.820	2.47535	3070.57	13.45	3.54	0.3	3024.18	9.59	5.42	0.6
2623.68	10.629	29.100	2.73790	3070.67	12.78	9.38	0.7	3024.28	8.52	4.81	0.6
2623.82	12.081	21.690	1.79537	3070.77	5.44	13.45	2.5	3024.38	7.12	3.59	0.5
2623.88	13.679	18.910	1.38238	3070.87	2.83	18.74	6.6	3024.48	3.72	1.99	0.5
2623.98	13.496	16.820	1.24634	3070.97	4.48	18.21	4.1	3024.58	3.81	2.30	0.6
2624.086	1.599	18.600	11.63085	3071.07	4.96	14.33	2.9	3024.78	3.02	6.45	2.1
2624.18	13.131	19.040	1.44998	3071.55	3.91	18.57	4.7	3024.88	5.30	2.93	0.6
2624.28	14.294	18.440	1.29007	3071.65	2.37	14.64	6.2	3024.98	4.36	1.16	0.3
2624.38	17.523	19.330	1.10310	3071.75	2.15	17.51	8.2	3025.08	5.44	2.18	0.4
2624.48	11.252	14.590	1.29661	3071.93	3.97	24.18	6.1	3025.18	5.63	4.29	0.8
2624.58	14.219	9.660	0.67939	3072.03	2.76	19.07	6.9	3025.28	7.37	4.96	0.7
2624.68	16.862	5.140	0.30483	3072.13	4.09	15.22	3.7	3025.48	8.74	4.79	0.5
2624.76	9.003	3.160	0.35098	3072.23	1.73	14.54	8.4	3025.68	5.63	4.88	0.9
2624.92	5.691	3.650	0.64142	3072.33	1.77	14.01	7.9	3025.88	9.04	3.86	0.4
2624.981	0.000	4.000	7.46447	3072.43	2.62	8.91	3.4	3026.18	4.87	2.47	0.5
2625.08	9.870	2.810	0.28469	3072.53	2.26	10.19	4.5	3026.28	5.98	2.68	0.4
2625.18	8.346	3.250	0.38942	3072.63	3.26	11.87	3.6	3026.38	5.98	4.08	0.7
2625.271	16.275	6.090	0.37420	3072.77	2.92	10.01	3.4	3026.48	10.48	3.63	0.3
2625.38	13.587	7.380	0.54315	3072.87	2.00	8.37	4.2	3026.58	5.55	4.29	0.8
2625.48	12.735	6.070	0.47662	3072.97	2.10	8.70	4.1	3026.68	5.55	4.37	0.8
2625.58	11.066	6.530	0.59012	3073.07	1.59	9.44	5.9	3026.78	6.72	5.61	0.8

2625.69	11.785	8.240	0.69919	3073.17	3.07	11.43	3.7	3026.88	8.67	3.88	0.4
2625.78	7.991	8.100	1.01360	3073.27	3.62	9.54	2.6	3026.98	8.65	2.18	0.3
2625.88	9.067	6.490	0.71580	3073.37	2.97	7.72	2.6	3027.18	5.37	2.69	0.5
2625.98	12.029	7.080	0.58860	3073.47	2.91	4.40	1.5	3027.28	4.91	2.51	0.5
2626	9.919	7.790	0.78535	3073.57	3.02	1.82	0.6	3027.38	4.64	3.43	0.7
				3073.67	2.96	1.12	0.4	3036.65	6.22	1.55	0.2
				3074.08	3.52	14.05	4.0	3036.75	6.96	1.55	0.2
				3074.18	3.19	13.82	4.3	3036.85	6.23	2.03	0.3
				3074.28	2.68	16.59	6.2	3038.65	3.44	3.09	0.9
				3074.38	1.35	18.26	13.5	3039.85	6.11	0.79	0.1
				3074.48	2.40	16.00	6.7	3039.95	7.46	0.88	0.1
				3074.58	3.01	10.16	3.4	3040.05	7.26	0.29	0.0
				3074.68	4.22	7.30	1.7	3040.15	4.77	0.74	0.2
				3074.78	3.16	6.60	2.1	3041.25	16.50	1.72	0.1
				3074.89	2.77	12.02	4.3	3041.65	4.01	2.36	0.6
				3074.99	3.77	10.23	2.7	3042.15	11.57	2.22	0.2
				3075.09	3.02	10.35	3.4	3042.25	11.61	1.09	0.1
				3075.19	2.66	9.62	3.6	3046.65	2.67	1.81	0.7
				3075.29	4.20	12.28	2.9	3046.75	2.89	1.65	0.6
				3075.39	3.61	9.70	2.7	3046.95	7.31	1.36	0.2
				3075.49	3.36	9.30	2.8	3047.15	3.27	1.84	0.6

				3075.59	4.71	8.11	1.7	3047.25	4.99	1.40	0.3
				3075.77	4.64	16.36	3.5	3047.35	1.39	1.93	1.4
				3075.87	3.72	17.19	4.6	3047.45	0.88	1.79	2.0
				3075.97	2.79	15.07	5.4	3047.65	0.64	0.62	1.0
				3076.07	4.64	15.86	3.4	3047.75	1.49	1.47	1.0
				3076.17	4.69	15.25	3.3	3047.85	2.30	1.74	0.8
				3076.27	3.09	13.29	4.3	3048.05	5.26	1.45	0.3
				3076.37	3.61	6.54	1.8	3048.15	5.26	1.88	0.4
				3076.47	2.66	4.25	1.6	3048.35	6.28	1.58	0.3
				3076.66	4.72	5.06	1.1	3048.45	6.28	1.50	0.2
				3076.76	4.13	6.64	1.6	3048.55	6.75	0.86	0.1
				3076.86	3.14	8.68	2.8	3048.65	7.52	1.75	0.2
				3076.96	3.03	12.10	4.0	3048.75	5.48	1.15	0.2
				3077.06	2.84	14.71	5.2	3048.85	8.35	1.05	0.1
				3077.16	4.08	15.72	3.8				
				3077.26	4.24	16.99	4.0				
				3077.36	4.42	13.73	3.1				
				3077.46	3.43	11.59	3.4				
				3077.56	3.63	7.48	2.1				
				3077.67	5.60	5.73	1.0				
				3077.77	5.34	6.26	1.2				
				3077.87	3.76	7.46	2.0				
				3077.97	6.02	7.95	1.3				
				3078.07	4.76	6.09	1.3				

				3078.17	5.62	3.08	0.5
				3078.27	5.96	1.37	0.2
				3078.37	2.42	1.43	0.6
				3078.47	1.24	1.28	1.0
				3078.67	2.87	7.62	2.7
				3078.77	1.40	6.81	4.9
				3078.87	1.93	7.14	3.7
				3078.97	5.01	8.53	1.7
				3079.07	3.78	10.41	2.8
				3079.17	3.41	7.67	2.2
				3079.27	4.28	2.88	0.7
				3079.37	5.11	0.00	0.1
				3079.47	4.97	0.00	0.0

Table 37. The distribution of the uranium concentration (U), the organic carbon (TOC) and the ratio U/TOC for the wells 7, 8, 6.

Depth, m	TOC thermal, %	U, ppm	U/TOC thermal	Depth, m	TOC thermal, %	U, ppm	U/TOC thermal	Depth, m	TOC thermal, %	U, ppm	U/TOC thermal
Well 7				Well 8				Well 6			
3120.05	12.28	21.72	1.8	2777.2	7.3	14.58	2.0	2694.30	1.34	11.50	8.6
3120.15	12.49	26.14	2.1	2777.3	5.2	12.44	2.4	2694.50	2.79	14.60	5.2
3120.25	13.79	32.56	2.4	2777.6	2.06	19.71	9.6	2694.70	9.19	26.50	2.9
3120.35	13.08	32.85	2.5	2777.7	3.47	14.73	4.2	2694.90	6.20	25.70	4.1
3120.45	12.33	27.55	2.2	2777.86	3.46	16.26	4.7	2695.30	4.34	15.70	3.6
3120.55	11.79	25.22	2.1	2777.96	8.08	21.14	2.6	2695.50	3.41	16.60	4.9
3120.65	11.55	25.73	2.2	2778.16	4.8	23.78	5.0	2695.70	4.42	17.50	4.0
3120.75	11.21	28.35	2.5	2778.26	7.05	28.57	4.1	2695.90	6.22	13.50	2.2
3120.85	12.25	33.40	2.7	2778.36	4.2	26.06	6.2	2696.30	4.13	17.60	4.3
3121.54	13.22	28.52	2.2	2778.46	3.83	20.69	5.4	2696.50	7.85	16.90	2.2
3121.64	11.61	32.08	2.8	2778.66	9.16	31.93	3.5	2696.70	5.24	18.30	3.5
3121.74	12.30	29.42	2.4	2778.76	8.7	40.63	4.7	2696.90	4.04	17.00	4.2
3121.84	13.07	32.51	2.5	2778.86	8.12	25.66	3.2	2697.10	6.76	19.20	2.8
3122.04	13.01	30.74	2.4	2778.96	9.67	26.6	2.8	2697.50	7.14	16.70	2.3
3122.14	12.40	32.99	2.7	2779.06	7.88	36.56	4.6	2697.70	4.56	23.20	5.1
3122.24	11.42	35.08	3.1	2779.16	6.3	40.98	6.5	2697.90	4.91	23.80	4.8
3122.34	11.42	36.08	3.2	2779.26	7.81	45.97	5.9	2698.10	7.75	25.60	3.3
3122.54	12.51	34.78	2.8	2779.56	7.8	50.2	6.4	2698.30	4.07	21.40	5.3
3122.64	12.10	36.64	3.0	2781.45	9.27	54.12	5.8	2698.70	5.91	22.50	3.8
3122.74	8.46	36.71	4.3	2781.55	8.78	49.63	5.7	2699.30	5.08	17.60	3.5
3122.84	5.71	31.29	5.5	2781.95	9.73	45.93	4.7	2699.70	4.87	30.20	6.2
3122.94	4.70	30.72	6.5	2782.05	8.87	42.31	4.8	2699.90	3.51	25.60	7.3
3123.14	6.32	56.23	8.9	2782.15	8.48	40.94	4.8	2700.30	3.60	31.40	8.7
3123.24	9.53	84.65	8.9	2782.25	10.08	39.54	3.9	2700.50	7.13	33.80	4.7
3123.38	11.45	51.20	4.5	2782.35	7.35	40.79	5.5	2700.70	8.93	44.40	5.0
3123.58	11.90	37.85	3.2	2782.45	5.72	44.36	7.8	2701.10	6.91	32.40	4.7
3123.68	12.00	40.13	3.3	2782.55	12.63	42.49	3.4	2701.30	9.69	35.30	3.6
3123.78	11.71	41.64	3.6	2782.65	10.02	47.21	4.7	2701.50	9.22	37.80	4.1
3123.98	10.75	45.76	4.3	2782.85	9.76	52.46	5.4	2701.70	10.54	49.60	4.7
3124.28	6.34	37.01	5.8	2783.25	9.32	62.97	6.8	2701.90	11.65	57.60	4.9

3124.49	13.31	36.68	2.8	2783.35	10.45	57	5.5	2702.30	7.99	38.40	4.8
3124.59	13.88	40.41	2.9	2783.65	12.08	68.7	5.7	2702.70	6.48	23.20	3.6
3124.89	13.69	31.87	2.3	2783.75	8.51	60.41	7.1	2702.90	7.83	23.30	3.0
3125.25	14.74	46.38	3.1	2783.85	12.37	66.68	5.4	2703.10	6.66	12.70	1.9
3125.36	12.32	40.03	3.2	2783.95	12.11	77.55	6.4	2703.30	8.85	10.90	1.2
3125.46	11.88	42.24	3.6	2784.05	9.16	82.5	9.0	2703.50	9.18	13.20	1.4
3125.56	13.00	42.69	3.3	2784.15	8.41	76.08	9.0	2703.90	11.20	11.80	1.1
3125.66	11.27	44.46	3.9	2785.88	12.48	57.52	4.6	2704.10	7.29	12.90	1.8
3125.96	13.11	45.70	3.5	2786.08	9.53	64.42	6.8	2704.30	8.00	13.00	1.6
3126.06	14.60	48.38	3.3	2786.18	11.54	83.16	7.2	2704.50	7.19	15.60	2.2
3126.26	13.91	53.55	3.9	2786.38	10.82	104.83	9.7	2705.10	8.69	17.30	2.0
3126.36	15.42	52.71	3.4	2786.58	20.96	69.39	3.3	2705.30	10.64	15.30	1.4
3126.46	15.99	56.60	3.5	2786.88	8.37	44.8	5.4	2705.50	8.88	8.60	1.0
3126.86	16.83	58.65	3.5	2786.98	7.51	43.21	5.8	2705.90	14.66	14.50	1.0
3126.96	16.40	57.95	3.5	2787.08	5.27	36.15	6.9	2706.10	6.83	47.10	6.9
3127.06	17.76	64.70	3.6	2787.18	8.75	40.89	4.7	2707.10	11.31	28.90	2.6
3127.26	17.75	60.93	3.4	2787.28	9.98	47.3	4.7	2707.30	15.12	25.60	1.7
3127.46	17.44	66.66	3.8	2787.38	9.29	41.36	4.5	2707.50	14.11	21.40	1.5
3127.56	17.53	65.82	3.8	2787.48	6.77	37.15	5.5	2707.70	4.66	23.90	5.1
3127.66	16.70	62.31	3.7	2787.58	4.1	42.48	10.4	2707.90	13.57	26.60	2.0
3127.76	14.45	63.15	4.4	2788.08	3.82	24.73	6.5	2708.10	14.76	34.40	2.3
3128.06	15.29	65.96	4.3	2788.28	3.83	22.09	5.8	2708.30	13.20	35.60	2.7
3128.16	14.91	58.18	3.9	2788.38	7.46	16.74	2.2	2708.50	14.28	36.60	2.6
3128.26	4.24	50.64	11.9	2788.48	2.53	16.1	6.4	2708.70	11.32	43.00	3.8
3128.46	7.50	61.89	8.3	2788.58	7.28	17.28	2.4	2708.90	16.45	40.70	2.5
3128.56	9.75	57.19	5.9	2788.77	3.79	28.45	7.5	2709.10	7.95	122.40	15.4
3128.66	3.58	51.53	14.4	2789.07	10.03	45.26	4.5	2709.30	6.59	47.70	7.2
3128.76	4.58	45.15	9.9	2789.17	11.41	41.68	3.7	2709.70	9.61	25.80	2.7
3128.86	1.93	44.26	22.9	2789.27	9.4	40.03	4.3	2709.90	9.09	34.80	3.8
3128.96	1.37	45.01	32.9	2789.47	11.41	37.74	3.3	2710.10	9.94	41.00	4.1
3129.06	3.76	39.63	10.5	2789.57	4.19	32.82	7.8	2710.30	9.84	32.80	3.3
3129.23	7.82	39.55	5.1	2789.97	5.85	20.28	3.5	2710.50	11.13	35.30	3.2
3129.33	2.50	37.88	15.2	2790.17	5.18	6	1.2	2710.70	8.95	42.00	4.7
3129.43	2.40	34.52	14.4	2790.27	9.32	5.48	0.6	2710.90	3.32	37.20	11.2
3129.73	3.31	31.20	9.4	2790.37	8.04	10.55	1.3	2711.10	3.76	14.10	3.7

3129.83	5.06	35.34	7.0	2790.47	6.42	24.19	3.8	2711.30	10.87	18.50	1.7
3129.93	6.94	31.66	4.6	2790.57	8.62	39.45	4.6	2711.50	8.50	27.70	3.3
3130.33	1.64	17.01	10.4	2790.67	8.31	39.21	4.7	2712.10	4.03	32.40	8.0
3130.53	0.94	14.66	15.6	2790.77	6.92	40.24	5.8	2712.30	9.17	34.30	3.7
3130.63	2.78	15.98	5.8	2790.87	5.99	37.59	6.3	2712.50	8.42	38.00	4.5
3130.73	1.80	20.57	11.5	2791.06	6.3	29.74	4.7	2712.70	8.73	39.10	4.5
3130.83	4.14	19.76	4.8	2791.16	4.12	28.61	6.9	2712.90	6.75	33.70	5.0
3130.93	1.33	16.77	12.6	2791.46	7.22	22.43	3.1	2713.10	10.97	38.10	3.5
3131.03	4.61	19.30	4.2	2791.76	7.88	37.35	4.7	2713.30	9.84	35.30	3.6
3131.13	2.54	20.34	8.0	2791.86	8.14	35.55	4.4	2713.50	9.08	41.20	4.5
3131.23	3.35	20.97	6.3	2791.96	8.91	35.66	4.0	2713.70	9.00	49.90	5.5
3131.33	3.27	27.26	8.3	2792.06	6.47	37.04	5.7	2713.90	11.26	47.40	4.2
3131.43	4.93	28.43	5.8	2792.26	8.33	36.17	4.3	2714.10	7.71	54.10	7.0
3131.53	4.50	21.21	4.7	2792.36	7.67	35.92	4.7	2715.50	7.76	12.20	1.6
3131.63	4.20	19.90	4.7	2792.46	6.83	36.05	5.3	2715.70	8.53	12.50	1.5
3131.73	5.56	23.06	4.1	2792.56	6.93	34.1	4.9	2716.10	0.95	7.80	8.2
3131.83	4.49	20.37	4.5	2792.66	6.48	30.42	4.7	2716.50	3.23	10.80	3.3
3131.93	4.03	22.98	5.7	2792.76	7.19	44.77	6.2	2716.70	3.76	16.50	4.4
3132.03	2.87	26.21	9.1	2792.86	7.23	36.96	5.1	2717.10	4.23	9.60	2.3
3132.13	3.26	19.58	6.0	2792.96	7.51	38.84	5.2	2717.30	3.12	13.40	4.3
3132.23	3.36	19.54	5.8	2793.14	7.27	40.17	5.5	2717.50	7.06	11.70	1.7
3132.43	5.49	24.82	4.5	2793.24	7.26	42.56	5.9	2717.70	2.95	15.10	5.1
3132.53	2.13	34.32	16.1	2793.34	9.12	44.27	4.9	2717.90	5.60	33.00	5.9
3132.63	3.33	41.52	12.5	2793.44	9.23	40.99	4.4	2718.10	1.19	10.90	9.2
3132.73	4.96	34.55	7.0	2793.54	8.64	43.68	5.1	2718.30	4.02	10.50	2.6
3132.83	3.51	29.76	8.5	2793.74	8.82	44.7	5.1	2718.50	4.75	6.70	1.4
3132.93	2.69	21.75	8.1	2793.94	8.99	46.87	5.2	2718.70	6.69	7.70	1.2
3133.45	2.32	10.95	4.7	2794.04	8.75	47.74	5.5	2718.90	4.55	6.80	1.5
3133.55	2.12	10.60	5.0	2794.14	8.75	49.97	5.7	2719.10	5.70	7.10	1.2
3133.65	3.05	9.31	3.1	2794.24	8.52	48.08	5.6	2719.30	2.21	6.90	3.1
3133.75	3.17	9.85	3.1	2794.44	9.46	32.35	3.4	2719.50	2.72	6.40	2.3
3133.85	1.05	8.11	7.7	2794.59	8.19	44.4	5.4	2720.10	7.10	8.70	1.2
3134.05	2.16	8.57	4.0	2794.79	9.05	49.8	5.5	2720.30	6.11	7.40	1.2
3134.23	3.41	9.81	2.9	2794.89	9.33	48.23	5.2	2720.50	3.84	6.10	1.6
3134.33	3.95	9.72	2.5	2794.99	8.82	52.25	5.9	2720.70	4.28	6.90	1.6

3134.43	3.62	10.35	2.9	2795.09	9.09	54.54	6.0	2720.90	2.20	5.90	2.7
3134.53	3.70	10.85	2.9	2795.29	9.79	49.61	5.1	2721.10	5.76	3.40	0.6
3134.63	2.13	9.01	4.2	2795.39	10.59	47.59	4.5	2721.30	7.34	8.80	1.2
3134.73	3.81	8.75	2.3	2795.81	10.15	51.6	5.1	2721.70	8.35	7.40	0.9
3134.83	3.50	9.09	2.6	2795.91	9.9	45.2	4.6	2721.90	3.24	6.30	1.9
3134.93	5.15	9.54	1.9	2798.63	5.11	25.34	5.0	2722.30	3.69	3.80	1.0
3135.03	5.29	10.82	2.0	2798.93	5.81	24.52	4.2	2722.50	5.06	5.80	1.1
3135.13	3.81	10.57	2.8	2799.13	1.79	30.37	17.0	2722.70	5.47	8.30	1.5
3135.23	4.40	10.17	2.3	2799.33	3.07	25.56	8.3	2722.90	3.15	5.50	1.7
3135.33	5.17	11.82	2.3	2799.43	4.87	31.16	6.4	2723.50	2.59	4.80	1.9
3135.47	4.97	11.97	2.4	2799.53	2.71	35.94	13.3	2723.70	3.46	4.80	1.4
3135.57	4.07	10.24	2.5	2800.63	4.02	14.35	3.6	2723.90	4.48	3.80	0.9
3135.67	2.98	8.04	2.7	2800.83	3.08	15.25	5.0	2724.10	5.75	4.60	0.8
3135.77	3.80	7.75	2.0	2802.13	4.39	4.54	1.0	2724.30	1.91	3.70	1.9
3135.87	5.31	6.28	1.2	2802.23	6.31	3.11	0.5	2724.50	4.59	3.10	0.7
3135.97	5.71	7.09	1.2	2802.33	1.71	4.21	2.5	2724.70	3.60	3.50	1.0
3136.07	5.38	8.50	1.6	2802.73	1.77	9.59	5.4	2724.90	0.55	3.90	7.0
3136.17	3.54	11.40	3.2	2803.23	0.53	8.52	16.1	2725.10	2.16	5.50	2.5
3136.27	5.01	11.57	2.3	2803.33	2.52	6.39	2.5				
3136.37	4.91	13.24	2.7	2803.53	4.37	8.01	1.8				
3136.47	3.48	10.88	3.1	2803.83	5.05	5.06	1.0				
3136.57	5.22	9.75	1.9	2803.93	3.54	5.22	1.5				
3136.67	4.10	9.86	2.4	2804.13	3.3	7.83	2.4				
3136.77	4.29	10.54	2.5	2804.53	2.05	6.47	3.2				
3136.87	4.47	12.79	2.9	2804.93	2.45	5.42	2.2				
3137.07	4.22	5.94	1.4	2805.33	3.98	1.67	0.4				
3137.17	2.54	6.08	2.4	2807.08	6.19	4.4	0.7				
3137.27	0.90	10.65	11.8	2807.28	3.22	3.13	1.0				
3137.41	5.60	11.76	2.1	2807.58	3.8	4.26	1.1				
3137.51	3.71	12.55	3.4								
3137.61	4.29	11.15	2.6								
3137.71	5.12	9.09	1.8								
3137.81	4.54	10.17	2.2								
3137.91	4.46	10.43	2.3								
3138.01	6.18	9.76	1.6								
3138.11	5.60	8.76	1.6								
3138.21	5.85	10.66	1.8								

3138.31	7.33	11.70	1.6
3138.41	6.37	12.88	2.0
3138.51	6.41	11.43	1.8
3138.61	6.39	10.20	1.6
3138.71	6.07	12.14	2.0
3138.81	4.68	12.05	2.6
3138.91	4.96	8.30	1.7
3139.01	3.70	8.22	2.2
3139.11	4.50	8.06	1.8
3139.28	6.91	10.91	1.6
3139.38	5.08	10.01	2.0
3139.48	5.22	10.73	2.1
3139.58	5.91	10.21	1.7
3139.68	5.27	10.95	2.1
3139.78	7.60	13.45	1.8
3139.88	5.65	8.64	1.5
3139.98	5.31	8.95	1.7
3140.08	5.31	10.23	1.9
3140.18	5.47	7.65	1.4
3140.28	5.77	7.57	1.3
3140.38	6.66	7.52	1.1
3140.49	5.08	5.26	1.0
3140.59	6.56	8.07	1.2
3140.69	5.43	5.71	1.1
3140.79	4.99	4.68	0.9
3140.89	7.05	5.05	0.7
3140.99	5.90	2.96	0.5
3141.05	5.09	5.88	1.2
3141.15	5.10	6.11	1.2
3141.25	4.58	5.20	1.1
3141.35	3.36	5.10	1.5
3141.45	4.73	6.72	1.4
3141.55	7.00	5.64	0.8
3141.65	5.64	6.32	1.1
3141.75	6.36	6.54	1.0
3141.85	8.52	7.04	0.8
3142.05	10.67	10.41	1.0
3142.15	7.81	12.66	1.6